The specific role of neutrophil- and epithelial cell-derived extracellular vesicles in antifungal defence against *Aspergillus fumigatus*

Dissertation

To Fulfil the Requirements

for the Degree of

„doctor rerum naturalium" (Dr. rer. nat.)

Submitted to the Council of the Faculty of Biological Sciences

of Friedrich Schiller University Jena

by Flora Rivieccio

Master of Science in Medical Biotechnology

born on August 8th, 1993 in Torre del Greco, Italy

2022

1. Gutachter: Prof. Dr. Axel A. Brakhage

Scientific Director, Leibniz Institute for Natural Product Research and Infection Biology – Hans-Knöll-Institute (HKI) Jena

2. Gutachter: Prof. Dr. Christine Skerka

Group leader, Leibniz Institute for Natural Product Research and Infection Biology – Hans-Knöll-Institute (HKI) Jena

3. Gutachter: Prof. Dr. med. Utz Reichard

Facharzt für Mikrobiologie und Infektionsepidemiologie in Göttingen

Datum der öffentlichen Verteidigung: 05/12/2022

Diese Arbeit wurde am Leibniz-Institut für Naturstoff-Forschung und Infektionsbiologie Hans-Knöll-Institut Jena, in der Abteilung Molekulare und Angewandte Mikrobiologie–Lehrstuhl für Mikrobiologie und Molekulare Biologie, Friedrich-Schiller-Universität Jena, unter
Leitung von Prof. Dr. Axel A. Brakhage angefertigt.

Table of Contents

Table of Contents I

List of Figures III

Zusammenfassung V

Summary VIII

1. Introduction 1

1.1 *Aspergillus fumigatus*: successful journey from the environment to the human host. 1

1.2 Defence against *A. fumigatus*: epithelial cells and alveolar macrophages coordinate antifungal response. 5

1.3 Neutrophils are essential immune cells against *A. fumigatus* 10

1.4 Extracellular vesicles: intercellular mediators in health and disease. 14

2. Research aims 18

3. Manuscripts 19

3.1 Manuscript A 19

3.2 Manuscript B 41

3.3 Manuscript C 53

3.4 Manuscript D 79

3.5 Manuscript E 109

4. Discussion 161

4.1 Neutrophil derived EVs are specific against *A. fumigatus* 161

4.1.1 DHN-melanin as inducer of antifungal EVs 162

4.1.2 Affinity of EVs for *A. fumigatus* hyphae and cargo delivery 163

4.1.3 C1q as a possible target molecule for fungal hyphae? 165

4.1.4 Immunosuppressing treatment affects neutrophil production of afEVs by neutrophils .. 167

4.2 PLB-985 cells: a valid model to investigate *A. fumigatus* 169

pathogenesis 169

4.3 Epithelial cells as key regulators of cytokine cascades 172

4.3.1 Bronchial epithelial cells-derived EVs: additional information carriers 174

4.3.2 *PyrG*-derived EVs as inducer of pro-inflammatory cytokines 175

5. References 178

6. Appendix 196

6.1 Additional results 196

6.2 Characterization of EVs derived from bronchial epithelial cells 196

6.2.1 Bronchial epithelial cells do not alter EVs production after infection. 196

6.2.2 Proteomic analyses show changes in the EV cargo only in the *ΔpksP*-derived EVs. 197

6.2.3 *PyrG*-induced EVs promote IL-6 secretion from unstimulated BECs 199

6.2.4 Infection of BECs with swollen conidia changes the content of EVs. 201

6.3 Contribution to Figures 204

Scientific contributions 213

Acknowledgements 215

Ehrenwörtliche Erklärung 216

List of Figures

Figure 1 *A. fumigatus* growth stages. 4

Figure 2 Interaction of *A. fumigatus* with innate immune cells. 7

Figure 3 Killing mechanisms of neutrophils. 13

Figure 4 Biogenesis of EVs and their composition. 15

Figure 5 Interaction of neutrophils with *A. fumigatus* WT conidia and production of afEVs. 166

Figure 6 Model summarizing the interaction of BECs with *A. fumigatus* conidia. 176

Figure 7 Concentration and size distribution of BEAS-2B cell-derived EVs. 197

Figure 8 Proteomic analysis on different subsets of EVs. 199

Figure 9 Evaluation of cytokines released from BEAS-2B cells. 201

Figure 10 Analysis of EVs derived from BEAS-2B cells infected with swollen conidia. 203

Zusammenfassung

Mit dieser Arbeit habe ich zur Aufklärung der Rolle und physiologischen Bedeutung von extrazellulären Vesikeln (EVs) beigetragen, die von verschiedenen Immunzellen nach Interaktion mit dem pathogenen Pilz *Aspergillus fumigatus* freigesetzt werden. Vor einigen Jahren wurde die Sekretion extrazellulärer Vesikel von neutrophilen Granulozyten beschrieben, die mit *A. fumigatus* konfrontiert waren. Insbesondere wurde gezeigt, dass EVs eine Reihe von antimikrobiellen Peptiden wie Azurocidin und Cathepsin G beherbergen und dass sie sich mit Pilzhyphen assoziieren können und sogar aufgenommen werden, wodurch das hyphale Wachstum gestoppt und Zellen abgetötet werden.

Mit meiner Arbeit habe ich weitere Aspekte dieser Wechselwirkung aufgeklärt und bin zu dem Befund gelangt, dass EVs, deren Bildung in Neutrophilen durch *A. fumigatus* Konidien induziert wurden, hochspezifisch sind und nur *A. fumigatus* abtöten, aber das Wachstum von Bakterien wie *Pseudomonas aeruginosa* oder sogar anderen nahen Verwandten wie *Aspergillus nidulans* nicht beeinflussen. Zusätzlich habe ich weiter starke Hinweise dafür erhalten, dass diese Spezifität durch das auf der Oberfläche von Konidien vorhandene Dihydroxynaphthalin (DHN) Melanin induziert wird. Wie bereits gezeigt, führte die Co-Inkubation von Neutrophilen mit einer nicht pigmentierten Mutante von *A. fumigatus*, der *ΔpksP*-Mutante, zur Produktion von EVs, die nicht mehr antimykotisch wirkten. Die Bedeutung von DHN-Melanin wurde durch die Konfrontation von Neutrophilen mit Melanin-Ghosts bestätigt: die so induzierten EVs wirkten toxisch auf *A. fumigatus*. Auch der DHN-Melanin-synthetisierende Pilz *Aspergillus clavatus* induziert die Produktion antimykotischer EVs, was die Bedeutung von DHN-Melanin unterstreicht, da dieser Pilz einer der wenigen ist, die gleichfalls DHN-Melanin enthalten. Die Bewertung der durch EVs induzierten Hyphenschädigung wurde mit umfangreicher konfokaler Bildgebung, bioinformatischer 3D-Rekonstruktion und Quantifizierung von Signalen und einem metabolischen Assay durchgeführt. Darüber hinaus habe ich gezeigt, dass die antimykotische EV-Population besonders viel Tetraspanin CD81 enthielt und dass ihre antimykotische Aktivität mit der Fähigkeit verbunden war, in Pilzhyphen einzudringen, was darauf hindeutet, dass eine intrazelluläre Lokalisation von EVs notwendig ist, um die antimykotische Fracht abzuliefern. Um die Rolle von EVs bei Gesundheits- und Krankheitszuständen zu untersuchen, wurden Neutrophile von

immunsupprimierten Patienten analysiert. Diese Analyse führte zu dem Befund, dass die Behandlung mit immunosuppriemerende Medikamenten die Fähigkeit von Neutrophilen, antimykotische EVs zu produzieren, vollständig aufhoben. Bemerkenswert ist, dass aus vergleichenden Proteom-Analysen von EVs, von Neutrophilen von gesunden Menschen und denjenigen immunsupprimierten Patienten geschlossen werden kann, dass einige Proteine in EVs von Neutrophilen von immunsupprimierten Patienten vollständig fehlen. Weitere Untersuchungen zu diesen Proteinen könnten Aufschluss über die antifungalen Abtötungsmechanismen geben, die von EVs ausgehen.

Des Weiteren wurde für die zukünftige Möglichkeit, EVs aus Neutrophilen in der Therapie gegen *A. fumigatus* gentechnisch zu manipulieren, ein Neutrophilen-ähnliches Zellmodell bestehend aus PLB985-Zell etabliert. Um das Potenzial dieser Zellen zu testen, sich wie primäre Neutrophile zu verhalten, wenn sie mit Konidien konfrontiert werden, habe ich Experimente zur Phagozytose, und Zytokin Freisetzung, durchgeführt. Zusammen mit Experimenten weiterer KollegInnen eröffnen diese Ergebnisse die Möglichkeit primären Neutrophilen durch die PLB985-Zelllinie zu ersetzen, um einiger Aspekte der *A. fumigatus*-Pathogenese untersuchen zu können.

Im Zuge meiner Forschung an EVs habe ich auch EVs aus Epithelzellen charakterisiert. Für Epithelzellen habe ich die Antwort von EVs nach Konfrontation mit ruhenden und geschwollenen Konidien und mit der *ΔpksP*-Mutante von *A. fumigatus* evaluiert. Die Analyse der EVs nach diesen verschiedenen Co-Inkubationen ergab, dass ihr Protein- und Zytokingehalt verändert ist. Insbesondere EVs von Zellen, die mit Wildtyp-Ruhekonidien infiziert waren, verstärkten die entzündungsfördernde Reaktion benachbarter Epithelzellen, während EVs, die nach Kontakt mit geschwollenen Konidien sekretiert wurden, mit Zytokinen angereichert waren, mit der potenziellen Rolle, mehr Zellen aus dem Blutkreislauf zu rekrutieren. Das zu EVs hier generierte Wissen könnte für eine zukünftige gezielte Therapie der invasiven Aspergillose genutzt werden, die spezifisch den Pilz, aber nicht das menschliche Gewebe schädigen und die Immunantwort verstärken würde.

Schließlich beleuchtete meine gemeinsame Arbeit mit anderen Autoren zu Virulenz-Determinanten von Pilzen den Einfluss von Temperatur- und Zeitwachstum auf die Oberflächenzusammensetzung von *Aspergillus*-Konidien und auch, wie die Expression grundlegender Virulenz Moleküle jedoch nicht verändert wird. Dabei

zeigte sich, dass sich der Pilz an unterschiedliche Umweltbedingungen anpassen kann, ohne seine „Unsichtbarkeit“ für das Immunzellen zu verlieren.

Summary

In this work I contributed to the elucidation of the role and physiological meaning of extracellular vesicles (EVs) released from epithelial cells and neutrophils after interaction with the pathogenic fungus *Aspergillus fumigatus*. Some years ago, the secretion of EVs from neutrophils confronted with *A. fumigatus* was described. In particular it was shown that EVs harbour an array of antimicrobial peptides like azurocidin and cathepsin G and that they can associate with fungal hyphae, or be internalized, leading to inhibition of fungal growth and cell death.

With my work I untangled more aspects of this interaction and came to the finding that EVs generated from neutrophils infected with *A. fumigatus* are highly specific in the killing of *A. fumigatus*, but do not kill bacteria, like *Pseudomonas aeruginosa*, or even other close fungal relatives like *Aspergillus nidulans*. Additionally, I received more evidence that this specificity is induced by dihydroxynaphthalene (DHN) melanin present on the surface of conidia. As already demonstrated co-incubation of neutrophils with a non-pigmented mutant of *A. fumigatus*, the *ΔpksP* mutant, led to the production of EVs which were no longer antifungal. The role of DHN-melanin was tested through the confrontation of neutrophils with melanin ghosts, and with the DHN-melanin synthesizing fungus, *Aspergillus clavatus*, which both induced the production of EVs toxic to *A. fumigatus*. Evaluation of the hyphal damage induced by EVs was performed with extensive imaging, based on confocal laser scanning microscopy, bioinformatic 3D reconstruction and quantification of signals, and a metabolic assay. Furthermore, I observed that the antifungal EV-population was enriched for the tetraspanin CD81 and that its antifungal activity was connected to the ability to enter fungal hyphae, suggesting that an intracellular localisation of EVs is necessary to deliver the antifungal cargo. To investigate the role of EVs in health and disease conditions, neutrophils from immunosuppressed patients were analysed. This analysis led to the result, that immunosuppressive treatments completely abolish the ability of neutrophils to produce antifungal EVs. Of note, comparing proteome analysis of EVs derived from neutrophils of healthy donors with EVs from neutrophils of immunosuppressed patients, revealed that some proteins are in the EVs from neutrophils of immunosuppressed patients completely absent. Further investigation on these proteins might shed a light on the antifungal killing mechanisms implemented by EVs.

Furthermore, for the future prospective of being able to genetically engineer EVs from neutrophils in the therapy against *A. fumigatus*, a neutrophil-like cell model, the PLB-985 cell line, was established. To test the potential of these cells to behave like primary neutrophils when confronted with conidia, I analysed the phagocytosis rate and cytokine release. My results, together with those of other colleagues, provide concrete evidence for the possibility of replacing primary neutrophils with the PLB-985 cell line, to investigate some aspect of *A. fumigatus* pathogenesis.

In the course of my research on extracellular vesicles I also characterized EVs from epithelial cells. I evaluated the cell response after confrontation with resting and swollen conidia and with the *ΔpksP* mutant of *A. fumigatus*. Analysing the EVs after these different co-incubations revealed that their protein and cytokine contents are changed. In particular EVs from cells infected with WT resting conidia boosted pro-inflammatory responses of neighbouring epithelial cells, while EVs secreted after contact with swollen conidia, were enriched in cytokines with the potential role of recruiting more cells from bloodstream.

The knowledge about EVs generated here, could be used for a future targeted therapy against invasive aspergillosis, which could specifically damage the fungus but not the human tissue and enhance the immune response.

Lastly my collaborative work with other authors, on fungal virulence determinants, highlighted the influence of temperature and time growth on shaping the surface composition of *Aspergillus* conidia and also how the expression of fundamental virulence molecules is however not changed. This indicates that the fungus adapts to different environmental conditions without losing its “invisibility” to immune cells.

1. Introduction

1.1 Aspergillus *fumigatus*: successful journey from the environment to the human host.

Aspergillus fumigatus is a ubiquitous saprophytic fungus belonging to the phylum Ascomycota. The natural niches where this mould can be found are soil, decomposing organic matter, or the compost pile (Tekaia & Latgé 2005). Several factors like the presence of nutrients or high oxygen levels, lead to its asexual sporulation (Mah & Yu 2006). During this process, airborne conidia, with a size of 2-3 μm, are formed from a specialized structure of *A. fumigatus* hyphae, called conidiophore (Figure 1) (Zhang et al 2021). It was estimated that a single conidiophore can generate up to 10^4 spores, which represent a real medical threat because they are efficiently dispersed into the air (van de Veerdonk et al 2017). Even if for hundred years it was believed that asexual sporulation was the only mean by which *A. fumigatus* could reproduce, recent advanced technologies in molecular genetics led to the discovery of mating-type and sex-related genes in its genome, which indicate that this fungus can also perform a fully functional sexual reproductive cycle (Latgé & Chamilos 2019, O'Gorman et al 2009, Paoletti et al 2005, Sugui et al 2011). *A. fumigatus* spreads and survives better than other Aspergillus species due to several fitness and virulence factors (Kwon-Chung & Sugui 2013). The conidia are in fact, highly hydrophobic, for the presence of a thick layer composed of a low molecular weight protein called RodA (Paris et al 2003, Valsecchi et al 2017). The rodlet layer makes them resistant to numerous environmental stressors like UV radiations and reactive oxygen species (ROS), plus it masks molecules recognized by our immune system (Aimanianda et al 2009, Bayry et al 2012, van de Veerdonk et al 2017). Another very prominent surface molecule is dihydroxynaphthalene (DHN) melanin which gives the typical grey-greenish color to the conidia (Figure 1) (Heinekamp et al 2013). It is biosynthesized by enzymes located in a gene cluster with a total of 6 genes: ayg1, arp1, arp2, abr1, abr2 and pksP (Langfelder et al 2003). All genes are essential for the biosynthesis of melanin but only the deletion of the polyketide synthase PksP, which is involved in the first step of polymerization of 1,8-DHN, produces a pigmentless strain (Akoumianaki et al 2016, Jahn et al 2000, Jahn et al 1997, Jahn et al 2002, Youngchim et al 2004). Conidia of this strain are much less virulent than the melanized one in an immunocompromised mouse infection model, demonstrating the important role of

melanin for immune evasion by *A. fumigatus* (Jahn et al 1997, Langfelder et al 1998). DHN-melanin interferes with immune cells by preventing recognition and phagocytosis of conidia from professional phagocytes, by modulating the secretion of cytokines, and even by blocking acidification of phagolysosomes (Aimanianda et al 2009, Chai et al 2010, Schmidt et al 2020, Schmidt et al 2018, Thywißen et al 2011).

Another peculiarity which makes *A. fumigatus* a successful opportunistic human pathogen is the thermotolerance (Bhabhra & Askew 2005). The temperatures at which the fungus can grow range from 20 to 60 °C, with 37 °C being the optimal temperature (Tansey & Brock 1972). In addition to its adaptation to human body temperature, *A. fumigatus* can very efficiently sequester elements like Fe^{2+} and Fe^{3+} (Brandon et al 2015, Misslinger et al 2021, Schrettl et al 2008), Zn (Amich & Calera 2014, Perez-Cuesta et al 2021) and Ca^{2+} (de Castro et al 2020, Juvvadi 2017) and produce additional secondary metabolites (Keller 2019, Raffa & Keller 2019) that contribute to the establishment of infection. Because of all these properties *A. fumigatus*, although not being the prevalent mould in the environment, is the most frequently isolated fungus from cultures of respiratory tract specimens, and its DNA is found in 37 % of lung biopsies from healthy individuals (Denning et al 2011, Máiz et al 2015, Mortensen et al 2011).

Pulmonary infections caused by *A. fumigatus* begin with the inhalation of conidia the concentration of which is quite high, both indoors and outdoors, ranging from 1 to 100 conidia per m^3 of air (O'Gorman 2011). However, the persistence of the fungus in the lungs and the outcome of an infection depends not only on the virulence characteristics of the fungus, but also on the immune status of the host (Cohen et al 1993, Hohl 2017, Ortiz et al 2022, Perfect et al 2001). In the presence of a healthy immune system the conidia are rapidly cleared from the lung parenchyma, but some clinical conditions and risk factors can favour the bypassing of immune defences (Dagenais & Keller 2009) (and & Langfelder 2002). Individuals with genetic defects like chronic granulomatosis disease (CGD) or cystic fibrosis (CF) are very often colonized with *A. fumigatus* and have a high risk of developing allergic conditions like allergic bronchial pulmonary aspergillosis (ABPA), or experience more severe complications like chronic obstructive pulmonary disease (COPD) and Invasive Aspergillosis (IA) (Guinea et al 2010, Hammond et al 2020, King et al 2016, Knutsen

& Slavin 2011, Marciano et al 2015). The immune system can also be impaired due to immunosuppressive treatments especially in patients with haematological malignancies or that underwent organ or stem-cell transplantations (Klein et al 2022, Lewis et al 2013, Little et al 2021, Post et al 2007, Rogacheva et al 2021). In these cohort of patients IA has a mortality rate between 40 and 90 % if not diagnosed in time and correctly treated (Lin et al 2001). Unfortunately, the diagnosis of IA, using non-invasive techniques, still relies on the simple, and most times inefficient, measurement of galactomannans or beta-glucan from blood samples or bronchoalveolar lavage fluid (BALF). A more precise detection is therefore based on histopathology performed on tissue biopsies, although the collection of these samples is not always feasible due to the critical conditions of the patients and the time needed to deliver the results, which can be several days (Lass-Flörl 2019, Ullmann et al 2018). The treatment of IA is also a major challenge for scientists and clinicians. Today, there are three classes of antifungal drugs available, *i.e.,* azoles, inhibitors of the ergosterol synthesis, echinocandins, inhibitors of beta 1-3 glucan synthesis in the cell wall and the polyenes which also bind ergosterol. The efficacy of all antifungals mostly depends on early and rapid treatment to prevent fungal colonization of the tissue (Jenks & Hoenigl 2018). In addition, combination therapy with antifungals must be used with caution due to hepatoxicity and nephrotoxicity of the individual agent and increasing fungal resistance (Campitelli et al 2017, Guegan et al 2021, Johnson & Perfect 2010, Pérez-Cantero et al 2020, Tverdek et al 2016). For all these reasons uncovering fundamental host-pathogen mechanisms, whose knowledge form the basis for developing novel strategies for the diagnosis and therapy of IA, is crucial and has been the focus of my doctoral research.

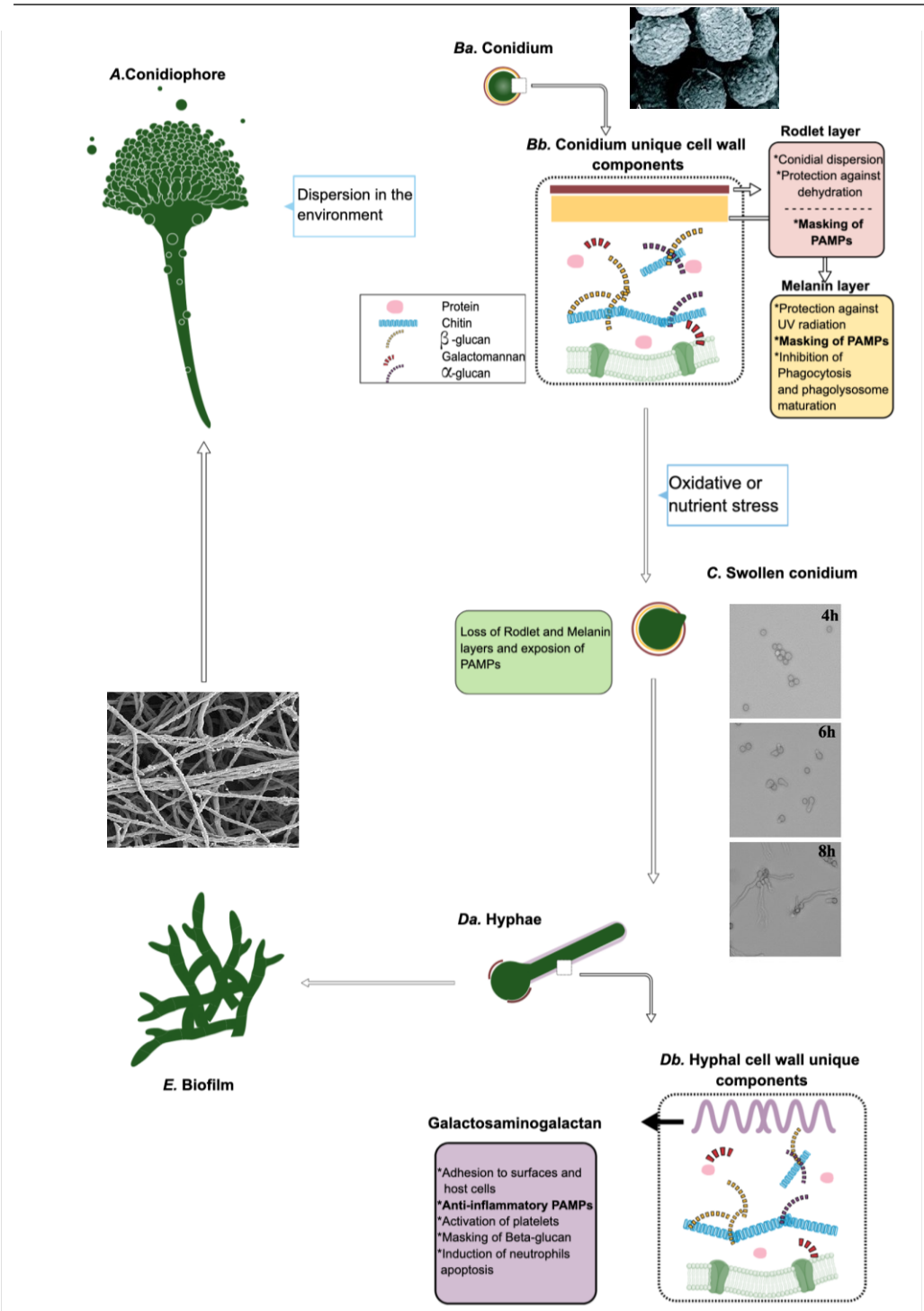

Figure 1 *A. fumigatus* growth stages.

A. fumigatus mostly reproduces asexually and releases the formed conidia from conidiophores to the air (A). The formed conidia are hydrophobic because of the presence of a rodlet and melanin layer as shown in Ba: SEM image of conidium surface (Credit to Pihet et al., (Pihet et al 2009)). The surface composition of conidia is unique (Bb) and it alters when the environmental conditions change (C). The rodlet and melanin layers are lost during swelling, leading to the formation of hyphae (Da). Hyphae also possess a peculiar cell wall composition (Db) and can form biofilms E: SEM picture of A. *fumigatus* biofilm (Credit to William et al., (Williams et al 2016)) Image created with Mindthegraph.com

1.2 Defence against *A. fumigatus*: epithelial cells and alveolar macrophages coordinate antifungal response.

After inhalation, the small-sized *A. fumigatus* conidia reach the human lungs (Figure 2) (Latgé & Chamilos 2019). In most cases, they are limited to the upper respiratory tract where they encounter bronchial epithelial cells (BECs) and are eliminated through mucociliary clearance (Osherov 2012). Besides producing mucus, the bronchial epithelium is able to phagocytose up to 20 % of conidia. A small percentage ends up in acidified phagolysosomes and is digested, but the majority is only contained for several hours within cells, leading eventually to conidial germination and their growth out of the epithelium (Ben-Ghazzi et al 2021, Bigot et al 2020a, Clark et al 2019, Culibrk et al 2019). Some molecules have been identified as fungal ligands on resting conidia, recognized by epithelial cells, like the lectin FleA which binds to mucins present in the airway mucus, or the protein CalA which interacts with integrin α5β1 on host cells (Kerr et al 2016, Liu et al 2016, Richard et al 2018). Moreover, epithelial cells can also strongly bind a polysaccharide exposed on swollen conidia, the beta 1-3 glucan, through the dectin-1 receptor (Sun et al 2012). Dectin-1 is a C-type lectin receptor, required for the defence against *A. fumigatus* (Romani 2011). Immunocompetent mice lacking this receptor showed increased susceptibility to intratracheal *A. fumigatus* infection compared to wild type mice and in humans a dysfunctional dectin-1 is connected to a high risk of developing IA (Ferwerda et al 2009, Sainz et al 2012, Werner et al 2009). Binding of dectin-1 to beta 1-3-glucan, initiates the transduction *via* the Syk/CARD9 and Raf-1 signalling pathways. Both cascades end with the induction of the nuclear factor (NF)-κB and transcription of pro-inflammatory genes (Drummond & Brown 2011, Geijtenbeek & Gringhuis 2009). Furthermore, the Syk kinase also activates the NLRP3 inflammasome triggering the cleavage of IL-1β and IL-18 from caspase-1 (Jeong et al 2018). Additionally, lung epithelial cells can sense the presence of *A. fumigatus* through Toll like receptors (TLRs) (Mayer et al 2007). The expression of all 10 TLRs was in fact detected *via* real time PCR in airway human epithelial cells, and mutations in TLR 2 and 4 are considered risk factors for development of IA (Balloy et al 2005, Bellocchio et al 2004a, Blease et al 2001, Sha et al 2004). Even though the molecule inducing their activation remains a mystery, they are known to respond by secreting pro-inflammatory mediators in a MyD88-NF-κB-dependent way (Balloy et al 2008). The generation of cytokines and chemokines from epithelial cells is crucial to establish an

efficient host response against *A. fumigatus* (Figure 2) (Ewald et al 2021, Øya et al 2019). Cytokines like IL-8 act on the recruitment of neutrophils by stimulating their chemotaxis, their degranulation and their ROS production (Balloy & Chignard 2009). IL-6 can promote mucus formation and maturation of T helper type 2 cells (Heijink et al 2002, Oosthuizen et al 2011, Shin et al 2006) and GM-CSF can function simultaneously on immature hematopoietic cells inducing their final differentiation, but also on mature neutrophils and macrophages to enhance their antimicrobial activities (Bigot et al 2020a, Kasahara et al 2016). In addition to recruiting factors epithelial cells produce soluble antimicrobial peptides capable of damaging the fungus directly. For example, human beta defensins are highly expressed in bronchial epithelial cells after exposure to *A. fumigatus* and lysosomal enzymes like N-Acetyl-β-d-glucosaminidase, Cathepsin B and D were found in the secretome of infected BECs (Alekseeva et al 2009, Fekkar et al 2012).

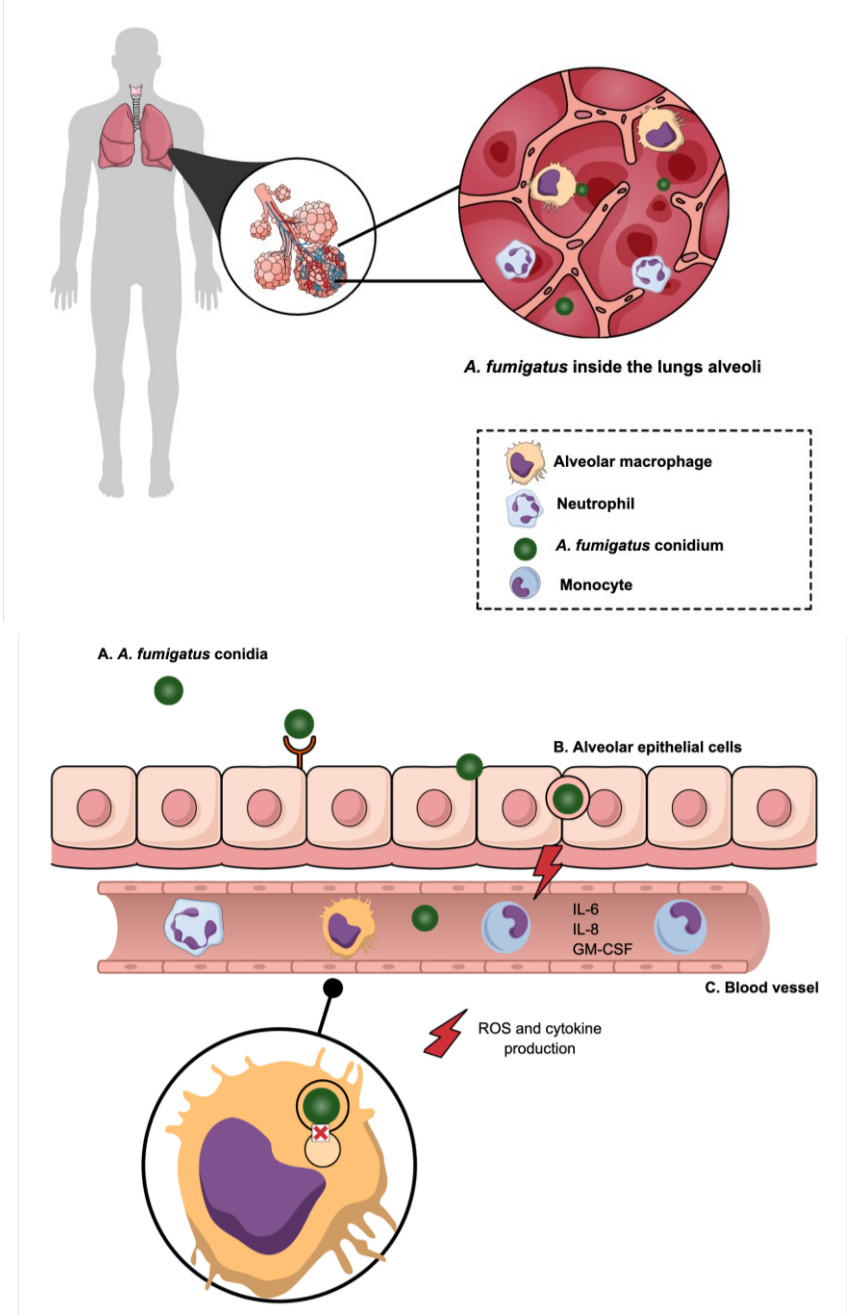

Figure 2 Interaction of *A. fumigatus* with innate immune cells.

After inhalation, the small conidia reach the lungs' alveoli. Upon contact with conidia, epithelial cells release anti-inflammatory cytokines to recruit neutrophils, macrophages, and monocytes from blood. Alveolar macrophages are important for the clearance of conidia due to their phagocytic ability. They also produce reactive oxygen species and cytokines to amplify the inflammation wave and boost the activity of other immune cells. In the case of *A. fumigatus*, the degradation following phagocytosis by macrophages is inhibited by the DHN-melanin on the surface of conidia. This molecule interferes with the assembly of the V-ATPase and acidification of phagolysosomes and allows conidia to survive for some time in macrophages. Image created with Mindthegraph.com

Alveolar macrophages are the first immune cells that encounter *A. fumigatus* inside the lungs alveoli (Dagenais & Keller 2009, Latgé & Chamilos 2019). Computer modeling systems predicted the presence of only one resident macrophage for every three alveoli, but even being in such a low number they have a notable role in the management of infection (Neupane et al 2020, Romani 2011). As professional phagocytes, they recognize the fungus through pattern recognition receptors (PRRs) (Brakhage et al 2010). In particular the dectin-1 receptor, like for epithelial cells, it´s also important for the binding of beta 1-3-glucan by macrophages (Brown et al 2002, Steele et al 2005). This binding is only possible when the carbohydrate is accessible on the surface of conidia that is mainly on swollen conidia or early germlings (Luther et al 2007). The activation of dectin-1 leads to reorganization of surface molecules, cytoskeleton rearrangements, and formation of the phagocytic cup to engulf the conidia (Goodridge et al 2011, Goodridge et al 2012). Furthermore, it promotes the release of cytokines and chemokines including TNF-α, IL-1β, IL-6, IL-8, macrophage inflammatory protein (MIP)-1α, and monocyte chemoattractant protein (MCP)-1 which are fundamental for recruitment and stimulation of other immune cells from the bloodstream (Brown et al 2003, Dubourdeau et al 2006, Phadke & Mehrad 2005). Generation of pro-inflammatory cytokines induced by dectin-1, in macrophages, requires the co-stimulation of the TLR2 and 4 (Braedel et al 2004, Faro-Trindade et al 2012, Gantner et al 2003, Gersuk et al 2006, Meier et al 2003). Knockouts of TLR2 or the MyD88 adaptor proteins, in macrophages, both in human and mouse cell lines, showed reduced cytokine production and phagocytosis. Conidia engage equally TLR2 and 4 but signalling through TLR4 is lost after formation of hyphae, suggesting a more important role of this receptor in late stages of infection (Chai et al 2009, Mambula et al 2002, Marr et al 2003, Netea et al 2003). Following ingestion, conidia are then processed by alveolar macrophages (Dagenais & Keller 2009). Killing is exerted through production of ROS and phagolysosomal acidification (Ibrahim-Granet et al 2003). The role of ROS was demonstrated in alveolar macrophages from $47^{phox-/-}$ CGD mice, or wild-type alveolar macrophages treated with chemical inhibitors of NADPH oxidase which were not able anymore to efficiently eliminate the fungus (Philippe et al 2003). Furthermore, mitochondrial ROS contribute also to this fungicidal activity (Shlezinger et al 2021). However, the role of ROS for killing is a matter of debate since mutant strains of *A. fumigatus* supersensitive for ROS are still virulent in a mouse infection model (Lessing et al 2007).

The last crucial step required for degradation of conidia is the maturation of phagosomes to functional phagolysosomes. Phagolysosomal acidification depends on the vATPase proton pump, which lowers the intraluminal pH thereby activating catalytic and proteolytic enzymes (Hackam et al 1999, Westman & Grinstein 2021). The assembly of the vATPase on the phagolysosomal membrane is delayed by DHN melanin of *A. fumigatus* allowing a longer intracellular survival of the fungus (Figure 2) (Schmidt et al 2020, Thywißen et al 2011). Regardless the significant role of epithelial cells and alveolar macrophages, immune cells that are absolutely essential for a complete clearance of *A. fumigatus* are neutrophils. Their defence strategies will be discussed in the following chapter.

1.3 Neutrophils are essential immune cells against *A. fumigatus*

Polymorphonuclear granulocytes (PMNs), or neutrophils, belong to the professional phagocytes of the human innate immune system (Mayadas et al 2014). They represent 60 % of the circulating white blood cells and circa 70 % of the whole leukocyte population (Li et al 2002). PMNs originate from myeloid pluripotent progenitors in the bone marrow. These cells undergo a series of differentiation steps, ending with the release of circa 10^{11} mature and terminally differentiated neutrophils per day in the bloodstream (Cowland & Borregaard 1999, Dancey et al 1976, Hidalgo et al 2019). Once they start circulating their life span is very short, between 4 and 18 h. After this time, they activate apoptosis and are mainly phagocytosed by resident macrophages of the liver, spleen, and bone marrow (Basu et al 2002, Bratton & Henson 2011, Lahoz-Beneytez et al 2016, Liew & Kubes 2019, Shi et al 2001). However, this rapid turnover does not affect the number of circulating neutrophils, which remains constant thanks to a perfect balance between production and elimination (Adrover et al 2016, von Vietinghoff & Ley 2008). Mature PMNs possess special features that distinguish them from all other cells: the polylobulated nuclei surrounded by small amounts of laminin A/C, which contributes to their plasticity and facilitates migration to the site of infection (Manley et al 2018, Rowat et al 2013), and the presence of granules in their cytoplasm (Borregaard & Cowland 1997b, Carvalho et al 2015, Rosales 2018). Granules start to form before the full maturation of neutrophils and continue this process until the very last step of segmentation (Borregaard & Cowland 1997a, Borregaard et al 1995). Based on their size, morphology, and protein content granules are divided into three classes (Bainton et al 1971). Primary, or azurophilic, granules carriers of potent hydrolytic enzymes like elastase, myeloperoxidases (MPO), and defensins. Secondary, or specific, granules enriched with the iron-binding protein lactoferrin, collagenase, lysozyme, and the cytochrome b558, and tertiary, or gelatinase granules harbouring matrix metalloproteinases, such as gelatinase (Borregaard & Cowland 1997a, Sheshachalam et al 2014).

The journey of mature neutrophils does not end in the bloodstream, in fact upon exposure of selectins from endothelial cells, they start rolling along the vessel´s wall and with an integrin-mediated movement, they transmigrate from the blood into the infected tissue, a process called extravasation (Schnoor et al 2021). Arrival and activation of PMNs in the lungs following *A. fumigatus* colonization are decisive for

the resolution of the infection. Their pivotal function is illustrated in neutropenic mouse models or neutropenic and CGD patients that have a very high susceptibility to this infection. (Cohen et al 1981, Gerson et al 1984, Pollock et al 1995, Svirshchevskaya et al 2009). Neutrophils respond to all the different fungal morphotypes with the help of various tools (Gazendam et al 2016), including phagocytosis (Lehrer & Jan 1970), degranulation (Levitz & Farrell 1990, Zarember et al 2007), generation of ROS (Boyle et al 2012, Prüfer et al 2014), production of neutrophils extracellular traps (NETs) (Bruns et al 2010, McCormick et al 2010), production of cytokine and chemokines (Hasenberg et al 2011, Mehrad et al 1999), and as more recently discovered, secretion of extracellular vesicles (Shopova et al 2020).

Recognition of the pathogen is the first step toward efficient phagocytosis. For this purpose neutrophils express on their surface different receptors: the C-type lectin receptors (CLRs) dectin-1 (Gringhuis et al 2012, Steele et al 2005, Werner et al 2009), dectin-2 and mincle, the Toll-like-receptors (TLRs) (Bellocchio et al 2004a, Bellocchio et al 2004b) and the complement receptors (CR1, CR2, CR3) (Braem et al 2015, Moalli et al 2010). Ingestion of resting conidia from human neutrophils is enhanced by opsonization. The opsonins present in blood and lung tissue are complement proteins and antibodies. Their function is to flag the surface of a pathogen making it visible to the professional phagocytes. IgG and IgM were shown to bind *A. fumigatus* conidia, and afterwards interact with the C1q complement protein. This protein initiates the classical complement pathway forming a complex with two serine-proteases C1r and C1s. Together they process the C4 and subsequentially, C2 protein generating the C3 convertase (Gaboriaud et al 2003, Venkatraman Girija et al 2013). The binding of C1q in some cases is mediated by the pentraxin 3 (PTX3) a soluble pattern recognition molecule (Parente et al 2020). *Moalli et al*. showed that the N- terminal domain of PTX3 is responsible for conidia detection but the full-length molecule is required to enhance the phagocytic activity of neutrophils (Moalli et al 2010).

Furthermore, conidia can be sensed by other opsonins present in the human serum called L-ficolins (Bidula et al 2015, Bidula et al 2016). Normally, ficolins are only initiators of the alternative complement pathway which also culminates with the formation of the C3 convertase, but during *Aspergillus* infection, they might exert additional functions, as ficolin-deficient mice display increased fungal burden and

severe illness compared to wild-type mice (Genster et al 2016). In this context, one study showed that ficolin-2 can bind directly to *A. fumigatus*, and subsequently interact with PTX3 modulating complement activation (Dumestre-Pérard et al 2008, Gout et al 2011, Ma et al 2009). All these opsonization patterns culminate with C3 deposition and CR3-mediated elimination of conidia through activation of the FCγRs receptors (Genster et al 2016). As discussed for epithelial cells and macrophages, neutrophils can also bind the beta 1-3-glucan once the conidia start swelling. Nevertheless, dectin-1 recognition of particles seems to be not the major contributor to phagocytosis and activation in human neutrophils (Gazendam et al 2016, van Bruggen et al 2009). On the contrary, the engagement of TLRs is crucial for the induction of some oxidative pathways, such as the release of granules and pro-inflammatory cytokines which contribute to the reduction of fungal burden (Bellocchio et al 2004b).

Once *Aspergillus* conidia have swollen, they become too large to be engulfed by PMNs. A series of mechanisms are initiated by neutrophils designed to inhibit fungal growth. One of these is the formation of neutrophil extracellular traps (NETs) (Diamond et al 1978). As a consequence of the drastic changes which brings in the cells, in particular their eventual death, NETosis is often referred to, as a cell death program (Fuchs et al 2007). Hallmarks of NETosis are decondensation of chromatin, loss of nuclear shape and disintegration of the nuclear membrane, homogenization of the nuclear and cytoplasmic content and their expulsion outside the cells (Brinkmann et al 2004). Fundamentally NETs represent a web of chromatin fibers, full of histone proteins and antimicrobial peptides like MPO, neutrophils elastase, and other degradative enzymes (Dąbrowska et al 2016). An important pathway for the generation of NETs in human neutrophils, is dependent on the activation of the NADPH oxidase as demonstrated by the inability of CGD patients and $p47^{phox-/-}$ mice, to control fungal infections (Remijsen et al 2011, Röhm et al 2014). Furthermore, the involvement of the Raf-MEK-ERK pathways is also required for their full engagement in NETs production and inhibition of apoptosis (Hakkim et al 2011).

Due to their non-specific content, NETs can be deleterious to tissues, and lead to hyperinflammation and eventually organ failure (Mutua & Gershwin 2021), therefore their formation must be limited. Additionally, in the context of aspergillosis, their function has been shown to be dispensable. In fact, their secretion from neutrophils

can be reduced by the hydrophobin RodA present on the surface of conidia and they are only mildly fungistatic against hyphae (Bruns et al 2010, McCormick et al 2010). For this reason, neutrophils must possess additional extracellular killing mechanisms to harm the fungus. These mechanisms will be the topic of the next chapter.

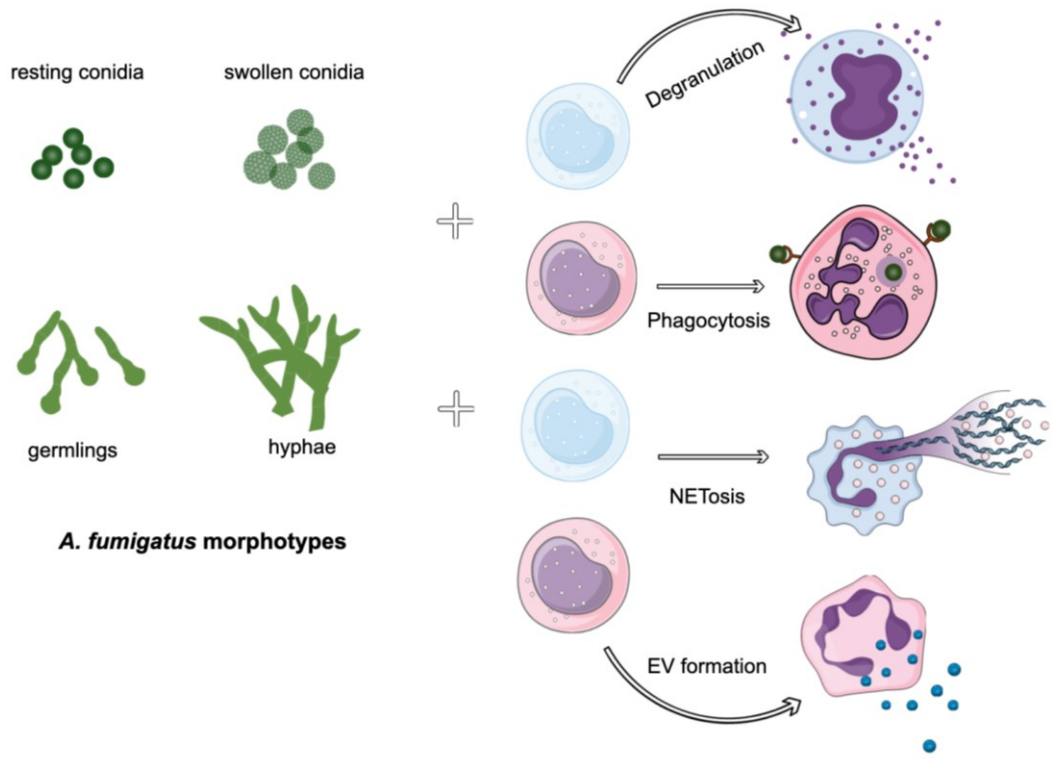

Figure 3 Killing mechanisms of neutrophils.

Neutrophils employ different strategies to kill *A. fumigatus* depending on the growth stages of the fungus. The first interaction with resting conidia coated with DHN-melanin, leads to phagocytosis and intracellular degradation. Nevertheless, as in alveolar macrophages, also in neutrophils the phagosome maturation is delayed by DHN-melanin. Degranulation as well as NET formation are induced by all three morphotypes and are followed by neutrophil cell death. NETs are webs of chromatin fibers is full of DNA and antimicrobial peptides which literally trap hyphae and hardly block their growth. Lastly, as recently showed, conidia can trigger the release of antifungal EVs. Image created with Mindthegraph.com.

1.4 Extracellular vesicles: intercellular mediators in health and disease.

Extracellular vesicles (EVs) are lipid-enclosed particles secreted from nearly every cell type and organism (Raposo & Stoorvogel 2013). Their main function is to transfer information, in the form of protein, DNA, RNA, or lipid, from one cell to another (Nederveen et al 2021). Based on their size and biogenesis they are classified into exosomes, microvesicles, apoptotic bodies, and more recently a new population of super-small particles (< 50 nm) named exomeres, was described (Anand et al 2021). Apoptotic bodies are the largest member of the EV family (500- 4000 nm) and they are normally secreted by cells undergoing apoptosis. This type of cell death is highly regulated and leads to the compartmentalization of all cellular components and their incorporation into apoptotic bodies. These are then released from the dying cell and phagocytosed by professional phagocytes to avoid induction of inflammation (Elmore 2007). Microvesicles are usually greater than 200 nm and originate from direct budding from the plasma membrane (Tricarico et al 2017), while the smallest family components, exosomes (< 150 nm) are first formed within a structure called the multivesicular body (MVB) and then released in the extracellular space by MVB fusion with the plasma membrane (Figure 4) (Latifkar et al 2019, Yokoi & Ochiya 2021). Independently from the way they are secreted from cells, the generation of all EVs requires the presence of the ESCRT (Endosomal Sorting Complex Responsible for Transport) machinery. This machinery consists of four main protein complexes, ESCRT 0, I, II, III, and some adaptor proteins. ESCRT-0 is the first one to associate with the endosomal membrane, shuttling through its Hrs subunit, ubiquitinated proteins. Afterward, the same Hrs compartment interacts with a subunit of the ESCRT-I protein complex called the tumor susceptibility gene 101 (TSG101), leading to the assembly of ESCRT-II. Through ESCRT-I incorporation with ESCRT-II, intraluminal vesicles (ILVs) invaginate into the MVB lumen. Later on, the ESCRT-III complex is also coupled and activated, playing a crucial role in EV formation by initiating membrane deformation and detachment of the MVBs from the plasma membrane (Frankel & Audhya 2018, Mir & Goettsch 2020).

Although ESCRTs are major contributors in exosome formation, they are not the only factors involved. More recently, cargo selection mechanisms independent of ESCRT, have been described. It was observed that increased ceramide levels, produced by sphingomyelinases can promote in different ways MVB maturation (Shamseddine et

al 2015), or that ILVs formation and cargo sorting could also be triggered by the tetraspanin CD63 in the absence of a functional ESCRT machinery (Edgar et al 2014, van Niel et al 2011).

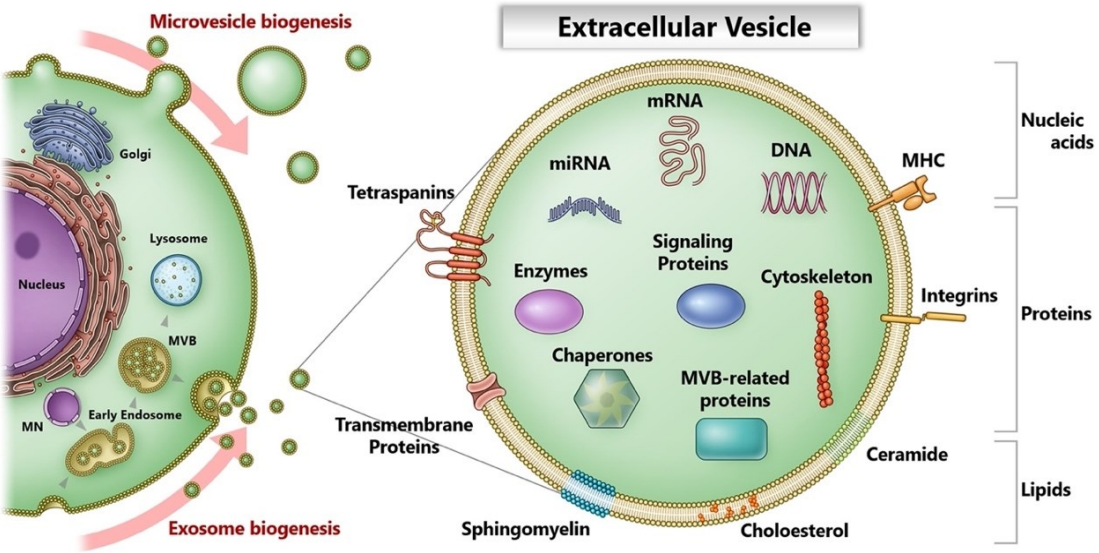

Figure 4 Biogenesis of EVs and their composition.

A. Microvesicles originate from reorganization of the plasma membrane and its outward blebbing. **B.** Exosomes are formed by invagination of intraluminal vesicles (ILVs) inside early endosomes, which then mature into a structure called multivesicular body (MVBs). The MVBs can fuse with the plasma membrane releasing exosomes in the extracellular space or fuse with lysosomes resulting in the degradation of their content. **C.** Exosomes are lipid bilayer-enclosed particles that can contain proteins, nucleic acids, or lipids. Their composition changes depending on the type and conditions of the releasing cell. (Image credit to Yokoi & Ochiya, 2021).

The importance of EVs lies in their multiple functions. However, to be functional, they must somehow be perceived by the recipient cell. In some cases, EVs have been shown to interact preferentially with certain cell types (French et al 2017). For example, EVs from leukemia cells were internalized through phagocytosis only by professional phagocytes but remained attached to the membrane of non-phagocytic cells (Feng et al 2010). Furthermore, the EVs selectivity was also observed *in vivo*, with their differential organ distribution (Lai et al 2014). The surface protein composition of EVs is in part accountable for this phenomenon. Tetraspanins such as CD81, CD63, and CD9 are regularly found on EVs and are considered “EV markers” (Simpson et al 2012).

In light of the heterogeneous distribution of tetraspanins across different EV populations, it is evident that these molecules do not just accumulate on the surface of EVs due to their involvement in protein recycling, but also because they can interact with molecules on the recipient cells (Jankovičová et al 2020). For instance, CD81 was shown to interact with the VCAM-1 integrin thereby strengthening the adhesiveness of monocytes to the vascular endothelium (Feigelson et al 2003). Besides tetraspanins, the EV surface is also enriched with integrins, proteoglycans, and lectins which play a crucial role in their docking and uptake (French et al 2017). What has also aroused great interest in the scientific community since the discovery of EVs, is their cargo, which consists of proteins, DNA, RNA, and lipids (Figure 4) (Anand et al 2019). The ability to decipher the cargo of an individual EV population through, transcriptomic, proteomic, or sequencing techniques opened up the possibility of manipulating this content to create genetically engineered vesicles that can be used as therapeutic agents (Li et al 2018).

Recent evidence has shown that EVs play also an important role in combating pathogens (Brakhage et al 2021). EVs secreted by mouse macrophages could reduce *Mycobacterium tuberculosis* infection both *in vivo* and *in vitro,* and dendritic cell-derived EVs, were able to activate the response of NK cells against the bacterium *Chlamydia psittaci* (García-Martínez et al 2019, Radomski et al 2019).

In addition to all the "lethal weapons" discussed in the previous paragraph, neutrophils can also produce EVs during inflammatory processes (Hong 2018). They were first characterized as phosphatidylserine-containing particles with a size between 100 and 2000 nm (Gasser et al 2003, Hess et al 1999, Stein & Luzio 1991).

Depending on the target cells, they can trigger either pro-inflammatory or anti-inflammatory reactions. In the context of rheumatoid arthritis, neutrophil-derived EVs (NDEVs) have been shown to be loaded with the anti-inflammatory protein annexin A1 which stimulates chondrocytes to produce extracellular matrix and cartilage, thus exerting a beneficial effect on joints (Headland et al 2015). Moreover, NDEVs were also able to decrease the inflammatory state of human macrophages and dendritic cells, primed with zymosan and LPS through the expression of phosphatidylserine (PS) in the outer membrane (Eken et al 2010). This phenotype was caused by the binding of PS with the Mer tyrosine kinase (MerTK) receptor and subsequent release of TGF-β1. However, blocking the binding between PS and MerTK did not completely abolish the secretion of TGF-β1, revealing an even higher level of

regulation induced by NDEVs, which was found to be the induction of $Ca^{(2+)}$ influxes and mobilization of stored TGF-β1 (Eken et al 2013). However, in some cases, the presence of neutrophils, as well as NDEVs, may have detrimental effects on the tissue (Pitanga et al 2014). Exposure of endothelial cells to NDEVs drove morphological changes and loss of their membrane integrity. In the effort to understand the cause of this effect, *Gomez et al*. identified a miRNA, *mir-155*, as the factor delivered by NDEVs to endothelial cells that promotes atherosclerosis plaque formation. This miRNA increases NF-κB expression by targeting its negative regulator BCL6 thereby initiating inflammation (Gomez et al 2020).

The function of NDEVs during pathogen-cell interactions has also been described. Stimulation of neutrophils with opsonized *Staphylococcus aureus* induced the release of antibacterial microvesicles. These vesicles caused the aggregation of bacteria and decreased their growth (Timár et al 2013). Moreover, the formation of EVs with antibacterial activity was induced by stimulation of the CR3 (Mac-1) receptor and was restricted to EVs secreted from activated neutrophils and not spontaneously released, probably due to the different protein cargo of the two EV subsets (Lőrincz Á et al 2015) (Szeifert et al 2021). Another explanation for this phenotype could be that PMNs are able to sense environmental factors, such as the presence of a pathogen or cytokines produced by neighbouring cells, and consequently, "customize" their EVs (Kolonics et al 2021).

The production of EVs from neutrophils after contact with *A. fumigatus* was only recently uncovered (Shopova et al 2020). These vesicles showed antifungal activity when applied to the fungus and the ability to bind to fungal hyphae. Proteomic analysis revealed that they are carriers of potent antimicrobial peptides like azurocidin and cathepsin G which might account for their inhibitory activity.

To summarize NDEVs exhibit diversified functions in health and disease making their study essential for harnessing their potential as therapeutic or diagnostic agents.

2. Research aims

Aspergillus fumigatus is an important human fungal pathogen causing life-threatening infections. The number of these infections continues to rise due to the lack of rapid diagnosis and highly effective therapies. Thus, to address this critical situation is essential to elucidate the mechanisms by which the immune system can prevent infection, as well as the virulence factors that allow the fungus to evade this immune response (Fisher et al 2022, Netzker et al 2018).

Since previously the meaning of afEVs (*A. fumigatus*-induced EVs) produced by neutrophilic granulocytes to target and kill *A. fumigatus* has been discovered, the aim of my PhD thesis was to understand the specificity of this response, *i.e.*, whether the afEVs are able to kill other pathogens, and whether the antifungal effect could be provided by a specific subpopulation of afEVs, enriched for a particular surface marker. A question very relevant, whose answer could benefit the treatment of invasive aspergillosis might be connected to afEVs: are they also effective when individuals are immunosuppressed?

The second major aim of my thesis was to analyze the response of epithelial cells, for the production of antifungal EVs and cytokine release, as little is known about their role during aspergillosis.

Finally, the induction of antifungal EVs could be triggered by surface molecules of *A. fumigatus*, hence my third aim was to investigate the modifications of the surface proteome under different growth conditions.

3. Manuscripts

3.1 Manuscript A

Dynamic surface proteomes of allergenic fungal conidia

Blango MG, Pschibul A, **Rivieccio F**, Krüger T, Rafiq M, Jia L, Zheng T, Goldmann M, Voltersen V, Li J, Panagiotou G, Kniemeyer O, Brakhage AA

Manuscript published in *Journal of Proteome Research*; 19(5), 2092-2104
Accepted March 2020

Summary:
The surface composition of the pathogenic fungus *A. fumigatus* is fundamental for its survival in the environment and adaptation to the human body.
Therefore, investigation on how this surface changes is crucial to understand which virulence determinants make this mold a successful pathogen compared to other fungi.
This paper investigates, through a trypsin shaving approach followed by LC-MS/MS analysis, the surface proteome of *A. fumigatus* expressed at various temperatures and different growth stages.
As a result, the two proteins ScwA and CweA were identified as the most abundant on the surface of conidia. However, knockout of these proteins had only minor effects on the fungal response to cell wall stressors, suggesting that, even being dynamic, the conidial surface composition is stable against disturbances.

Contribution to the manuscript:
Flora Rivieccio was involved in the generation of complemented strain of *ΔscwA* and *ΔcweA* and in their characterization together with the knockout strains. She also contributed to editing the manuscript.

Estimated contribution in percentage:

Author	Conceptual	Data analysis	Experimental	Writing the manuscript	Provision of material
Blango MG.	35%	35%	30%	40%	0%
Pschibul A.	10%	20%	20%	20%	0%
Rivieccio F.	**5%**	**14%**	**20%**	**5%**	**0%**
Krüger T.	0%	8%	13%	2%	0%
Rafiq M.	0%	8%	12%	2%	0%
Brakhage A.A	45%	10%	0%	25%	100%
Others	5%	5%	5%	6%	0%
Total:	100%	100%	100%	100%	100%

Journal of proteome research

pubs.acs.org/jpr Article

Dynamic Surface Proteomes of Allergenic Fungal Conidia

Matthew G. Blango, Annica Pschibul, Flora Rivieccio, Thomas Krüger, Muhammad Rafiq, Lei-Jie Jia, Tingting Zheng, Marie Goldmann, Vera Voltersen, Jun Li, Gianni Panagiotou, Olaf Kniemeyer,* and Axel A. Brakhage*

Cite This: https://dx.doi.org/10.1021/acs.jproteome.0c00013 Read Online

ACCESS | Metrics & More | Article Recommendations | Supporting Information

ABSTRACT: Fungal spores and hyphal fragments play an important role as allergens in respiratory diseases. In this study, we performed trypsin shaving and secretome analyses to identify the surface-exposed proteins and secreted/shed proteins of *Aspergillus fumigatus* conidia, respectively. We investigated the surface proteome under different conditions, including temperature variation and germination. We found that the surface proteome of resting *A. fumigatus* conidia is not static but instead unexpectedly dynamic, as evidenced by drastically different surface proteomes under different growth conditions. Knockouts of two abundant *A. fumigatus* surface proteins, ScwA and CweA, were found to function only in fine-tuning the cell wall stress response, implying that the conidial surface is very robust against perturbations. We then compared the surface proteome of *A. fumigatus* to other allergy-inducing molds, including *Alternaria alternata*, *Penicillium rubens*, and *Cladosporium herbarum*, and performed comparative proteomics on resting and swollen conidia, as well as secreted proteins from germinating conidia. We detected 125 protein ortholog groups, including 80 with putative catalytic activity, in the extracellular region of all four molds, and 42 nonorthologous proteins produced solely by *A. fumigatus*. Ultimately, this study highlights the dynamic nature of the *A. fumigatus* conidial surface and provides targets for future diagnostics and immunotherapy.

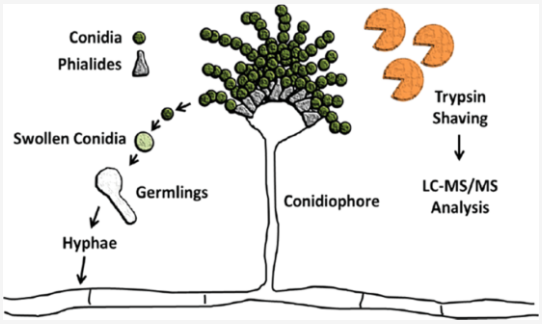

KEYWORDS: *Aspergillus fumigatus, Alternaria alternata, Penicillium rubens, Cladosporium herbarum, proteome, spore, germling, hyphae, LC−MS/MS, secreted proteins*

INTRODUCTION

120 000 fungal species have been described to date; however, only a few hundred of these fungi are able to cause illness in humans.[1] These diseases range from mild allergic reactions to life-threatening systemic infection. In terms of allergy, more than 80 mold genera have been associated with hypersensitive responses in allergic patients.[2] Within this group, species of the genera *Alternaria* and *Cladosporium* represent the most important outdoor allergens, while species of *Penicillium* and *Aspergillus* are reported to be the most common indoor airborne fungi.[3] *A. fumigatus* is associated with different forms of allergic diseases, including allergic bronchopulmonary aspergillosis (ABPA[4]), a persistent colonization of the bronchi known to frequently occur in patients with asthma and cystic fibrosis (CF). In addition, *A. fumigatus* is the most common species within the mold fungi to cause invasive infections in the lungs of immunocompromised patients, which is designated invasive aspergillosis.[5−7]

The *A. fumigatus* infectious lifecycle starts with the inhalation of conidia, 2−3 μm asexual spores, produced by mature conidiophores.[8] After deposition in the lungs, conidia undergo germination, whereby they initially swell, extend germ tubes, and finally form hyphae.[9] The small size and ubiquitous nature of these fungal spores require that the human innate immune system must continuously defend against inhaled conidia. Epithelial cells are the likely source of first contact in the mammalian lung, but recruitment of alveolar macrophages and neutrophils quickly follows.[10] Recognition by macrophages typically results in phagocytosis of conidia, while recruitment of neutrophils provides an additional level of antifungal defense.[11] In immunocompromised patients, specifically those with neutropenia, these host defenses are impaired and result in unregulated fungal growth with dangerous clinical manifestations.[12] Far less is known about the adaptive immune response to *A. fumigatus*, but CD4+ and CD8+ T cells have been shown to play important roles in antifungal defense.[13,14] The balance of host adaptive immune cell subsets appears to

Received: January 13, 2020
Published: April 1, 2020

ACS Publications © XXXX American Chemical Society

play an important role in susceptibility to fungal disease, as was recently shown for the accumulation of Th17 cells in ABPA, chronic obstructive pulmonary disease, and CF patients with acute airway inflammation.[15,16] Interestingly, tolerance to inhaled conidia was found to be mainly mediated by antigen-specific FOXP3+ regulatory T cells.[17]

In addition to *Aspergilli*, species of *Alternaria*, *Cladosporium*, and *Penicillium* are among the most commonly inhaled ascomycete molds capable of causing allergic diseases in humans.[2,18] Organisms in the genus *Penicillium* are genetically closely related to the *Aspergilli* and exhibit similar lifecycles; however, *Penicillium* species rarely cause infectious disease but rather asthma and allergic rhinitis in adults and children.[19] *Alternaria* and *Cladosporium* species are a major source of disease in plants, but they also represent important environmental allergens associated with asthma and asthma exacerbations.[3] Due to their abundance in nature, it is not surprising that conidia and/or hyphal fragments containing immune-activating allergenic proteins from these fungi are thought to be a major source of fungal-induced allergy.[20] Many allergens have been identified from each organism, with *A. fumigatus* containing 25 known allergen proteins, and *A. alternata*, *C. herbarum*, and *P. chrysogenum* (*rubens*) ranging from 6 to 17 protein antigens.[2,21] Despite this knowledge of allergens, our understanding of the complex interplay between fungus and host remains limited. The protein, lipid, and carbohydrate composition of a conidium has a direct impact on its recognition by the immune system and the following response of either tolerance or inflammation.[8,13,22]

The conidium of *A. fumigatus* is the best-studied mold spore to date.[23] Previous studies have elucidated the cell wall and surface proteome of *A. fumigatus* conidia to understand the molecules that likely interact with the host.[24−26] Throughout germination, the surface of the fungi changes dramatically, in terms of both the cell wall proteome and carbohydrate organization.[27,28] One major protein on the surface of conidia is the RodA hydrophobin, which encases resting conidia in a hydrophobic coat to minimize interactions with potential hazards. This hydrophobic rodlet layer is composed of a regular arrangement of the RodA protein interwoven among a layer of dihydroxynaphthalene (DHN)-melanin pigment. Upon encountering favorable growth conditions, resting conidia begin germination, a process that is highlighted by disassembly of the rodlet layer and degradation of the DHN-melanin polymer.[29−31] Despite this key function, RodA is not required for virulence in a mammalian infection model.[30,32] Aside from RodA, the functions of a few other *A. fumigatus* surface-exposed proteins are known. In many cases, these proteins seem to play important, but enigmatic, roles in fungal biology, as is the case with the recently described CcpA protein, which serves as a conidial protein important for virulence in a mouse infection model.[24] CcpA appears to have a structural role that normally masks other antigenic structures in the conidial cell wall. Despite our increasing understanding of the biology of fungal conidia, our ability to rapidly detect, diagnose, and treat fungal pathogens remains limited.[33] Our capacity to detect airborne fungi remains particularly limited and slow, despite the obvious importance of fungal conidia in initiating invasive lung infections or allergic reactions in susceptible populations.[34−36] As the burden of fungal pathogens in the clinic increases, improvements in each of these realms are desperately needed.[37]

In this study, we further elucidated the surface-exposed proteome and secreted/shed proteins of allergy-inducing fungal conidia to reveal new fungal surface antigens as potential diagnostic or therapeutic targets. In addition, similarities and differences between the mold species were discovered, as well as the influence of environmental factors like temperature on the composition of the conidial surface proteome. We also focused on the biology of two particularly abundant, previously uncharacterized cell wall proteins of *A. fumigatus*, Afu4g09600 and Afu4g09310, which are denoted here as "Cell Wall Enriched A" (CweA) and "Small Cell Wall Peptide A" (ScwA), respectively.

■ EXPERIMENTAL PROCEDURES

Fungal Strains and Cultivation

All strains used in this study are listed in Table S1. Cultivation of *A. alternata* (Fries) Keissler (ATCC 66981), *P. rubens* WIS 54-1255 (ATCC 28089; formerly *P. chrysogenum WIS* 54-1255), and *A. fumigatus* CEA10 was performed on *Aspergillus* minimal medium (AMM; 70 mM $NaNO_3$, 11.2 mM KH_2PO_4, 7 mM KCl, 2 mM $MgSO_4$, and 1 μL/mL trace element solution (pH 6.5)) agar plates with 1% (w/v) glucose for 7 days at room temperature for the comparative analysis. The trace element solution was composed of 1 g of $FeSO_4{\cdot}7H_2O$, 8.8 g of $ZnSO_4{\cdot}7H_2O$, 0.4 g of $CuSO_4{\cdot}5_2O$, 0.15 g of $MnSO_4{\cdot}H_2O$, 0.1 g of $NaB_4O_7{\cdot}10H_2O$, 0.05 g of $(NH_4)_6Mo_7O_{24}{\cdot}4H_2O$, and ultrafiltrated water to 1000 mL.[38,39] *C. herbarum* Link : Fries (ATCC MYA-4682) was cultivated on malt agar plates for 7 days at room temperature for the comparative analysis as AMM was not a permissible growth condition. All conidia were harvested in sterile, ultrafiltrated water without surfactants to minimize disruption of the surface proteome. Resting conidia from three 10 cm plates (~1×10^9 conidia) were used immediately after collection for all trypsin-shaving experiments. For the *A. fumigatus* germination experiment, resting conidia of *A. fumigatus* collected from three 10 cm plates grown for 7 days at 37 °C were germinated with shaking in RPMI 1640 (Lonza) liquid media supplemented with glucose to a final concentration of 2% (w/v) at 37 °C to produce swollen conidia (5 h), germlings (8 h), and hyphae (14 h). For the comparative analysis between *A. fumigatus*, *P. rubens*, *A. alternata*, and *C. herbarum*, resting conidia were prepared at room temperature for 7 days as described above and then transferred to 50 mL of RPMI media shaking (200 rpm) at 37 °C for 5 h in Erlenmeyer flasks. Fungal conidia were enumerated using a CASY Cell Counter (Omni Life Science) with care taken to resuspend thoroughly to avoid clumps.

Extraction of Surface Proteins by Trypsin Shaving

Surface proteins were extracted as described previously.[24] Briefly, resting conidia, swollen conidia, germlings, and/or hyphae of *A. fumigatus*, *A. alternata*, *C. herbarum*, and *P. rubens* were each washed twice with 25 mM ammonium bicarbonate and collected by centrifugation (1800*g* for 10 min at room temperature). Samples were resuspended in 800 μL of 25 mM ammonium bicarbonate and treated with 5 μg of MS-approved trypsin (Serva) for 5 min at 37 °C with gentle agitation. Samples were then immediately passed through a 0.2 μm cellulose acetate filter (Sartorius) and collected in a micro-centrifuge tube, followed by washing of the syringe filter with 200 μL of 25 mM ammonium bicarbonate. Then, 9 μL of 89% (v/v) formic acid was added to stop the tryptic digestion. The

https://dx.doi.org/10.1021/acs.jproteome.0c00013
J. Proteome Res. XXXX, XXX, XXX−XXX

samples were dried using a SpeedVac Concentrator (Thermo-Fisher), resuspended in 25 μL of 2% (v/v) ACN and 0.05% (v/v) trifluoroacetic acid (TFA), and centrifuged for 15 min through a 10 kDa cutoff microfuge column (VWR Scientific). For the liquid chromatography−tandem mass spectrometry (LC−MS/MS) method # 2 described in detail below, the 10 kDa cutoff centrifugation step was replaced with centrifugation through a 0.22-μm-pore-size Spin X cellulose acetate spin filter (Corning Costar). Resting conidia and germinating conidia after 8 h were collected after trypsin treatment and tested for lysis using a brief (15 min) staining with 40 μM propidium iodide followed by imaging with a Zeiss Axio Imager.M2 microscope (Zeiss).

Purification of Secreted Proteins from Swollen Conidia

For the identification of secreted proteins, ~2 × 10^9 resting conidia were germinated as described above for 5 h, before collection of the supernatant by filtration through a 0.22 μm filter and addition of TFA to a final concentration of 0.1% (v/v). Protein was purified by SPE with a Chromabond SPE-C4 cartridge (Macherey-Nagel, Germany). Briefly, columns were washed with 4 mL of methanol and reconstituted with 4 mL of 0.1% (v/v) TFA. Sample supernatants were aspirated through columns, washed with 2 mL of 5% (v/v) MeOH/0.1% (v/v) TFA, and eluted in 4 mL of 0.1% (v/v) TFA 80/20 ACN/H_2O (v/v). Samples were then dried by SpeedVac, resolubilized in 100 μL of denaturation buffer (50 mM triethylammonium bicarbonate (TEAB) in 50/50 trifluoroethanol (TFE)/H_2O (v/v)), sonicated for 15 min, and homogenized by Vortex mixing. Following 10 min at 90 °C, samples were collected by centrifugation (1800*g* for 10 min at room temperature) and cooled on ice. Protein content was measured with a Merck Millipore Direct Detect spectrometer. The samples were then reduced by adding 2 μL of reduction buffer (500 mM tris(2-carboxyethyl)phosphine in 100 mM TEAB) to 100 μL of the sample (<1 μg/μL) for 1 h at 55 °C. Then, 2 μL of fresh alkylation buffer (625 mM iodoacetamide) was added to each sample and incubated for 30 min at room temperature, in the dark. Following evaporation by SpeedVac, the samples were resolubilized in 95 μL of 100 mM TEAB and sonicated for 10 min. The samples were treated with 2 μg of MS-approved trypsin (Serva) for 18 h at 37 °C. The reaction was stopped with 10 μL of 10% (v/v) formic acid and again evaporated using the SpeedVac. Peptides were resolubilized in 25 μL of 0.05% (v/v) TFA in 2/98 ACN/H_2O (v/v) and sonicated for 15 min in a water bath before being transferred to a 10 kDa molecular weight cutoff filter (VWR Scientific). After 15 min of centrifugation at 14 000*g* (20 °C), the samples were transferred to HPLC vials and stored at −20 °C.

LC−MS/MS Analysis

Three similar methods (denoted M#1, M#2, and M#3) were used for LC−MS/MS analysis due to advances in our proteomics approaches over time and differences in sample processing, e.g., trypsin-shaving versus secretome analysis. A wild-type control was always included in each new analysis for comparison. LC−MS/MS analyses of trypsin-shaved surface peptides (M#1, M#2) and tryptic peptides of secreted proteins (M#3) were performed on an Ultimate 3000 RSLC nano instrument coupled to either a QExactive Plus (M#1, M#3) or an HF mass spectrometer (M#2; Thermo Fisher Scientific) as described previously.[24] Tryptic peptides were trapped for 4 min on an Acclaim Pep Map 100 column (2 cm × 75 μm, 3 μm) at a flow rate of 5 μL/min. The peptides were then separated on an Acclaim Pep Map column (50 cm × 75 μm, 2 μm) using a binary gradient (A: 0.1% (v/v) formic acid in H_2O; B: 0.1% (v/v) formic acid in 90:10 (v/v) ACN/H_2O). M#1: 0−4 min at 4% B, 10 min at 7% B, 40 min at 10% B, 60 min at 15% B, 80 min at 25% B, 90 min at 35% B, 110 min at 50% B, 115 min at 60% B, 120−125 min at 96% B, 125.1−150 min at 4% B. M#2: 0−4 min at 4% B, 5 min at 8% B, 20 min at 12% B, 30 min at 18% B, 40 min at 25% B, 50 min at 35% B, 57 min at 50% B, 62−65 min at 96% B, 65.1−90 min at 4% B. M#3: 0−5 min at 4% B, 30 min at 7% B, 60 min at 10% B, 100 min at 15% B, 140 min at 25% B, 180 min at 45% B, 200 min at 65% B, 210−215 min at 96% B, 215.1−240 min at 4% B. Positively charged ions were generated by a Nanospray Flex Ion Source (Thermo Fisher Scientific) using a stainless steel emitter with 2.2 kV spray voltage. Ions were measured in the Full MS/dd MS2 (Top10) mode, i.e., precursors were scanned at m/z 300−1500 (R: 70 000 FWHM (M#1/#3): 60 000 FWHM (M#2); AGC target: 1•10^6; max. IT: 120 ms (M#1/#3)/100 ms (M#2)). Fragment ions generated in the HCD cell at 30% normalized collision energy using N_2 were scanned (R: 17,500 FWHM (M#1/#3)/15 000 FWHM (M#2); AGC target: 2e5; max. IT: 120 ms (M#1/#3)/100 ms (M#2)) in a data-dependent manner (dynamic exclusion: 30 s).

Database Search and Data Analysis of Trypsin-Shaved Surface Peptides

The MS/MS data were searched against the *A. fumigatus* Af293 genome of the *Aspergillus* Genome Database (AspGD); Uniprot Proteome ID UP000000724 for *P. rubens*; Uniprot Proteome ID UP000077248 for *A. alternata*; and the Joint Genome Institute MycoCosm annotation against the proteome of the related organism *C. fulvum* (described in[40,41]) for *C. herbarum*, using Proteome Discoverer 1.4 and 2.2 and the algorithms of Mascot 2.4.1, Sequest HT, and MS Amanda as described previously.[24] Briefly, we allowed for two missed cleavages for tryptic peptides, a precursor mass tolerance set to 10 ppm, and a fragment mass tolerance set to 0.02 Da. The dynamic modification was set as oxidation of Met. For secretome analysis (M#3), the static modification was set to carbamidomethylation of Cys. In all cases, at least two peptides per protein and a strict target false discovery rate (FDR) of <1% were required for positive protein hits. In all cases, experiments were performed as three biological replicates with multiple technical replicates in the LC−MS/MS device. Proteins had to be identified in at least two of three replicates of a given condition to be included in the presented analyses, including Supporting Information tables.

Data Availability

The mass spectrometry proteomics data have been deposited to the ProteomeXchange Consortium via the PRIDE partner repository[42] with the dataset identifier PXD017067.

Genetic Manipulation of *A. fumigatus*

All oligonucleotides utilized in this study are listed in Table S2. The genetic deletions of *cweA* (Afu4g09600) and *scwA* (Afu4g09310) were generated using a 3-fragment polymerase chain reaction (PCR) method, as previously described.[43] ScwA, a small protein, was reannotated in *A. fumigatus* CEA10 as indicated in Figure S1A (V. Valiante, personal communication). For the knockout constructs, flanking regions of ~1 kb were amplified for each gene using *A. fumigatus* CEA17 genomic DNA as the template and the appropriate primer pairs (p1/p2 and p3/p4 indicated in Figure S1B,C). The

https://dx.doi.org/10.1021/acs.jproteome.0c00013
J. Proteome Res. XXXX, XXX, XXX−XXX

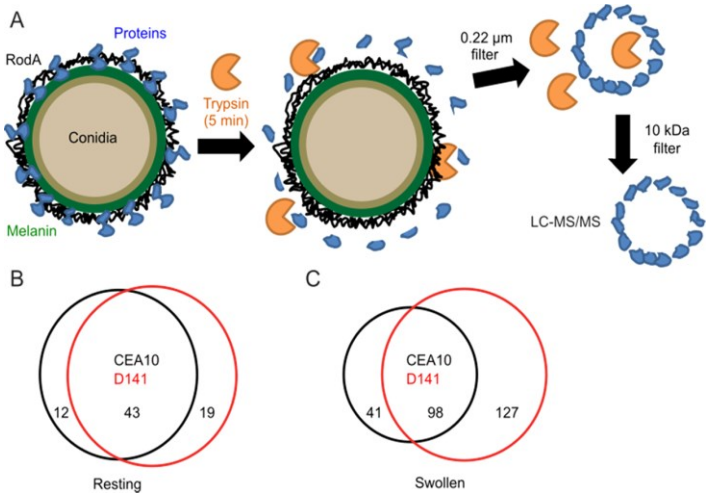

Figure 1. Trypsin-shaving proteomics of allergy-inducing fungi. (A) Model of the trypsin-shaving proteomics approach to identify surface-exposed peptides. Scaled Venn diagrams produced using Biovenn software[54] show intersection of proteins identified by trypsin shaving of (B) resting and (C) swollen conidia from the *A. fumigatus* strain CEA10 with D141 (D141 data described in ref 24). Trypsin-shaving proteomics was performed as three separate biological replicates with multiple technical replicates measured by LC−MS/MS. To be included in the analysis, proteins had to be identified in at least two of three biological replicates.

pyrithiamine resistance marker (*ptrA*) was amplified from the pSK275 plasmid using primers ptrA-F/R. Using Phusion polymerase (Thermo Scientific) and equimolar amounts of the three fragments as the template, primers p1 and p4 directed amplification of the entire construct (Figure S1D). Knockouts of *A. fumigatus* were generated by homologous recombination following the transformation of protoplasts.[44] Knockouts were verified by PCR and Southern blot according to standard procedures as described below (Figure S1E,F).

Complemented strains were produced by knocking in the gene of interest to the endogenous locus of the corresponding knockout strain (Figure S1G−J). Constructs were produced by fusion PCR using primers listed in Table S2. Briefly, to complement strains CEA17Δ*scwA* and CEA17Δ*cweA*, plasmids *pUC*19_*scwAc* and *pUC*19_*cweAc* were produced and transformed into protoplasts as previously described.[44] Both plasmids were generated using a Gibson cloning and assembly kit (BioLabs) according to the manufacturer's instructions. For *pUC*19_*scwAc*, the DNA fragments were generated as follows: the *scwA* gene and its 3′ flanking region were PCR amplified using primers scwA_F/scwA_hph_R and scwA_hph_F/scwA_R, respectively. The hygromycin resistance cassette (*hph*) was amplified from the *pJWx*41 plasmid with primers hph_scwA_F/hph_scwA_R, and the plasmid *pUC*19 backbone was amplified by PCR using primers pUC19_F/pUC19_R. The construct from transformation was amplified using the primer pair scwA_F and scwA_R. For *pUC*19_*cweAc*, the *cweA* gene and its 3′ flanking region were PCR amplified using primers cweA_F/cweA_hph_R and cweA_hph_F/cweA_R, respectively. The hygromycin resistance cassette (*hph*) was amplified from the *pJWx*41 plasmid with primers hph_cweA_F/hph_cweA_R, and the plasmid *pUC*19 backbone was amplified by PCR using primers pUC19_F/pUC19_R. The primer pair cweA_F/cweA_R was used for amplification of the construct for transformation.

Southern Blot Analysis

Southern blots to validate genetic deletion were carried out according to standard protocols.[45] All sequence information was obtained from the Ensembl Fungi Database.[46] Genomic DNA of *A. fumigatus* was isolated using the MasterPure Yeast DNA Purification Kit (Epicentre). Genomic DNA of *A. fumigatus* was digested with the appropriate restriction enzymes (New England Biolabs). DNA fragments were separated on an agarose gel followed by blotting onto Hybond N+ nylon membranes (GE Healthcare Bio-Sciences). DNA probes were amplified with digoxigenin-UTP (DIG-UTP) in the PCR reaction using primer pairs cweA-1/2, scwA-3/4, cweA_hph_F/cweA_R, and scwA_F/scwA_hph_R for Δ*cweA*, Δ*scwA*, *cweAc*, and *scwAc*, respectively (primers in Table S2). Genomic DNA of candidates Δ*cweA*, Δ*scwA*, *cweAc*, and *scwAc* was digested using restriction enzymes *Cla*I, *Hin*dIII, *Bam*HI, and *Eco*RI, respectively, hybridized to the appropriate probe in DIG Easy Hyb (Roche Applied Science) and detected using the CDP-Star ready-to-use kit (Roche Applied Science), according to the manufacturers' recommendations. Chemiluminescence signals were detected by a Fusion-FX CCD camera (Vilbert Lourmat).

Growth Assays of *A. fumigatus* Knockouts

Wild-type and knockout conidia were collected in water from AMM agar plates after 5 days of growth. Conidia were counted using a CASY Cell Counter (Omni Life Science), diluted in droplet solution (0.9% (v/v) NaCl, 0.1% (v/v) Agar, 0.01% (v/v) Tween 20), and added to plates in 5 μL drops containing 10^2, 10^3, 10^4, or 10^5 conidia. Growth was monitored over time at 37 °C, and images were collected before overgrowth of the plate. Cell stress was induced using common stressors[47,48] including caffeine (Fluka), caspofungin acetate (Cancidas, MSD), calcofluor white (Sigma), congo red (Sigma), and SDS (Serva), all dissolved in water (except for calcofluor white, which was dissolved in Tris−HCl) and added directly to cooling agar at the concentrations denoted in the text. Plates were prepared fresh for each experiment, and growth was

https://dx.doi.org/10.1021/acs.jproteome.0c00013
J. Proteome Res. XXXX, XXX, XXX−XXX

allowed to continue for 72 h. Germination assays were performed as above by microscopically determining the ratio of spores undergoing germination (germ-tube formation) at each time point.

Bioinformatic Analyses

Phylogenetic analyses were performed using sequences gathered from FungiDB[49] for each ortholog of *A. fumigatus* CweA and ScwA. Additional protein−protein BLAST (blastp) searches were performed to confirm the collection of all orthologs. Alignments and phylogenetic trees were then produced using the DNAStar MegAlign software package (DNASTAR Inc.) using a ClustalW alignment.

The InParanoid algorithm was used to identify ortholog clusters for pairwise species comparison.[50] The default algorithm parameters were used: a score cutoff of 40 bits, an overlap cutoff of 50%, and a segment cutoff of 25%. The proteins with an ortholog score <0.95 contained in the ortholog clusters were excluded from the analysis. "One to many" and "many to many" orthologous relationships were included in the ortholog clusters. An ortholog group among three or four species was found only if the ortholog group was identified for all of the pairings. Furthermore, the InParanoid-defined ortholog clusters with at least one expressed protein were also identified.

■ RESULTS AND DISCUSSION

A. fumigatus Surface Proteome is Dynamic across Germination

In this study, we sought to expand the repertoire of *A. fumigatus* conidial surface and secreted proteins that potentially trigger allergy or promote infection and compare the proteins exposed on the surface of *A. fumigatus* conidia with other important allergenic molds. Initially, we utilized a previously described trypsin-shaving proteomics approach[24] to identify surface-exposed proteins throughout germination of the filamentous fungus, *A. fumigatus* strain CEA10 (Figure 1A). Samples were collected from resting (0 h) conidia grown at 37 °C on AMM agar plates and swollen conidia (5 h), germlings (8 h), and hyphae (14 h) germinated at 37 °C in RPMI liquid media. We identified 177 unique proteins across all germination time points; 75/177 proteins had a predicted signal peptide cleavage site using the SignalP program,[51] 15/177 contained at least one predicted transmembrane helix using TMHMM Server v. 2.0 (services.healthtech.dtu.dk),[52] and 13/177 contained putative GPI anchors using PredGPI (Table S3[53]). When compared to previous trypsin-shaving data from the literature, 43/55 proteins from CEA10 were found on the surface of *A. fumigatus* strain D141 resting conidia under similar growth conditions, whereas in swollen conidia, 98/139 CEA10 proteins were on the surface of D141 swollen conidia (Figure 1B−C;[24]). These results suggest that the surface proteome of different *A. fumigatus* strains exhibits high similarities under standard growth conditions. The differences still observed could be due to slight differences in growth media. The surface proteins identified have a diverse array of cellular localizations and activities using Gene Ontology Enrichment (fungidb.org). These include localization to the cell wall (72/177; GO:0005618), cytoplasm (71/177; GO:0005737), and external encapsulating structure (72/177; GO:0030312) with activities related to catalytic activity (89/177; GO:0003824), binding (78/177; GO:0005488), oxidoreductase activity (22/177; GO:0016491), and nucleic acid binding activity (16/177; GO:0003676), among others.

Over the course of germination, 55 proteins were identified on resting conidia (see Table 1 for Top 20), 140 on swollen conidia, 56 on germlings, and 109 on hyphae. In direct comparisons between samples, 35 proteins were found in all four stages of the germination time course, including the conidial hydrophobin, RodA (Figure 2). RodA exhibited the highest levels of normalized abundance throughout germination, ranging from 16.8 to 7.7% of the normalized peptide spectrum matches (PSMs) per length and consistent with previous studies.[26,32] The majority of conidia underwent germination in our assays; however, a small fraction of conidia failed to germinate, which likely contributed to the abundance of RodA at later time points. In agreement, localization studies with a polyclonal RodA antibody revealed the presence of RodA on the surface of conidia, in biofilm cell walls, and in phialides during sporulation.[32]

Table 1. Top 20 *A. fumigatus* Proteins Identified on Resting Conidia Ranked by Normalized Spectral Abundance Factor (NSAF)

accession number	protein name	NSAF	description
Afu5g09580	RodA	0.126	conidial hydrophobin
Afu6g03210	ConJ	0.093	uncharacterized protein
Afu2g09030	DppV	0.055	secreted dipeptidyl-peptidase
Afu6g14470	Afu6g14470	0.045	uncharacterized protein
Afu2g05635	Afu2g05635	0.041	uncharacterized protein
Afu1g13670	CcpA	0.040	conidial cell wall protein
Afu4g09310	Afu4g09310	0.037	uncharacterized protein
Afu4g09280	Afu4g09280	0.033	uncharacterized protein
Afu5g14210	Grg1	0.033	glucose-repressible gene
Afu1g14560	MsdS	0.030	putative 1,2-α-mannosidase
Afu8g01980	Afu8g01980	0.027	uncharacterized protein
Afu5g03540	Afu5g03540	0.024	putative flavin-linked sulfhydryl oxidase activity
Afu2g17530	Abr2	0.023	laccase
Afu8g05020	NagA	0.022	putative secreted N-acetylhexosaminidase
Afu3g07160	Afu3g07160	0.020	putative family 18 chitinase
Afu2g00680	Afu2g00680	0.020	uncharacterized protein
Afu1g13550	Afu1g13550	0.019	uncharacterized protein
Afu4g09600	Afu4g09600	0.018	putative glycophosphatidylinositol (GPI)-anchored cell wall protein
Afu4g01290	Csn	0.016	glycosyl hydrolase family 75 chitosanase
Afu5g09240	Sod1	0.016	Cu/Zn superoxide dismutase

In addition to RodA, the other most prevalent proteins on the surface of resting conidia, as determined using the normalized spectral abundance factor (NSAF;[55,56]), were the proteins of unknown function, ConJ, Afu6g14470, and Afu2g05635; the serine protease, DppV; and the previously described surface protein, CcpA. ConJ shows high similarity to the conidiation-specific, light-induced protein 10 of *Neurospora crassa*, and its transcripts are upregulated during early conidial development and murine infection with *A. fumigatus*.[26] Afu6g14470 and Afu2g05635 remain relatively unstudied, but each contains a signal peptide cleavage site according to SignalP,[51] and Afu6g14470 was previously detected by 2D-gel electrophoresis on the conidial surface of *A. fumigatus*.[25] The protein DppV is a secreted dipeptidyl-peptidase and non-

https://dx.doi.org/10.1021/acs.jproteome.0c00013
J. Proteome Res. XXXX, XXX, XXX−XXX

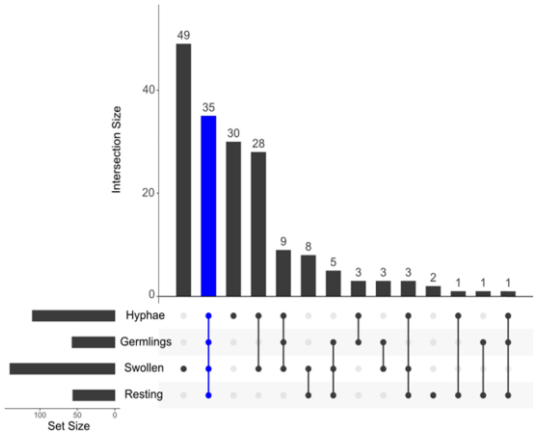

Figure 2. Trypsin-shaving proteomics elucidate surface proteome of *A. fumigatus* conidia after germination in RPMI. Four-way comparison indicating the intersection of surface-exposed proteins from resting (0 h) and swollen conidia (5 h), germlings (8 h), and hyphae (14 h). The experiment was performed as three separate biological replicates with multiple technical replicates measured by LC−MS/MS, and to be included in the analysis, proteins had to be identified in at least two of three biological replicates. Plot produced using the R package UpSet.

classical serine protease,[57] which is known to be targeted by the T-cell response in mice surviving *A. fumigatus* infection.[58] The surface of swollen conidia exposed more proteins (140 unique proteins identified) than what was found on the surface of the other time points, which is consistent with previous studies comparing resting and swollen conidia.[24] It is possible that reorganization of the conidial surface during germination results in the temporary availability of cell wall proteins to trypsin cleavage in some circumstances. The surface proteome of germlings was less complex, with no proteins unique to only germlings, suggesting that perhaps there is a restriction to the surface proteome in germlings. In hyphae, we again see slightly higher numbers of surface-exposed proteins, with 30 proteins found that were not identified in the other samples (Figure 2).

Knockout of Abundant Conidial Surface Proteins Does Not Alter Surface Proteome

We were interested in further studying several of the more highly abundant surface proteins from *A. fumigatus*. The putative GPI-anchored cell wall protein CweA (Afu4g09600, 980 amino acids) and the protein ScwA (Afu4g09310, 93 amino acids) were both predicted to encode a signal peptide for entry into the secretory pathway (SignalP) but otherwise lacked recognizable conserved domains or characterized orthologs. In addition to being highly abundant, CweA and ScwA were observed on the surface throughout germination by trypsin shaving (Table S3) and were previously found on the conidial surface in other studies.[24,59] Interestingly, *cweA* contains multiple coding tandem repeats, and its transcript was shown to be upregulated upon membrane stress.[60]

Since ScwA is such a small protein, we first confirmed the annotation of the genetic loci in the CEA10 genome by multisequence alignment to related organisms after a resequencing of CEA10 *scwA* (Figure S1A). ScwA appears to exclusively belong to a small subset of the *Aspergillus* genus (Figure S2A), while CweA is widely found in both the *Aspergillus* and *Penicillium* genera (Figure S2B), with an ortholog expressed in *P. rubens*. Genetic deletions of *cweA* (Afu4g09600) and *scwA* (Afu4g09310) were produced in *A. fumigatus* CEA17 by homologous recombination following transformation of protoplasts (Figure S1B−F). Both knockouts grew normally on AMM and malt agar plates (Figure S3A). The genetic deletion of *cweA* provided a growth advantage relative to the wild type on Congo Red agar plates, a known cell wall stressor,[47,48] whereas Δ*scwA* exhibited only a minor growth inhibition (Figure 3A). This finding is consistent with data from the literature showing that *cweA* was downregulated in response to Congo Red stress.[60] Under calcofluor white stress, the Δ*scwA* strain exhibited a slight advantage, whereas Δ*cweA* exhibited a more robust growth advantage, all of which could be complemented (Figure 3A). Challenge with other cell wall and membrane stressors, including caffeine, caspofungin, and SDS, revealed no obvious defects by the droplet growth inhibition assay (Figure S3B). Taken together, these results

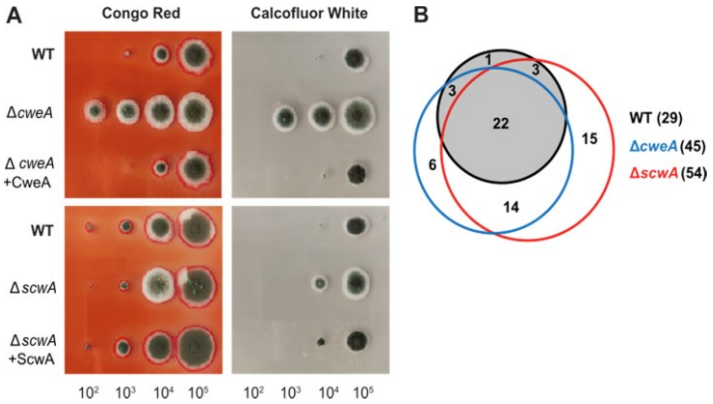

Figure 3. Phenotypic analysis of *A. fumigatus* conidial surface proteins. (A) Droplet growth inhibition assays for wild-type, Δ*cweA*, and Δ*scwA* knockout strains grown on AMM agar plates supplemented with 35 μg/mL Congo red or 50 μg/mL calcofluor white. Images are representative of three separate experiments. (B) Scaled Venn diagram indicating intersection of surface proteins identified by trypsin shaving of wild-type, Δ*cweA*, and Δ*scwA* knockout strains. Trypsin-shaving proteomics was performed as three separate biological replicates with multiple technical replicates measured by LC−MS/MS, and to be included in the analysis, proteins had to be identified in at least two of three biological replicates.

https://dx.doi.org/10.1021/acs.jproteome.0c00013
J. Proteome Res. XXXX, XXX, XXX−XXX

suggest that the abundant surface proteins ScwA and CweA are important for fine-tuning the conidial response to stress.

Our previous characterization of the surface protein CcpA revealed an altered conidial surface proteome after growth on AMM agar plates.[24] In this case, it was postulated that CcpA functions to mask other cell wall proteins or other surface molecules that are normally hidden in the conidial cell wall. To explore if other cell wall protein knockouts resulted in a similar alteration to the surface proteome of resting conidia, we performed trypsin shaving on the Δ*cweA* and Δ*scwA* knockout strains compared to the wild-type CEA17 *akuB*^{KU80} strain used to create the knockouts.[61] In both cases, we saw very little change to the exposed surface proteome, suggesting that the function of CcpA in masking surface-exposed proteins is not a common feature of all abundant surface proteins but rather a specific feature of CcpA (Table S4 and Figure 3B). Ultimately, these results suggest that the cell surface is quite robust and adaptable, as even the removal of abundant cell surface proteins like CweA and ScwA yields few major phenotypes and little changes in the overall structure. Further study will be required to fully understand the redundancy of conidial surface proteins in cell wall maintenance and stress response.

Growth Time and Temperature Dictate the Surface Proteome of *A. fumigatus* Conidia

As described above, the surface proteome undergoes dynamic changes during the germination process. Previous studies showed that environmental conditions during conidiation affect the stress tolerance of *A. fumigatus* conidia.[62] We thus wanted to understand if and how the temperature during conidiation influences the surface proteome of *A. fumigatus* resting conidia. We performed trypsin-shaving proteomics on resting conidia grown for 7 days at room temperature, 37, or 42 °C and for 14 days at room temperature or 37 °C. Surprisingly, conidia produced at room temperature and 42 °C had more surface-exposed proteins than spores grown at 37 °C after 7 days of growth (Figure 4A and Table S5). After 14 days

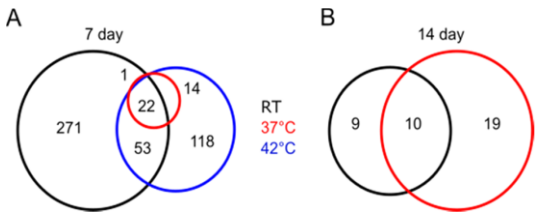

Figure 4. Temperature and time influence the *A. fumigatus* surface proteome. (A) Scaled Venn diagrams show the intersection of proteins identified by trypsin shaving on the surface of resting conidia after (A) 7 days at 37, 42 °C, or room temperature or (B) 14 days at 37 °C or room temperature. Experiments were performed in triplicate with multiple technical replicates, and to be included in the analysis, proteins had to be identified in at least two of three biological replicates.

of incubation, conidia grown at room temperature and at 37 °C both exhibited far fewer proteins on the surface, 19 and 29, respectively (Figure 4B and Table S5). These results suggest that the surface proteome of conidia is potentially restricted or degraded over developmental time. In agreement with this idea of a surface proteome restriction is a previous work showing that the whole conidial proteome has a lower complexity at 15 days compared to conidia after 3 or 30 days of growth.[63] It remains unclear how changes to the intracellular proteome might influence the surface proteome during conidial development, but one explanation is that more cytosolic proteins contaminate the conidial surface at 7 days compared to 14 days, at which time additional proteolytic degradation has occurred. It is also possible that as the RodA coat and melanin layers become more contiguous during development, it is harder for trypsin to penetrate into the cell wall to release surface-exposed peptides. Similarly, increases in hydrophobicity during development may result in decreased ability of the trypsin protease to reach the surface. We hope that future studies will be able to better define the exact mechanism by which the surface proteome is limited during development.

Interestingly, the ScwA protein appears to be only on the surface of conidia grown at 37 °C, and not room temperature, suggesting a possible role in temperature adaptation. However, we see no obvious growth difference for the knockout strain at 37 °C or room temperature. Five proteins were identified on resting conidia grown at all tested time points and temperatures (Table 2), including one previously uncharacterized

Table 2. *A. fumigatus* Proteins Identified on Resting Conidia at All Tested Time Points and Temperatures

accession number	protein name	description
Afu5g09580	RodA	conidial hydrophobin
Afu1g07440	Hsp70	molecular chaperone
Afu8g01980	Afu8g01980	uncharacterized protein
Afu2g17530	Abr2	laccase
Afu1g05630	Afu1g05630	40S ribosomal protein S3, putative

protein, Afu8g01980, which is a putative phosphotriesterase containing a TolB-like six-bladed β-propeller domain (https://www.ebi.ac.uk/interpro/).[64] Overall, these results have obvious implications for the study of *A. fumigatus* pathogenesis and reaffirm that the growth temperature of conidia can have a drastic effect on surface protein expression.[62] One partial explanation for the observed temperature-dependent effects is the difference in the growth rate of *A. fumigatus* on agar plates at room temperature and 37 °C, where sporulation requires several additional days at room temperature. At 14 days of incubation, the conidia are mature under both conditions, and at this time point, we observe a similar number of proteins on the surface of conidia (Figure 4B). Despite a comparable number of surface proteins, 19 for spores grown at room temperature and 29 for spores cultivated at 37 °C, the composition of the surface proteome is not the same at 14 days (10 shared proteins), suggesting some temperature-dependent regulation of surface-exposed proteins.

Comparative Proteomics Uncovers Proteins on the Surface/Shed from Allergenic Fungal Conidia

To refine our understanding of the surface-exposed cell wall proteins that might contribute to the initiation of allergic inflammation in the lung, we leveraged the power of comparative proteomics. To this end, the surface-exposed proteomes of 7-day-old resting conidia of *A. fumigatus* (CEA10) and three other prevalent allergy-inducing fungi, *A. alternata* (ATCC 66981), *C. herbarum* (ATCC MYA-4682), and *P. rubens* (ATCC 28089), grown at room temperature were assessed by trypsin-shaving proteomics. We first confirmed that the short trypsin treatment did not result in cell lysis in all cases for resting conidia and germlings by staining with the cell-impermeable dye propidium iodide

https://dx.doi.org/10.1021/acs.jproteome.0c00013
J. Proteome Res. XXXX, XXX, XXX−XXX

Journal of Proteome Research pubs.acs.org/jpr Article

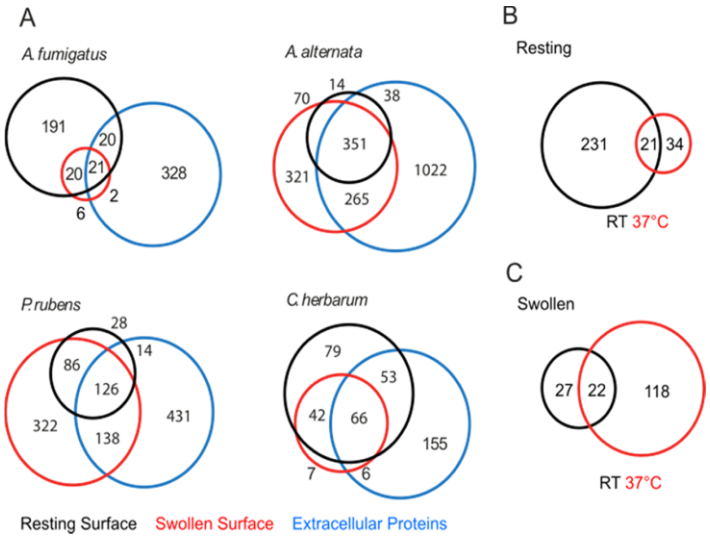

Figure 5. Comparative analysis reveals conserved surface proteins. (A) Scaled Venn diagrams show the intersection of surface-exposed proteins of resting conidia and swollen conidia (5 h) and extracellular proteins (5 h) from *A. fumigatus*, *P. rubens*, *A. alternata*, and *C. herbarum* (annotated using *C. fulvum* genome) germinated at 37 °C in RPMI. Although the experimental setup for *A. fumigatus* CEA10 grown at room temperature for 7 days shown in A (black circle) was the same as that described in Figure 4A (black circle), it was redone for this experiment as an additional control. (B) Scaled Venn diagrams indicate difference in surface proteome between *A. fumigatus* resting conidia isolated from mycelia grown at room temperature or 37 °C. (C) Scaled Venn diagrams indicate differences in the surface proteome between *A. fumigatus* swollen conidia isolated from mycelia grown at room temperature or 37 °C. Experiments were performed in triplicate with multiple technical replicates, and to be included in the analysis, proteins had to be identified in at least two of three biological replicates.

(Figure S4). *A. alternata* and *C. herbarum* conidial populations contained a noticeable fraction of dead cells, which were permeable to propidium iodide in both the presence and absence of trypsin (Figure S4). Therefore, we believe that these data sets provide more information about trypsin-accessible proteins (and likely immune-accessible proteins) and less information about the exact surface composition of *A. alternata* and *C. herbarum*. Unfortunately, an annotated genome of *C. herbarum* is not available, so we relied on the mapping of peptides to the annotated *C. fulvum* genome for these analyses, which potentially results in the omission of some *C. herbarum*-specific surface proteins. *C. herbarum* was also unable to sporulate on AMM agar plates, and thus some of the observed differences may be due to differences between growth media. After growth at room temperature, conidia were collected and transferred to RPMI media at 37 °C. This temperature and growth substrate switch was designed to better mimic the likely change in an environment from growth outdoors or in a hospital environment to that of the lung of an immunocompromised patient.

LC−MS/MS analysis revealed 252 surface-exposed proteins on resting conidia of *A. fumigatus*, 473 on *A. alternata*, 240 on *C. herbarum*, and 254 on *P. rubens* (Figure 5A and Tables S6−S9). On swollen conidia, we observed 49 surface-exposed proteins on *A. fumigatus*, 1,007 on *A. alternata*, 121 on *C. herbarum*, and 672 on *P. rubens*. *A. fumigatus* conidia harvested from cultures grown at room temperature again exhibited more proteins on the surface than conidia obtained from cultures grown at 37 °C (Figure 5B). These results are also consistent with previous studies that link fungal growth variability to cultivation temperature[62] and again highlight the importance of selecting appropriate and consistent growth conditions. Interestingly, we observed that conidia from mycelia grown at room temperature or 37 °C for 7 days responded differently to germination in RPMI, such that swollen conidia exhibited vastly different surface proteomes after 5 h at 37 °C (Figure 5C). In particular, swollen conidia grown initially at room temperature responded by restricting their surface proteomes, whereas conidia grown initially at 37 °C expanded their surface proteomes. The mechanism of this phenotype remains unknown but provides an interesting view of the dynamics of the surface proteome.

In addition to surface-exposed proteins, we were also interested in proteins secreted from swollen conidia that may serve as allergens. Our previous proteomics analyses revealed an abundance of *A. fumigatus* proteins available for trypsin cleavage on swollen conidia.[24] To test the hypothesis that a subset of these newly surface-exposed proteins might also be secreted or shed from conidia, we performed solid-phase extraction of spent cell culture supernatant after 5 h of germination. Using this method, we were able to identify 371 *A. fumigatus* proteins secreted/shed after 5 h of incubation, 1676 from *A. alternata*, 280 from *C. herbarum*, and 709 from *P. rubens* (Figure 5A and Tables S6−S9). These findings highlight that many proteins exposed on the surface of germinating conidia are also secreted/shed into the local environment, where they may serve as potential allergens to activate or inhibit host responses. In fact, 13 known allergens were identified in *A. fumigatus*, including Asp f 1, Asp f 9, and Asp f 12. Of these 13 allergens, nine were found only secreted/shed during swelling, two allergens were specific to resting conidia (Asp f 12, Asp f 23), and one was detected in all three conditions (Asp f 1). Three known allergens were identified in *A. alternata*, with two on the surface of resting and swollen conidia as well as secreted/shed from swelling conidia (Alt a 6, Alt a 7) and one found only secreted/shed from swelling

https://dx.doi.org/10.1021/acs.jproteome.0c00013
J. Proteome Res. XXXX, XXX, XXX−XXX

Journal of Proteome Research pubs.acs.org/jpr Article

Table 3. Ortholog Analysis on Surface/Secreted Proteins of Allergy-Inducing Fungi Grown at Room Temperature[a]

organism A	organism B	organism C	organism D	total ortholog groups from detected proteins	ortholog groups w/orthologs detected in all organisms
A. fumigatus	*P. rubens*	*C. herbarum*	*A. alternata*	1617	125
A. fumigatus	*P. rubens*	*C. herbarum*		1050	134
A. fumigatus	*P. rubens*		*A. alternata*	1773	289
A. fumigatus		*C. herbarum*	*A. alternata*	1589	146
	P. rubens	*C. herbarum*	*A. alternate*	1657	258
A. fumigatus	*P. rubens*			1146	351
A. fumigatus		*C. herbarum*		664	156
A. fumigatus			*A. alternata*	1737	377
	P. rubens		*A. alternata*	1835	726
	P. rubens	*C. herbarum*		992	276
		C. herbarum	*A. alternata*	1739	359

[a]See also Table S10 in the supplements.

conidia (Alt a 1). Four allergens were identified in analyses of *P. rubens*: Pc20g10360 (β-hexosaminidase), Pc21g16950 (transaldolase), and Pc21g16970 (vacuolar serine proteinase) were found on resting conidia, swollen conidia, and secreted/shed from swelling conidia and the protein of unknown function Pc12g10650 was found only secreted/shed from swelling conidia.

Fungal secreted proteases are known to drive allergic airway diseases by hydrolyzing the glycoprotein complex fibrinogen (FGB), which leads to the activation of a TLR4-mediated immune response via the integrin Mac-1.[65] The secreted serine protease, Alp1 (Asp f 13) of *A. fumgiatus*, is a known promoter of airway hyperresponsiveness.[66] Our proteomic data reveal that Alp1 is secreted from swollen conidia of *A. fumigatus*, like the serine protease Pc21g16970 of *P. rubens* (40% sequence similarity). No orthologs of Alp1 were found in the secretome of *A. alternata* or *C. herbarum*. However, *A. fumigatus* secretes an arsenal of other peptidases (Afu3g08290, Afu3g11400, Afu5g04330, AFu7g05930) whose orthologs are also detectable in the secretomes of all other investigated molds. All have the potential to initiate allergic and antifungal immunity.

Ortholog Analysis Reveals a Conserved Surface Proteome among Allergenic Fungi

Next, we used the InParanoid software package to assign ortholog groups between the different fungi in our comparative proteomics data sets.[50,67] The aim was to identify proteins that were conserved across all four organisms as well as to define proteins that were specific to one organism. We were able to identify 125 orthologous surface/secreted protein groups detected in all four organisms (Tables 3 and S10). In *A. fumigatus*, these orthologs corresponded mostly to proteins in the cytosol (91/125; GO:0005737), but a small subset was found in the extracellular region (37/125; GO:0005576) by Gene Ontology Enrichment (fungidb.org). The large number of proteins from the cytosol is indicative of the prevalent contamination of the cellular surface with proteins from the intracellular space by each of the four tested fungi. Many represent ribosomal proteins, chaperones, and metabolic enzymes, some of which have been shown to exhibit antigenic activity.[68] It is possible that some of these proteins have moonlighting functions in the extracellular environment, as has been observed in other systems.[8] For example, Asp f 22 (enolase) was recently shown to bind human plasma complement proteins to damage epithelial cell layers.[69] Interestingly, 42 *A. fumigatus* proteins were detected in this experiment that had no ortholog in the related allergy-inducing species, including the Asp f 1 allergen. In total, 102 proteins were specific to the extracellular space of *P. rubens*, 206 proteins unique to *A. alternata*, and nine to *C. herbarum* (Table S10). Of note, we did observe the *P. rubens* orthologs of *A. fumigatus* CweA and CcpA on *P. rubens* conidia, perhaps suggesting a conserved function for these proteins in *P. rubens*.

Airborne fungi, especially in outdoor and hospital environments, remain difficult to rapidly detect, despite their potential to contribute to invasive fungal disease and allergic exacerbation in susceptible patient populations.[34,35] Therefore, improved methods for rapid detection of airborne fungi are greatly needed in managing allergic responses and invasive fungal disease. The ortholog analysis presented here provides numerous candidate proteins likely accessible to both the immune system and potential diagnostic assays. Our comparative proteomics approach and ortholog comparison also revealed that much overlap exists between *A. fumigatus* and other allergy-inducing fungi, further complicating the development of future diagnostics and highlighting the issue of cross-reactivity between organisms. The dynamic nature of the surface proteome of fungi adds an additional complexity to this challenging problem. Despite these hurdles, we hope that the data sets assembled here will serve as a resource in guiding future endeavors into the biology of the conidial surface and selection of diagnostic targets, particularly with regard to antibody-based detection and chimeric antigen receptor T-cell-based therapeutics, which are proving to be more versatile in combatting infectious diseases.[70]

■ CONCLUSIONS

The surface of fungal conidia is a dynamic meshwork of macromolecules, including a number of important proteins.[8] In this study, we identified the surface-exposed and secreted proteome of resting conidia from several allergenic fungal pathogens and searched for orthologs between these organisms. We find that the surfaces of germinating fungi are quite variable, which creates unique challenges for the identification of these organisms during allergy and infection and further confirms that these fungi have sophisticated ways of managing diverse environments. In fact, we show that temperature has a great effect on the surface proteome of *A. fumigatus*, a factor that must be considered in the design of future experiments. We were able to significantly add to our collective knowledge of the surface proteome of allergenic fungi in the early stages of germination and now have a

https://dx.doi.org/10.1021/acs.jproteome.0c00013
J. Proteome Res. XXXX, XXX, XXX−XXX

resource that will aid in the design of future diagnostics and therapeutics.

■ ASSOCIATED CONTENT

Supporting Information

The Supporting Information is available free of charge at https://pubs.acs.org/doi/10.1021/acs.jproteome.0c00013.

Figure S1, production of Δ*cweA* and Δ*scwA* knockouts in *A. fumigatus*; Figure S2, phylogenetic analysis of *A. fumigatus* cell surface proteins; Figure S3, growth characterization of the Δ*cweA* and Δ*scwA* knockouts; Figure S4, trypsin does not induce major changes in fungal permeability; Table S1, fungal strains used in this study; Table S2, oligonucleotides and plasmids used in this study; Table S3, surface proteome of germinating *A. fumigatus* conidia; Table S4, surface proteome of Δ*scwA* and Δ*cweA* deletion strains; Table S5, time- and temperature-dependent surface proteome of *A. fumigatus* conidia; Table S6, surface proteome and secretome of resting and swollen *A. fumigatus* conidia; Table S7, surface proteome and secretome of resting and swollen *P. rubens* conidia; Table S8, surface proteome and secretome of resting and swollen *A. alternata* conidia; Table S9, surface proteome and secretome of resting and swollen *C. herbarum* conidia; Table S10, ortholog analysis performed using the InParanoid software package (PDF)

Surface proteome of germinating *A. fumigatus* conidia (XLSX)

Surface proteome of ΔscwA and ΔcweA deletion strains (XLSX)

Time and temperature-dependent surface proteome of *A. fumigatus* conidia (XLSX)

Surface proteome and secretome of resting and swollen *A. fumigatus* conidia (XLSX)

Surface proteome and secretome of resting and swollen *P. rubens* conidia (XLSX)

Surface proteome and secretome of resting and swollen *A. alternata* conidia (XLSX)

Surface proteome and secretome of resting and swollen *C. herbarum* conidia (XLSX)

Ortholog analysis performed using InParanoid software package (XLSX)

■ AUTHOR INFORMATION

Corresponding Authors

Olaf Kniemeyer − *Department of Molecular and Applied Microbiology, Leibniz Institute for Natural Product Research and Infection Biology—Hans Knöll Institute (Leibniz-HKI), Jena 07745, Germany; Department of Microbiology and Molecular Biology, Institute of Microbiology, Friedrich Schiller University, Jena 07745, Germany;* orcid.org/0000-0002-9493-6402; Phone: +49 (0)3641-532 1071; Email: olaf.kniemeyer@leibniz-hki.de

Axel A. Brakhage − *Department of Molecular and Applied Microbiology, Leibniz Institute for Natural Product Research and Infection Biology—Hans Knöll Institute (Leibniz-HKI), Jena 07745, Germany; Department of Microbiology and Molecular Biology, Institute of Microbiology, Friedrich Schiller University, Jena 07745, Germany;* orcid.org/0000-0002-8814-4193; Phone: +49 (0)3641-532 1001; Email: axel.brakhage@leibniz-hki.de

Authors

Matthew G. Blango − *Department of Molecular and Applied Microbiology, Leibniz Institute for Natural Product Research and Infection Biology—Hans Knöll Institute (Leibniz-HKI), Jena 07745, Germany;* orcid.org/0000-0001-8015-9019

Annica Pschibul − *Department of Molecular and Applied Microbiology, Leibniz Institute for Natural Product Research and Infection Biology—Hans Knöll Institute (Leibniz-HKI), Jena 07745, Germany; Department of Microbiology and Molecular Biology, Institute of Microbiology, Friedrich Schiller University, Jena 07745, Germany*

Flora Rivieccio − *Department of Molecular and Applied Microbiology, Leibniz Institute for Natural Product Research and Infection Biology—Hans Knöll Institute (Leibniz-HKI), Jena 07745, Germany; Department of Microbiology and Molecular Biology, Institute of Microbiology, Friedrich Schiller University, Jena 07745, Germany;* orcid.org/0000-0002-1009-5328

Thomas Krüger − *Department of Molecular and Applied Microbiology, Leibniz Institute for Natural Product Research and Infection Biology—Hans Knöll Institute (Leibniz-HKI), Jena 07745, Germany*

Muhammad Rafiq − *Department of Molecular and Applied Microbiology, Leibniz Institute for Natural Product Research and Infection Biology—Hans Knöll Institute (Leibniz-HKI), Jena 07745, Germany; Department of Microbiology and Molecular Biology, Institute of Microbiology, Friedrich Schiller University, Jena 07745, Germany;* orcid.org/0000-0002-6018-3318

Lei-Jie Jia − *Department of Molecular and Applied Microbiology, Leibniz Institute for Natural Product Research and Infection Biology—Hans Knöll Institute (Leibniz-HKI), Jena 07745, Germany*

Tingting Zheng − *Department of Systems Biology and Bioinformatics, Leibniz Institute for Natural Product Research and Infection Biology—Hans Knöll Institute (Leibniz-HKI), Jena 07745, Germany*

Marie Goldmann − *Department of Molecular and Applied Microbiology, Leibniz Institute for Natural Product Research and Infection Biology—Hans Knöll Institute (Leibniz-HKI), Jena 07745, Germany; Department of Microbiology and Molecular Biology, Institute of Microbiology, Friedrich Schiller University, Jena 07745, Germany*

Vera Voltersen − *Department of Molecular and Applied Microbiology, Leibniz Institute for Natural Product Research and Infection Biology—Hans Knöll Institute (Leibniz-HKI), Jena 07745, Germany*

Jun Li − *Department of Infectious Diseases and Public Health, Jockey Club College of Veterinary Medicine and Life Sciences and School of Data Science, City University of Hong Kong, Kowloon, Hong Kong S.A.R., China*

Gianni Panagiotou − *Department of Systems Biology and Bioinformatics, Leibniz Institute for Natural Product Research and Infection Biology—Hans Knöll Institute (Leibniz-HKI), Jena 07745, Germany*

Complete contact information is available at: https://pubs.acs.org/10.1021/acs.jproteome.0c00013

Notes

The authors declare no competing financial interest.

https://dx.doi.org/10.1021/acs.jproteome.0c00013
J. Proteome Res. XXXX, XXX, XXX−XXX

■ ACKNOWLEDGMENTS

We would like to thank Laura Broschat for excellent technical assistance and Antje Häder for her assistance in creating the Δ*cweA* knockout strain. We would also like to thank Vito Valiante for providing an updated gene annotation for *scwA* and Volker Schwartze for thoughtful discussions throughout this project. We thank Amelia Barber for critical reading of this manuscript. M.G.B. was funded by the Federal Ministry of Education and Research (BMBF; https://www.bmbf.de/), Germany, project EXASENS (13N13861). This work was supported by the Deutsche Forschungsgemeinschaft (DFG)-funded Collaborative Research Center/Transregio 124 Fungi-Net (projects A1, B5 and Z2) and the DFG-funded ANR project AfuInf (316898429). The authors declare no conflicts of interest.

■ REFERENCES

(1) Hawksworth, D. L.; Lucking, R. Fungal Diversity Revisited: 2.2 to 3.8 Million Species. *Microbiol. Spectr.* **2017**, *5*, 1422−1432.

(2) Simon-Nobbe, B.; Denk, U.; Poll, V.; Rid, R.; Breitenbach, M. The spectrum of fungal allergy. *Int. Arch. Allergy Immunol.* **2008**, *145*, 58−86.

(3) Fukutomi, Y.; Taniguchi, M. Sensitization to fungal allergens: Resolved and unresolved issues. *Allergol. Int.* **2015**, *64*, 321−31.

(4) Kousha, M.; Tadi, R.; Soubani, A. O. Pulmonary aspergillosis: a clinical review. *Eur. Respir. Rev.* **2011**, *20*, 156−174.

(5) Brown, G. D.; Denning, D. W.; Gow, N. A.; Levitz, S. M.; Netea, M. G.; White, T. C. Hidden killers: human fungal infections. *Sci. Transl. Med.* **2012**, *4*, No. 165rv13.

(6) Steinbach, W. J.; Marr, K. A.; Anaissie, E. J.; Azie, N.; Quan, S. P.; Meier-Kriesche, H. U.; Apewokin, S.; Horn, D. L. Clinical epidemiology of 960 patients with invasive aspergillosis from the PATH Alliance registry. *J. Infect.* **2012**, *65*, 453−464.

(7) Kontoyiannis, D. P.; Marr, K. A.; Park, B. J.; Alexander, B. D.; Anaissie, E. J.; Walsh, T. J.; Ito, J.; Andes, D. R.; Baddley, J. W.; Brown, J. M.; Brumble, L. M.; Freifeld, A. G.; Hadley, S.; Herwaldt, L. A.; Kauffman, C. A.; Knapp, K.; Lyon, G. M.; Morrison, V. A.; Papanicolaou, G.; Patterson, T. F.; Perl, T. M.; Schuster, M. G.; Walker, R.; Wannemuehler, K. A.; Wingard, J. R.; Chiller, T. M.; Pappas, P. G. Prospective surveillance for invasive fungal infections in hematopoietic stem cell transplant recipients, 2001-2006: overview of the Transplant-Associated Infection Surveillance Network (TRANS-NET) Database. *Clin. Infect. Dis.* **2010**, *50*, 1091−1100.

(8) Blango, M. G.; Kniemeyer, O.; Brakhage, A. A. Conidial surface proteins at the interface of fungal infections. *PLoS Pathog.* **2019**, *15*, No. e1007939.

(9) Dagenais, T. R.; Keller, N. P. Pathogenesis of *Aspergillus fumigatus* in Invasive Aspergillosis. *Clin. Microbiol. Rev.* **2009**, *22*, 447−465.

(10) Pollmacher, J.; Timme, S.; Schuster, S.; Brakhage, A. A.; Zipfel, P. F.; Figge, M. T. Deciphering the Counterplay of *Aspergillus fumigatus* Infection and Host Inflammation by Evolutionary Games on Graphs. *Sci. Rep.* **2016**, *6*, 27807.

(11) Mircescu, M. M.; Lipuma, L.; van Rooijen, N.; Pamer, E. G.; Hohl, T. M. Essential role for neutrophils but not alveolar macrophages at early time points following *Aspergillus fumigatus* infection. *J Infect Dis* **2009**, *200*, 647−656.

(12) Denning, D. W. Invasive aspergillosis. *Clin. Infect. Dis.* **1998**, *26*, 781−803.

(13) Latge, J. P.; Chamilos, G. *Aspergillus fumigatus* and Aspergillosis in 2019. *Clin. Microbiol. Rev.* **2019**, *33*, No. 310.

(14) Hebart, H.; Bollinger, C.; Fisch, P.; Sarfati, J.; Meisner, C.; Baur, M.; Loeffler, J.; Monod, M.; Latge, J. P.; Einsele, H. Analysis of T-cell responses to *Aspergillus fumigatus* antigens in healthy individuals and patients with hematologic malignancies. *Blood* **2002**, *100*, 4521−4528.

(15) Bacher, P.; Hohnstein, T.; Beerbaum, E.; Rocker, M.; Blango, M. G.; Kaufmann, S.; Rohmel, J.; Eschenhagen, P.; Grehn, C.; Seidel, K.; Rickerts, V.; Lozza, L.; Stervbo, U.; Nienen, M.; Babel, N.; Milleck, J.; Assenmacher, M.; Cornely, O. A.; Ziegler, M.; Wisplinghoff, H.; Heine, G.; Worm, M.; Siegmund, B.; Maul, J.; Creutz, P.; Tabeling, C.; Ruwwe-Glosenkamp, C.; Sander, L. E.; Knosalla, C.; Brunke, S.; Hube, B.; Kniemeyer, O.; Brakhage, A. A.; Schwarz, C.; Scheffold, A. Human Anti-fungal Th17 Immunity and Pathology Rely on Cross-Reactivity against *Candida albicans*. *Cell* **2019**, *176*, 1340.e15−1355.e15.

(16) Dewi, I. M. W.; van de Veerdonk, F. L.; Gresnigt, M. S. The Multifaceted Role of T-Helper Responses in Host Defense against *Aspergillus fumigatus*. *J. Fungi* **2017**, *3*, No. 55.

(17) Bacher, P.; Heinrich, F.; Stervbo, U.; Nienen, M.; Vahldieck, M.; Iwert, C.; Vogt, K.; Kollet, J.; Babel, N.; Sawitzki, B.; Schwarz, C.; Bereswill, S.; Heimesaat, M. M.; Heine, G.; Gadermaier, G.; Asam, C.; Assenmacher, M.; Kniemeyer, O.; Brakhage, A. A.; Ferreira, F.; Wallner, M.; Worm, M.; Scheffold, A. Regulatory T Cell Specificity Directs Tolerance versus Allergy against Aeroantigens in Humans. *Cell* **2016**, *167*, 1067.e16−1078.e16.

(18) de Ana, S. G.; Torres-Rodriguez, J. M.; Ramirez, E. A.; Garcia, S. M.; Belmonte-Soler, J. Seasonal distribution of *Alternaria*, *Aspergillus*, *Cladosporium* and *Penicillium* species isolated in homes of fungal allergic patients. *J. Invest. Allergol. Clin. Immunol.* **2006**, *16*, 357−63.

(19) Caillaud, D.; Leynaert, B.; Keirsbulck, M.; Nadif, R. Indoor mould exposure, asthma and rhinitis: findings from systematic reviews and recent longitudinal studies. *Eur. Respir. Rev.* **2018**, *27*, 170137.

(20) Bozek, A.; Pyrkosz, K. Immunotherapy of mold allergy: A review. *Hum. Vaccines Immunother.* **2017**, *13*, 2397−2401.

(21) Bowyer, P.; Denning, D. W. Genomic analysis of allergen genes in *Aspergillus* spp: the relevance of genomics to everyday research. *Med. Mycol.* **2007**, *45*, 17−26.

(22) Hohl, T. M.; Van Epps, H. L.; Rivera, A.; Morgan, L. A.; Chen, P. L.; Feldmesser, M.; Pamer, E. G. *Aspergillus fumigatus* triggers inflammatory responses by stage-specific beta-glucan display. *PLoS Pathog.* **2005**, *1*, No. e30.

(23) Baltussen, T. J. H.; Zoll, J.; Verweij, P. E.; Melchers, W. J. G. Molecular Mechanisms of Conidial Germination in *Aspergillus* spp. *Microbiol. Mol. Biol. Rev.* **2020**, *84*, No. 19.

(24) Voltersen, V.; Blango, M. G.; Herrmann, S.; Schmidt, F.; Heinekamp, T.; Strassburger, M.; Kruger, T.; Bacher, P.; Lother, J.; Weiss, E.; Hunniger, K.; Liu, H.; Hortschansky, P.; Scheffold, A.; Loffler, J.; Krappmann, S.; Nietzsche, S.; Kurzai, O.; Einsele, H.; Kniemeyer, O.; Filler, S. G.; Reichard, U.; Brakhage, A. A. Proteome Analysis Reveals the Conidial Surface Protein CcpA Essential for Virulence of the Pathogenic Fungus *Aspergillus fumigatus*. *mBio* **2018**, *9*, No. e01557-18.

(25) Asif, A. R.; Oellerich, M.; Amstrong, V. W.; Riemenschneider, B.; Monod, M.; Reichard, U. Proteome of conidial surface associated proteins of *Aspergillus fumigatus* reflecting potential vaccine candidates and allergens. *J. Proteome Res.* **2006**, *5*, 954−62.

(26) Suh, M. J.; Fedorova, N. D.; Cagas, S. E.; Hastings, S.; Fleischmann, R. D.; Peterson, S. N.; Perlin, D. S.; Nierman, W. C.; Pieper, R.; Momany, M. Development stage-specific proteomic profiling uncovers small, lineage specific proteins most abundant in the *Aspergillus fumigatus* conidial proteome. *Proteome Sci.* **2012**, *10*, 30.

(27) Cagas, S. E.; Jain, M. R.; Li, H.; Perlin, D. S. The proteomic signature of *Aspergillus fumigatus* during early development. *Mol. Cell. Proteomics* **2011**, *10*, No. M111 010108.

(28) Erwig, L. P.; Gow, N. A. Interactions of fungal pathogens with phagocytes. *Nat. Rev. Microbiol.* **2016**, *14*, 163−176.

(29) Paris, S.; Debeaupuis, J. P.; Crameri, R.; Carey, M.; Charles, F.; Prevost, M. C.; Schmitt, C.; Philippe, B.; Latge, J. P. Conidial hydrophobins of *Aspergillus fumigatus*. *Appl. Environ. Microbiol.* **2003**, *69*, 1581−1588.

https://dx.doi.org/10.1021/acs.jproteome.0c00013
J. Proteome Res. XXXX, XXX, XXX−XXX

(30) Thau, N.; Monod, M.; Crestani, B.; Rolland, C.; Tronchin, G.; Latge, J. P.; Paris, S. rodletless mutants of *Aspergillus fumigatus*. *Infect. Immun.* **1994**, *62*, 4380−4388.
(31) Dague, E.; Alsteens, D.; Latge, J. P.; Dufrene, Y. F. High-resolution cell surface dynamics of germinating *Aspergillus fumigatus* conidia. *Biophys. J.* **2008**, *94*, 656−660.
(32) Valsecchi, I.; Dupres, V.; Stephen-Victor, E.; Guijarro, J. I.; Gibbons, J.; Beau, R.; Bayry, J.; Coppee, J. Y.; Lafont, F.; Latge, J. P.; Beauvais, A. Role of Hydrophobins in *Aspergillus fumigatus*. *J. Fungi* **2017**, *4*, No. 2.
(33) Kozel, T. R.; Wickes, B. Fungal diagnostics. *Cold Spring Harbor Perspect. Med.* **2014**, *4*, No. a019299.
(34) Li, X.; Zhang, X.; Liu, Q.; Zhao, W.; Liu, S.; Sui, G. Microfluidic System for Rapid Detection of Airborne Pathogenic Fungal Spores. *ACS Sens.* **2018**, *3*, 2095−2103.
(35) Tong, X.; Xu, H.; Zou, L.; Cai, M.; Xu, X.; Zhao, Z.; Xiao, F.; Li, Y. High diversity of airborne fungi in the hospital environment as revealed by meta-sequencing-based microbiome analysis. *Sci Rep* **2017**, *7*, No. 39606.
(36) Ghajari, A.; Lotfali, E.; Azari, M.; Fateh, R.; Kalantary, S. Fungal Airborne Contamination as a Serious Threat for Respiratory Infection in the Hematology Ward. *Tanaffos* **2015**, *14*, 257−261.
(37) Rhodes, J. Rapid Worldwide Emergence of Pathogenic Fungi. *Cell Host Microbe* **2019**, *26*, 12−14.
(38) Brakhage, A. A.; Van den Brulle, J. Use of reporter genes to identify recessive trans-acting mutations specifically involved in the regulation of *Aspergillus nidulans* penicillin biosynthesis genes. *J. Bacteriol.* **1995**, *177*, 2781−2788.
(39) Maerker, C.; Rohde, M.; Brakhage, A. A.; Brock, M. Methylcitrate synthase from *Aspergillus fumigatus*. Propionyl-CoA affects polyketide synthesis, growth and morphology of conidia. *FEBS J* **2005**, *272*, 3615−3630.
(40) de Wit, P. J.; van der Burgt, A.; Okmen, B.; Stergiopoulos, I.; Abd-Elsalam, K. A.; Aerts, A. L.; Bahkali, A. H.; Beenen, H. G.; Chettri, P.; Cox, M. P.; Datema, E.; de Vries, R. P.; Dhillon, B.; Ganley, A. R.; Griffiths, S. A.; Guo, Y.; Hamelin, R. C.; Henrissat, B.; Kabir, M. S.; Jashni, M. K.; Kema, G.; Klaubauf, S.; Lapidus, A.; Levasseur, A.; Lindquist, E.; Mehrabi, R.; Ohm, R. A.; Owen, T. J.; Salamov, A.; Schwelm, A.; Schijlen, E.; Sun, H.; van den Burg, H. A.; van Ham, R. C.; Zhang, S.; Goodwin, S. B.; Grigoriev, I. V.; Collemare, J.; Bradshaw, R. E. The genomes of the fungal plant pathogens *Cladosporium fulvum* and *Dothistroma septosporum* reveal adaptation to different hosts and lifestyles but also signatures of common ancestry. *PLoS Genet.* **2012**, *8*, No. e1003088.
(41) Ohm, R. A.; Feau, N.; Henrissat, B.; Schoch, C. L.; Horwitz, B. A.; Barry, K. W.; Condon, B. J.; Copeland, A. C.; Dhillon, B.; Glaser, F.; Hesse, C. N.; Kosti, I.; LaButti, K.; Lindquist, E. A.; Lucas, S.; Salamov, A. A.; Bradshaw, R. E.; Ciuffetti, L.; Hamelin, R. C.; Kema, G. H.; Lawrence, C.; Scott, J. A.; Spatafora, J. W.; Turgeon, B. G.; de Wit, P. J.; Zhong, S.; Goodwin, S. B.; Grigoriev, I. V. Diverse lifestyles and strategies of plant pathogenesis encoded in the genomes of eighteen *Dothideomycetes* fungi. *PLoS Pathog.* **2012**, *8*, No. e1003037.
(42) Perez-Riverol, Y.; Csordas, A.; Bai, J.; Bernal-Llinares, M.; Hewapathirana, S.; Kundu, D. J.; Inuganti, A.; Griss, J.; Mayer, G.; Eisenacher, M.; Perez, E.; Uszkoreit, J.; Pfeuffer, J.; Sachsenberg, T.; Yilmaz, S.; Tiwary, S.; Cox, J.; Audain, E.; Walzer, M.; Jarnuczak, A. F.; Ternent, T.; Brazma, A.; Vizcaino, J. A. The PRIDE database and related tools and resources in 2019: improving support for quantification data. *Nucleic Acids Res.* **2019**, *47*, D442−D450.
(43) Szewczyk, E.; Nayak, T.; Oakley, C. E.; Edgerton, H.; Xiong, Y.; Taheri-Talesh, N.; Osmani, S. A.; Oakley, B. R. Fusion PCR and gene targeting in *Aspergillus nidulans*. *Nat. Protoc.* **2006**, *1*, 3111−3120.
(44) Weidner, G.; d'Enfert, C.; Koch, A.; Mol, P. C.; Brakhage, A. A. Development of a homologous transformation system for the human pathogenic fungus *Aspergillus fumigatus* based on the *pyrG* gene encoding orotidine 5′-monophosphate decarboxylase. *Curr. Genet.* **1998**, *33*, 378−385.
(45) Sambrook, J.; Russell, D. W. *Molecular Cloning: A Laboratory Manual*; Cold Spring Harbor Laboratory Press, 2001.
(46) Howe, K. L.; Contreras-Moreira, B.; De Silva, N.; Maslen, G.; Akanni, W.; Allen, J.; Alvarez-Jarreta, J.; Barba, M.; Bolser, D. M.; Cambell, L.; Carbajo, M.; Chakiachvili, M.; Christensen, M.; Cummins, C.; Cuzick, A.; Davis, P.; Fexova, S.; Gall, A.; George, N.; Gil, L.; Gupta, P.; Hammond-Kosack, K. E.; Haskell, E.; Hunt, S. E.; Jaiswal, P.; Janacek, S. H.; Kersey, P. J.; Langridge, N.; Maheswari, U.; Maurel, T.; McDowall, M. D.; Moore, B.; Muffato, M.; Naamati, G.; Naithani, S.; Olson, A.; Papatheodorou, I.; Patricio, M.; Paulini, M.; Pedro, H.; Perry, E.; Preece, J.; Rosello, M.; Russell, M.; Sitnik, V.; Staines, D. M.; Stein, J.; Tello-Ruiz, M. K.; Trevanion, S. J.; Urban, M.; Wei, S.; Ware, D.; Williams, G.; Yates, A. D.; Flicek, P. Ensembl Genomes 2020-enabling non-vertebrate genomic research. *Nucleic Acids Res.* **2019**, *48*, D689−D695.
(47) Chang, P. K.; Zhang, Q.; Scharfenstein, L.; Mack, B.; Yoshimi, A.; Miyazawa, K.; Abe, K. *Aspergillus flavus* GPI-anchored protein-encoding ecm33 has a role in growth, development, aflatoxin biosynthesis, and maize infection. *Appl. Microbiol. Biotechnol.* **2018**, *102*, 5209−5220.
(48) Valiante, V.; Heinekamp, T.; Jain, R.; Hartl, A.; Brakhage, A. A. The mitogen-activated protein kinase MpkA of *Aspergillus fumigatus* regulates cell wall signaling and oxidative stress response. *Fungal Genet. Biol.* **2008**, *45*, 618−627.
(49) Basenko, E. Y.; Pulman, J. A.; Shanmugasundram, A.; Harb, O. S.; Crouch, K.; Starns, D.; Warrenfeltz, S.; Aurrecoechea, C.; Stoeckert, C. J., Jr.; Kissinger, J. C.; Roos, D. S.; Hertz-Fowler, C. FungiDB: An Integrated Bioinformatic Resource for Fungi and Oomycetes. *J. Fungi* **2018**, *4*, No. 39.
(50) O'Brien, K. P.; Remm, M.; Sonnhammer, E. L. Inparanoid: a comprehensive database of eukaryotic orthologs. *Nucleic Acids Res.* **2005**, *33*, D476−D480.
(51) Nielsen, H.; Engelbrecht, J.; Brunak, S.; von Heijne, G. Identification of prokaryotic and eukaryotic signal peptides and prediction of their cleavage sites. *Protein Eng.* **1997**, *10*, 1−6.
(52) Krogh, A.; Larsson, B.; von Heijne, G.; Sonnhammer, E. L. Predicting transmembrane protein topology with a hidden Markov model: application to complete genomes. *J. Mol. Biol.* **2001**, *305*, 567−580.
(53) Pierleoni, A.; Martelli, P. L.; Casadio, R. PredGPI: a GPI-anchor predictor. *BMC Bioinformatics* **2008**, *9*, 392.
(54) Hulsen, T.; de Vlieg, J.; Alkema, W. BioVenn—a web application for the comparison and visualization of biological lists using area-proportional Venn diagrams. *BMC Genomics* **2008**, *9*, 488.
(55) Zybailov, B.; Mosley, A. L.; Sardiu, M. E.; Coleman, M. K.; Florens, L.; Washburn, M. P. Statistical analysis of membrane proteome expression changes in *Saccharomyces cerevisiae*. *J. Proteome Res.* **2006**, *5*, 2339−2347.
(56) Florens, L.; Carozza, M. J.; Swanson, S. K.; Fournier, M.; Coleman, M. K.; Workman, J. L.; Washburn, M. P. Analyzing chromatin remodeling complexes using shotgun proteomics and normalized spectral abundance factors. *Methods* **2006**, *40*, 303−311.
(57) Beauvais, A.; Monod, M.; Wyniger, J.; Debeaupuis, J. P.; Grouzmann, E.; Brakch, N.; Svab, J.; Hovanessian, A. G.; Latge, J. P. Dipeptidyl-peptidase IV secreted by *Aspergillus fumigatus*, a fungus pathogenic to humans. *Infect Immun* **1997**, *65*, 3042−3047.
(58) Beauvais, A.; Monod, M.; Debeaupuis, J. P.; Diaquin, M.; Kobayashi, H.; Latge, J. P. Biochemical and antigenic characterization of a new dipeptidyl-peptidase isolated from *Aspergillus fumigatus*. *J. Biol. Chem.* **1997**, *272*, 6238−6244.
(59) Levdansky, E.; Kashi, O.; Sharon, H.; Shadkchan, Y.; Osherov, N. The *Aspergillus fumigatus* cspA gene encoding a repeat-rich cell wall protein is important for normal conidial cell wall architecture and interaction with host cells. *Eukaryotic Cell* **2010**, *9*, 1403−1415.
(60) Levdansky, E.; Romano, J.; Shadkchan, Y.; Sharon, H.; Verstrepen, K. J.; Fink, G. R.; Osherov, N. Coding tandem repeats generate diversity in *Aspergillus fumigatus* genes. *Eukaryotic Cell* **2007**, *6*, 1380−1391.
(61) da Silva Ferreira, M. E.; Kress, M. R.; Savoldi, M.; Goldman, M. H.; Hartl, A.; Heinekamp, T.; Brakhage, A. A.; Goldman, G. H. The akuB(KU80) mutant deficient for nonhomologous end joining is a

https://dx.doi.org/10.1021/acs.jproteome.0c00013
J. Proteome Res. XXXX, XXX, XXX−XXX

powerful tool for analyzing pathogenicity in *Aspergillus fumigatus*. *Eukaryotic Cell* **2006**, *5*, 207−211.
(62) Hagiwara, D.; Sakai, K.; Suzuki, S.; Umemura, M.; Nogawa, T.; Kato, N.; Osada, H.; Watanabe, A.; Kawamoto, S.; Gonoi, T.; Kamei, K. Temperature during conidiation affects stress tolerance, pigmentation, and trypacidin accumulation in the conidia of the airborne pathogen *Aspergillus fumigatus*. *PLoS One* **2017**, *12*, No. e0177050.
(63) Anjo, S. I.; Figueiredo, F.; Fernandes, R.; Manadas, B.; Oliveira, M. A proteomic and ultrastructural characterization of *Aspergillus fumigatus*' conidia adaptation at different culture ages. *J. Proteomics* **2017**, *161*, 47−56.
(64) Mitchell, A. L.; Attwood, T. K.; Babbitt, P. C.; Blum, M.; Bork, P.; Bridge, A.; Brown, S. D.; Chang, H. Y.; El-Gebali, S.; Fraser, M. I.; Gough, J.; Haft, D. R.; Huang, H.; Letunic, I.; Lopez, R.; Luciani, A.; Madeira, F.; Marchler-Bauer, A.; Mi, H.; Natale, D. A.; Necci, M.; Nuka, G.; Orengo, C.; Pandurangan, A. P.; Paysan-Lafosse, T.; Pesseat, S.; Potter, S. C.; Qureshi, M. A.; Rawlings, N. D.; Redaschi, N.; Richardson, L. J.; Rivoire, C.; Salazar, G. A.; Sangrador-Vegas, A.; Sigrist, C. J. A.; Sillitoe, I.; Sutton, G. G.; Thanki, N.; Thomas, P. D.; Tosatto, S. C. E.; Yong, S. Y.; Finn, R. D. InterPro in 2019: improving coverage, classification and access to protein sequence annotations. *Nucleic Acids Res.* **2019**, *47*, D351−D360.
(65) Landers, C. T.; Tung, H. Y.; Knight, J. M.; Madison, M. C.; Wu, Y.; Zeng, Z.; Porter, P. C.; Rodriguez, A.; Flick, M. J.; Kheradmand, F.; Corry, D. B. Selective cleavage of fibrinogen by diverse proteinases initiates innate allergic and antifungal immunity through CD11b. *J. Biol. Chem.* **2019**, *294*, 8834−8847.
(66) Balenga, N. A.; Klichinsky, M.; Xie, Z.; Chan, E. C.; Zhao, M.; Jude, J.; Laviolette, M.; Panettieri, R. A., Jr.; Druey, K. M. A fungal protease allergen provokes airway hyper-responsiveness in asthma. *Nat. Commun.* **2015**, *6*, No. 6763.
(67) Remm, M.; Storm, C. E.; Sonnhammer, E. L. Automatic clustering of orthologs and in-paralogs from pairwise species comparisons. *J. Mol. Biol.* **2001**, *314*, 1041−1052.
(68) Teutschbein, J.; Simon, S.; Lother, J.; Springer, J.; Hortschansky, P.; Morton, C. O.; Loffler, J.; Einsele, H.; Conneally, E.; Rogers, T. R.; Guthke, R.; Brakhage, A. A.; Kniemeyer, O. Proteomic Profiling of Serological Responses to *Aspergillus fumigatus* Antigens in Patients with Invasive Aspergillosis. *J. Proteome Res.* **2016**, *15*, 1580−1591.
(69) Dasari, P.; Koleci, N.; Shopova, I. A.; Wartenberg, D.; Beyersdorf, N.; Dietrich, S.; Sahagun-Ruiz, A.; Figge, M. T.; Skerka, C.; Brakhage, A. A.; Zipfel, P. F. Enolase From *Aspergillus fumigatus* Is a Moonlighting Protein That Binds the Human Plasma Complement Proteins Factor H, FHL-1, C4BP, and Plasminogen. *Front. Immunol.* **2019**, *10*, 2573.
(70) Parida, S. K.; Poiret, T.; Zhenjiang, L.; Meng, Q.; Heyckendorf, J.; Lange, C.; Ambati, A. S.; Rao, M. V.; Valentini, D.; Ferrara, G.; Rangelova, E.; Dodoo, E.; Zumla, A.; Maeurer, M. T-Cell Therapy: Options for Infectious Diseases. *Clin. Infect. Dis.* **2015**, *61*, S217−S224.

https://dx.doi.org/10.1021/acs.jproteome.0c00013
J. Proteome Res. XXXX, XXX, XXX−XXX

Supplemental information

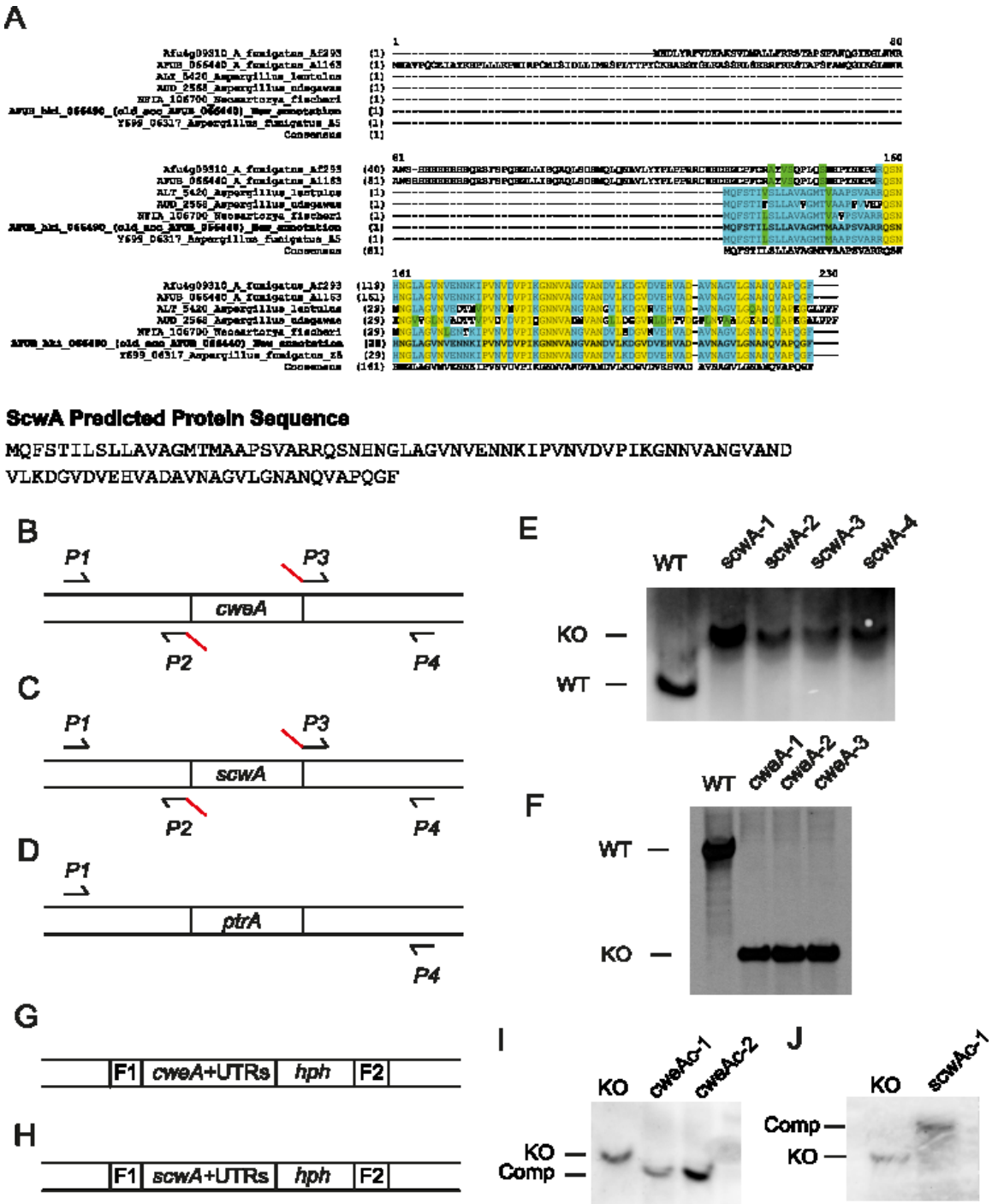

Figure S1. Production of Δ*cweA* and Δ*scwA* knockouts in *A. fumigatus*. A) Reannotation of *scwA* (Afu4g09310) from *A. fumigatus* CEA10. For production of genetic deletions of B) *cweA* and C) *scwA* flanking DNA sequences were amplified using the appropriate primers p1-p4. D) The flanking DNA sequences were then combined with the *ptrA* resistance marker by Phusion polymerase and primers p1/4 to produce a construct with gene flanking regions surrounding the resistance marker. Genetic deletions of E) *scwA* and F) *cweA* were then confirmed by Southern blot analysis after digestion of genomic DNA with *Hin*dIII or *Cla*I, respectively. Complemented strains for G) *cweA* and H) *scwA* were produced by introducing a construct containing a 5' flanking sequence (F1), the gene with both 5' and 3' UTRs, a hygromycin resistance cassette (*hph*), and a 3' flanking sequence (F2) into the original locus of the corresponding knockout strain *via* homologous recombination. Southern blots were performed to confirm complementation of I) *cweA* after digestion of genomic DNA using restriction enzyme *Bam*HI and J) *scwA* using restriction enzyme *Eco*RI.

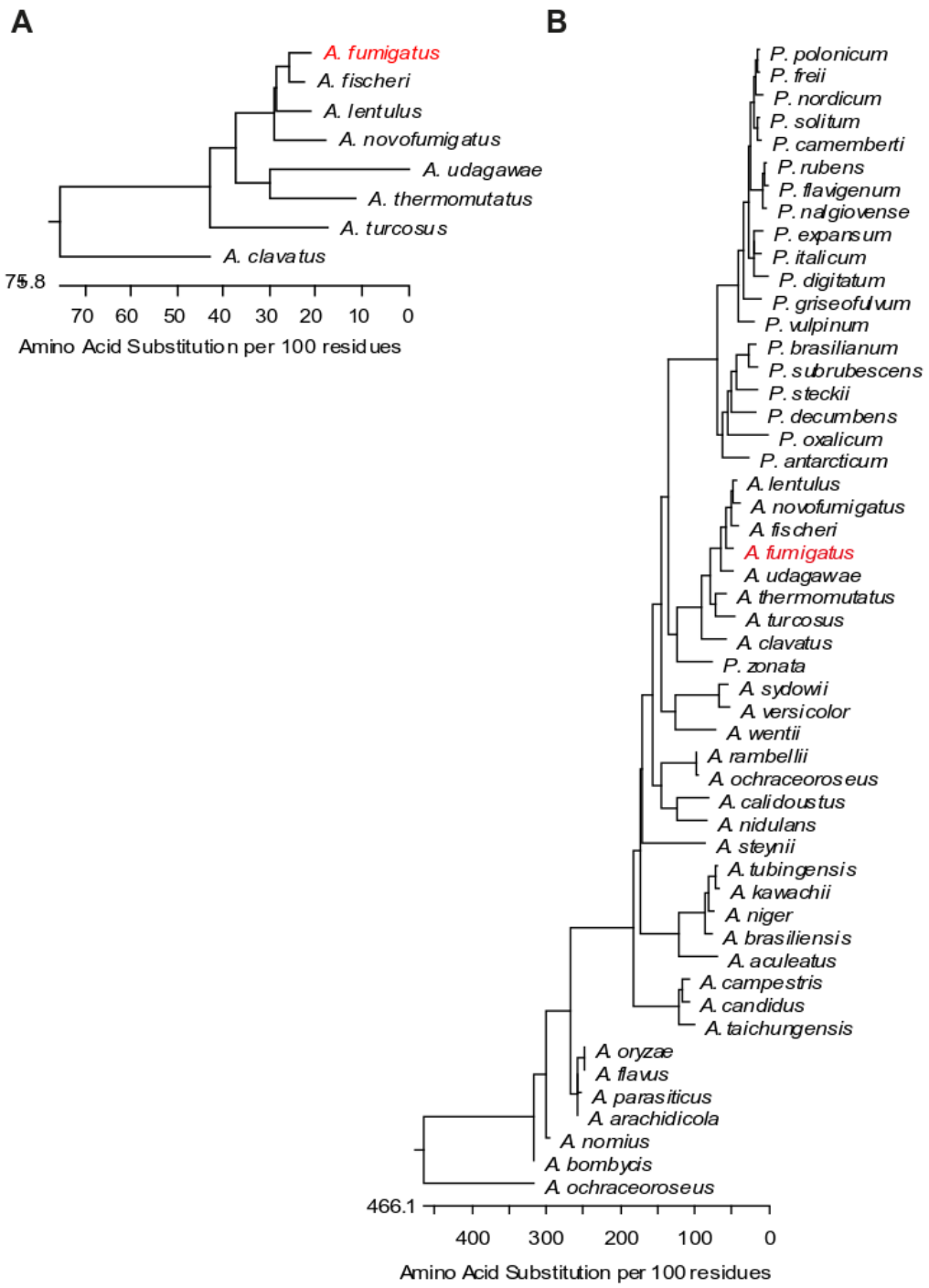

Figure S2. Phylogenetic analysis of *A. fumigatus* cell surface proteins. A) Phylogenetic tree of ScwA sequences produced using the DNAStar MegAlign software with a ClustalW alignment of all sequences deemed significant by NCBI Blastp suite. B) Phylogenetic tree of CweA sequences produced using the DNAStar MegAlign software with a ClustalW alignment of all sequences deemed significant by NCBI Blastp suite.

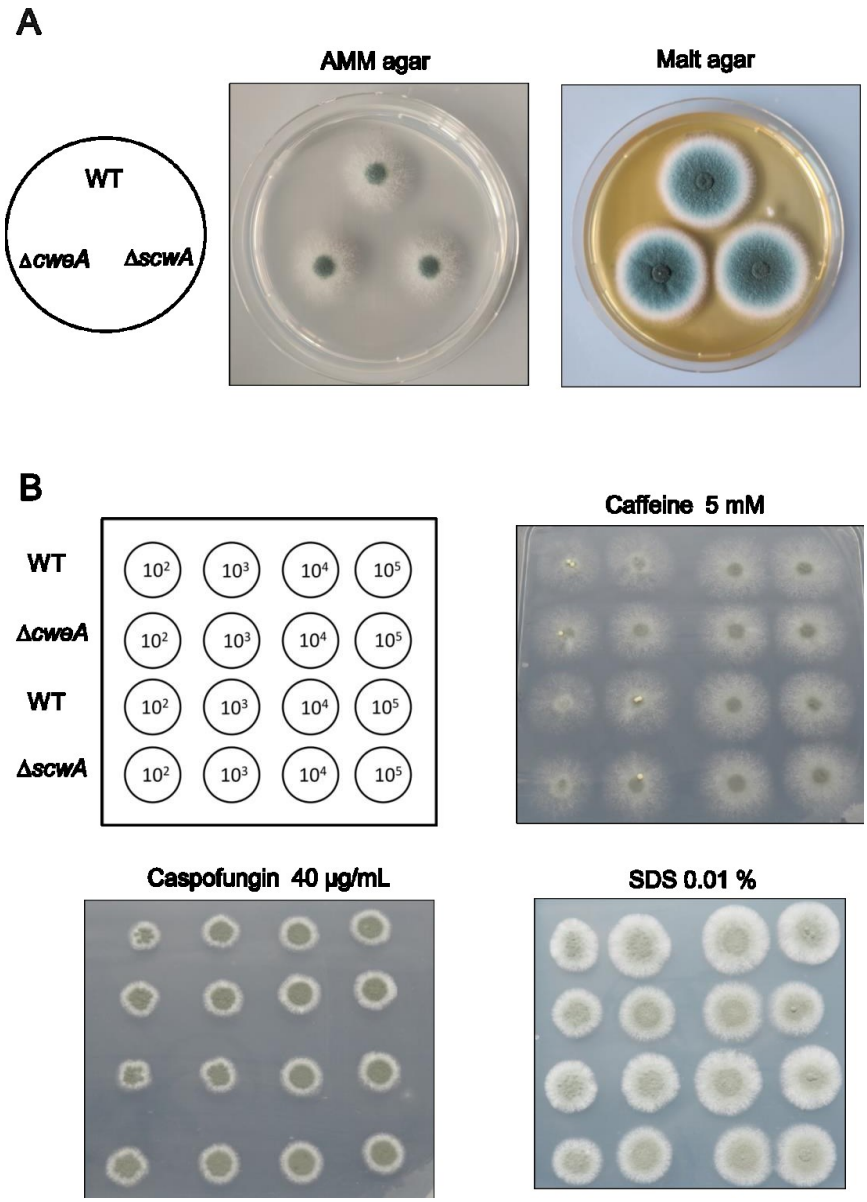

Figure S3. Growth characterization of the Δ*cweA* and Δ*scwA* knockouts. A) Growth on AMM and malt agar plates for 48 h. B) Strains were serially diluted and spotted onto AMM agar with the addition of the indicated stressors and grown for 72 h. Experiments are representative data from three separate experiments.

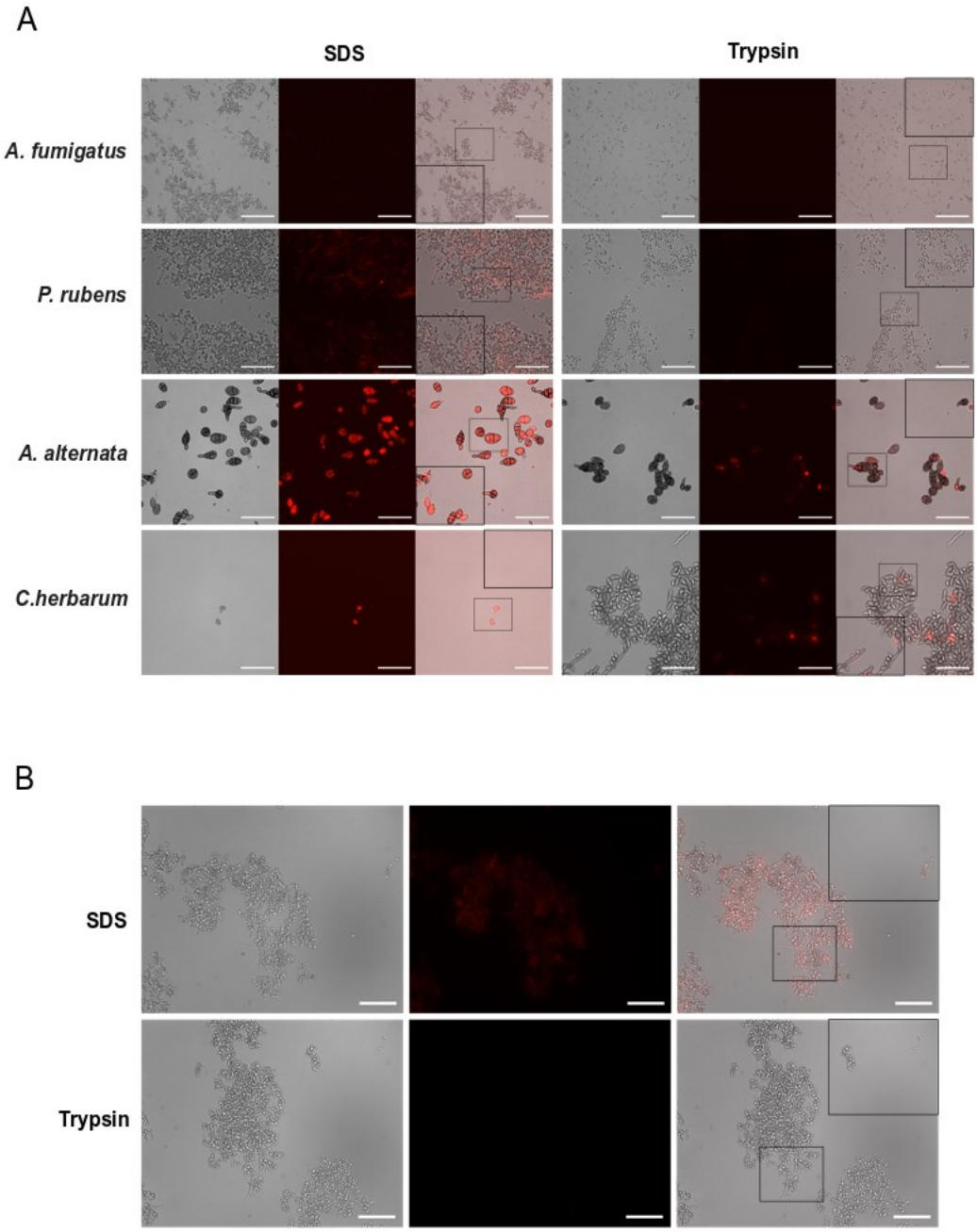

Figure S4. Trypsin does not induce major changes in fungal conidial permeability. A) Images show representative fungal conidia stained for 15 min with the cell-impermeable dye propidium iodide (red) following treatment with 1% (w/v) SDS (left) or 5 µg/mL trypsin for 5 min at 37°C (right). B) After 8 hours of incubation, germlings (with hyphal extensions) and swollen conidia also show no lysis after trypsin treatment as performed in A). All scale bars are 50 µm.

Table S1. Fungal strains used in this study.

Strain	Genotype/Phenotype	Source
CEA10	*A. fumigatus* wild type	Fungal Genetics Stock Center (A1163)
CEA17	*A. fumigatus akuB*^{KU80} deletion in CEA10	Da Silva Ferreira et al., 2006
CEA17*ΔcweA*	Derived from CEA17; *Afu4g09600*::*ptrA*; PtrA^{R}, Δ*Afu4g09600*	This study
CEA17*ΔcweA* + CweA	*ΔcweA* complemented strain	This study
CEA17*ΔscwA*	Derived from CEA17; *Afu4g09310*::*ptrA*; PtrA^{R}, Δ*Afu4g09310*	This study
CEA17*ΔscwA* + ScwA	*ΔscwA* complemented strain	This study
ATCC 66981	*A. alternata* wild type	American Type Culture Collection
ATCC 28089	*P. rubens* wild type	American Type Culture Collection
ATCC MYA-4682	*C. herbarum* wild type	American Type Culture Collection

Table S2. Oligonucleotides and plasmids used in this study.

Oligonucleotide	Sequence (5'—3')	Target
Gene Deletion		
cweA-1	TAACAGAACCTGCCACGACC	*cweA*
cweA-2	GGCCTGAGTGGCCATCGAATTCTTCCTCCGACCAGACCCTTC	*cweA*
cweA-3	GAGGCCATCTAGGCCATCAAGCGCTGTCATTCGTGCCGTTGA	*cweA*
cweA-4	GCAAGCGCAGCAAGATAAGG	*cweA*
scwA-1	GCCCACATGCCTCTAGACTC	*scwA*
scwA-2	GGCCTGAGTGGCCATCGAATTCCGATCAGCACTCTGGTACTG	*scwA*
scwA-3	GAGGCCATCTAGGCCATCAAGCGGAGATGGCTGGATATAGTC	*scwA*
scwA-4	GCGAGAACCAGAGCGCAAAC	*scwA*
prtA-1	GAATTCGATGGCCACTCAGGCC	*ptrA*
prtA-2	GCTTGATGGCCTAGATGGCCTC	*ptrA*
Complementation		
scwA_F	TATCACGAGGCCCTTTCGTCAAGCAAGACCAGAACCTGAAATC	*scwA*
scwA_hph_R	GCTCCCCAGGGCTTCTAGTGGATATCTG	*scwA*
scwA_hph_F	GCAAAGGAATATGAAGGGCTTTCCCGAAAG	*scwA*
scwA_R	CATCGTCACCAACCACACGTCGCGCGTTTCGGTGATGAC	*scwA*
hph_scwA_F	GGGCTTCTAGTGGATATCTGCAGAATTCGC	*hph*
hph_scwA_R	GTCCGAGGGCAAAGGAATATGAAGGGCT	*hph*
pUC19_F	TCGCGCGTTTCGGTGATG	*pUC19*
pUC19_R	GTATCACGAGGCCCTTTCGTC	*pUC19*
cweA_F	TATCACGAGGCCCTTTCGTCCTAACAGAACCTGCCACG	*cweA*
cweA_hph_R	CTAGCTTACGAAGATCAAGAATTTCGCCAGTGTG	*cweA*
cweA_hph_F	CAAAGGAATAGTCAGCCATGTGTGGTCTC	*cweA*
cweA_R	CATGAGTTTATTAGGGAGCATGAGTCGCGCGTTTCGGTGATGAC	*cweA*
hph_cweA_F	TCAAGAATTTCGCCAGTGTGATGGATATC	*hph*
hph_cweA_R	GTCCGAGGGCAAAGGAATAGTCAGCCATG	*hph*
Plasmids	***Source***	
pUC19	New England Biolabs	
pUC19_scwAc	Complementation plasmid produced in this study	
pUC19_cweAc	Complementation plasmid produced in this study	

3. Manuscripts

3.2 Manuscript B

Host-derived extracellular vesicles for antimicrobial defense

Brakhage A.A, Zimmermann A-K, **Rivieccio F**, Visser C, Blango MG.

Manuscript published in *microLife*, Volume 2, April 2021.

Summary:
This review gives an overview on the role of extracellular vesicles in the host defense against pathogens. In particular it highlights how, many organisms, like plants or human cells, utilize extracellular vesicles packed with antimicrobial cargo, to extracellularly kill fungi or bacteria. Ultimately it provides examples of extracellular vesicles-based therapeutics.

Contribution to the manuscript:
Flora Rivieccio was involved in writing the introduction and the chapter "Microbes produce extracellular vesicles against other microbes". Furthermore, she designed and generated the first the figure.

Estimated contribution in percentage:

Author	Conceptual	Data analysis	Experimental	Writing the manuscript	Provision of material
Brakhage A.A	20%	0%	0%	20%	0%
Zimmermann A-K	20%	0%	0%	20%	0%
Rivieccio F.	**20%**	**0%**	**0%**	**20%**	**0%**
Visser C.	20%	0%	0%	20%	0%
Blango MG.	20%	0%	0%	20%	0%
Total:	100%	0%	0%	100%	100%

microLife, 2, 2021, uqab003

doi: 10.1093/femsml/uqab003
Advance Access Publication Date: 16 April 2021
Short Review

SHORT REVIEW

Host-derived extracellular vesicles for antimicrobial defense

Axel A. Brakhage[1,2,*], Ann-Kathrin Zimmermann[1,2,†], Flora Rivieccio[1,2], Corissa Visser[1,2,‡] and Matthew G. Blango[3,*,#]

[1]Department of Molecular and Applied Microbiology, Leibniz Institute for Natural Product Research and Infection Biology—Hans Knöll Institute (Leibniz-HKI), Adolf-Reichwein-Straße 23, 07745, Jena, Germany, [2]Department of Microbiology and Molecular Biology, Institute of Microbiology, Friedrich Schiller University Jena, Adolf-Reichwein-Straße 23, 07745, Jena, Germany and [3]Junior Research Group RNA Biology of Fungal Infections, Leibniz Institute for Natural Product Research and Infection Biology—Hans Knöll Institute (Leibniz-HKI), Adolf-Reichwein-Straße 23, 07745, Jena, Germany

*Corresponding author: Junior Research Group RNA Biology of Fungal Infections, Leibniz Institute for Natural Product Research and Infection Biology—Hans Knöll Institute (Leibniz-HKI), Adolf-Reichwein-Straße 23, 07745, Jena, Germany. Tel: +49 (0)3641-532 1072; E-mail: matthew.blango@leibniz-hki.de; Tel: +49 (0)3641-532 1001; E-mail: axel.brakhage@leibniz-hki.de

One sentence summary: Antimicrobial extracellular vesicles produced by organisms ranging from bacteria to humans contribute to host defense against microbes and offer new strategies for the development of therapeutics.

†Ann-Kathrin Zimmermann, http://orcid.org/0000-0003-1750-5091
‡Corissa Visser, http://orcid.org/0000-0001-7218-701X
#Matthew G. Blango, http://orcid.org/0000-0001-8015-9019

ABSTRACT

Extracellular vesicles are of increasing importance in the clinic, as diagnostics for complex diseases and as potential delivery systems for therapeutics. Over the past several decades, extracellular vesicles have emerged as a widespread, conserved mechanism of intercellular and interkingdom communication. The ubiquitous distribution of extracellular vesicles across life offers at least two compelling opportunities: first a path forward in the design of targeted antimicrobial delivery systems; and second, a new way to view host pathogenesis during infection. Both avenues of research are well underway. In particular, preliminary studies showing that plant and human host-derived extracellular vesicles can deliver natural antimicrobial cargos to invading fungal and bacterial pathogens are captivating. Further, modification of host extracellular vesicle populations may ultimately lead to enhanced killing and serve as a starting point for the development of more advanced therapeutic options, especially against difficult to treat pathogens. Despite the rapid pace of growth surrounding extracellular vesicle biology, many questions remain unanswered. For example, the heterogeneity of vesicle populations continues to be a confounding factor in ascribing clear functions to a vesicular subset, and the molecular cargos responsible for specific antimicrobial actions of extracellular vesicles during infection remain especially poorly described. In this short review, we will summarize the current state of affairs surrounding the antimicrobial function, and potential, of host-derived extracellular vesicles.

Received: 5 March 2021; **Accepted:** 13 April 2021

© The Author(s) 2021. Published by Oxford University Press on behalf of FEMS. This is an Open Access article distributed under the terms of the Creative Commons Attribution-NonCommercial License (http://creativecommons.org/licenses/by-nc/4.0/), which permits non-commercial re-use, distribution, and reproduction in any medium, provided the original work is properly cited. For commercial re-use, please contact journals.permissions@oup.com

Downloaded from https://academic.oup.com/microlife/article/doi/10.1093/femsml/uqab003/6228840 by guest on 25 May 2021

Keywords: extracellular vesicle; antimicrobial; cross-kingdom RNAi; intercellular communication; bacteria; fungi

INTRODUCTION

Extracellular vesicles were originally described in 1967 as 'platelet dust,' which was physically separable from platelets by ultracentrifugation (Wolf 1967). In the intervening years, research into these small particles has grown rapidly, in large part due to their involvement in a wide array of diseases and their obvious potential as biomarkers (Hargett and Bauer 2013). The term 'extracellular vesicle' was a later addition to the field, but now broadly encompasses a heterogenous group of cell-derived, lipid-bilayer-enclosed particles important for both intercellular and inter-organismal communication in all domains of life (Colombo, Raposo and Thery 2014; van Niel, D'Angelo and Raposo 2018). In prokaryotes, extracellular vesicles are abundantly produced by both Gram-negative and Gram-positive bacteria and typically referred to as outer membrane vesicles or more broadly bacterial extracellular vesicles, respectively (MacDonald and Kuehn 2012; Toyofuku, Nomura and Eberl 2019). In the Eukaryota, exosomes, microvesicles, and apoptotic cell-derived extracellular vesicles (frequently referred to as apoptotic bodies) are the terms most-widely accepted to describe the three major groups based on their biogenesis through multivesicular bodies, membrane shedding, and apoptosis, respectively (Lorincz *et al.* 2015). However, it is clear that even these terms are too simple for the description of the eukaryotic extracellular vesicle population in its entirety, as additional layers of complexity can be observed with further purification (Jeppesen *et al.* 2019). In general, extracellular vesicles carry a combination of lipids, nucleic acids, proteins, and metabolites, and the particular cargo found within a subset appears to be tightly regulated and highly dependent on cell of origin and isolation method (Kolonics *et al.* 2020b; He *et al.* 2021). Thus, in an effort to standardize research into extracellular vesicles, the International Society for Extracellular Vesicles (ISEV) has released several position statements, most recently in 2019, to define the minimal requirements to report findings on extracellular vesicles (Thery *et al.* 2018; Russell *et al.* 2019). The community is slowly implementing these guidelines, and the quality of reporting and reproducibility appears to be generally improving.

Even with these new guidelines, the size distributions of extracellular vesicles are still contested in the literature. The majority of researchers agree that exosomes are typically less than 150 nm in diameter (Fig. 1; Russell *et al.* 2019) and formed by invagination of late endosomal membranes to create intraluminal vesicles, within a structure known as a multivesicular body (Table 1; Latifkar *et al.* 2019). The multivesicular body then fuses with the plasma membrane to release the exosomes into the extracellular space. We now know that biogenesis and cargo loading of exosomes are linked through the action of the Endosomal Sorting Complex Required for Transport (ESCRT) family of proteins, which are important for membrane bending/budding (Juan and Furthauer 2018). However, the ESCRTs are not the only factors that contribute to exosome cargo loading, as more recently, ESCRT-independent mechanisms of cargo selection have also been described, including mechanisms reliant on lipid raft formation or dependent on ceramide-mediated recruitment (Li *et al.* 2018). Microvesicles, typically greater than 200 nm in diameter, are shed directly from the plasma membrane after distinct, localized changes in lipid content (Haraszti *et al.* 2016; Tricarico, Clancy and D'Souza-Schorey 2017). Interestingly, microvesicles also exhibit selective enrichment for certain cargo, despite budding directly from the plasma membrane. Apoptotic cell-derived extracellular vesicles, a heterogeneous fraction of 50–5000 nm diameter vesicles, are less well defined but are again formed during the highly regulated cellular process of apoptotic cell disassembly (Caruso and Poon 2018). This diverse class of extracellular vesicles also includes more specific subsets, including the apoptotic bodies (1000–5000 nm in diameter; Table 1) and apoptotic microvesicles (50–1000 nm in diameter). Although the biogenesis of each subset of extracellular vesicles appears to be biochemically distinct, many features are shared across subsets, including a high level of regulation and the specificity of cargo selection.

Nearly every cell-type tested has been shown to produce extracellular vesicles, and many different functions have been ascribed to this diverse category of small particles. In addition to intercellular signaling, extracellular vesicles have also been shown to be important in microbial communication, disease, and host pathogenesis (Buck *et al.* 2014; Bielska *et al.* 2018; Genschmer *et al.* 2019; Munhoz da Rocha *et al.* 2020). The function of extracellular vesicles during infectious disease depends on the particular host and pathogen. In many cases, extracellular vesicles have been shown to play a role in propagating the immune response against invading pathogens (Rybak and Robatzek 2019; Kolonics *et al.* 2020b). The contribution of extracellular vesicles to pathogenesis is not one-sided, as many pathogens including bacteria, fungi, and parasites also depend on activities encased in extracellular vesicles to exploit their host (Kim *et al.* 2015; Ofir-Birin, Heidenreich and Regev-Rudzki 2017; Kuipers *et al.* 2018; Liu *et al.* 2018; Bielska *et al.* 2019; Ofir-Birin and Regev-Rudzki 2019). Interestingly, extracellular vesicles are even relied upon by the host to control viral infection, as vesicles containing the RNA editing enzyme APOBEC3G are known to help the host fight against HIV infection (Khatua *et al.* 2009). Bacteria have been observed on several occasions to increase production of outer membrane vesicles as cellular decoys in defense against phage infection or even to counteract attacks by the host complement system (Manning and Kuehn 2011; Roier *et al.* 2016; Reyes-Robles *et al.* 2018; McNamara and Dittmer 2020). Collectively, these examples highlight just a few of the many roles of extracellular vesicles in mediating the outcome of infection.

In this short review, we focus not on the pathogen or the propagation of host immunity by extracellular vesicles, but instead on how extracellular vesicles may function as discrete containers to deliver antimicrobials to their competitors and enemies. We intend to define the common antimicrobial theme present in each of these systems as we provide an outlook for the future development of antimicrobial therapeutics based on knowledge gained from the study of extracellular vesicles.

HUMAN HOSTS PRODUCE ANTIMICROBIAL EXTRACELLULAR VESICLES AGAINST BACTERIAL PATHOGENS

Although hypothesized earlier (Hess *et al.* 1999; Gonzalez-Cano *et al.* 2010), the first reported experimental demonstration of an antibacterial function for host-derived extracellular vesicles

Downloaded from https://academic.oup.com/microlife/article/doi/10.1093/femsml/uqab003/6228840 by guest on 25 May 2021

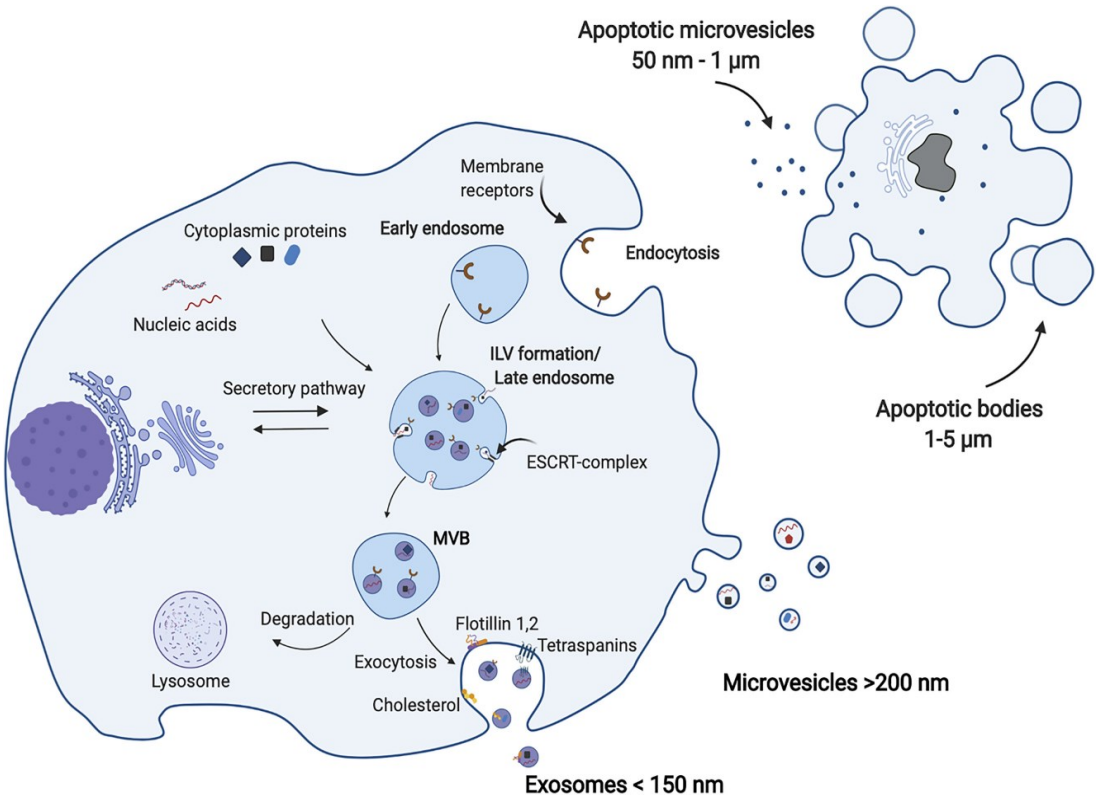

Figure 1. Biogenesis of extracellular vesicles. Extracellular vesicles are produced through a variety of different cellular processes, including budding of plasma membrane (microvesicles), release of intraluminal vesicles (ILV) from multivesicular bodies (exosomes), and apoptotic cell disassembly (apoptotic cell-derived extracellular vesicles). Created with BioRender.com.

Table 1. Nomenclature and origin of commonly described extracellular vesicle populations.

Extracellular vesicle category		Characteristic diameter (nm)	Cellular origin	Reference
Mammalian-derived	Exosome	<150	Multivesicular body	Russell *et al.* (2019)
	Microvesicle	>200	Plasma membrane	Tricarico, Clancy and D'Souza-Schorey (2017)
	Apoptotic cell-derived extracellular vesicles	>50	Broad biogenesis derived from apoptotic cells (includes apoptotic bodies)	Caruso and Poon (2018)
	Apoptotic microvesicles	50–1000	Biogenesis unclear	Caruso and Poon (2018)
	Apoptotic bodies	1000–5000	Apoptotic cell plasma membrane blebbing	Caruso and Poon (2018)
Plant-derived	Exosomes/Exosome-like (PEN1-, TET8- and EXPO-positive subsets)	<500	Multivesicular body, exocyst-positive organelles (EXPO)	Rutter and Innes (2017); Cui *et al.* (2020); He *et al.* (2021)
Microbe-associated	Bacterial outer membrane vesicles	20–400	Budding of outer membrane of Gram-negative bacteria	Toyofuku, Nomura and Eberl (2019)
	Gram-positive bacterial extracellular vesicles	10–400	The biogenesis remains disputed	Liu *et al.* (2018)
	Fungal-derived extracellular vesicles	50–1000	Diverse, poorly understood class; similarities to higher eukaryotes	Joffe *et al.* (2016)
	Protozoa-derived extracellular vesicles	30–500	Diverse pathways; similarities to higher eukaryotes	Ofir-Birin and Regev-Rudzki (2019)

Downloaded from https://academic.oup.com/microlife/article/doi/10.1093/femsml/uqab003/6228840 by guest on 25 May 2021

came from the study of microvesicles released from human neutrophilic granulocytes in response to infection with *Staphylococcus aureus* (Fig. 2; Timar *et al.* 2013). The antibacterial activity of microvesicles was shown to depend on opsonization of the bacteria via activation of opsonin receptors, PLCγ2 and extracellular calcium, in a manner distinct from that of spontaneously released extracellular vesicles (Lorincz *et al.* 2015, 2019). Further investigation revealed that the Mac-1 integrin complex, also known as Complement Receptor 3, is essential to initiate the production of these antibacterial extracellular vesicles (Lorincz *et al.* 2020). Surprisingly, the activation of pathogen recognition receptors or immunoglobulin binding Fc receptors was not sufficient for production of antibacterial extracellular vesicles.

The antimicrobial activity observed in response to *S. aureus* infection was not limited to *S. aureus* alone, as *Escherichia coli* was also inhibited by neutrophil-derived vesicles (Timar *et al.* 2013). In contrast, these antibacterial extracellular vesicles produced in response to opsonized *S. aureus* infection had no antibacterial activity against *Proteus mirabilis*, suggesting some level of specificity (Timar *et al.* 2013). Extracellular vesicles that were formed spontaneously by neutrophils, or in response to treatment with phorbolmyristate acetate, showed less antibacterial activity. The antimicrobial activity of extracellular vesicles was not reliant on toxic reactive oxygen intermediates or the opsonization status of the target bacteria, but instead required an intact cytoskeleton and metabolic activity within the extracellular vesicles (Timar *et al.* 2013). Since these initial studies were only performed using chemical inhibitors, further studies will be required to definitely determine the function of the cytoskeleton and active metabolism in antibacterial extracellular vesicles.

The inability of extracellular vesicles to produce superoxide like their parent neutrophils was a bit of a surprise, as superoxide radicals are a major mechanism known to target many pathogens (Lorincz *et al.* 2015). One possible explanation of this phenotype is that extracellular vesicles act indirectly by promoting the inflammatory response in neighboring cells. In fact, it was shown that opsonized zymosan particles induced neutrophils to produce extracellular vesicles that facilitated neutrophil interleukin 8 secretion and reactive oxygen species production (Kolonics *et al.* 2020a). This explanation agrees with studies of *Mycobacterium tuberculosis* pathogenesis, where pathogen-induced extracellular vesicles from neutrophils were shown to increase superoxide production by macrophages (Alvarez-Jimenez *et al.* 2018). Interestingly, extracellular vesicles released spontaneously from macrophages led to a stronger reduction of bacterial load than *M. tuberculosis*-infected macrophages, suggesting an active inhibition of antimicrobial activity of extracellular vesicles by the bacteria (Garcia-Martinez *et al.* 2019).

Importantly, there appeared to be no sensitization of neutrophils to extracellular vesicle induction, as repeated exposure to opsonized *S. aureus* led to additional production of antibacterial extracellular vesicles (Timar *et al.* 2013). Of potential relevance to future therapeutic design, the antimicrobial function of neutrophil-derived extracellular vesicles over time was shown to depend on storage temperature (Lorincz *et al.* 2014). At -80°C the activity was quite stable, whereas at 4°C or 20°C, the activity rapidly declined.

The *in vivo* relevance of extracellular vesicles has been an important question from the start of the field. In terms of an antibacterial function, early studies showed that extracellular vesicles derived from neutrophils could be found in the circulation (Timar *et al.* 2013). However, when extracellular vesicles from the murine macrophage cell line J774A.1 were applied exogenously to *M. tuberculosis*-infected mice, there was no major change in survival, despite a reduction in bacterial load (Garcia-Martinez *et al.* 2019). Additional experiments using extracellular vesicles from patient samples are needed to fully understand the *in vivo* relevance during infection.

The exact mechanism of action for antibacterial extracellular vesicles remains unknown, but we are starting to have an idea of what is possible. In fact, a recent study showed that extracellular vesicles derived from *M. tuberculosis*-infected macrophages contained molecules derived from the pathogen itself (Cheng and Schorey 2019). In this case, bacterial RNA was transferred from the macrophages in extracellular vesicles and activated microtubule-associated protein 1A/1B-light chain 3 (LC3)-associated phagosome maturation via a retinoic acid-inducible gene I (RIG-I)/mitochondrial antiviral-signaling protein (MAVS)-dependent signaling pathway in recipient cells. This sharing of bacterial RNA between cells ultimately led to increased killing of the intracellular bacteria.

A similar strategy is also employed by the host to transfer cytokines for immune activation in response to infection. In particular, extracellular vesicles from dendritic cells carried the proinflammatory cytokine TNF-α and were able to activate epithelial cells, which resulted in the release of additional inflammatory mediators (Obregon *et al.* 2009). More recent work showed that the induction of proinflammatory cytokines by host-derived extracellular vesicles can further activate antibacterial immunity (Radomski *et al.* 2019). In this study, *Chlamydia psittaci*-infected dendritic cells were shown to release vesicles capable of inducing IFN-γ production in natural killer-cells via a TNF-α/TNF receptor interaction. Interestingly, in this case, the extracellular vesicles produced by infected dendritic cells contained no discernable bacterial material, suggesting a process mediated by host factors alone. Ultimately, it was shown that dendritic cell-derived extracellular vesicles worked in concert with natural killer cell-derived IFN-γ and TNF-α to limit the growth of *C. psittaci* in infected epithelial cells. These studies highlight the complicated interplay of extracellular vesicles with other well-described immune reactions and highlight that much work remains to fully understand the antibacterial activity of extracellular vesicles and their role in propagating the immune response.

PLANT HOSTS PRODUCE EXTRACELLULAR VESICLES AND EFFECTOR SMALL RNAS AGAINST PATHOGENS

In plants, extracellular vesicles were only first isolated in 2009 from water-imbibed seeds of the sunflower, *Helianthus annuus* (Regente *et al.* 2009). This is despite the initial ultrastructural observations from carrot cell culture having occurred more than 50 years prior (Halperin and Jensen 1967). The antimicrobial nature of these plant-derived extracellular vesicles was not immediately obvious, and remains, like the entire field of antimicrobial extracellular vesicles, a work in progress (Rutter and Innes 2020). The first hints of an importance for extracellular vesicles during plant infection came from the discovery that paramural vesicles of barley were enriched around sites of infection of the powdery mildew fungus *Blumeria graminis* (An *et al.* 2006). Paramural vesicles are produced from multivesicular bodies, similar to the mammalian exosomes, and reside between the plant cell membrane and cell wall. It was therefore hypothesized that the vesicles that accumulate around the pathogen might in some instances be released from the cell wall to serve

Downloaded from https://academic.oup.com/microlife/article/doi/10.1093/femsml/uqab003/6228840 by guest on 25 May 2021

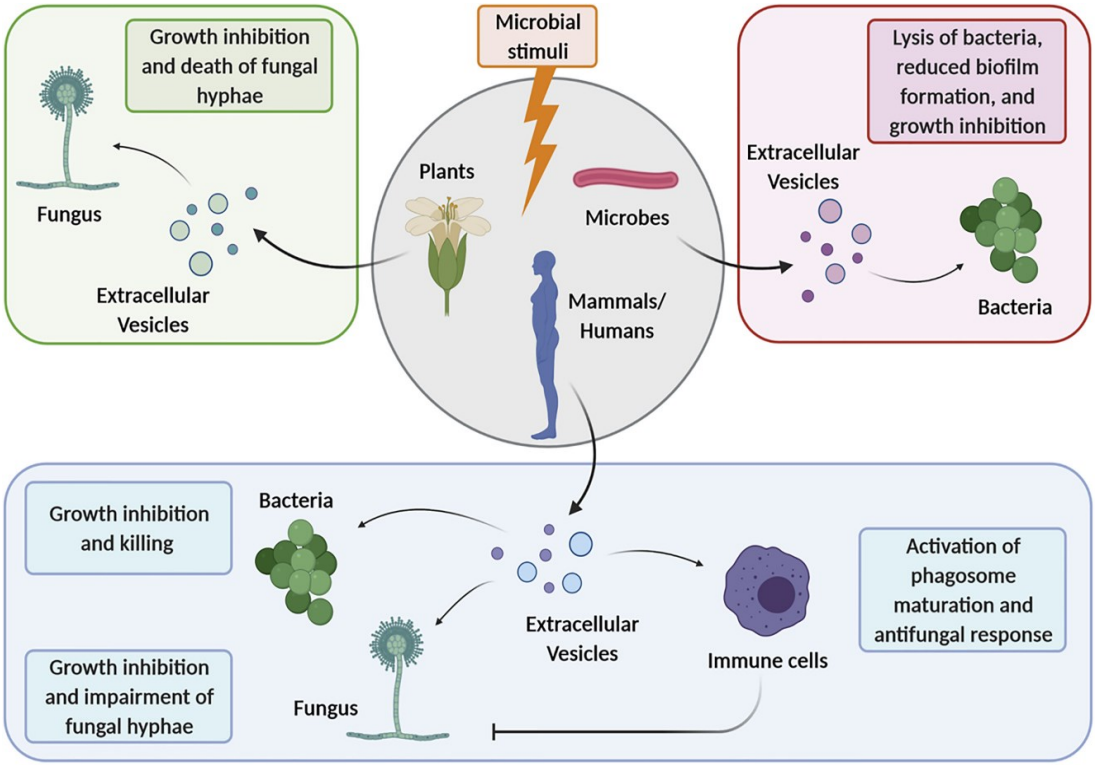

Figure 2. Antimicrobial functions of extracellular vesicles. Extracellular vesicles with antimicrobial cargo are routinely produced as a response to microbial competitors or in response to infection of a host. Extracellular vesicles produced by plants influence the outcome of infection by fungi and oomycetes. Humans use a similar strategy to control fungal and bacterial infections. Finally, microbes often produce extracellular vesicles to modulate neighbors and gain an advantage over competitors. Created with BioRender.com.

as antimicrobial extracellular vesicles in response to infection (An, van Bel and Huckelhoven 2007; Samuel *et al.* 2015). Another clue came from the first experimental isolation of the extracellular vesicles derived from *Arabidopsis thaliana* apoplastic fluid (Rutter and Innes 2017). These extracellular vesicles were enriched for proteins involved in host defense and stress adaptation, including proteins important for reactive oxygen species signaling and bioactive metabolite transport, again suggesting a role in plant immunity. Consistent with the suspected role in host defense, the syntaxin, PENETRATION-1 (PEN1)-specific extracellular vesicle fraction was shown to increase in abundance in response to the bacterial plant pathogen, *Pseudomonas syringae*. Surprisingly, the composition of the extracellular vesicles did not change after infection, suggesting that some organisms may constitutively produce antimicrobial extracellular vesicles to ward off potential pathogens.

The antimicrobial nature of plant-derived extracellular vesicles was demonstrated soon thereafter, when extracellular vesicles again derived from seedlings of the sunflower, *H. annuus*, were demonstrated to be antifungal against the phytopathogenic fungus, *Sclerotinia sclerotiorum* (Regente *et al.* 2017). In this case, extracellular vesicles released during infection were enriched in defense proteins and cell wall remodeling enzymes. Upon confrontation, host-derived extracellular vesicles were taken up by *S. sclerotiorum* spores and hyphae, which resulted in growth inhibition and potentially death of hyphae as observed by incorporation of the cell impermeable dyes propidium iodide and Evans blue. In this case, the exact source of the antifungal activity remains to be uncovered.

Perhaps the most compelling examples of antimicrobial extracellular vesicles come from studies of bidirectional cross-kingdom RNA interference. In this phenomenon, small RNAs produced by both the host and the pathogen are thought to be transferred to the opposing organism to modulate the outcome of infection. Most small RNAs are produced by cleavage of a double-stranded RNA precursor by a dicer or a dicer-like protein before loading into an argonaute protein for gene silencing (Wilson and Doudna 2013). The small RNA/argonaute complex is the core component of the RNA induced silencing complex that recognizes target genes based on sequence complementarity between the small RNA and target to drive mRNA degradation or translational repression. Cross-kingdom RNA interference takes advantage of the conserved nature of the RNA interference machinery across eukaryotes to facilitate silencing between organisms after transfer of small RNAs.

An early example of cross-kingdom RNA interference came from the study of the grey mold, *Botrytis cinerea*, which is capable of infecting a wide array of plant species. The small RNAs of *B. cinerea* were identified during infection of two plant hosts, *A. thaliana* and *Solanum lycopersicum*, where they were shown to be transferred from the fungus to the host to silence plant immunity genes (Weiberg *et al.* 2013). Deletion of either the fungal dicer-like proteins or the *A. thaliana* argonaute proteins resulted in diminished virulence, suggesting that the small RNAs were

Downloaded from https://academic.oup.com/microlife/article/doi/10.1093/femsml/uqab003/6228840 by guest on 25 May 2021

produced in the fungus, but capable of trafficking to and hijacking the plant RNA interference machinery for virulence. Follow-up work indicated that the host plant also uses a similar approach to fight back against fungal infection. It was demonstrated that tetraspanin 8 (TET8) and 9 (TET9)-positive exosome-like extracellular vesicles were used by the plant as a vehicle for delivery of plant-derived effector small RNAs into the fungus (Cai *et al.* 2018). These endogenous small RNAs produced by *A. thaliana* are transferred to *B. cinerea* to target the mRNAs of conserved vesicle pathways important to virulence, thus limiting the virulence potential of the organism upon knockdown (Cai *et al.* 2018). Although there has been some discussion over the exact subsets of extracellular vesicles, or possibly even ribonucleoprotein particles, that are responsible for small RNA transfer (Rutter and Innes 2020), a recent publication provided support for small RNAs at least being contained within the TET8-positive extracellular vesicle fraction (He *et al.* 2021).

In the study from He *et al.* (2021), proteomic analysis revealed that the TET8-positive extracellular vesicle subset was enriched for diverse RNA binding proteins, including the argonaute protein AGO1, the DEAD-box RNA helicases RH11 and RH37, as well as the annexins ANN1 and ANN2. Within the cell these RNA-binding proteins colocalized with multivesicular bodies, likely to facilitate their loading into the plant exosome-like extracellular vesicles. Investigation of the RNA binding capacity uncovered the selective binding of AGO1, RH11, and RH37 to small RNAs previously found to be enriched in TET8-positive extracellular vesicles, indicating their involvement in the specific sorting of RNA molecules into plant extracellular vesicles. The abundant annexin proteins on the other hand were hypothesized to play a role in the stabilization of RNA within the extracellular vesicle compartment. Particularly compelling were the findings that plants lacking these RNA binding proteins displayed lower levels of small RNAs loaded into their extracellular vesicles and a higher susceptibility to *B. cinerea* infection. Several other examples also support the use of small RNAs by plants to target fungal pathogens. In particular, cotton plants were shown to export microRNAs to inhibit the virulence of *Verticillium dahliae* (Zhang *et al.* 2016), and wheat plants to suppress the invasion of *Fusarium graminearum* again using microRNAs (Jiao and Peng 2018). It remains unknown if extracellular vesicles are the true transporters of small RNAs in all cases, but it seems clear that small RNAs play a role in equipping extracellular vesicles with an antimicrobial capacity in some instances.

In response to infection by the evolutionarily distinct oomycetes, plants again seem to rely on small RNAs in extracellular vesicles to target pathogen virulence genes. For example, study of the oomycete, *Phytophthora capsici* has revealed that *A. thaliana* responds to infection with production of extracellular vesicles capable of delivering small interfering RNAs to potentially silence pathogen genes (Hou *et al.* 2019). *P. capsici* suppressed this host-induced gene-silencing reaction using the effector molecule PSR2, which blocks biogenesis of secondary small interfering RNAs. The strategy of delivering antimicrobial RNAs seems to be conserved against different oomycetes, as *Hyaloperonospora arabidopsidis* infection is also inhibited by *A. thaliana* using small RNAs (Bilir *et al.* 2019), in an interaction that provides another example of bidirectional cross-kingdom RNA interference (Dunker *et al.* 2020). Not surprisingly, and despite these clear examples of plant-derived antifungal extracellular vesicles, there are also cases of host-pathogenesis where extracellular vesicles do not seem to play an obvious role, as shown during the interaction of wheat plants and the *Zymoseptoria tritici* fungus (Ma, Wiedmer and Palma-Guerrero 2019). In the future, additional work will be required to better define the subsets of extracellular vesicles involved in the transfer of small RNAs into invading pathogens. It seems likely that both extracellular vesicle-dependent and -independent mechanisms will be discovered to facilitate transfer.

MAMMALIAN HOSTS PRODUCE EXTRACELLULAR VESICLES AGAINST FUNGAL PATHOGENS

In contrast to the studies in plants, the role of mammalian host-derived extracellular vesicles in combating fungal infections remains relatively unexplored. However, recent studies have started to shed light on the host response to two important human fungal pathogens, *Aspergillus fumigatus* and *Candida albicans*. In the first case, neutrophils were recently shown to produce antifungal extracellular vesicles in response to *A. fumigatus* infection *ex vivo* (Shopova *et al.* 2020). These extracellular vesicles limited the growth of fungal conidia when applied *in vitro* and were also able to bind, enter and seemingly kill fungal hyphae. LC-MS/MS proteomics analysis of these antifungal extracellular vesicles revealed an abundance of antifungal cargo proteins like cathepsin G and azurocidin. Surprisingly, a mutant strain of *A. fumigatus* lacking dihydroxynaphthalene-melanin, an important polymer and virulence factor in the spore cell wall, induced production of some extracellular vesicle subsets and a similar protein cargo, but these vesicles were no longer antifungal, again suggesting some level of host specificity against particular fungal pathogens. More work is required to fully understand the breadth of this specificity in the control of fungal pathogens. Finally, it was shown that inducible, heterologous overexpression of the human extracellular vesicle proteins cathepsin G or azurocidin by the fungus was toxic upon induction. Albeit artificial, this finding provided a proof-of-principle that the presence of antifungal peptides inside of a fungus, as would be delivered by an extracellular vesicle, could prove toxic in sufficient concentrations. These results also suggest that different cargo molecules might be responsible for the antimicrobial action of extracellular vesicles depending on the subset and doses delivered. In agreement, it was recently shown that opsonized fungal zymosan particles induced neutrophils to produce pro-inflammatory extracellular vesicles, whereas resting and apoptotic neutrophils produced anti-inflammatory and coagulation-promoting extracellular vesicles, respectively (Kolonics *et al.* 2020a).

In response to *C. albicans* infection, extracellular vesicles from primary monocytes appear to serve yet another function. It was recently shown that soluble β-glucan released from *C. albicans* binds to Complement Receptor 3 to induce the release of TGF-β1-transporting vesicles that are anti-inflammatory in nature (Halder *et al.* 2020). Rather than serving an antimicrobial function as in *S. aureus* or *A. fumigatus* infection, these extracellular vesicles seem to facilitate niche establishment for *C. albicans*; a difference that might reflect the frequent role of *C. albicans* as a human commensal.

MICROBES PRODUCE EXTRACELLULAR VESICLES AGAINST OTHER MICROBES

The antimicrobial features of some extracellular vesicles are not only found in eukaryotes. In fact, many examples of antimicrobial extracellular vesicles come from studies of microbe–microbe communication. Outer membrane vesicles, a particularly well-studied class of extracellular vesicles derived from

Downloaded from https://academic.oup.com/microlife/article/doi/10.1093/femsml/uqab003/6228840 by guest on 25 May 2021

Gram-negative bacteria have been well-studied in this regard (Olsen and Amano 2015; Lynch and Alegado 2017). As early as the late 1990s, naturally produced outer membrane vesicles of Gram-negative bacteria were shown to have an antibacterial activity due in large part to hydrolytic enzyme cargo (Kadurugamuwa and Beveridge 1996; Li, Clarke and Beveridge 1998). In particular, it was shown that *Pseudomonas aeruginosa*, an opportunistic lung pathogen, can release extracellular vesicles containing autolysin (Kadurugamuwa and Beveridge 1996). This 26 kDa protein can lyse a wide range of Gram-negative bacteria and, surprisingly, also some Gram-positive bacteria, including the genus of *Mycobacterium* (MacDonald and Beveridge 2002). Interestingly, when *P. aeruginosa* was treated with an antimicrobial agent such as gentamicin, a small amount of the molecule was encapsulated in extracellular vesicles, which further enhanced the growth inhibition of bacteria. Later on, it was made clear that the antibacterial activity of these extracellular vesicles was specific, relying on the peptidoglycan content in the outer membrane and the absence of O-acetylation (Kadurugamuwa and Beveridge 1996; Li, Clarke and Beveridge 1998; Moynihan and Clarke 2011).

The ability of extracellular vesicles to encapsulate antimicrobial agents opened a wide range of possible applications, one of which was to facilitate bacterial biofilm disassembly. In agreement, it was shown that outer membrane vesicles play a fundamental role in the biofilm formation of some bacteria, like *P. aeruginosa* and *Helicobacter pylori* (Yonezawa *et al.* 2011; Murphy *et al.* 2014), making the outer membrane vesicle machinery a potential target for future therapeutics. Studies based on *P. aeruginosa* hypothesized that outer membrane vesicles produced from one species in a biofilm may also be able to lyse neighboring bacteria, thus releasing nutrients for growth and DNA for the biofilm matrix (Beveridge *et al.* 1997). The experimental evidence for this hypothesis is still somewhat lacking, but the ability of outer membrane vesicles to influence neighboring bacteria has been strengthened over time. For example, bacterial-secreted vesicles can be deadly to other bacteria as shown by the study of the Gram-positive bacteria *Lactobacillus acidophilus*. Vesicles secreted from this bacterium contain and can deliver bacteriocin peptides to the opportunistic pathogen *Lactobacillus delbrueckii*. The final effect is to inhibit *L. delbrueckii* growth and compromise membrane integrity (Dean *et al.* 2020). A recent report extended the idea of biofilm dissolution further by showing that outer membrane vesicles from nonpathogenic *Burkholderia thailandensis* are loaded with antimicrobial and antibiofilm compounds such as 4-hydroxy-3-methyl-2-(2-nonenyl)-quinoline that can limit the growth and biofilm formation of drug-sensitive and drug-resistant bacteria like *S. aureus*, but have no effect on closely related *P. aeruginosa* (Wang *et al.* 2020). Many groups are now focused on trying to leverage outer membrane vesicles as bio delivery containers for small interfering RNA or antimicrobial molecules (Gujrati and Jon 2014; Gerritzen *et al.* 2017; Jan 2017). This approach may ultimately provide a strategy for promoting biofilm disassembly via targeting by specialized outer membrane vesicles; however, further research is still required to reach these goals.

In some cases, bacteria can also utilize outer membrane vesicles to kill and prey on other bacteria as a nutrition source. This is the case for the soil bacterium, *Myxococcus xanthus*, which relies on outer membrane vesicles to kill *E. coli* prey, again using hydrolytic enzymes, in addition to proteases, phosphatases and secondary metabolites (Evans *et al.* 2012). These outer membrane vesicles were shown to fuse with the outer membrane of Gram-negative bacteria, in a process that was further facilitated by the presence of glyceraldehyde-3-phosphatase dehydrogenase, an enzyme actively secreted by *M. xanthus*. The inherent antibacterial activity of Myxobacteria outer membrane vesicles makes them intriguing leads for the development of potential delivery systems for antibacterial therapeutics (Schulz *et al.* 2018). One of the major problems with the development of antimicrobials remains the inability to distinguish between pathogen and commensal. Properly targeted extracellular vesicles may eventually offer a strategy for targeting a particular antimicrobial cargo to a pathogen of interest in a sick patient.

There are a number of other intriguing examples of antimicrobials delivered by extracellular vesicles during bacterial communication. *Chromobacterium violaceum* delivers violacein, a hydrophobic antibiotic, to other microbes in membrane vesicles (Choi *et al.* 2020; Wettstadt 2020). Not only do the extracellular vesicles provide a transport mechanism, they also offer a clever solution to the problem of solubility of hydrophobic compounds like violacein, a bisindole with antibiotic capacity. Similarly, the linearmycin family of polyketides, with antifungal and antibacterial activity, are also known to be packaged in extracellular vesicles and released by bacteria of the genus *Streptomyces* (Stubbendieck and Straight 2015; Stubbendieck *et al.* 2018). The linearmycins were even found to be important for the biogenesis of the vesicle, and the disruption of linearmycin production led to the inhibition of vesicle biogenesis (Hoefler *et al.* 2017). There is great potential for the identification of new therapeutics for treatment of human disease from the antimicrobial extracellular vesicles produced by bacteria. Future studies into this realm will likely continue to reveal novel mechanisms important to extracellular biology as well as intriguing new options for the development of therapeutics.

CONCLUSIONS: THE FUTURE OF EXTRACELLULAR VESICLE-BASED THERAPEUTICS

The examples provided in this short review show a reality where extracellular vesicles are used throughout the kingdoms of life to manage interkingdom communication. Extracellular vesicles produced by plants are able to contribute to defense against highly destructive fungi, humans rely on extracellular vesicles to manage bacterial and fungal infections, and microbes even use extracellular vesicles to deter invading competitors. All of these examples point to the fantastic potential of extracellular vesicles as future therapeutic delivery systems for the treatment of human infectious diseases. In fact, these systems are already exploited for the protection of crops and in human medicine. For example, in host-induced gene silencing, the expression of small RNAs in plants that are capable of targeting common virulence gene-encoding mRNAs of pathogens resulted in extracellular vesicle-mediated silencing of pathogen genes (Cai *et al.* 2018). Recent work showing the importance of the TET8-positive extracellular fraction in small RNA delivery pushes us further towards a mechanistic understanding of this phenomenon (He *et al.* 2021). Another interesting case is the antifungal drug formulation, AmBisome (amphotericin B liposomal), which relies on lipid-enclosed Amphotericin B to maximize uptake and limit off target effects (Walker *et al.* 2018). Although AmBisome is not technically an extracellular vesicle in the classical sense, it is a strong proof-of-principle that approaches based on lipid-encapsulation of drugs offer a promising path forward. With the additional specificity granted by a better understanding of

Downloaded from https://academic.oup.com/microlife/article/doi/10.1093/femsml/uqab003/6228840 by guest on 25 May 2021

the surface receptors of extracellular vesicles, we will hopefully be able to directly target extracellular vesicles to pathogens of interest in the near future. Another approach in this vein will be to coat nanoparticles with extracellular vesicle membrane constituents, as has been used in the fight against *S. aureus* (Gao *et al.* 2019; Witwer and Wolfram 2021).

We are also learning a lot about the antimicrobial potential of extracellular vesicles through detailed analyses of the cargo of extracellular vesicles. Advanced proteomics and RNA sequencing technologies are now allowing for elucidation of components found at even fleeting amounts in these populations (Cheng and Schorey 2019; Shopova *et al.* 2020). As our understanding of the cargo within extracellular vesicles increases, so will our ability to leverage these cargos for therapeutic design. In many of the examples described throughout this review, the exact molecules resulting in the observed antimicrobial activity remain elusive, likely due to a combined action of many different factors. We like to think of extracellular vesicles as a toolbox, capable of using many different tools to address many different situations. For the development of therapeutics, we will likely have to increase the relative abundance of particular tools, cargo, in order to create a consistent treatment option against infectious diseases. We suspect that small RNAs might be the easiest species to manipulate for this purpose, as they can be easily and cheaply synthesized for therapeutic purposes (O'Brien *et al.* 2020).

Extracellular vesicles are not an easy class of particles with which to work. Their low abundance and small size make tracking their biogenesis and distribution difficult. This becomes increasingly complex in situations with more than one or two partners; for example, amongst the gut microbiota or during the coordinated immune response by multiple immune cell types. Understanding the complex interaction between pathogens and hosts in the context of the entire environment during infection will be a challenge for the future. As our ability to identify and track extracellular vesicles improves, so too will our understanding of the role of these small particles in transferring information between organisms. New systems will likely have to be established to better understand how host-derived extracellular vesicles produced in response to large consortia of microbes target specific pathogens to influence the outcome infection.

There are many other unanswered questions surrounding the antimicrobial function of extracellular vesicles. For example, in many cases we still do not know whether extracellular vesicle abundance, cargo, or surface receptor specificity play a pivotal role in function. Even, the delivery of specific cargo to extracellular vesicles remains a mystery in many cases. However, there is an emerging body of data that suggests the loading of extracellular vesicle cargo is a highly tailored process. For example, in the work described above, the Mac-1 receptor mediates the activation of a tailoring process in neutrophils that ultimately results in antibacterial extracellular vesicles being produced in response to *S. aureus* infection (Lorincz *et al.* 2020) and proteins like AGO1, RH11, and RH37 are important for antifungal RNA loading into TET8-positive extracellular vesicles in plants (He *et al.* 2021). We expect that examples of precision-loading will prove to be widespread throughout host pathogenesis.

We also find the hypothesis compelling that extracellular vesicles of hosts and pathogens are likely under strong evolutionary pressure to adapt to the near-constant evolutionary arms race of host-pathogenesis, as has been postulated previously (Correa *et al.* 2020). It remains to be seen whether pathogens influence or take advantage of the production of extracellular vesicles by the host or commensals to their benefit to promote pathogenesis. Ultimately, we believe that there is a wealth of information to gain from increased scrutiny of the role of extracellular vesicles during infection. The coming years will likely see a surge in the use of extracellular vesicles as both diagnostics for cancers, metabolic diseases, and infectious diseases, but also as starting points for the development of novel therapeutics.

ACKNOWLEDGMENTS

The work presented here was generously supported by the Deutsche Forschungsgemeinschaft (DFG)-funded Collaborative Research Center/Transregio FungiNet 124 'Pathogenic fungi and their human host: Networks of Interaction' (210879364, project A1) and by the Federal Ministry for Education and Research (BMBF: https://www.bmbf.de/), Germany, Project FKZ 01K12012 'RFIN—RNA-Biologie von Pilzinfektionen.' The funders had no role in the design of the study, data collection and analysis, the decision to publish, or the preparation of the manuscript.

Conflicts of Interest. None declared.

REFERENCES

Alvarez-Jimenez VD, Leyva-Paredes K, Garcia-Martinez M *et al.* Extracellular vesicles released from *Mycobacterium tuberculosis*-Infected neutrophils promote macrophage autophagy and decrease intracellular mycobacterial survival. *Front Immunol* 2018;**9**:272.

An Q, Huckelhoven R, Kogel KH *et al.* Multivesicular bodies participate in a cell wall-associated defence response in barley leaves attacked by the pathogenic powdery mildew fungus. *Cell Microbiol* 2006;**8**:1009–19.

An Q, van Bel AJ, Huckelhoven R. Do plant cells secrete exosomes derived from multivesicular bodies? *Plant Signal Behav* 2007;**2**:4–7.

Beveridge TJ, Makin SA, Kadurugamuwa JL *et al.* Interactions between biofilms and the environment. *FEMS Microbiol Rev* 1997;**20**:291–303.

Bielska E, Birch PRJ, Buck AH *et al.* Highlights of the mini-symposium on extracellular vesicles in inter-organismal communication, held in Munich, Germany, August 2018. *J Extracell Vesicles* 2019;**8**:1590116.

Bielska E, Sisquella MA, Aldeieg M *et al.* Pathogen-derived extracellular vesicles mediate virulence in the fatal human pathogen *Cryptococcus gattii*. *Nat Commun* 2018;**9**:1556.

Bilir O, Telli O, Norman C *et al.* Small RNA inhibits infection by downy mildew pathogen *Hyaloperonospora arabidopsidis*. *Mol Plant Pathol* 2019;**20**:1523–34.

Buck AH, Coakley G, Simbari F *et al.* Exosomes secreted by nematode parasites transfer small RNAs to mammalian cells and modulate innate immunity. *Nat Commun* 2014;**5**:5488.

Cai Q, Qiao L, Wang M *et al.* Plants send small RNAs in extracellular vesicles to fungal pathogen to silence virulence genes. *Science* 2018;**360**:1126–9.

Caruso S, Poon IKH. Apoptotic cell-derived extracellular vesicles: more than just debris. *Front Immunol* 2018;**9**:1486.

Cheng Y, Schorey JS. Extracellular vesicles deliver *Mycobacterium* RNA to promote host immunity and bacterial killing. *EMBO Rep* 2019;**20**. DOI: 10.15252/embr.201846613.

Choi SY, Lim S, Cho G *et al.* *Chromobacterium violaceum* delivers violacein, a hydrophobic antibiotic, to other microbes in membrane vesicles. *Environ Microbiol* 2020;**22**:705–13.

Downloaded from https://academic.oup.com/microlife/article/doi/10.1093/femsml/uqab003/6228840 by guest on 25 May 2021

Colombo M, Raposo G, Thery C. Biogenesis, secretion, and intercellular interactions of exosomes and other extracellular vesicles. *Annu Rev Cell Dev Biol* 2014;**30**:255–89.

Correa R, Caballero Z, De Leon LF *et al.* Extracellular vesicles could carry an evolutionary footprint in Interkingdom communication. *Front Cell Infect Microbiol* 2020;**10**:76.

Cui Y, Gao J, He Y *et al.* Plant extracellular vesicles. *Protoplasma* 2020;**257**:3–12.

Dean SN, Rimmer MA, Turner KB *et al.* *Lactobacillus acidophilus* membrane vesicles as a vehicle of bacteriocin delivery. *Front Microbiol* 2020;**11**:710.

Dunker F, Trutzenberg A, Rothenpieler JS *et al.* Oomycete small RNAs bind to the plant RNA-induced silencing complex for virulence. *Elife* 2020;**9**. DOI: 10.7554/eLife.56096.

Evans AGL, Davey HM, Cookson A *et al.* Predatory activity of *Myxococcus xanthus* outer-membrane vesicles and properties of their hydrolase cargo. *Microbiology* 2012;**158**:2742–52.

Gao F, Xu L, Yang B *et al.* Kill the real with the fake: eliminate intracellular *Staphylococcus aureus* using nanoparticle coated with its extracellular vesicle membrane as active-targeting drug carrier. *ACS Infect Dis* 2019;**5**:218–27.

Garcia-Martinez M, Vazquez-Flores L, Alvarez-Jimenez VD *et al.* Extracellular vesicles released by J774A.1 macrophages reduce the bacterial load in macrophages and in an experimental mouse model of tuberculosis. *Int J Nanomed* 2019;**14**:6707–19.

Genschmer KR, Russell DW, Lal C *et al.* Activated PMN exosomes: pathogenic entities causing matrix destruction and disease in the lung. *Cell* 2019;**176**:113–26 e115.

Gerritzen MJH, Martens DE, Wijffels RH *et al.* Bioengineering bacterial outer membrane vesicles as vaccine platform. *Biotechnol Adv* 2017;**35**:565–74.

Gonzalez-Cano P, Mondragon-Flores R, Sanchez-Torres LE *et al.* *Mycobacterium tuberculosis* H37Rv induces ectosome release in human polymorphonuclear neutrophils. *Tuberculosis* 2010;**90**:125–34.

Gujrati VB, Jon S. Bioengineered bacterial outer membrane vesicles: what is their potential in cancer therapy? *Nanomedicine* 2014;**9**:933–5.

Halder LD, Jo EAH, Hasan MZ *et al.* Immune modulation by complement receptor 3-dependent human monocyte TGF-beta1-transporting vesicles. *Nat Commun* 2020;**11**:2331.

Halperin W, Jensen WA. Ultrastructural changes during growth and embryogenesis in carrot cell cultures. *J Ultrastruct Res* 1967;**18**:428–43.

Haraszti RA, Didiot MC, Sapp E *et al.* High-resolution proteomic and lipidomic analysis of exosomes and microvesicles from different cell sources. *J Extracell Vesicles* 2016;**5**:32570.

Hargett LA, Bauer NN. On the origin of microparticles: from "platelet dust" to mediators of intercellular communication. *Pulm Circ* 2013;**3**:329–40.

He B, Cai Q, Qiao L *et al.* RNA-binding proteins contribute to small RNA loading in plant extracellular vesicles. *Nature Plants* 2021. DOI: 10.1038/s41477-021-00863-8.

Hess C, Sadallah S, Hefti A *et al.* Ectosomes released by human neutrophils are specialized functional units. *J Immunol* 1999;**163**:4564–73.

Hoefler BC, Stubbendieck RM, Josyula NK *et al.* A link between linearmycin biosynthesis and extracellular vesicle genesis connects specialized metabolism and bacterial membrane physiology. *Cell Chem Biol* 2017;**24**:1238–49 e1237.

Hou Y, Zhai Y, Feng L *et al.* A phytophthora effector suppresses Trans-Kingdom RNAi to promote disease susceptibility. *Cell Host Microbe* 2019;**25**:153–65 e155.

Jan AT. Outer Membrane Vesicles (OMVs) of Gram-negative bacteria: a perspective update. *Front Microbiol* 2017; **8**:1053.

Jeppesen DK, Fenix AM, Franklin JL *et al.* Reassessment of exosome composition. *Cell* 2019;**177**:428–45 e418.

Jiao J, Peng D. Wheat microRNA1023 suppresses invasion of *Fusarium graminearum* via targeting and silencing FGSG_03101. *J Plant Interact* 2018;**13**:514–21.

Joffe LS, Nimrichter L, Rodrigues ML *et al.* Potential roles of fungal extracellular vesicles during infection. *mSphere* 2016;**1**. DOI: 10.1128/mSphere.00099-16.

Juan T, Furthauer M. Biogenesis and function of ESCRT-dependent extracellular vesicles. *Semin Cell Dev Biol* 2018;**74**:66–77.

Kadurugamuwa JL, Beveridge TJ. Bacteriolytic effect of membrane vesicles from *Pseudomonas aeruginosa* on other bacteria including pathogens: conceptually new antibiotics. *J Bacteriol* 1996;**178**:2767–74.

Khatua AK, Taylor HE, Hildreth JE *et al.* Exosomes packaging APOBEC3G confer human immunodeficiency virus resistance to recipient cells. *J Virol* 2009;**83**:512–21.

Kim JH, Lee J, Park J *et al.* Gram-negative and Gram-positive bacterial extracellular vesicles. *Semin Cell Dev Biol* 2015;**40**: 97–104.

Kolonics F, Kajdacsi E, Farkas VJ *et al.* Neutrophils produce proinflammatory or anti-inflammatory extracellular vesicles depending on the environmental conditions. *J Leukoc Biol* 2020a. DOI: 10.1002/JLB.3A0320-210R.

Kolonics F, Szeifert V, Timar CI *et al.* The functional heterogeneity of Neutrophil-Derived extracellular vesicles reflects the status of the parent cell. *Cells* 2020b;**9**. DOI: 10.3390/cells9122718.

Kuipers ME, Hokke CH, Smits HH *et al.* Pathogen-derived extracellular vesicle-associated molecules that affect the host immune system: an overview. *Front Microbiol* 2018; **9**:2182.

Latifkar A, Hur YH, Sanchez JC *et al.* New insights into extracellular vesicle biogenesis and function. *J Cell Sci* 2019;**132**:jcs222406.

Li SP, Lin ZX, Jiang XY *et al.* Exosomal cargo-loading and synthetic exosome-mimics as potential therapeutic tools. *Acta Pharmacol Sin* 2018;**39**:542–51.

Liu Y, Defourny KAY, Smid EJ *et al.* Gram-positive bacterial extracellular vesicles and their impact on health and disease. *Front Microbiol* 2018;**9**:1502.

Li Z, Clarke AJ, Beveridge TJ. Gram-negative bacteria produce membrane vesicles which are capable of killing other bacteria. *J Bacteriol* 1998;**180**:5478–83.

Lorincz AM, Bartos B, Szombath D *et al.* Role of Mac-1 integrin in generation of extracellular vesicles with antibacterial capacity from neutrophilic granulocytes. *J Extracell Vesicles* 2020;**9**:1698889.

Lorincz AM, Schutte M, Timar CI *et al.* Functionally and morphologically distinct populations of extracellular vesicles produced by human neutrophilic granulocytes. *J Leukoc Biol* 2015;**98**:583–9.

Lorincz AM, Szeifert V, Bartos B *et al.* Different calcium and Src family kinase signaling in Mac-1 dependent phagocytosis and extracellular vesicle generation. *Front Immunol* 2019;**10**:2942.

Lorincz AM, Timar CI, Marosvari KA *et al.* Effect of storage on physical and functional properties of extracellular vesicles derived from neutrophilic granulocytes. *J Extracell Vesicles* 2014;**3**:25465.

Downloaded from https://academic.oup.com/microlife/article/doi/10.1093/femsml/uqab003/6228840 by guest on 25 May 2021

Lynch JB, Alegado RA. Spheres of hope, packets of doom: the good and bad of outer membrane vesicles in interspecies and ecological dynamics. *J Bacteriol* 2017;**199**. DOI: 10.1128/JB.00012-17.

MacDonald IA, Kuehn MJ. Offense and defense: microbial membrane vesicles play both ways. *Res Microbiol* 2012;**163**:607–18.

MacDonald KL, Beveridge TJ. Bactericidal effect of gentamicin-induced membrane vesicles derived from *Pseudomonas aeruginosa* PAO1 on gram-positive bacteria. *Can J Microbiol* 2002;**48**:810–20.

Manning AJ, Kuehn MJ. Contribution of bacterial outer membrane vesicles to innate bacterial defense. *BMC Microbiol* 2011;**11**:258.

Ma X, Wiedmer J, Palma-Guerrero J. Small RNA bidirectional crosstalk during the interaction between wheat and *Zymoseptoria tritici*. *Front Plant Sci* 2019;**10**:1669.

McNamara RP, Dittmer DP. Extracellular vesicles in virus infection and pathogenesis. *Curr Opin Virol* 2020;**44**:129–38.

Moynihan PJ, Clarke AJ. O-Acetylated peptidoglycan: controlling the activity of bacterial autolysins and lytic enzymes of innate immune systems. *Int J Biochem Cell Biol* 2011;**43**:1655–9.

Munhoz da Rocha IF, Amatuzzi RF, Lucena ACR *et al.* Cross-kingdom extracellular vesicles EV-RNA communication as a mechanism for host-pathogen interaction. *Front Cell Infect Microbiol* 2020;**10**:593160.

Murphy K, Park AJ, Hao Y *et al.* Influence of O polysaccharides on biofilm development and outer membrane vesicle biogenesis in *Pseudomonas aeruginosa* PAO1. *J Bacteriol* 2014;**196**: 1306–17.

O'Brien K, Breyne K, Ughetto S *et al.* RNA delivery by extracellular vesicles in mammalian cells and its applications. *Nat Rev Mol Cell Biol* 2020;**21**:585–606.

Obregon C, Rothen-Rutishauser B, Gerber P *et al.* Active uptake of dendritic cell-derived exovesicles by epithelial cells induces the release of inflammatory mediators through a TNF-alpha-mediated pathway. *Am J Pathol* 2009;**175**:696–705.

Ofir-Birin Y, Heidenreich M, Regev-Rudzki N. Pathogen-derived extracellular vesicles coordinate social behaviour and host manipulation. *Semin Cell Dev Biol* 2017;**67**:83–90.

Ofir-Birin Y, Regev-Rudzki N. Extracellular vesicles in parasite survival. *Science* 2019;**363**:817–8.

Olsen I, Amano A. Outer membrane vesicles - offensive weapons or good Samaritans? *J Oral Microbiol* 2015;**7**:27468.

Radomski N, Karger A, Franzke K *et al.* *Chlamydia psittaci*-Infected dendritic cells communicate with NK cells via exosomes to activate antibacterial immunity. *Infect Immun* 2019;**88**. DOI: 10.1128/IAI.00541-19.

Regente M, Corti-Monzon G, Maldonado AM *et al.* Vesicular fractions of sunflower apoplastic fluids are associated with potential exosome marker proteins. *FEBS Lett* 2009;**583**: 3363–6.

Regente M, Pinedo M, San Clemente H *et al.* Plant extracellular vesicles are incorporated by a fungal pathogen and inhibit its growth. *J Exp Bot* 2017;**68**:5485–95.

Reyes-Robles T, Dillard RS, Cairns LS *et al.* *Vibrio cholerae* outer membrane vesicles inhibit bacteriophage infection. *J Bacteriol* 2018;**200**. DOI: 10.1128/JB.00792-17.

Roier S, Zingl FG, Cakar F *et al.* A novel mechanism for the biogenesis of outer membrane vesicles in Gram-negative bacteria. *Nat Commun* 2016;**7**:10515.

Russell AE, Sneider A, Witwer KW *et al.* Biological membranes in EV biogenesis, stability, uptake, and cargo transfer: an ISEV position paper arising from the ISEV membranes and EVs workshop. *J Extracell Vesic* 2019;**8**:1684862.

Rutter BD, Innes RW. Extracellular vesicles isolated from the leaf apoplast carry stress-response proteins. *Plant Physiol* 2017;**173**:728–41.

Rutter BD, Innes RW. Growing pains: addressing the pitfalls of plant extracellular vesicle research. *New Phytol* 2020;**228**:1505–10.

Rybak K, Robatzek S. Functions of extracellular vesicles in immunity and virulence. *Plant Physiol* 2019;**179**:1236–47.

Samuel M, Bleackley M, Anderson M *et al.* Extracellular vesicles including exosomes in cross kingdom regulation: a viewpoint from plant-fungal interactions. *Front Plant Sci* 2015;**6**:766.

Schulz E, Goes A, Garcia R *et al.* Biocompatible bacteria-derived vesicles show inherent antimicrobial activity. *J Control Rel* 2018;**290**:46–55.

Shopova IA, Belyaev I, Dasari P *et al.* Human neutrophils produce antifungal extracellular vesicles against *Aspergillus fumigatus*. *mBio* 2020;**11**. DOI: 10.1128/mBio.00596-20.

Stubbendieck RM, Brock DJ, Pellois JP *et al.* Linearmycins are lytic membrane-targeting antibiotics. *J Antibiot (Tokyo)* 2018;**71**:372–81.

Stubbendieck RM, Straight PD. Escape from lethal bacterial competition through coupled activation of antibiotic resistance and a mobilized subpopulation. *PLos Genet* 2015;**11**:e1005722.

Thery C, Witwer KW, Aikawa E *et al.* Minimal information for studies of extracellular vesicles 2018 (MISEV2018): a position statement of the International Society for Extracellular Vesicles and update of the MISEV2014 guidelines. *J Extracell Vesicles* 2018;**7**:1535750.

Timar CI, Lorincz AM, Csepanyi-Komi R *et al.* Antibacterial effect of microvesicles released from human neutrophilic granulocytes. *Blood* 2013;**121**:510–8.

Toyofuku M, Nomura N, Eberl L. Types and origins of bacterial membrane vesicles. *Nat Rev Microbiol* 2019;**17**:13–24.

Tricarico C, Clancy J, D'Souza-Schorey C. Biology and biogenesis of shed microvesicles. *Small GTPases* 2017;**8**:220–32.

van Niel G, D'Angelo G, Raposo G. Shedding light on the cell biology of extracellular vesicles. *Nat Rev Mol Cell Biol* 2018;**19**: 213–28.

Walker L, Sood P, Lenardon MD *et al.* The viscoelastic properties of the fungal cell wall allow traffic of AmBisome as intact liposome vesicles. *mBio* 2018;**9**. DOI: 10.1128/mBio.02383-17.

Wang Y, Hoffmann JP, Chou CW *et al.* *Burkholderia thailandensis* outer membrane vesicles exert antimicrobial activity against drug-resistant and competitor microbial species. *J Microbiol* 2020;**58**:550–62.

Weiberg A, Wang M, Lin FM *et al.* Fungal small RNAs suppress plant immunity by hijacking host RNA interference pathways. *Science* 2013;**342**:118–23.

Wettstadt S. Death in a sphere: *C hromobacterium violaceum* secretes outer membrane vesicles filled with antibiotics. *Environ Microbiol Rep* 2020;**12**:255–7.

Wilson RC, Doudna JA. Molecular mechanisms of RNA interference. *Annu Rev Biophys* 2013;**42**:217–39.

Witwer KW, Wolfram J. Extracellular vesicles versus synthetic nanoparticles for drug delivery. *Nat Rev Mater* 2021;**6**:103–6.

Wolf P. The nature and significance of platelet products in human plasma. *Br J Haematol* 1967;**13**:269–88.

Yonezawa H, Osaki T, Woo T *et al.* Analysis of outer membrane vesicle protein involved in biofilm formation of *Helicobacter pylori*. *Anaerobe* 2011;**17**:388–90.

Zhang T, Zhao YL, Zhao JH *et al.* Cotton plants export microRNAs to inhibit virulence gene expression in a fungal pathogen. *Nat Plants* 2016;**2**:16153.

Downloaded from https://academic.oup.com/microlife/article/doi/10.1093/femsml/uqab003/6228840 by guest on 25 May 2021

3. Manuscripts

3.3 Manuscript C

PLB-985 Neutrophil-Like cells as a model to study *Aspergillus fumigatus* pathogenesis

Rafiq M*, **Rivieccio F***, Zimmermann A-K*, Visser C, Bruch A, Krüger T, González Rojas K, Kniemeyer O, Blango MG, Brakhage A.A.
*These authors contributed equally

Manuscript published on *mSphere* journal. 7(1):e0094021. January 2022.

Summary:
Polymorphonuclear leukocytes are important immune cells against the pathogenic fungus *A. fumigatus*. However, the only way to investigate their response to the fungus, is to isolate them freshly from healthy donors. This can be challenging due to the limited amount of blood, restricted number of donors and above all to the short half-life of these cells after isolation. In this work a neutrophil cells line model in the context of *A. fumigatus* infection was established. To this aim different aspects of the neutrophil's interplay with conidia and hyphae, in differentiated PLB-985 cells, were investigated. This analysis revealed that differentiated PLB-985 cells are a valid model for substitution of primary cells to study *A. fumigatus* pathogenesis.

Contribution to the manuscript:
Flora Rivieccio analyzed phagocytosis and cytokines production from PLB-985 cells and primary neutrophils. She also contributed to writing and editing figures and text of the manuscript.

Estimated contribution in percentage:

Author	Conceptual	Data analysis	Experimental	Writing the manuscript	Provision of material
Rafiq M*	15%	20%	20%	15%	0%
Rivieccio F.*	**15%**	**20%**	**20%**	**15%**	**0%**
Zimmermann A-K*	15%	20%	20%	15%	0%
Visser C.	10%	10%	15%	5%	0%
González Rojas K	5%	8%	10%	5%	0%
Blango MG.	15%	7%	5%	20%	0%
Brakhage A.A	25%	10%	0%	20%	100%
Others	0%	5%	10%	5%	0%
Total:	100%	100%	100%	100%	100%

AMERICAN SOCIETY FOR MICROBIOLOGY | mSphere®

RESEARCH ARTICLE

PLB-985 Neutrophil-Like Cells as a Model To Study *Aspergillus fumigatus* Pathogenesis

Muhammad Rafiq,[a,b] Flora Rivieccio,[a,b] Ann-Kathrin Zimmermann,[a,b] Corissa Visser,[a,b] Alexander Bruch,[c] Thomas Krüger,[a] Katherine González Rojas,[a,b] Olaf Kniemeyer,[a,b] Matthew G. Blango,[c] Axel A. Brakhage[a,b]

[a]Department of Molecular and Applied Microbiology, Leibniz Institute for Natural Product Research and Infection Biology - Hans Knöll Institute (Leibniz-HKI), Jena, Germany

[b]Department of Microbiology and Molecular Biology, Institute of Microbiology, Friedrich Schiller University, Jena, Germany

[c]Junior Research Group RNA Biology of Fungal Infections, Leibniz Institute for Natural Product Research and Infection Biology - Hans Knöll Institute (Leibniz-HKI), Jena, Germany

Muhammad Rafiq, Flora Rivieccio, and Ann-Kathrin Zimmermann contributed equally to the manuscript and are listed alphabetically.

ABSTRACT Fungal infections remain a major global concern. Emerging fungal pathogens and increasing rates of resistance mean that additional research efforts and resources must be allocated to advancing our understanding of fungal pathogenesis and developing new therapeutic interventions. Neutrophilic granulocytes are a major cell type involved in protection against the important fungal pathogen *Aspergillus fumigatus*, where they employ numerous defense mechanisms, including production of antimicrobial extracellular vesicles. A major drawback to work with neutrophils is the lack of a suitable cell line system for the study of fungal pathogenesis. To address this problem, we assessed the feasibility of using differentiated PLB-985 neutrophil-like cells as an *in vitro* model to study *A. fumigatus* infection. We find that dimethylformamide-differentiated PLB-985 cells provide a useful recapitulation of many aspects of *A. fumigatus* interactions with primary human polymorphonuclear leukocytes. We show that differentiated PLB-985 cells phagocytose fungal conidia and acidify conidia-containing phagolysosomes similar to primary neutrophils, release neutrophil extracellular traps, and also produce antifungal extracellular vesicles in response to infection. In addition, we provide an improved method for the isolation of extracellular vesicles produced during infection by employing a size exclusion chromatography-based approach. Advanced liquid chromatography-tandem mass spectrometry (LC-MS/MS) proteomics revealed an enrichment of extracellular vesicle marker proteins and a decrease of cytoplasmic proteins in extracellular vesicles isolated using this improved method. Ultimately, we find that differentiated PLB-985 cells can serve as a genetically tractable model to study many aspects of *A. fumigatus* pathogenesis.

IMPORTANCE Polymorphonuclear leukocytes are an important defense against human fungal pathogens, yet our model systems to study this group of cells remain very limited in scope. In this study, we established that differentiated PLB-985 cells can serve as a model to recapitulate several important aspects of human polymorphonuclear leukocyte interactions with the important human fungal pathogen *Aspergillus fumigatus*. The proposed addition of a cultured neutrophil-like cell line to the experimental toolbox to study fungal pathogenesis will allow for a more mechanistic description of neutrophil antifungal biology. In addition, the easier handling of the cell line compared to primary human neutrophils allowed us to use PLB-985 cells to provide an improved method for isolation of neutrophil-derived extracellular vesicles using size exclusion chromatography. Together, these results provide significant tools and a baseline knowledge for the future study of neutrophil-derived extracellular vesicles in the laboratory.

Editor Aaron P. Mitchell, University of Georgia

Copyright © 2022 Rafiq et al. This is an open-access article distributed under the terms of the Creative Commons Attribution 4.0 International license.

Address correspondence to Axel A. Brakhage, axel.brakhage@leibniz-hki.de.

The authors declare no conflict of interest.

Received 19 November 2021
Accepted 13 December 2021
Published 5 January 2022

KEYWORDS *Aspergillus fumigatus*, PLB-985, phagocytosis, fungal pathogens, extracellular vesicles, HL-60

Fungal infections remain a tremendous source of global morbidity and mortality. More than 1 billion individuals are affected per year, with invasive infections killing numbers comparable to other leading bacterial pathogens (>1.5 million per year [gaffi.org] [1]). Deadly invasive infections are caused by a relatively small number of fungi, with most of these attributed to members of the genera *Candida*, *Pneumocystis*, *Cryptococcus*, and *Aspergillus* (2). *Aspergillus fumigatus* is the major cause of aspergillosis and is particularly dangerous to immunocompromised individuals suffering from neutropenia (3). There is also emerging evidence to suggest that invasive aspergillosis may contribute to coronavirus disease 2019 (COVID-19)-related deaths (4, 5), but challenges in safely obtaining bronchoalveolar lavage samples from these patients have often made confirmatory diagnosis difficult. Despite the obvious importance of *A. fumigatus* in the clinic, our understanding of this important pathogen remains lacking in many aspects, in part due to a lack of tractable experimental systems in the laboratory.

Mammals are continuously challenged by fungal pathogens. In fact, asexual spores of *A. fumigatus*, termed conidia, are thought to be inhaled by humans on a scale of hundreds per day (6). For most fungi, the body temperature of mammals is too high to allow for growth, but for organisms like *A. fumigatus* that thrive in compost piles at high temperatures, the human host provides fertile ground in the absence of a functional immune system (7). However, humans do have multiple additional defenses, including a mucociliary escalator to remove particles from the lungs, a robust epithelium, resident alveolar macrophages that eliminate the majority of the remaining fungal conidia, and infiltrating polymorphonuclear leukocytes (PMNs) that aid in clearance of conidia and destruction of fungal hyphae, among others (3, 8). Neutrophils play an essential role in antifungal defense, due to their importance in killing fungal hyphae. This is well illustrated by the high susceptibility of neutropenic patients to *A. fumigatus* infections in clinics (reviewed in references 3 and 9).

Studies of primary human neutrophils have revealed the capacity of these cells to phagocytose conidia and release granules, neutrophil extracellular traps (NETs), and extracellular vesicles in response to invading pathogens (10–12). Phagocytosis occurs in conjunction with recognition of pathogen-associated molecular patterns by host pathogen recognition receptors. Studies of zebrafish and mice have shown that these internalized conidia can even be passed from neutrophils to macrophages for destruction of the fungus (13), implying complex intracellular trafficking. In neutrophils and macrophages however, internalized wild-type *A. fumigatus* conidia are capable of stalling phagolysosomal acidification to facilitate outgrowth (14).

In addition to phagocytosis, NETs are an important mechanism of defense against *A. fumigatus* that are produced in response to fungal recognition in a CD11b-dependent manner (11, 15). NET production is most abundant against hyphae, but NETs are also sometimes produced in response to resting and swollen conidia (16). *In vivo*, NETs were shown to be present in mouse lungs during infection but were generally dispensable for fungal clearance (16, 17), suggesting that alternative measures are required to eliminate fungal hyphae that escaped phagocytosis as conidia.

Neutrophilic granules and extracellular vesicles are two heterogeneous subcellular populations that also contribute widely to the antimicrobial response. Proteins associated with granules like lactoferrin are known to inhibit *A. fumigatus* conidial germination due to iron sequestration (18), and the abundant granule protein myeloperoxidase inhibits fungal hyphal growth (19). Extracellular vesicles were also shown to provide an antifungal mechanism against *A. fumigatus* hyphae and conidia (10). Antifungal extracellular vesicles produced by neutrophils in response to infection are capable of associating with the fungal cell wall and are in some cases internalized to deliver an unknown antifungal cargo. Intriguingly, the antifungal effect of these extracellular vesicles appeared to be tailored to the infecting pathogen, as spontaneously released

vesicles and vesicles released in response to infection with a knockout strain deficient in production of the conidial pigment dihydroxynaphthalene (DHN)-melanin were not antifungal against wild-type fungus (10).

The molecular mechanisms behind these differences in antifungal potential are difficult to discern in the absence of a tractable model system for the genetic manipulation of neutrophils. Despite the importance of neutrophils in antifungal defense, the majority of studies are still performed in primary human PMNs isolated from venous blood, a resource that can be used only for small-scale studies and is unfortunately highly variable between blood donors. A laborious isolation procedure and limited half-life of about 19 h *ex vivo* (20) also make more mechanistic studies difficult. For these reasons, establishment of a cell culture line to study *A. fumigatus* pathogenesis in neutrophils or neutrophil-like cells would be highly advantageous. In recent years, some options to investigate specific aspects of neutrophil biology in culture have emerged (21). In particular, the myeloid cell line PLB-985, a derivative of HL-60 granulocytic cells, seems a tractable model to study NET formation in response to bacterial infection after differentiation into neutrophil-like cells (22, 23). Of note, the related HL-60 cell line has also been used to deliver azole drugs to *A. fumigatus*-infected mice (24), but not to our knowledge in studies of *A. fumigatus* pathogenesis.

Here, we hypothesized that differentiated human PLB-985 neutrophil-like cells could serve as a model system to study the host pathogenesis of *A. fumigatus* in a blood donor-independent manner. We tested this hypothesis by defining the phagocytosis and intracellular trafficking of *A. fumigatus* conidia by PLB-985 cells, the production of neutrophil extracellular traps, and the release of extracellular vesicles produced in response to fungal infection. We find numerous similarities between this cell line and primary neutrophils that suggest differentiated PLB-985 cells can serve as a tractable *in vitro* model system for further study of some aspects of *A. fumigatus* pathogenesis.

RESULTS

Differentiated PLB-985 neutrophil-like cells phagocytose opsonized *A. fumigatus* conidia. We set out to assess the feasibility of using *N*,*N*-dimethylformamide (DMF)-differentiated PLB-985 (dPLB) cells as a model for neutrophil phagocytosis, NET production, and extracellular vesicle release in response to *A. fumigatus* infection. Upon infection, neutrophils are known to rapidly phagocytose and process *A. fumigatus* conidia. We therefore challenged dPLB cells with opsonized *A. fumigatus* resting conidia and assessed various parameters of infection.

First, we determined the phagocytic capacity of PLB-985 cells using confocal laser scanning microscopy following incubation of cells with fluorescein isothiocyanate (FITC)-labeled, opsonized conidia (green). We observed that dPLBs were capable of phagocytosis, as evidenced by a phagosomal membrane surrounding the conidia (Fig. 1A). A similar result was confirmed for primary human PMNs with this experimental setup (see Fig. S1A in the supplemental material). The dPLB cells only infrequently phagocytosed unopsonized conidia, highlighting the importance of opsonization and consistent with previous findings in primary human neutrophils (25). To better quantify phagocytosis, we analyzed 5,000 host cells postinfection with opsonized conidia by single-cell analysis using imaging flow cytometry. To do this, we counterstained with calcofluor white (CFW; blue) to elucidate nonphagocytosed conidia (Fig. 1B and Fig. S1B and S1C). Quantification revealed that approximately 22% of wild-type and 26% of nonpigmented Δ*pksP* conidia were phagocytosed by dPLBs after 2 h, while undifferentiated PLB-985 cells exhibited limited phagocytosis of both wild-type and nonpigmented conidia (Fig. 1C). As expected, these phagocytosis percentages were lower than those of primary human PMNs, which aggressively phagocytosed conidia (Fig. S1D). To determine whether infection also resulted in an activated immune response, we measured proinflammatory cytokine levels by an enzyme-linked immunosorbent assay (ELISA). Coincubation of dPLB cells with wild-type spores resulted in production of significantly increased levels of interleukin 8 (IL-8), but not IL-1β after 24 h of coincubation, comparable to time points with primary human PMNs (Fig. 1D and Fig. S2). Together, these

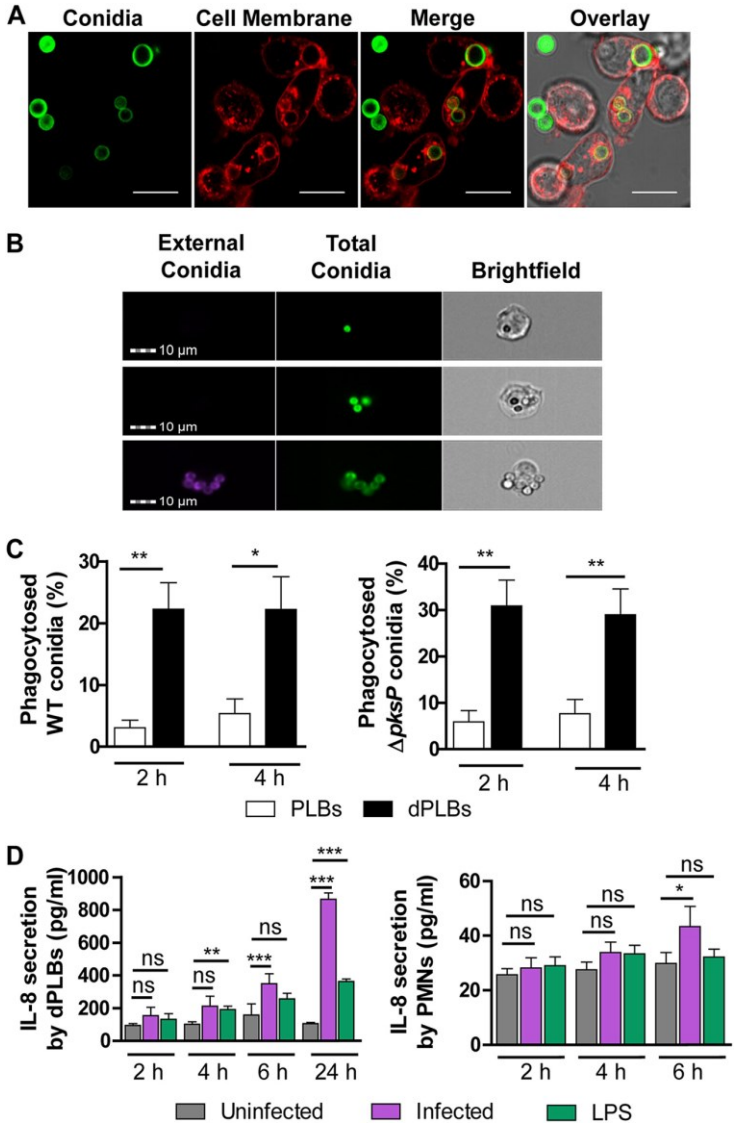

FIG 1 Phagocytosis of *A. fumigatus* conidia by PLB-985 cells. (A) Confocal microscopy images of wild-type conidia (FITC stained; green) phagocytosed by dPLB cells after 4 h coincubation. Membranes were stained with Cell Mask (red). Images are representative of three independent biological experiments. Bars, 10 μm. (B) Representative images of wild-type FITC-stained conidia phagocytosed by dPLB cells after 4 h coinfection obtained by imaging flow cytometry (top two rows). External conidia are visualized by counterstaining with CFW (purple), as seen in the bottom row. Images are representative of three independent experiments. (C) Quantification of PLB-985 cell phagocytosis using the IDEAS software on 5,000 cells per condition with either wild-type (WT) or Δ*pksP* conidia. Values are means plus standard errors of the means (SEM) (error bars) of four independent experiments. (D) ELISA detection of IL-8 cytokine released from infected dPLBs and primary human PMNs at different time points. Lipopolysaccharide (LPS) was included for comparison of a bacterial stimulus. Data are presented as means ± SEM from six biological replicates. Statistical significance is indicated as follows: *, $P \leq 0.05$; **, $P \leq 0.01$, ***, $P \leq 0.001$; ns, not significant.

results suggested that DMF-differentiated PLB-985 cells could serve as a suitable model for *A. fumigatus* pathogenesis and warranted further investigation.

Internalized *A. fumigatus* conidia are processed inside dPLB phagolysosomes. Following internalization of conidia by professional phagocytes like macrophages and

neutrophils, conidia-containing phagosomes fuse with lysosomes to acidify the compartment and aid in fungal killing. Numerous additional enzymes are activated upon phagolysosomal acidification to degrade and digest the internalized fungal conidia. The acidification and maturation of phagolysosomes are regulated by protein complexes assembled on the phagolysosomal membrane, including lysosome-associated membrane protein 1 (LAMP-1), 2, and 3; several vacuolar ATPases (V-ATPases); Ras-related protein 5 (RAB5) and 7; flotillin 1 and 2; and numerous others (26). DHN-melanin on the surface of conidia can interfere with these processes in alveolar macrophages, monocytes, and primary neutrophils to delay fungal processing and phagolysosomal acidification (14). To test whether dPLB cells process conidia similarly to primary human PMNs, we first stained the cells with LAMP-1, a general endocytic marker on the membranes of phagolysosomes. LAMP-1 showed a clear signal around phagolysosomes of infected cells (Fig. 2A), and the intensity of the signal did not differ between wild-type and Δ*pksP* conidia (Fig. 2B). Furthermore, loading of dPLB cells with Lysotracker, a weak base that becomes fluorescent under acidic conditions, showed that the Δ*pksP* conidia-containing phagosomes were significantly more acidified than those containing wild-type conidia, revealing that DHN-melanin can also block the acidification process in the dPLB model as well (Fig. 2C to D).

The interference of the acidification pathway in alveolar macrophages by fungal DHN-melanin occurs through the inhibition of V-ATPase assembly (27, 28). This multiprotein complex plays a major role in lowering the pH from 6 to <4.5 by pumping H^+ ions across the phagolysosomal membrane. Staining of the V-ATPase V1 subunit in dPLB cells revealed that the percentage of recruitment to conidia-containing phagolysosomes was fairly similar for wild-type and Δ*pksP* conidia (Fig. S3A and S3B), suggesting that other proton pumps may contribute to acidification of these phagolysosomes in neutrophil-like cells. An additional defense mechanism for intraphagosomal degradation of pathogens occurs via reactive oxygen species (ROS) production. As expected, we observed dPLB cells to be capable of producing ROS after staining with CellROX Orange (Fig. S3C), consistent with the literature (29, 30).

***A. fumigatus* triggers formation of NETs from dPLB cells.** One defense mechanism employed by neutrophilic granulocytes to fight against pathogens is the formation of NETs. These structures consist of condensed chromatin and various enzymes that are released into the extracellular space and typically correlate with death of the cell (31). NETs contain several antifungal proteins, which are responsible for the fungistatic effect against *A. fumigatus* hyphae (16). To test whether dPLBs are also able to form NETs in response to *A. fumigatus* and serve as a model for this pathway, we coincubated dPLB cells with hyphae and stained for nucleic acid with 4′,6-diamidino-2-phenylindole (DAPI) (Fig. 3A). For a positive control, we induced NET formation using phorbol myristate acetate, a known trigger of NET formation in PLB-985 cells (Fig. 3B) (22, 32). We observed the presence of histone H3 embedded in the DNA fibers and an association of NETs with fungal hyphae (Fig. 3B). Taken together, these results showed that *A. fumigatus* is able to trigger NET formation in dPLB cells and that these NETs are specifically directed against the hyphae.

dPLB cells produce extracellular vesicles in response to infection. Recently, a new defense mechanism from neutrophilic granulocytes was discovered, the production of antimicrobial extracellular vesicles (33, 34). These small lipid-enclosed nanoparticles are released from primary PMNs after contact with microorganisms and, in the case of *A. fumigatus* conidia, can inhibit fungal growth after coincubation (10). This effect is likely due in part to their protein cargo, which consists of antimicrobial peptides such as myeloperoxidase, azurocidin, and cathepsin G. To assess whether dPLB cells can produce extracellular vesicles spontaneously or in response to *A. fumigatus*, we incubated cells with or without conidia for 2 and 4 h. Next, we isolated extracellular vesicles using two different methods; first using a previously described differential centrifugation-based approach (DC) (10) that enriches for medium-sized extracellular vesicles and a second approach that relies on size exclusion chromatography (SEC) to purify a more selective population of smaller extracellular vesicles. Using these methods, dPLB cells were observed to actively secrete extracellular

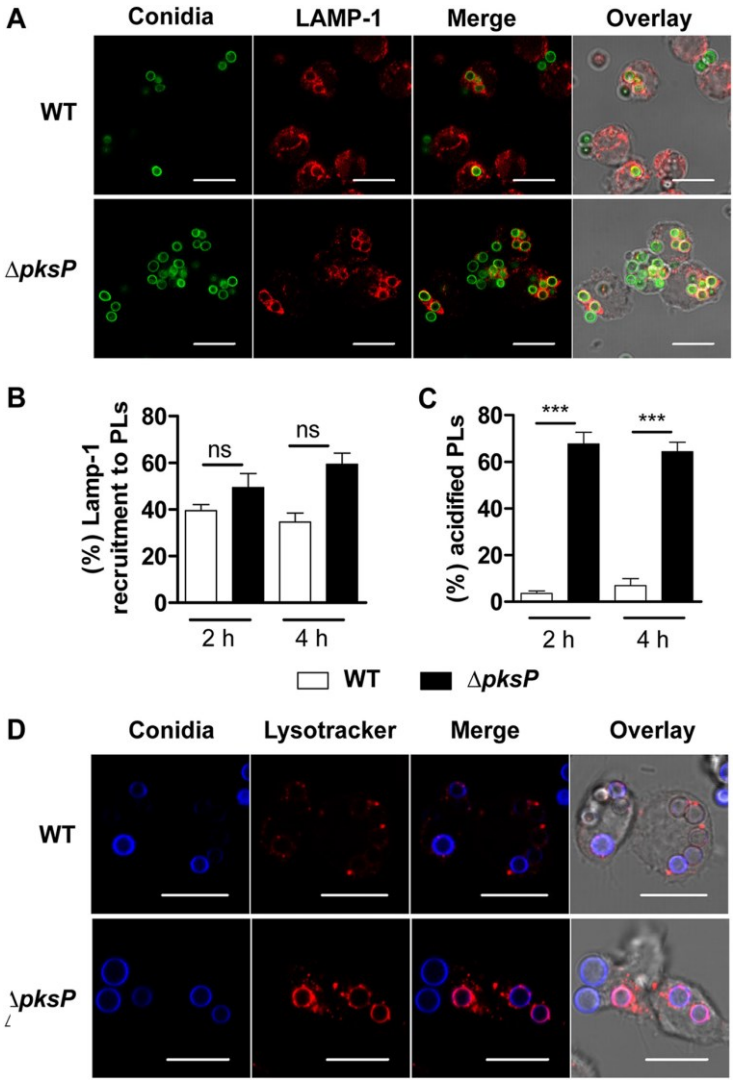

FIG 2 Processing of *A. fumigatus* conidia inside phagolysosomes. (A) dPLB cells were stained with LAMP-1 (red) after infection with wild-type (WT) or Δ*pksP* conidia (FITC labeled; green) for 4 h. Images are representative of three biological replicates. (B and C) Quantification of LAMP-1 colocalization with CFW-labeled conidia in phagolysosomes (B) and percentage of acidified conidia in dPLB cells after 2 and 4 h postinfection with wild-type and Δ*pksP* conidia (C). Data for panels B and C are presented as means plus SEM. Statistical significance is indicated as follows: *** = $P < 0.001$; ns, not significant. (D) Colocalization of conidia (CFW; blue) in acidified compartments labeled with Lysotracker (red). Images are representative of three biological replicates. Bars, 10 μm.

vesicles over time in a manner comparable to primary human PMNs (Fig. 4A and B). Using nanoparticle tracking analysis, we observed the median size of particles to be around 200 nm, similar to extracellular vesicles derived from primary neutrophils, a feature that was comparable between infection-derived and spontaneously released extracellular vesicles (Fig. 4C to D).

We next compared the protein content of dPLB-derived extracellular vesicles isolated at the 2-h time point using each isolation method with and without fungal infection by LC-MS/MS-based proteomics analysis. We were able to identify 1,984 unique proteins across all four samples (see Data Set S1 in the supplemental material). The majority of identified proteins (737 proteins) were found in all four samples (Fig. 5A). We

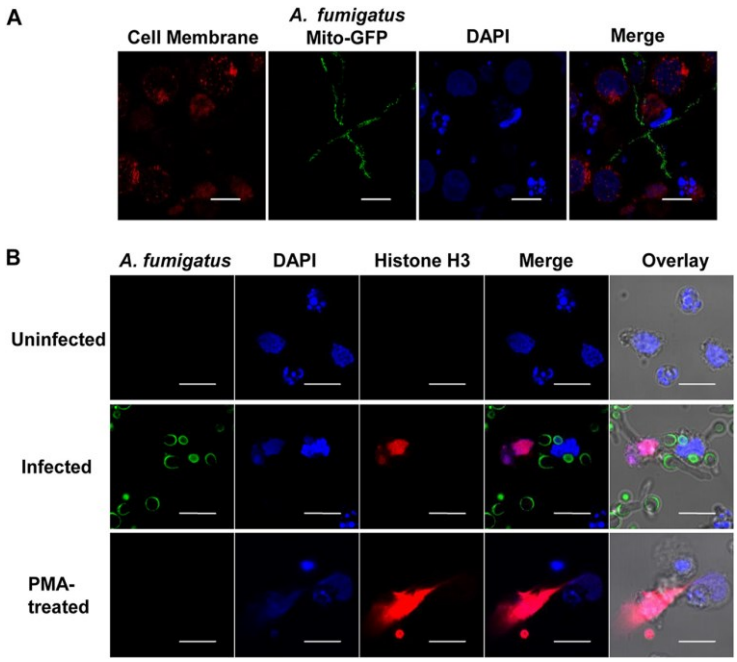

FIG 3 Production of NETs in response to *A. fumigatus* infection. (A) Confocal scanning laser microscopy of nucleic acid stained with DAPI (blue) released from dPLB cells stained with Cell Mask (red) after challenge with fungal hyphae containing a mitochondrial GFP reporter (*A. fumigatus* strain AfS35/pJW103 expressing a mitochondrial GFP reporter; green). Phorbol myristate acetate (PMA) was used as a positive control. Data are representative of three biological replicates. (B) Confocal micrographs of NET markers, histone H3 (red) and nucleic acid stained with DAPI (blue), produced by dPLB cells after contact with *A. fumigatus* hyphae (FITC labeled; green). Images are representative of three biological replicates. Bars, 10 μm.

expected that isolation using size exclusion chromatography would improve the quality of the isolated particles as has been shown previously (35), and this was in fact the case. We observed an increase in extracellular vesicle markers like the CD63 and CD81 tetraspanins and tumor susceptibility gene 101 (TSG101), and a decrease in cytoplasmic proteins like calnexin (CANX) (Table 1).

Extracellular vesicles produced by primary PMNs in response to *A. fumigatus* infection are known to be enriched for antimicrobial cargo proteins like azurocidin, cathepsin G, and defensin (10). In line with the primary neutrophil data, we found that dPLBs also contained many of the same proteins in both infection-derived and spontaneously released extracellular vesicles (Table 1), as evidenced by an UpSetR plot showing overlapping protein cohorts (Fig. S4) (10), albeit with some exceptions. For example, dPLBs appeared to lack defensin, neutrophil elastase, and some histone proteins previously observed. Ultimately, improvements in LC-MS/MS technology and the advantage of higher input amounts of extracellular vesicle protein using large amounts of dPLB cells in culture resulted in significantly more proteins detected here compared to efforts using primary neutrophils (10), proving that dPLBs offer a scalable system for the elucidation of novel mechanisms of neutrophil extracellular vesicle biology.

dPLB extracellular vesicles produced against *A. fumigatus* limit fungal growth. The most compelling feature of infection-derived extracellular vesicles of human neutrophils is likely their antifungal capacity, as we previously reported (10). We set out to determine whether the extracellular vesicles produced by dPLB cells in response to opsonized *A. fumigatus* conidia are antifungal to a mitochondrial-GFP (green fluorescent protein) reporter strain used previously as a marker of fungal

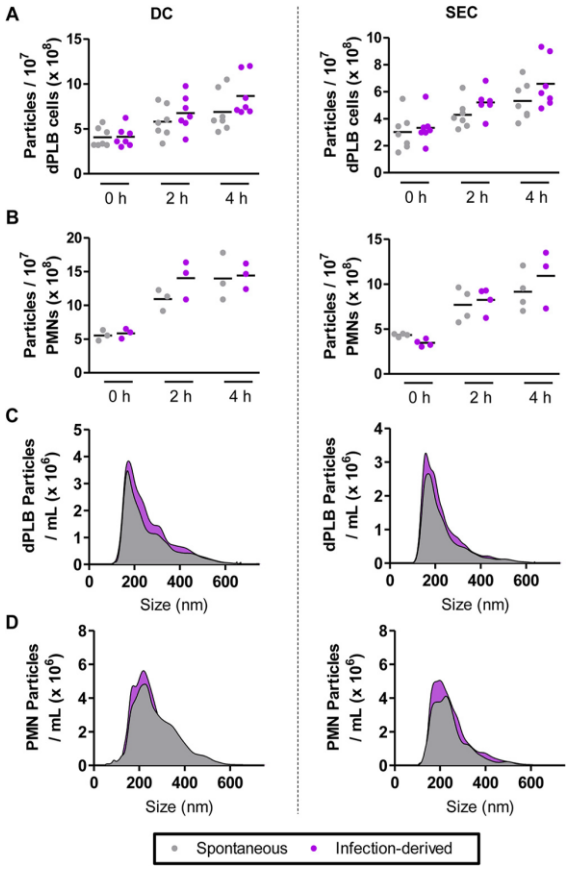

FIG 4 dPLB cells produce extracellular vesicles comparable in size to primary human PMNs. Extracellular vesicles released spontaneously or produced in response to infection with opsonized *A. fumigatus* conidia were isolated using a differential centrifugation-based approach (DC) or a size exclusion chromatography-based approach (SEC) and quantified using nanoparticle tracking analysis. (A and B) Extracellular vesicles were quantified from dPLB cells (A) or primary human PMNs (B) at 0, 2, and 4 h postinfection and show the mean of at least six biological replicates and three biological replicates, respectively. Each point indicates the value acquired in a single biological replicate. (C and D) Representative size histograms from five biological replicates are shown for extracellular vesicles derived from dPLB cells (C) and primary human PMNs (D).

viability (36). First, we incubated the reporter strain with dPLB cells and primary human PMNs and assessed the capacity of the cells to control infection. PMNs were capable of minimizing fungal outgrowth after 22 h, whereas dPLBs did not completely contain fungal growth (Fig. 6A). We then assessed the antifungal capacity of the dPLB extracellular vesicles. For this experiment, extracellular vesicles from equal numbers of dPLBs and primary human PMNs were isolated using differential centrifugation and found to be antifungal against the mitochondrial-GFP reporter strain. This was evidenced by fragmentation of fungal mitochondria after administration of extracellular vesicles to germinating conidia, which were allowed to germinate for 6 h prior to overnight incubation with extracellular vesicles, 3 mM H_2O_2 as a positive control, or left untreated as a negative control (Fig. 6B). Although the mitochondrial reporter clearly indicated fragmentation, the extracellular vesicles from dPLBs did appear to be in some cases less effective in limiting the length of hyphae than those from primary PMNs. It is important to note that dPLBs produced slightly fewer extracellular vesicles, which could partially explain the decreased antifungal activity in these assays (Fig. 6B). Additional representative images of dPLB-derived extracellular

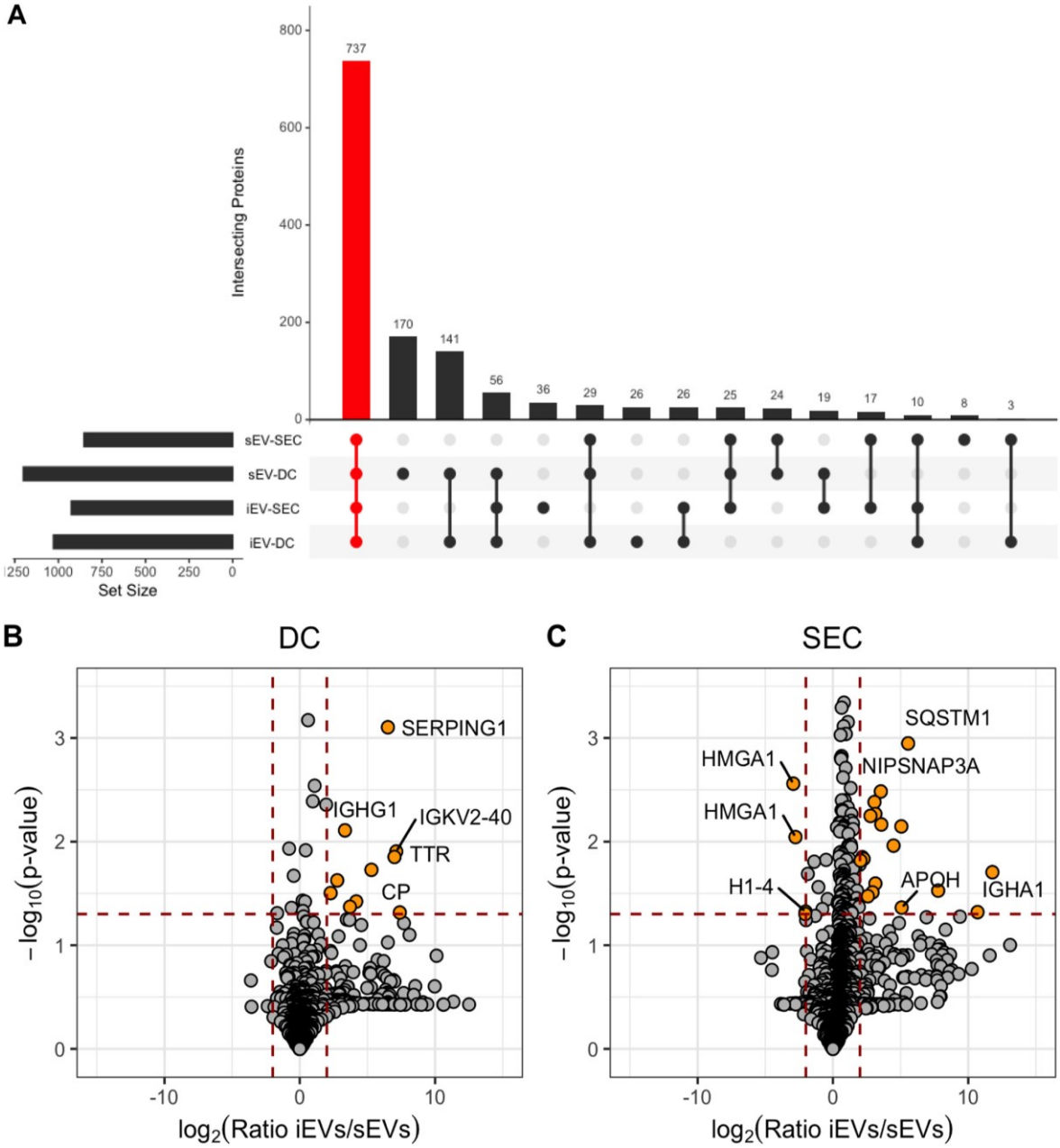

FIG 5 SEC enriches for extracellular vesicle populations. LC-MS/MS proteomics analysis was performed on extracellular vesicles isolated from dPLB cells using a differential centrifugation-based approach (DC) or a size exclusion chromatography-based approach (SEC) in the presence or absence of infection with opsonized *A. fumigatus* conidia. (A) Proteins identified in spontaneously released extracellular vesicles (sEVs) and infection-derived extracellular vesicles (iEVs) from at least two replicates of a given sample were intersected using UpSetR. The red bar indicates proteins that were found in all four samples. (B and C) Volcano plots show the $\log_2$ ratio of infection-derived extracellular vesicles (iEVs) versus spontaneously released EVs (sEVs) for DC-based isolation (B) and SEC-based isolation (C). Input data included values from all replicates using the RMN data included in Data Set S1 in the supplemental material. Plots were created using ggplot2 in R. Proteomics data are from three analytical replicates of three independent biological replicates. Orange circles represent proteins with greater than twofold change and *P* value of ≤0.05. Selected proteins are named for clarity.

vesicles are shown to indicate the spectrum of phenotypes observed for each experimental condition (Fig. S5). Collectively, these results suggest that dPLB infection-derived extracellular vesicles can limit *A. fumigatus* hyphal growth, similar to primary human PMNs (10).

TABLE 1 RMN fold change of selected proteins identified in extracellular vesicles from dPLB cells[a]

Marker type and gene	Accession no.	No. of infection-derived EVs (DC)/no. of spontaneous EVs (DC)	No. of infection-derived EVs (SEC)/no. of spontaneous EVs (SEC)	No. of infection-derived EVs (SEC)/no. of infection-derived EVs (DCs)	No. of spontaneous EVs (SEC)/no. of spontaneous EVs (DC)
EV markers					
CD63	F8VWK8	1.274	1.424	1.478	1.323
TSG101	F5H442	1.215	1.630	1.554	1.158
CD81	E9PRJ8	1.150	1.413	2.055	1.673
Non-EV markers					
CANX (calnexin)	P27824	−1.031	−1.082	−1.468	−1.398
MPO (myeloperoxidase)	P05164	−1.024	1.026	2.063	1.963
CTSG (cathepsin G)	P08311	1.045	1.042	1.117	1.120
AZU1 (azurocidin)	P20160	−1.141	1.029	1.521	1.295

[a]Abbreviations: EVs, extracellular vesicles; DC, differential centrifugation-based approach; SEC, size exclusion chromatography-based approach.

DISCUSSION

Neutrophils are critical players in the immune response to fungal pathogens stemming from their numerous antimicrobial capacities (10, 37). To study neutrophil functions, numerous cell lines that model these abilities *in vitro* have been considered with limited success. The most promising are the HL-60 leukemia cell line and PLB-985 sublineage, which have been used as models for aspergillosis and bacterial killing (22–24, 29). In this study, we analyzed different aspects of the interaction between DMF-differentiated PLB-985 myeloid cells and the fungus *A. fumigatus* for the first time, making frequent comparisons with data from primary neutrophils.

Primary neutrophils are capable of phagocytosing and processing *A. fumigatus* conidia, features that were maintained in dPLB cells. As expected for cultured cells, the observed phagocytosis rate of *A. fumigatus* conidia by dPLB cells was lower than that of primary human PMNs. It is possible that additional differentiation methods will ultimately reveal higher rates of phagocytosis, as PLB-985 cells differentiated with DMF are known to exhibit lower phagocytic activity than cells differentiated with dimethyl sulfoxide (38). In terms of cytokine release, we observed increased release of IL-8 from dPLBs after infection with opsonized *A. fumigatus* conidia, but not IL-1β, consistent with our observations of human PMNs. These results are also in agreement with those collected from primary PMNs coincubated with L-ficolin-opsonized conidia for 8 h, where secretion of IL-8 was also much higher than secretion of IL-1β (39).

We next stained dPLB cells for the endosomal marker LAMP-1 and measured the acidification of the phagolysosomes via Lysotracker to assess intracellular processing of fungal conidia. These experiments confirmed that around 20% of wild-type conidia are completely internalized inside the phagosomes and that lysosomal fusion occurs as a next step of conidial processing. Interestingly, and as already demonstrated for primary monocytes and neutrophils (14), melanized conidia showed less acidification around the phagolysosomal membrane than the mutant lacking DHN-melanin. This effect in monocytes is caused by inhibition of V-ATPase assembly. Surprisingly, staining for the V1 subunit of the V-ATPase did not reveal a significant difference between the wild-type and Δ*pksP* strains in dPLB cells as has been observed in other cell systems. These results suggest that neutrophils potentially employ additional mechanisms to acidify phagolysosomes in neutrophilic granulocytes after *A. fumigatus* infection or that the methods used were not sufficiently sensitive to detect slight differences in acidification. Together, these results suggest that dPLBs can serve as an intriguing model to study various aspects of neutrophil phagocytosis and intracellular processing in a more tractable *in vitro* model system.

A conidium that escapes phagocytosis can sometimes germinate into a hypha, a morphotype that is much more difficult to eliminate and requires the antifungal activity of neutrophils. One mechanism that aids in control of *A. fumigatus* hyphae is the release of fungistatic NETs composed of DNA and antimicrobial proteins. By staining for extracellular DNA and NET constituent histone H3, we could clearly show that dPLB cells also produce NETs in response to *A. fumigatus* hyphae, comparable to primary

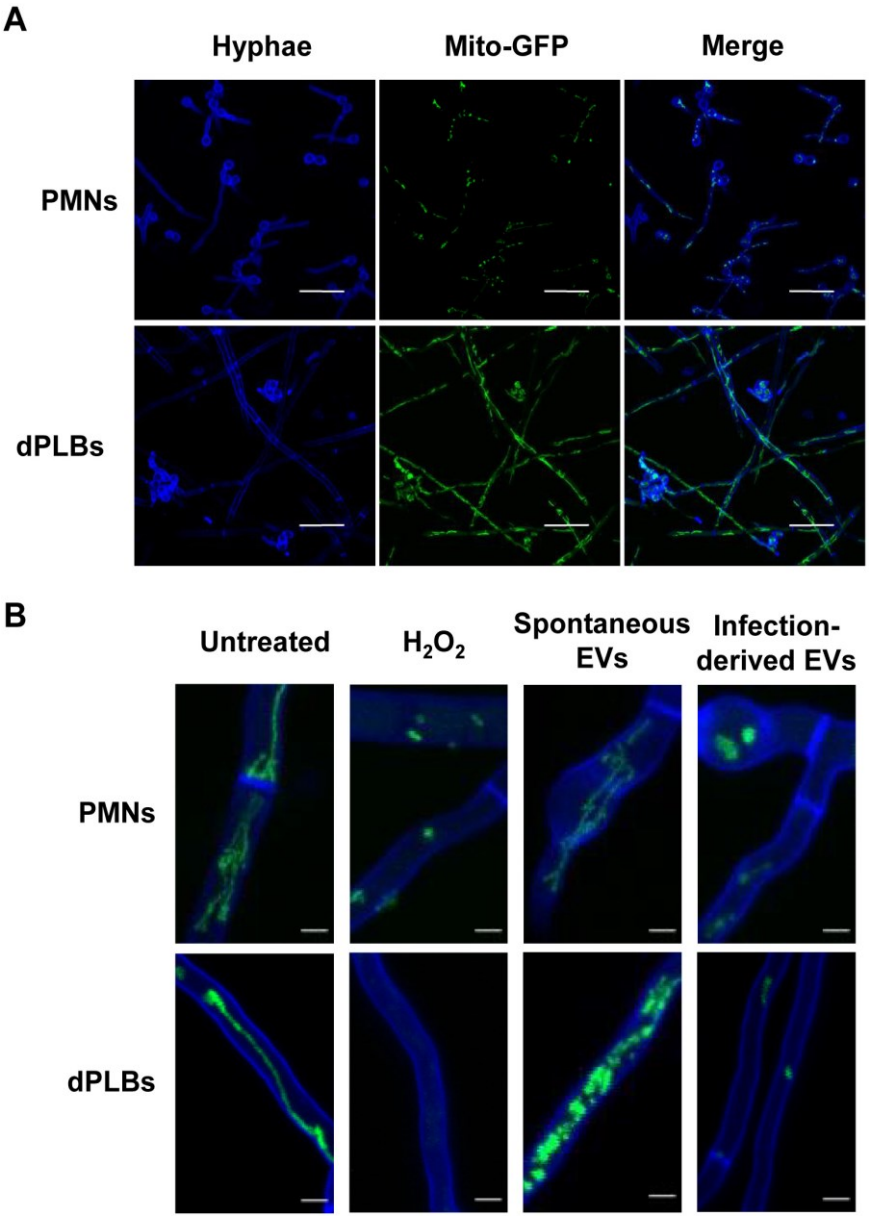

FIG 6 Infection-derived extracellular vesicles from dPLBs are antifungal to *A. fumigatus* hyphae. (A) Conidia from *A. fumigatus* strain AfS35 containing plasmid pJW103 expressing a mitochondrial GFP reporter (green) were opsonized and coincubated with freshly harvested human PMNs or dPLBs. After overnight incubation (22 h), samples were stained with CFW for 10 min, and images were taken using a Zeiss LSM 780 confocal microscope. Bars, 20 μm. (B) The *A. fumigatus* strain AfS35 expressing a mitochondrial GFP reporter (green) was first grown for 6 h and then incubated overnight with spontaneously released extracellular vesicles or infection-derived extracellular vesicles isolated from primary human PMNs or dPLBs. Fungal hyphae were then stained with CFW. For a control, untreated hyphae and hyphae treated with 3 mM H_2O_2 to induce cell death are included. An intact mitochondrial network is shown by a filamentous network, whereas a disrupted network is shown by fragmentation or the lack of green signal. Bars, 5 μm.

human PMNs and in agreement with other studies challenging dPLBs with bacterial pathogens (22, 23).

Production of extracellular vesicles from primary neutrophils coincubated with *Aspergillus* conidia or bacteria like *Staphylococcus aureus* is an important defense

strategy against microorganisms (10, 33). We found that dPLB cells were also able to generate comparable populations of extracellular vesicles to PMNs upon contact with opsonized conidia. Accumulation of extracellular vesicles of approximately 200 nm in diameter was observed over time, independently of the isolation method we applied. Proteomics analysis revealed that by using a size exclusion chromatography-based isolation approach, the extracellular vesicle population could be enriched for extracellular vesicle marker proteins like CD63, CD81, and TSG101. We observed that the samples obtained by this method had a higher abundance of proteins and showed more differences between the spontaneously released and infection-derived extracellular vesicles. In particular, infection-derived extracellular vesicles were enriched in immunoglobulins and complement factors compared to spontaneously released vesicles. These serum proteins may be introduced to the infection system during opsonization of the fungal conidia despite thorough washing. It remains unclear whether these immunoglobulins and complement factors play an important role in extracellular vesicle biology during *A. fumigatus* infection. As a hint for such a role, the association of immunoglobulins and complement proteins was shown previously to be important in systemic lupus erythematosus (SLE) disease, where extracellular vesicles with immunoglobulin cargo acted as immune complexes to mediate inflammation (40, 41).

In the proteomics analysis of extracellular vesicles derived from primary neutrophils infected with *A. fumigatus*, several antimicrobial peptides, such as cathepsin G and azurocidin, were detected (10). Coincubation of these extracellular vesicles from primary neutrophils with fungal hyphae arrested growth, which we confirmed here. Using dPLB cells, we identified extracellular vesicles containing cathepsin G and azurocidin; however, the distribution remained relatively equal between spontaneously released and infection-derived extracellular vesicles. We suspect that this is due to the differentiation procedure of dPLB cells with DMF, which provides a mild inflammatory stimulus. Nevertheless, we observed mitochondrial damage in hyphae treated with infection-derived but not spontaneously released extracellular vesicles. We can postulate several reasons for this result. First, it is possible that immunoglobulins are playing a role in targeting extracellular vesicles to fungal hyphae. In this case, the protein cargo may be the same, but targeting would be inefficient in spontaneously released extracellular vesicles. Of note, opsonization of the bacterial pathogen *Staphylococcus aureus* was not found to influence the antimicrobial capacity of neutrophil-derived extracellular vesicles (33). A second option is that additional extracellular vesicle cargo molecules such as RNA or lipids may play a role in the antifungal activity. It has been shown in many instances that extracellular vesicles can contain small RNAs that exert distinct functions during infection, especially in regard to plant fungal pathogens (42, 43). We believe that a combination of factors is likely involved in the antifungal effect of extracellular vesicles.

Part of the explanation may also come from similarities between neutrophilic granules and extracellular vesicles. Granules and extracellular vesicles are distinct cellular features, but they do share some biogenesis pathways and cargo molecules. For example, the azurophilic granules contain myeloperoxidase to aid in pathogen killing in the endocytic pathway via fusion of the granules to pathogen-containing phagosomes (44), but myeloperoxidase is also released in a CD63-negative population of extracellular vesicles known as microvesicles (45). Based on the proteomics analysis of this study, as well as our previous work (10), it seems possible that microvesicle cargo proteins like myeloperoxidase contribute at least in part to the antifungal activity. However, the presence of myeloperoxidase in spontaneously released extracellular vesicles and the lack of susceptibility of patients lacking myeloperoxidase to fungal infections (46) hint that other factors are also involved. Besides, the shared marker protein CD63 nicely highlights another link between granules and extracellular vesicles, the shared biogenesis from multivesicular bodies of azurophilic granules and the extracellular vesicle subset called exosomes (47).

In conclusion, our results suggest that DMF-differentiated PLB-985 cells can be used as a model to study aspects of the interaction of the human-pathogenic fungus

A. fumigatus with neutrophilic granulocytes. Although they will never substitute for all experiments with neutrophils, we do believe that this system will serve as a useful tool for the genetic dissection of *A. fumigatus* pathogenesis in the future.

MATERIALS AND METHODS

Fungal strain cultivation and opsonization. Cultivation of *A. fumigatus* strains CEA10 (Fungal Genetics Stock Center; A1163), CEA17 Δ*akuB*^{ku80} Δ*pksP* (48), and AfS35/pJW103 (36) was performed on malt agar plates (Sigma-Aldrich) supplemented to a final concentration of 2% (wt/vol) agar for 5 days at 37°C. Conidia were harvested in sterile, ultrafiltrated water filtered through a 30-μm pore filter (MACS, Miltenyi Biotec). Prior to confrontation with PLB-985 cells, conidia were opsonized with normal human serum (Merck Millipore). Briefly, 900 μl of spore suspension was mixed with 100 μl of normal human serum and incubated in a thermomixer at 37°C for 30 min shaking at 500 rpm. The spore suspension was washed three times by collecting spores via centrifugation at 1,800 × *g* for 1 min at 4°C and resuspending in fresh phosphate-buffered saline (PBS). Following washing, spores were enumerated in a Thoma chamber in preparation for infection assays.

Cell culture cultivation, differentiation, and infection. PLB-985 cells were maintained in Roswell Park Memorial Institute medium 1640 (RPMI; Gibco) supplemented with 10% (vol/vol) fetal bovine serum (FBS; HyClone, GE Life Science), 100 U/ml penicillin-streptomycin antibiotic solution (Lonza), and 2 mM UltraGlutamine (alanyl L-glutamine; Gibco). For differentiation into a neutrophilic granulocyte cell type, 4×10^5 cells/ml were resuspended in supplemented RPMI containing 2.5% (vol/vol) FBS and 0.5% DMF (Sigma-Aldrich) for 4 days at 37°C with 5% (vol/vol) CO_2. On day 4, fresh differentiation medium was added, and the cells were incubated for 3 additional days. On day 7, cells were collected, centrifuged at 300 × *g* for 5 min, and then seeded in wells for experiments at the appropriate concentrations. The medium used for all the assays was composed of RPMI supplemented with 1% (vol/vol) exosome-depleted FBS (Life Technologies GmbH), 2 mM UltraGlutamine, and 0.5% (vol/vol) DMF.

Isolation of human PMNs. Fresh venous blood was drawn from adult healthy volunteers, aged 20 to 35 years, after obtaining written consent. This study was approved by the Jena University Hospital Institutional Review Board (approval number 5074-02/17) in agreement with the Declaration of Helsinki. Blood was collected in EDTA BD Vacutainer tubes (BD Biosciences) and mixed with PBS. Six milliliters of this solution was carefully layered onto (avoiding any mixing) 5 ml (1:1 [vol/vol]) of PolymorphPrep solution (Progen) and centrifuged 50 min at 500 × *g* for gradient separation. After centrifugation, the neutrophil layer was collected, mixed with an equal volume of 0.5% PBS, and recentrifuged for 15 min at 400 × *g*. To limit contamination of red blood cells, the pellet was lysed with the ACK lysis buffer (Gibco) and centrifuged as before. The PMNs were finally resuspended in RPMI medium without phenol red (Thermo Fisher Scientific) and after addition of trypan blue counted with a Luna automated cell counter (Logos Biosystem). For each experiment, the viability of neutrophils was ≥95%.

Phagocytosis assays. To assess phagocytic ability, we used a combination of imaging flow cytometry and confocal fluorescence microscopy. For both methods, the conidia were first stained with fluorescein isothiocyanate (FITC) and then after confrontation of dPLBs or primary neutrophils, counterstained with calcofluor white (CFW; Sigma-Aldrich). The FITC solution was obtained by dissolving FITC powder (Sigma-Aldrich) in 5 ml of 0.1 M sodium carbonate (Na_2CO_3), followed by filtration through a 0.22-μm-pore-size filter (Carl Roth). Afterwards 1 ml of this solution was mixed with 500 μl of spore suspension and incubated for 30 min at 37°C while shaking at 1,000 rpm in the dark. The spores were then pelleted and washed three times with PBS with 0.001% (vol/vol) Tween 20 (Carl Roth). During the last washing step, Tween was removed to avoid residual detergent in the samples (14, 49). Before counting, the conidia were opsonized following the protocol described above. Spores were then added to cells and coincubated for 2 and 4 h at 37°C with 5% (vol/vol) CO_2. At each time point, CFW was added to a final concentration of 1 μg/ml and incubated for 1 min. Afterwards the cell suspension was transferred to microcentrifuge tubes, centrifuged at 600 × *g* for 2 min at 4°C, and washed with PBS twice. After the supernatant was discarded, the pellet was fixed with 150 μl of 3.7% (vol/vol) formaldehyde in PBS at room temperature for 15 min and subsequently washed as described above. For imaging flow cytometry measurements, the cells were resuspended in 150 μl of PBS and analyzed immediately or stored at 4°C for no more than 24 h. Four independent experiments were performed, and for each replicate, 5,000 cells were analyzed using the ImageStream X Mark II (Luminex). A 488-nm laser was used to detect FITC staining, and a 405-nm laser was used to detect CFW staining. The laser voltage was adjusted depending on the sample. For wild-type conidia, we used 10 mW of 488-nm laser and 2 mW for the 405-nm laser, and for Δ*pksP* conidia, we used 1 and 2 mW of the respective lasers. The fluorescence intensities of the samples were compensated and analyzed with the IDEAS software (Luminex). An example of the gating strategy used for analysis is provided (see Fig. S1B and S1C in the supplemental material). For the fluorescence microscopy analysis, cells were seeded in 8-well μ-slides (Ibidi) and visualized using a Zeiss LSM 780 confocal microscope (Carl Zeiss) from at least three biological replicates.

Immunofluorescence assays. For immunofluorescence assays, cells were allowed to adhere in a 24-well plate with poly-L-lysine-coated glass coverslips for 1 h (Merck). After infection with labeled *A. fumigatus* spores and incubation for the noted times, cells were fixed using 3.7% (vol/vol) formaldehyde in PBS for 10 min, rinsed three times with PBS, permeabilized for 15 min using 0.1% (vol/vol) Triton X-100 in PBS or 0.1% (wt/vol) saponin in PBS, and then blocked for 30 min with 2% (wt/vol) bovine serum albumin (BSA). After permeabilization, washed cells were incubated with primary rabbit anti-Lamp-1 antibody (Abcam ab24170; 1:100 dilution), anti-V-ATPase V1 subunit antibody (Abcam ab73404; 1:100 dilution), or anti-histone H3 (Cell Signaling DIH2; 1:200 dilution) antibody in 1% (wt/vol) BSA in PBS,

followed by incubation with secondary goat anti-rabbit IgG antibody DyLight 633 (Thermo Fisher Scientific). The glass coverslips were mounted onto microscopy slides and visualized using a Zeiss LSM 780 confocal microscope (Carl Zeiss). LAMP-1 recruitment was quantified by comparing the positive signal from stained phagolysosomes to nonstained phagolysosomes.

Reactive oxygen species measurements. ROS production was detected in dPLB cells by seeding cells in 8-well μ-slides (Ibidi) coated with poly-L-lysine followed by infection with *A. fumigatus* conidia at a multiplicity of infection (MOI) of 5 for either 2 or 4 h. CellROX Orange Reagent (Thermo Fisher Scientific) was added 30 min prior to the end of the infection time points, and ROS production was imaged using a Zeiss LSM 780 confocal microscope (Carl Zeiss) for fluorescent intensity.

Cytokine measurement. For the detection of IL-8 and IL-1β, 2×10^5 dPLB cells or primary neutrophils were seeded in 24-well plates. After the addition of conidia at an MOI of 5, plates were incubated at 37°C with 5% (vol/vol) CO_2 for 2, 4, or 6 h. An additional 24-h time point was included for dPLB cells. For a positive control, cells were treated with 5 μg/ml of lipopolysaccharide (LPS; Sigma-Aldrich L4516). At the appropriate endpoint, samples were collected, centrifuged at $300 \times g$ for 5 min to remove cell debris, frozen at −20°C, and analyzed within 3 days. Cytokines were measured using human ELISA Max deluxe kits (BioLegend) according to the manufacturer's instruction.

Acidification assays. Acidification assays were performed as mentioned previously (28). Briefly, the cells were incubated with 50 nM Lysotracker DND-99 (Thermo Fisher Scientific) for 1 h prior to infection. After that, FITC-labeled conidia were added to the cells for 2 or 4 h and imaged using Zeiss LSM 780 confocal microscope (Carl Zeiss). For quantification, 200 conidia-containing phagolysosomes were counted and evaluated for acidification. The values represent the means ± standard errors of the means (SEM) of three separate experiments.

Extracellular vesicle isolation. After infection with *A. fumigatus*, the supernatant of dPLB cells was collected, and extracellular vesicles were isolated using two different methods: a differential centrifugation-based approach or a size exclusion chromatography-based approach. The first method was described previously for the isolation of neutrophil-derived extracellular vesicles (10, 33). In both approaches, samples were centrifuged at $3{,}000 \times g$ for 15 min at 4°C and filtered through 5-μm-pore-size filters (Carl Roth). In the first method, samples were then centrifuged at $19{,}500 \times g$ for 20 min at 4°C to collect extracellular vesicles. For the second approach, the clarified filtrate was concentrated using Amicon Ultra-15 centrifugal filters (Merck) with a molecular mass cutoff (MWCO) of 100 kDa for 10 min at 4°C and $3{,}220 \times g$ and loaded on size exclusion chromatography qEV 70-nm columns (Izon). After the 3-ml void volume was discarded, 1.5 ml of extracellular vesicle sample was collected and measured. When necessary, extracellular vesicles were further concentrated using 10-kDa cutoff Amicon Ultra 0.5-ml filters (Merck). Extracellular vesicles were used fresh for most of the downstream experiments except for proteomics analysis where they were frozen at −20°C.

Nanoparticle tracking analysis. Particle concentration and size distribution were analyzed using a nanoparticle tracking analysis (NTA) NS300 device with a 650-nm laser (Malvern Instruments Ltd.). Fresh samples were measured with a constant flow rate of 20 and a temperature set at 25°C. Five 60-s videos were recorded with a camera level of 11. Videos were then analyzed with the NTA 3.2.16 software using a detection threshold of 4.

Protein preparation for LC-MS/MS. Isolated extracellular vesicles were delipidated as described previously (10) using the protein precipitation protocol of Wessel and Flügge (50). Delipidated extracellular vesicles were resolubilized in 100 μl of 50 mM triethyl ammonium bicarbonate (TEAB) in 1:1 (vol/vol) trifluoroethanol-water. For reduction of cysteine thiols, the solution was mixed with 10 mM Tris(2-carboxyethyl) phosphine and alkylated with 12.5 mM chloroacetamide at 70°C for 30 min in the dark. Proteins were digested for 18 h at 37°C with trypsin-LysC mix (Promega) at a protein-to-protease ratio of 25:1. Tryptic peptides were first completely evaporated using a vacuum concentrator (Eppendorf) and then resolubilized in 0.05% (vol/vol) trifluoroacetic acid (TFA) in 2:98 (vol/vol) acetonitrile-water. Finally, the samples were filtered through Ultrafree-MC hydrophilic polytetrafluoroethylene (PTFE) membrane (0.2-μm pore size) spin filters (Millipore) and stored at −20°C until measurement. Each sample was measured in triplicate (three analytical replicates of three biological replicates) as follows.

LC-MS/MS analysis. LC-MS/MS analysis was performed on an Ultimate 3000 nano RSLC system connected to a QExactive HF mass spectrometer (both Thermo Fisher Scientific). Peptide trapping for 5 min on an Acclaim Pep Map 100 column (2 cm × 75 μm, 3 μm) at 5 μl/min was followed by separation on an analytical Acclaim Pep Map RSLC nano column (50 cm × 75 μm, 2 μm). Mobile phase gradient elution of eluent A (0.1% [vol/vol] formic acid in water) mixed with eluent B (0.1% [vol/vol] formic acid in 90/10 acetonitrile/water) was performed as follows: 0 min at 4% eluent B, 30 min at 12% eluent B, 75 min at 30% eluent B, 85 min at 50% eluent B, 90 to 95 min at 96% eluent B, and 95.1 to 120 min at 4% eluent B.

Positively charged ions were generated at spray voltage of 2.2 kV using a stainless-steel emitter attached to the Nanospray Flex Ion Source (Thermo Fisher Scientific). The quadrupole/orbitrap instrument was operated in full MS/data-dependent MS2 (Top15) mode. Precursor ions were monitored at m/z 300 to 1,500 at a resolution of 120,000 FWHM (full width at half maximum) using a maximum injection time (ITmax) of 120 ms and an AGC (automatic gain control) target of 3×10^6. Precursor ions with a charge state of $z = 2$ to 5 were filtered at an isolation width of m/z 1.6 atomic mass units (amu) for further higher-energy collisional dissociation (HCD) fragmentation at 27% normalized collision energy (NCE). MS2 ions were scanned at 15,000 FWHM (ITmax = 100 ms; AGC = 2×10^5). Dynamic exclusion of precursor ions was set to 25 s, and the underfill ratio was set to 1.0%. The LC-MS/MS instrument was controlled by Chromeleon 7.2, QExactive HF Tune 2.8, and Xcalibur 4.0 software.

Database search and data analysis. Tandem mass spectra were searched against the UniProt database of *Homo sapiens* (https://www.uniprot.org/proteomes/UP000005640; 17 May 2021) and *Neosartorya fumigata* (https://www.uniprot.org/proteomes/UP000002530; 17 May 2021) using Proteome Discoverer (PD) 2.4 (Thermo) and the algorithms of Mascot 2.4.1 (Matrix Science), Sequest HT (version of PD2.2), MS Amanda 2.0, and MS Fragger 3.2. Two missed cleavages were allowed for tryptic digestion. The precursor mass tolerance was set at 10 ppm, and the fragment mass tolerance was set at 0.02 Da. Modifications were defined as dynamic Met oxidation and protein N-terminal acetylation with and without methionine loss as well as static Cys carbamidomethylation. A strict false discovery rate (FDR) of $<1\%$ (peptide and protein level) were required for positive protein hits. If only one peptide per protein has been identified, the hit was accepted if the Mascot score was >30 or the MS Amanda score was >300 or the Sequest score was >4 or the MS Fragger score was >8. The Percolator node of PD2.4 and a reverse decoy database was used for *q* value validation of spectral matches. Only rank 1 proteins and peptides of the top scored proteins were counted. Label-free protein quantification was based on the Minora algorithm of PD2.2 using a signal-to-noise ratio of >5. Imputation of missing quantification values was applied by setting the abundance to 75% of the lowest abundance identified for each sample. Normalization was based on a replicate median total peptide sum approach, which was calculated based on the sum of all identified peptide abundance values per replicate sample. The sums of each of the three replicates from the four sample groups were used to calculate median values. Normalization factors were calculated by dividing median values of the respective sample group by the abundance sum of each sample. Normalization factors were multiplied with single protein abundance values of each replicate/sample. The *P* values are based on a Student`s *t* test. Ratio-adjusted *P* values were calculated by dividing *P* values with the $\log_4$ ratio of the protein abundance levels. Significant differences in protein abundance were defined when the following three requirements were reached: at least a fourfold change in abundance (up and down), a ratio-adjusted *P* value of <0.05, and identified in at least two of three replicates of the sample group with the highest abundance. Intersection plots were created using the UpSetR package (51) and include only proteins that were detected in at least two replicates of a given sample. Volcano plots were created using ggplot2 in R using the replicate median total peptide sum normalized (RMN) data for all proteins detected in Data Set S1 in the supplemental material.

Fungal mitochondrial reporter inhibition assay. To characterize growth inhibition and killing of hyphae by fungus-induced extracellular vesicles, an *A. fumigatus* strain expressing a mitochondrial GFP reporter (AfS35/pJW103 [36]) has been used as described previously (10). Extracellular vesicles produced by 1×10^7 dPLB cells or PMNs were isolated and coincubated with the reporter strain. After 16 h of incubation, samples were stained with CFW, and images were taken using Zeiss LSM 780 confocal microscope (Carl Zeiss).

Statistical analysis. Data were plotted and statistically analyzed using GraphPad Prism software 5.0 (GraphPad Software) unless otherwise noted. The Student's *t* test was used for significance testing when comparing two groups. Differences between the groups were considered significant at a *P* value of <0.05. Throughout the article, significance is denoted as follows: *, $P \leq 0.05$; **, $P \leq 0.01$, ***, $P \leq 0.001$; ns, not significant.

Ethics statement. Peripheral human blood was collected from healthy volunteers only after written informed consent was provided. The study was conducted in accordance with the Declaration of Helsinki and approved by the Ethics Committee of the University Hospital Jena (approval number 5074-02/17).

Data availability. The mass spectrometry proteomics data have been deposited to the ProteomeXchange Consortium via the PRIDE partner repository (52) with the data set identifier PXD027032.

SUPPLEMENTAL MATERIAL

Supplemental material is available online only.

DATA SET S1, XLSX file, 18.9 MB.

FIG S1, TIF file, 2.6 MB.

FIG S2, TIF file, 0.7 MB.

FIG S3, PDF file, 0.2 MB.

FIG S4, TIF file, 1 MB.

FIG S5, TIF file, 2 MB.

TABLE S1, DOCX file, 0.01 MB.

ACKNOWLEDGMENTS

We thank Johannes Wagener for providing the *A. fumigatus* mitochondrial GFP reporter strain and Natascha Wilker for excellent technical assistance.

The work presented here was generously supported by the Deutsche Forschungsgemeinschaft (DFG)-funded Collaborative Research Center/Transregio FungiNet 124 "Pathogenic fungi and their human host: Networks of Interaction" (210879364, project A1 and Z2), the DFG-funded ANR project (316898429, project AfuInf), and the Federal Ministry for Education and Research (BMBF: https://www.bmbf.de/), Germany, Project FKZ 01K12012 "RFIN – RNA-Biologie von Pilzinfektionen."

We declare that we have no conflicts of interest.

REFERENCES

1. Brown GD, Denning DW, Gow NA, Levitz SM, Netea MG, White TC. 2012. Hidden killers: human fungal infections. Sci Transl Med 4:165rv13. https://doi.org/10.1126/scitranslmed.3004404.
2. Schmiedel Y, Zimmerli S. 2016. Common invasive fungal diseases: an overview of invasive candidiasis, aspergillosis, cryptococcosis, and Pneumocystis pneumonia. Swiss Med Wkly 146:w14281. https://doi.org/10.4414/smw.2016.14281.
3. Latge JP, Chamilos G. 2019. *Aspergillus fumigatus* and aspergillosis in 2019. Clin Microbiol Rev 33:e00140-18. https://doi.org/10.1128/CMR.00140-18.
4. Nasir N, Farooqi J, Mahmood SF, Jabeen K. 2020. COVID-19-associated pulmonary aspergillosis (CAPA) in patients admitted with severe COVID-19 pneumonia: an observational study from Pakistan. Mycoses 63:766–770. https://doi.org/10.1111/myc.13135.
5. Salmanton-Garcia J, Sprute R, Stemler J, Bartoletti M, Dupont D, Valerio M, Garcia-Vidal C, Falces-Romero I, Machado M, de la Villa S, Schroeder M, Hoyo I, Hanses F, Ferreira-Paim K, Giacobbe DR, Meis JF, Gangneux JP, Rodriguez-Guardado A, Antinori S, Sal E, Malaj X, Seidel D, Cornely OA, Koehler P, FungiScope European Confederation of Medical Mycology/The International Society for Human and Animal Mycology Working Group. 2021. COVID-19-associated pulmonary aspergillosis, March-August 2020. Emerg Infect Dis 27:1077–1086. https://doi.org/10.3201/eid2704.204895.
6. Rivera A, Hohl TM, Collins N, Leiner I, Gallegos A, Saijo S, Coward JW, Iwakura Y, Pamer EG. 2011. Dectin-1 diversifies *Aspergillus fumigatus*-specific T cell responses by inhibiting T helper type 1 CD4 T cell differentiation. J Exp Med 208:369–381. https://doi.org/10.1084/jem.20100906.
7. Brakhage AA, Langfelder K. 2002. Menacing mold: the molecular biology of *Aspergillus fumigatus*. Annu Rev Microbiol 56:433–455. https://doi.org/10.1146/annurev.micro.56.012302.160625.
8. Drummond RA, Gaffen SL, Hise AG, Brown GD. 2014. Innate defense against fungal pathogens. Cold Spring Harb Perspect Med 5:a019620. https://doi.org/10.1101/cshperspect.a019620.
9. Mircescu MM, Lipuma L, van Rooijen N, Pamer EG, Hohl TM. 2009. Essential role for neutrophils but not alveolar macrophages at early time points following *Aspergillus fumigatus* infection. J Infect Dis 200:647–656. https://doi.org/10.1086/600380.
10. Shopova IA, Belyaev I, Dasari P, Jahreis S, Stroe MC, Cseresnyes Z, Zimmermann AK, Medyukhina A, Svensson CM, Kruger T, Szeifert V, Nietzsche S, Conrad T, Blango MG, Kniemeyer O, von Lilienfeld-Toal M, Zipfel PF, Ligeti E, Figge MT, Brakhage AA. 2020. Human neutrophils produce antifungal extracellular vesicles against *Aspergillus fumigatus*. mBio 11:e00596-20. https://doi.org/10.1128/mBio.00596-20.
11. McCormick A, Heesemann L, Wagener J, Marcos V, Hartl D, Loeffler J, Heesemann J, Ebel F. 2010. NETs formed by human neutrophils inhibit growth of the pathogenic mold *Aspergillus fumigatus*. Microbes Infect 12:928–936. https://doi.org/10.1016/j.micinf.2010.06.009.
12. Brogan TD. 1964. Effect of complement and of the carbohydrate components of sputum on phagocytosis by human polymorphonuclear leucocytes. Immunology 7:626–638.
13. Pazhakh V, Ellett F, Croker BA, O'Donnell JA, Pase L, Schulze KE, Greulich RS, Gupta A, Reyes-Aldasoro CC, Andrianopoulos A, Lieschke GJ. 2019. Beta-glucan-dependent shuttling of conidia from neutrophils to macrophages occurs during fungal infection establishment. PLoS Biol 17:e3000113. https://doi.org/10.1371/journal.pbio.3000113.
14. Thywißen A, Heinekamp T, Dahse H-M, Schmaler-Ripcke J, Nietzsche S, Zipfel PF, Brakhage AA. 2011. Conidial dihydroxynaphthalene melanin of the human pathogenic fungus *Aspergillus fumigatus* interferes with the host endocytosis pathway. Front Microbiol 2:96. https://doi.org/10.3389/fmicb.2011.00096.
15. Silva JC, Rodrigues NC, Thompson-Souza GA, Muniz VS, Neves JS, Figueiredo RT. 2020. Mac-1 triggers neutrophil DNA extracellular trap formation to *Aspergillus fumigatus* independently of PAD4 histone citrullination. J Leukoc Biol 107:69–83. https://doi.org/10.1002/JLB.4A0119-009RR.
16. Bruns S, Kniemeyer O, Hasenberg M, Aimanianda V, Nietzsche S, Thywissen A, Jeron A, Latge JP, Brakhage AA, Gunzer M. 2010. Production of extracellular traps against *Aspergillus fumigatus* in vitro and in infected lung tissue is dependent on invading neutrophils and influenced by hydrophobin RodA. PLoS Pathog 6:e1000873. https://doi.org/10.1371/journal.ppat.1000873.
17. Clark HL, Abbondante S, Minns MS, Greenberg EN, Sun Y, Pearlman E. 2018. Protein deiminase 4 and CR3 regulate *Aspergillus fumigatus* and beta-glucan-induced neutrophil extracellular trap formation, but hyphal killing is dependent only on CR3. Front Immunol 9:1182. https://doi.org/10.3389/fimmu.2018.01182.
18. Zarember KA, Sugui JA, Chang YC, Kwon-Chung KJ, Gallin JI. 2007. Human polymorphonuclear leukocytes inhibit *Aspergillus fumigatus* conidial growth by lactoferrin-mediated iron depletion. J Immunol 178:6367–6373. https://doi.org/10.4049/jimmunol.178.10.6367.
19. Gazendam RP, van Hamme JL, Tool AT, Hoogenboezem M, van den Berg JM, Prins JM, Vitkov L, van de Veerdonk FL, van den Berg TK, Roos D, Kuijpers TW. 2016. Human neutrophils use different mechanisms to kill *Aspergillus fumigatus* conidia and hyphae: evidence from phagocyte defects. J Immunol 196:1272–1283. https://doi.org/10.4049/jimmunol.1501811.
20. Lahoz-Beneytez J, Elemans M, Zhang Y, Ahmed R, Salam A, Block M, Niederalt C, Asquith B, Macallan D. 2016. Human neutrophil kinetics: modeling of stable isotope labeling data supports short blood neutrophil half-lives. Blood 127:3431–3438. https://doi.org/10.1182/blood-2016-03-700336.
21. Blanter M, Gouwy M, Struyf S. 2021. Studying neutrophil function in vitro: cell models and environmental factors. J Inflamm Res 14:141–162. https://doi.org/10.2147/JIR.S284941.
22. Marin-Esteban V, Turbica I, Dufour G, Semiramoth N, Gleizes A, Gorges R, Beau I, Servin AL, Lievin-Le Moal V, Sandre C, Chollet-Martin S. 2012. Afa/Dr diffusely adhering *Escherichia coli* strain C1845 induces neutrophil extracellular traps that kill bacteria and damage human enterocyte-like cells. Infect Immun 80:1891–1899. https://doi.org/10.1128/IAI.00050-12.
23. Amulic B, Knackstedt SL, Abu Abed U, Deigendesch N, Harbort CJ, Caffrey BE, Brinkmann V, Heppner FL, Hinds PW, Zychlinsky A. 2017. Cell-cycle proteins control production of neutrophil extracellular traps. Dev Cell 43:449–462.e5. https://doi.org/10.1016/j.devcel.2017.10.013.
24. Baistrocchi SR, Lee MJ, Lehoux M, Ralph B, Snarr BD, Robitaille R, Sheppard DC. 2017. Posaconazole-loaded leukocytes as a novel treatment strategy targeting invasive pulmonary aspergillosis. J Infect Dis 215:1734–1741. https://doi.org/10.1093/infdis/jiw513.
25. Braem SG, Rooijakkers SH, van Kessel KP, de Cock H, Wosten HA, van Strijp JA, Haas PJ. 2015. Effective neutrophil phagocytosis of *Aspergillus fumigatus* is mediated by classical pathway complement activation. J Innate Immun 7:364–374. https://doi.org/10.1159/000369493.
26. Goyette G, Boulais J, Carruthers NJ, Landry CR, Jutras I, Duclos S, Dermine JF, Michnick SW, LaBoissiere S, Lajoie G, Barreiro L, Thibault P, Desjardins M. 2012. Proteomic characterization of phagosomal membrane microdomains during phagolysosome biogenesis and evolution. Mol Cell Proteomics 11:1365–1377. https://doi.org/10.1074/mcp.M112.021048.
27. Heinekamp T, Schmidt H, Lapp K, Pahtz V, Shopova I, Koster-Eiserfunke N, Kruger T, Kniemeyer O, Brakhage AA. 2015. Interference of *Aspergillus fumigatus* with the immune response. Semin Immunopathol 37:141–152. https://doi.org/10.1007/s00281-014-0465-1.
28. Schmidt F, Thywißen A, Goldmann M, Cunha C, Cseresnyés Z, Schmidt H, Rafiq M, Galiani S, Gräler MH, Chamilos G, Lacerda JF, Campos A, Eggeling C, Figge MT, Heinekamp T, Filler SG, Carvalho A, Brakhage AA. 2020. Flotillin-dependent membrane microdomains are required for functional phagolysosomes against fungal infections. Cell Rep 32:108017. https://doi.org/10.1016/j.celrep.2020.108017.
29. Pedruzzi E, Fay M, Elbim C, Gaudry M, Gougerot-Pocidalo MA. 2002. Differentiation of PLB-985 myeloid cells into mature neutrophils, shown by degranulation of terminally differentiated compartments in response to N-formyl peptide and priming of superoxide anion production by granulocyte-macrophage colony-stimulating factor. Br J Haematol 117:719–726. https://doi.org/10.1046/j.1365-2141.2002.03521.x.
30. Volk AP, Barber BM, Goss KL, Ruff JG, Heise CK, Hook JS, Moreland JG. 2011. Priming of neutrophils and differentiated PLB-985 cells by pathophysiological concentrations of TNF-alpha is partially oxygen dependent. J Innate Immun 3:298–314. https://doi.org/10.1159/000321439.
31. Branzk N, Papayannopoulos V. 2013. Molecular mechanisms regulating NETosis in infection and disease. Semin Immunopathol 35:513–530. https://doi.org/10.1007/s00281-013-0384-6.
32. Xie K, Varatnitskaya M, Maghnouj A, Bader V, Winklhofer KF, Hahn S, Leichert LI. 2020. Activation leads to a significant shift in the intracellular redox homeostasis of neutrophil-like cells. Redox Biol 28:101344. https://doi.org/10.1016/j.redox.2019.101344.
33. Timar CI, Lorincz AM, Csepanyi-Komi R, Valyi-Nagy A, Nagy G, Buzas EI, Ivanyi Z, Kittel A, Powell DW, McLeish KR, Ligeti E. 2013. Antibacterial effect of microvesicles released from human neutrophilic granulocytes. Blood 121:510–518. https://doi.org/10.1182/blood-2012-05-431114.

34. Brakhage AA, Zimmermann A-K, Rivieccio F, Visser C, Blango MG. 2021. Host-derived extracellular vesicles for antimicrobial defense. microLife 2: uqab003. https://doi.org/10.1093/femsml/uqab003.
35. Lane RE, Korbie D, Trau M, Hill MM. 2019. Optimizing size exclusion chromatography for extracellular vesicle enrichment and proteomic analysis from clinically relevant samples. Proteomics 19:e1800156. https://doi.org/10.1002/pmic.201800156.
36. Ruf D, Brantl V, Wagener J. 2018. Mitochondrial fragmentation in *Aspergillus fumigatus* as early marker of granulocyte killing activity. Front Cell Infect Microbiol 8:128. https://doi.org/10.3389/fcimb.2018.00128.
37. Feldmesser M. 2006. Role of neutrophils in invasive aspergillosis. Infect Immun 74:6514–6516. https://doi.org/10.1128/IAI.01551-06.
38. Pivot-Pajot C, Chouinard FC, El Azreq MA, Harbour D, Bourgoin SG. 2010. Characterisation of degranulation and phagocytic capacity of a human neutrophilic cellular model, PLB-985 cells. Immunobiology 215:38–52. https://doi.org/10.1016/j.imbio.2009.01.007.
39. Bidula S, Sexton DW, Schelenz S. 2016. Serum opsonin ficolin-A enhances host-fungal interactions and modulates cytokine expression from human monocyte-derived macrophages and neutrophils following *Aspergillus fumigatus* challenge. Med Microbiol Immunol 205:133–142. https://doi.org/10.1007/s00430-015-0435-9.
40. Buzas EI, Toth EA, Sodar BW, Szabo-Taylor KE. 2018. Molecular interactions at the surface of extracellular vesicles. Semin Immunopathol 40: 453–464. https://doi.org/10.1007/s00281-018-0682-0.
41. Perez-Hernandez J, Redon J, Cortes R. 2017. Extracellular vesicles as therapeutic agents in systemic lupus erythematosus. Int J Mol Sci 18:717. https://doi.org/10.3390/ijms18040717.
42. Cai Q, Qiao L, Wang M, He B, Lin FM, Palmquist J, Huang SD, Jin H. 2018. Plants send small RNAs in extracellular vesicles to fungal pathogen to silence virulence genes. Science 360:1126–1129. https://doi.org/10.1126/science.aar4142.
43. He B, Cai Q, Qiao L, Huang C-Y, Wang S, Miao W, Ha T, Wang Y, Jin H. 2021. RNA-binding proteins contribute to small RNA loading in plant extracellular vesicles. Nat Plants 7:342–352. doi:10.1038/s41477-021-00863-8. https://doi.org/10.1038/s41477-021-00863-8.
44. Klebanoff SJ, Kettle AJ, Rosen H, Winterbourn CC, Nauseef WM. 2013. Myeloperoxidase: a front-line defender against phagocytosed microorganisms. J Leukoc Biol 93:185–198. https://doi.org/10.1189/jlb.0712349.
45. Hess C, Sadallah S, Hefti A, Landmann R, Schifferli JA. 1999. Ectosomes released by human neutrophils are specialized functional units. J Immunol 163:4564–4573.
46. Desai JV, Lionakis MS. 2018. The role of neutrophils in host defense against invasive fungal infections. Curr Clin Microbiol Rep 5:181–189. https://doi.org/10.1007/s40588-018-0098-6.
47. Edgar JR. 2016. Q&A: what are exosomes, exactly? BMC Biol 14:46. https://doi.org/10.1186/s12915-016-0268-z.
48. Hillmann F, Novohradska S, Mattern DJ, Forberger T, Heinekamp T, Westermann M, Winckler T, Brakhage AA. 2015. Virulence determinants of the human pathogenic fungus *Aspergillus fumigatus* protect against soil amoeba predation. Environ Microbiol 17:2858–2869. https://doi.org/10.1111/1462-2920.12808.
49. Kraibooj K, Schoeler H, Svensson CM, Brakhage AA, Figge MT. 2015. Automated quantification of the phagocytosis of *Aspergillus fumigatus* conidia by a novel image analysis algorithm. Front Microbiol 6:549. https://doi.org/10.3389/fmicb.2015.00549.
50. Wessel D, Flügge UI. 1984. A method for the quantitative recovery of protein in dilute solution in the presence of detergents and lipids. Anal Biochem 138:141–143. https://doi.org/10.1016/0003-2697(84)90782-6.
51. Lex A, Gehlenborg N, Strobelt H, Vuillemot R, Pfister H. 2014. UpSet: visualization of intersecting sets. IEEE Trans Vis Comput Graph 20:1983–1992. https://doi.org/10.1109/TVCG.2014.2346248.
52. Perez-Riverol Y, Xu QW, Wang R, Uszkoreit J, Griss J, Sanchez A, Reisinger F, Csordas A, Ternent T, Del-Toro N, Dianes JA, Eisenacher M, Hermjakob H, Vizcaino JA. 2016. PRIDE Inspector Toolsuite: moving toward a universal visualization tool for proteomics data standard formats and quality assessment of ProteomeXchange datasets. Mol Cell Proteomics 15: 305–317. https://doi.org/10.1074/mcp.O115.050229.

Supplemental information

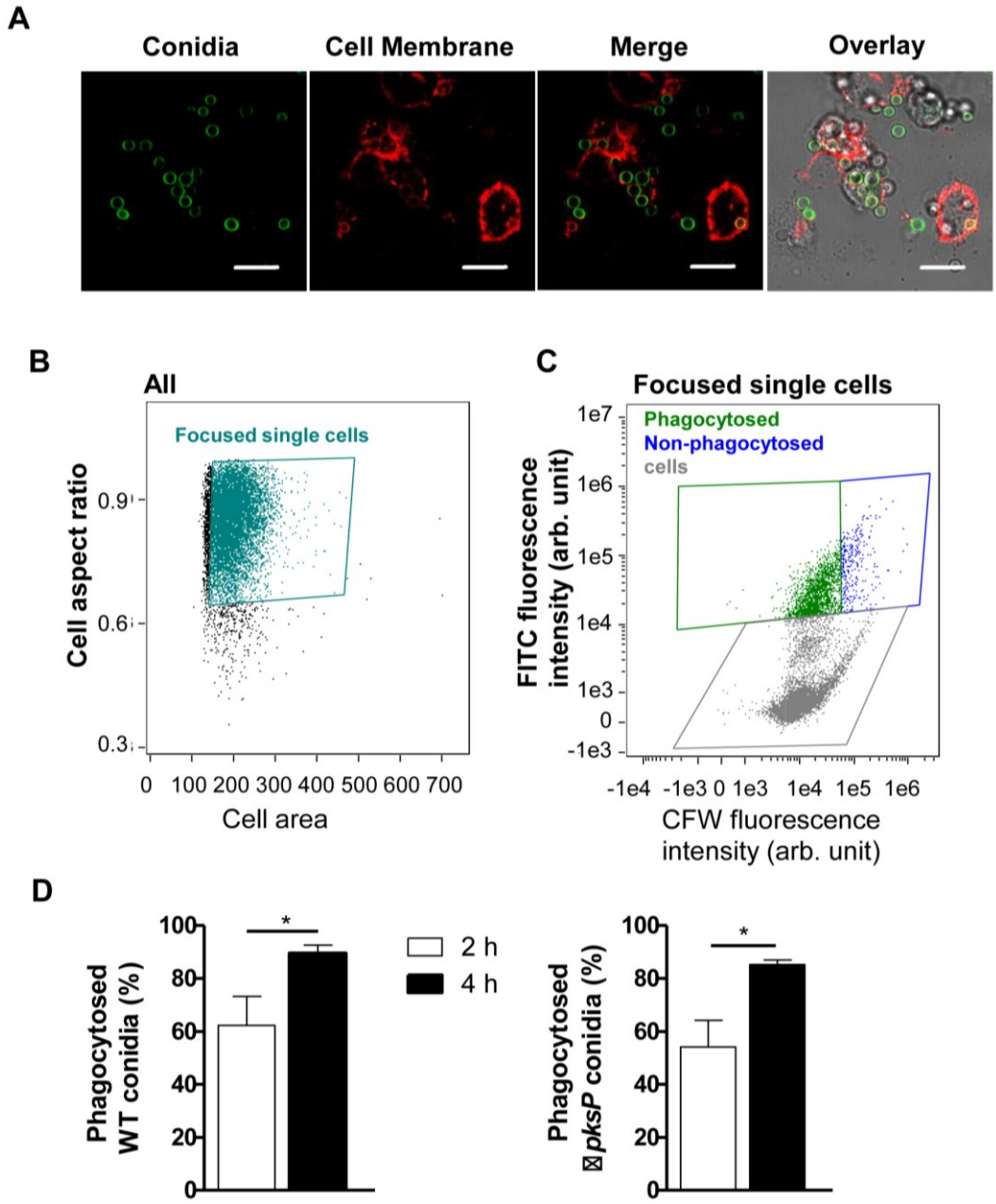

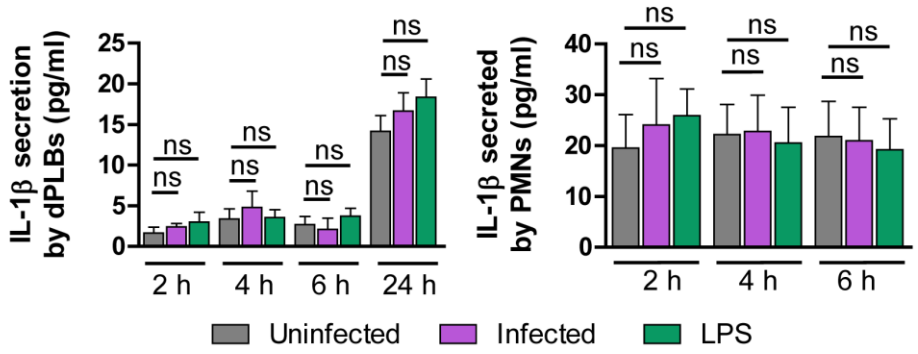
IL-1β secretion by dPLBs (pg/ml)
25
20
15
10
5
0
ns
ns
ns
ns
ns
ns
ns
ns
2 h
4 h
6 h
24 h
IL-1β secreted by PMNs (pg/ml)
40
30
20
10
0
ns
ns
ns
ns
ns
ns
2 h
4 h
6 h
Uninfected
Infected
LPS

Δ

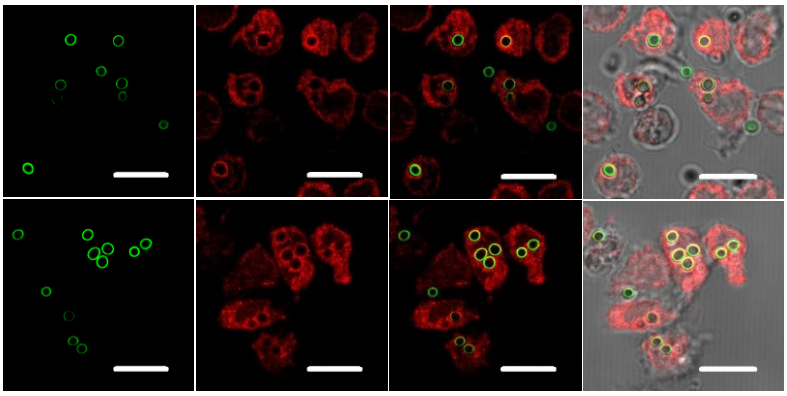

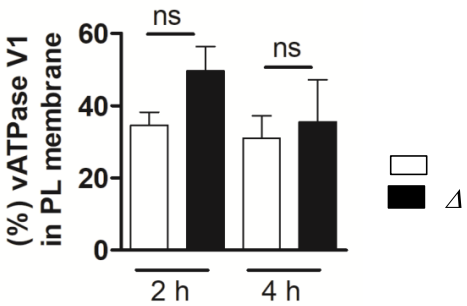

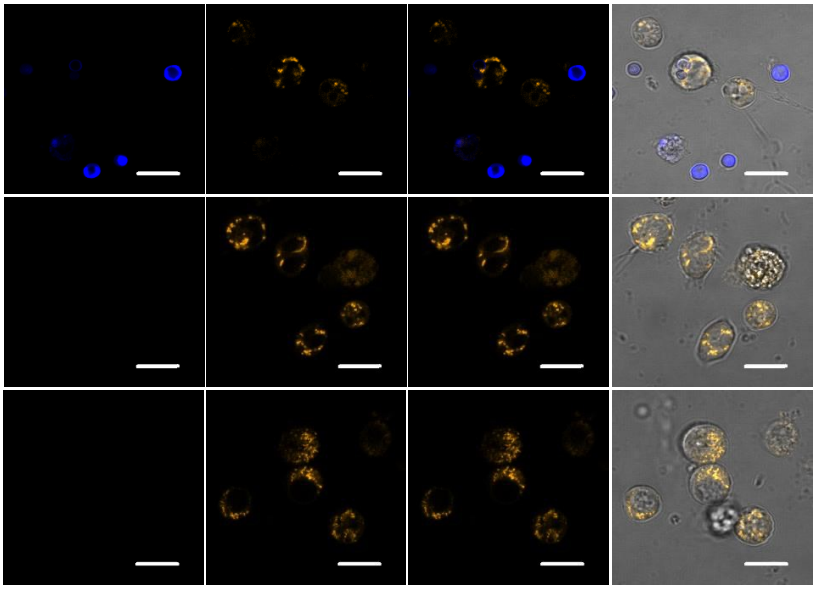

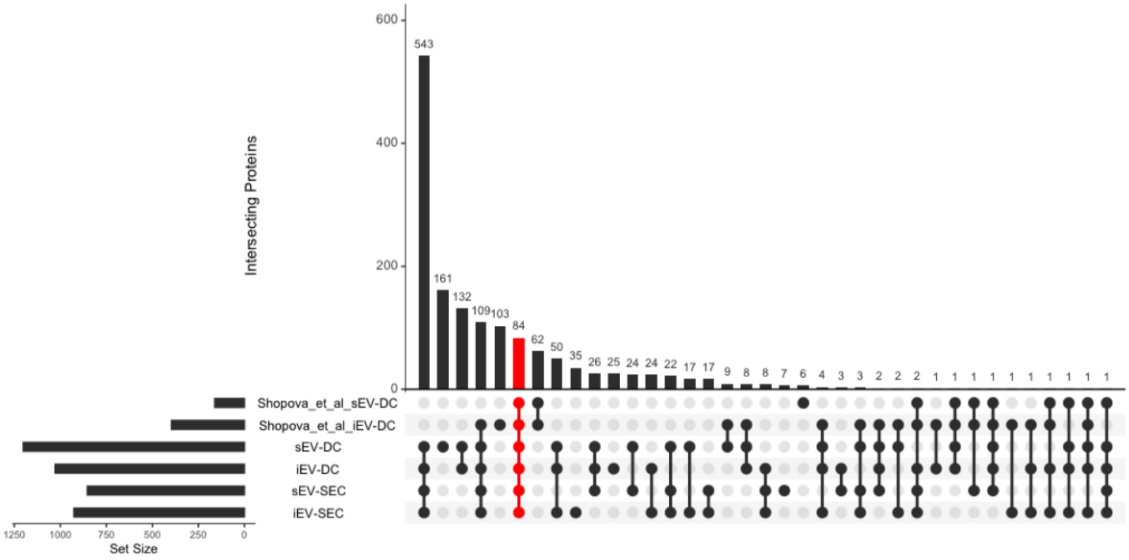
Intersecting Proteins
600
400
200
0
543
161
132
109
103
84
62
50
35
26
25
24
24
22
17
17
9
8
8
7
6
4
3
3
2
2
2
1
1
1
1
1
1
1
1
1
1
Shopova_et_al_sEV-DC
Shopova_et_al_iEV-DC
sEV-DC
iEV-DC
sEV-SEC
iEV-SEC
1250
1000
750
500
250
0
Set Size

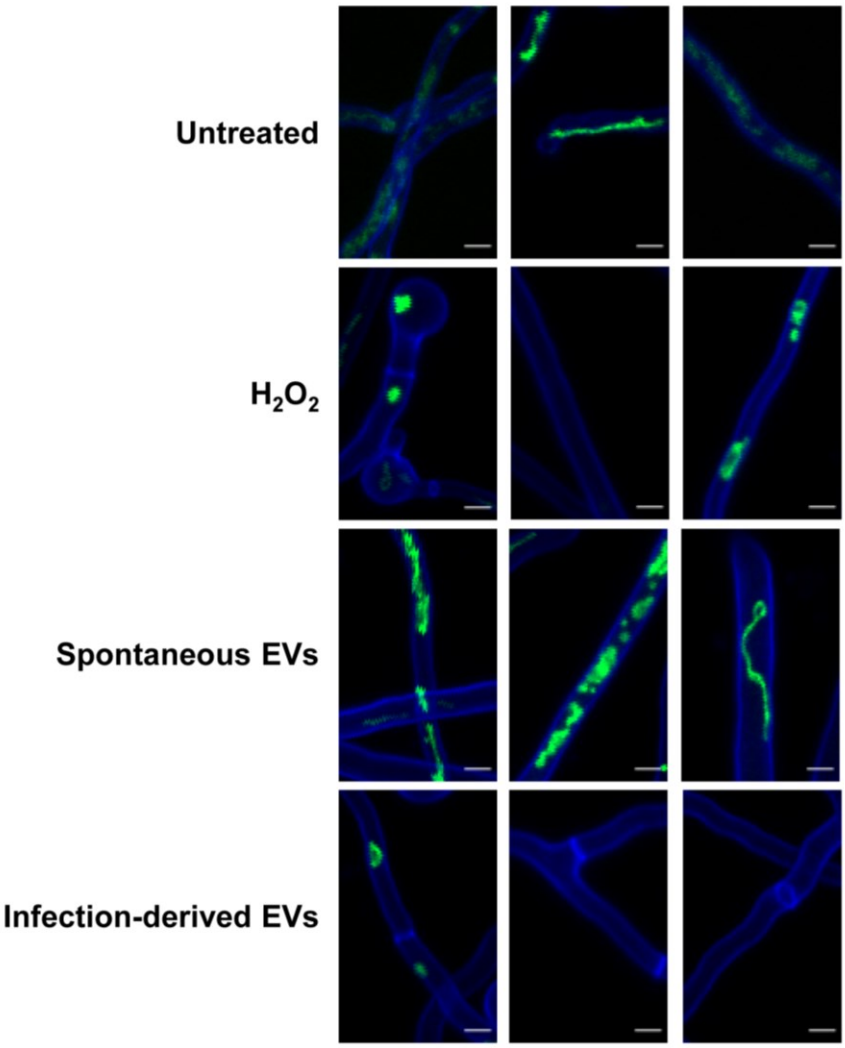
Untreated
H_2O_2
Spontaneous EVs
Infection-derived EVs

Table S1

Gene	Accession	Description	(PSMs/AAs)*(Cov%/100)
IGKC	P01834	Immunoglobulin kappa constant	3.45421
APOA1	P02647	Apolipoprotein A-I	1.73397
IGHM	P01871	Immunoglobulin heavy constant mu	1.26349
IGLC2	P0DOY2	Immunoglobulin lambda constant 2	0.82453
IGHG1	P01857	Immunoglobulin heavy constant gamma 1	0.51688
HBB	P68871	Hemoglobin subunit beta	0.43599
IGHG2	A0A286YEY4	Immunoglobulin heavy constant gamma 2 (Fragment)	0.27205
APOB	P04114	Apolipoprotein B-100	0.26471
IGHA1	P01876	Immunoglobulin heavy constant alpha 1	0.16677
C1QB	P02746	Complement C1q subcomponent subunit B	0.16126
NPTN	Q9Y639	Neuroplastin	0.12879
APCS	P02743	Serum amyloid P-component	0.12233
C1QC	P02747	Complement C1q subcomponent subunit C	0.07286
APOH	P02749	Beta-2-glycoprotein 1	0.06858
APOD	P05090	Apolipoprotein D	0.06349
EMB	D6RDX7	Embigin	0.04667
CFH	P08603	Complement factor H	0.02729
IGKV2-40	A0A087WW87	Immunoglobulin kappa variable 2-40	0.02545
DNAJA1	P31689	DnaJ homolog subfamily A member 1	0.01884
HPX	P02790	Hemopexin	0.01541
C4B	F5GXS0	C4a anaphylatoxin	0.00783
FN1	P02751	Fibronectin	0.00560
C3	P01024	Complement C3	0.00394
C8A	P07357	Complement component C8 alpha chain	0.00394
AHSG	P02765	Alpha-2-HS-glycoprotein	0.00229
C1R	B4DPQ0	Complement subcomponent C1r	0.00118

3. Manuscripts

3.4 Manuscript D

Dynamic optimization reveals alveolar epithelial cells as key mediators of host defense in invasive aspergillosis

Ewald J*, **Rivieccio F***, Radosa L, Schuster S, Brakhage A.A, Kaleta C.
* These authors contributed equally

Manuscript published on *Plos Computational biology* 17(12): e1009645; December 2021.

Summary:
Lung epithelial cells belong to the first line of defense of humans against the fungal pathogen *Aspergillus fumigatus*. However, until their role has been neglected. In this paper a dynamic optimization model, corroborated by experimental data, reveals the importance of fungal virulence factors, like germination rate, for the outcome of infection, and also the crucial role of epithelial cells in cytokine release in later stages of infection, after depletion of alveolar macrophages.

Contribution to the manuscript:
Flora Rivieccio was involved in the experimental part of the study, performing LDH assays, germination assays**,** isolation and cultivation of murine primary cells and cytokine measurements. Furthermore, she contributed to writing and editing the manuscript.

Estimated contribution in percentage:

Author	Conceptual	Data analysis	Experimental	Writing the manuscript	Provision of material
Ewald J.*	15%	25%	35%	20%	0%
Rivieccio F.*	**15%**	**25%**	**35%**	**20%**	**0%**
Radosa L.	5%	5%	15%	10%	0%
Schuster S	15%	10%	0%	20%	0%
Brakhage A.A	10%	5%	0%	10%	50%
Kaleta C.	40%	20%	15%	20%	50%
Total:	100%	100%	100%	100%	100%

PLOS COMPUTATIONAL BIOLOGY

RESEARCH ARTICLE

Dynamic optimization reveals alveolar epithelial cells as key mediators of host defense in invasive aspergillosis

Jan Ewald[1,2☯]*, **Flora Rivieccio**[3,4☯], **Lukáš Radosa**[3], **Stefan Schuster**[1]*, **Axel A. Brakhage**[3,4‡]*, **Christoph Kaleta**[5‡]

1 Department of Bioinformatics, Friedrich Schiller University Jena, Jena, Germany, **2** Center for Scalable Data Analytics and Artificial Intelligence (ScaDS.AI), University of Leipzig, Leipzig, Germany, **3** Department of Molecular and Applied Microbiology, Leibniz Institute for Natural Product Research and Infection Biology - Hans Knöll Institute (HKI), Jena, Germany, **4** Department of Microbiology and Molecular Biology, Institute of Microbiology, Friedrich Schiller University Jena, Jena, Germany, **5** Research Group Medical Systems Biology, Institute of Experimental Medicine, Kiel University, Kiel, Germany

☯ These authors contributed equally to this work.
‡ AAB and CK also contributed equally to this work.
* jan.ewald@uni-leipzig.de (JE); stefan.schu@uni-jena.de (SS); axel.brakhage@leibniz-hki.de (AAB)

Check for updates

OPEN ACCESS

Citation: Ewald J, Rivieccio F, Radosa L, Schuster S, Brakhage AA, Kaleta C (2021) Dynamic optimization reveals alveolar epithelial cells as key mediators of host defense in invasive aspergillosis. PLoS Comput Biol 17(12): e1009645. https://doi.org/10.1371/journal.pcbi.1009645

Editor: Amber M Smith, University of Tennessee Health Science Center College of Medicine Memphis, UNITED STATES

Received: June 30, 2021

Accepted: November 15, 2021

Published: December 13, 2021

Copyright: © 2021 Ewald et al. This is an open access article distributed under the terms of the Creative Commons Attribution License, which permits unrestricted use, distribution, and reproduction in any medium, provided the original author and source are credited.

Data Availability Statement: Origin of parameter values are described in detail in the Supporting information. The related model is submitted to BioModels Database, accession number: MODEL2105110001. Source code files to perform dynamic optimization was archived in https://doi.org/10.1101/2021.05.12.443764.

Funding: We acknowledge support by the Deutsche Forschungsgemeinschaft (DFG, German Research Foundation) CRC/Transregio 124

Abstract

Aspergillus fumigatus is an important human fungal pathogen and its conidia are constantly inhaled by humans. In immunocompromised individuals, conidia can grow out as hyphae that damage lung epithelium. The resulting invasive aspergillosis is associated with devastating mortality rates. Since infection is a race between the innate immune system and the outgrowth of *A. fumigatus* conidia, we use dynamic optimization to obtain insight into the recruitment and depletion of alveolar macrophages and neutrophils. Using this model, we obtain key insights into major determinants of infection outcome on host and pathogen side. On the pathogen side, we predict *in silico* and confirm *in vitro* that germination speed is an important virulence trait of fungal pathogens due to the vulnerability of conidia against host defense. On the host side, we found that epithelial cells, which have been underappreciated, play a role in fungal clearance and are potent mediators of cytokine release. Both predictions were confirmed by *in vitro* experiments on established cell lines as well as primary lung cells. Further, our model affirms the importance of neutrophils in invasive aspergillosis and underlines that the role of macrophages remains elusive. We expect that our model will contribute to improvement of treatment protocols by focusing on the critical components of immune response to fungi but also fungal virulence traits.

Author summary

Fungal infections are an increasing problem and threat for individuals which suffer from an impairment of immune functions due to immunosuppressive therapies or diseases. In those patients the innate immune response is not able to efficiently clear fungal cells from body surfaces and stop an invasive growth into tissues and bloodstream infections.

'Pathogenic fungi and their human host: Networks of interaction' (support code 210879364) sub project B1 (J.E. and S.S.) and A1 (F.R. and A.B.). Further, C.K. acknowledges support by the DFG under Germany´s Excellence Strategy 'Precision Medicine in Chronic Inflammation' – EXC 2167 – Project-ID 390884018 and L.R. under Germany´s Excellence Strategy 'Balance of the Microverse' – EXC 2051 – Project-ID 390713860. The funders had no role in study design, data collection and analysis, decision to publish, or preparation of the manuscript.

Competing interests: The authors have declared that no competing interests exist.

Aspergillus fumigatus is a ubiquitous mold as well as potent pathogen causing life-threatening infections, invasive aspergillosis, via lung inhalation of fungal spores (conidia). The innate immune response against conidia in the lung alveoli is a highly dynamic process and involves the interplay of immune cells like macrophages and neutrophils as well as lung epithelial cells. In the presented study, we used the mathematical approach of dynamic optimization to understand the roles of human cells and virulence factors of *A. fumigatus* in a quantitative and time-resolved manner. Our model predicts that lung epithelial cells play an important role in fungal clearance and contribute to pro-inflammatory signaling by cytokine release upon conidial stimulation. Further, this so far underappreciated role of epithelial cells and other findings are supported by experiments with established cell lines and primary lung cells of mice as model host organism.

Introduction

Since we constantly inhale microorganisms, the human lung is an entry point for opportunistic pathogens, like the mold *Aspergillus fumigatus* [1, 2]. Besides being a saphrophyte involved in the decay of organic matter in soil, *A. fumigatus* possesses virulence characteristics such as small spores (conidia), a fast growth at body temperature and the production of specific proteins, carbohydrates and secondary metabolites allowing its immune evasion [3–7]. These traits enable *A. fumigatus* to reach the lung's alveoli and cause invasive aspergillosis by filamentous growth (hyphae) into the tissue and dissemination into the host [5, 8]. In immunocompetent hosts this is prevented by the fast and efficient clearance of conidia by the innate immune system within a few hours [7, 9]. However, once *A. fumigatus* grows invasively facilitated by a suppressed immune system, mortality is very high (30–95%) due to non-efficient diagnostics and limited treatment options [10–13].

Along with the advances in medical care the number of patients with defects and suppression of their immune system is expected to grow. Major causes for this trend are the increasing number of cancer patients receiving chemotherapy [14, 15], organ transplant recipients [16] or patients with acquired immune deficiency syndrome (AIDS) [17]. Most recently, a high number of COVID-19 patients in intensive care units with extensive ventilation has been accompanied with secondary fungal infections due to *Aspergillus spp.* [13, 18].

The race between fungal growth and host immune response is complex and involves many cells like alveolar epithelial cells (AEC), alveolar macrophages (AM) and recruited neutrophils [7, 9]. To better understand this spatial and dynamic process computational modeling has proven to be of value [19–24]. These models are based on agent-based modelling or differential equation systems and contribute to a better understanding of the immune response. In particular, the meaning of spatial-dynamics of AM clearing conidia [20, 22, 23, 25] as well as the influence of the initial fungal burden on clearance and persistence of *A. fumigatus* were studied [19]. A major achievement and advantage of *in silico* models is the integration of existing biological knowledge and the generation of new hypotheses by disclosing knowledge gaps.

Despite extensive modeling and experimental investigations, the relative contribution of individual host immune cell types in invasive aspergillosis remains elusive [8]. For example, AM were identified as phagocytes of conidia [26] and release cytokines upon fungal infection [27]. Yet, AM depletion in mice at early phases of infection showed no effect on mortality while depletion of neutrophils was accompanied with low survival rates [28]. Current models and their analysis are based on immune cells and virtually neglect the contribution of AEC to cytokine release and fungal clearance. Experimental data obtained *in vitro*, however, suggest

that AEC can act as potent phagocytes [29] and release a significant amount of cytokines during their interaction with conidia [30]. Additionally, the importance of AEC in the promotion of neutrophil recruitment has been shown *in vivo* [31] and it has been postulated that AEC represent a 'neglected portal entry of *Aspergillus*' [7]. Therefore, the focus of our presented model here, is to dissect the contributions of AEC and innate immune cells for defense against *A. fumigatus*.

To elucidate the dynamic process of invasive aspergillosis during the first 24h, we propose a model using dynamic optimization as a mathematical approach. The mathematical concept of a dynamic system described by differential equations and regulated by control variables matches the dynamics of the innate immune response with recruitment and depletion of neutrophils and AM (mainly by maturation of monocytes). Due to this advantage, dynamic optimization has also been used to model other host-pathogen interactions and immune responses [24, 32–34] and makes use of the fact that these energy-demanding processes are highly optimized during evolution [35]. Our presented model, in addition, not only elucidates the complex recruitment dynamics of immune cells, but we also studied the role of AEC during early stages of fungal infection. To proof key variables of the model and thus its validity, major findings like fungal germination and cytokine release were experimentally evaluated.

Results

Model overview

The aim and scope of our modeling are a better understanding of the decisive parameters and interactions contributing to infection by *A. fumigatus* in the first 24h. To this end, we model the different growth states of *A. fumigatus* and their interaction with the innate immune response in the lung alveoli during the first hours of infection (see Fig 1). In addition, we explicitly model AEC as interactive cells and consider a single dose scenario of fungal conidia exposure. The latter modeling decision enables comparison of results and parameters to experimental animal models, which mainly use single dose regimes [36, 37].

Our model based on ordinary differential equations (ODE) considers time-dependent transition kinetics to describe the process of swelling and germination of conidia (detailed description in Subsection Model formulation). After germination, growth of *A. fumigatus* as hyphae depends on the presence of AEC as resource. Importantly, we accurately model interaction of each cell type with all host cell types. Resting conidia are far less recognized or killed due to their coating and swollen conidia are phagocytosed and killed by AM, neutrophils and AEC. Since AM and AEC are unable to phagocytose and kill larger hyphae at reasonable rates [38, 39], we only model killing of hyphae by neutrophils.

Host cell dynamics are characterized by damage, host or pathogen mediated, and transmigration of immune cells. In our dynamic optimization model, AEC face lysis by hyphae and damage by activated immune cells. While AM and neutrophils like AEC show cell death upon interaction with fungal cells, their transmigration upon infection is modeled by recruitment and depletion. In fact, the changes in cell number in our model can reflect also cell proliferation or programmed cell death. However, for simplicity we refer in the following to it as transmigration by recruitment and depletion including all other processes of host cell number control.

The maximal rate of recruitment and depletion is linked to the presence of pro-inflammatory cytokines and is optimized in our dynamic optimization approach via the control variables u_{1-4} (see Fig 1 and *cf.* Materials and methods, Subsection Model formulation). In our model we capture the release of cytokines by AM as well as AEC to reveal their respective contribution during infection.

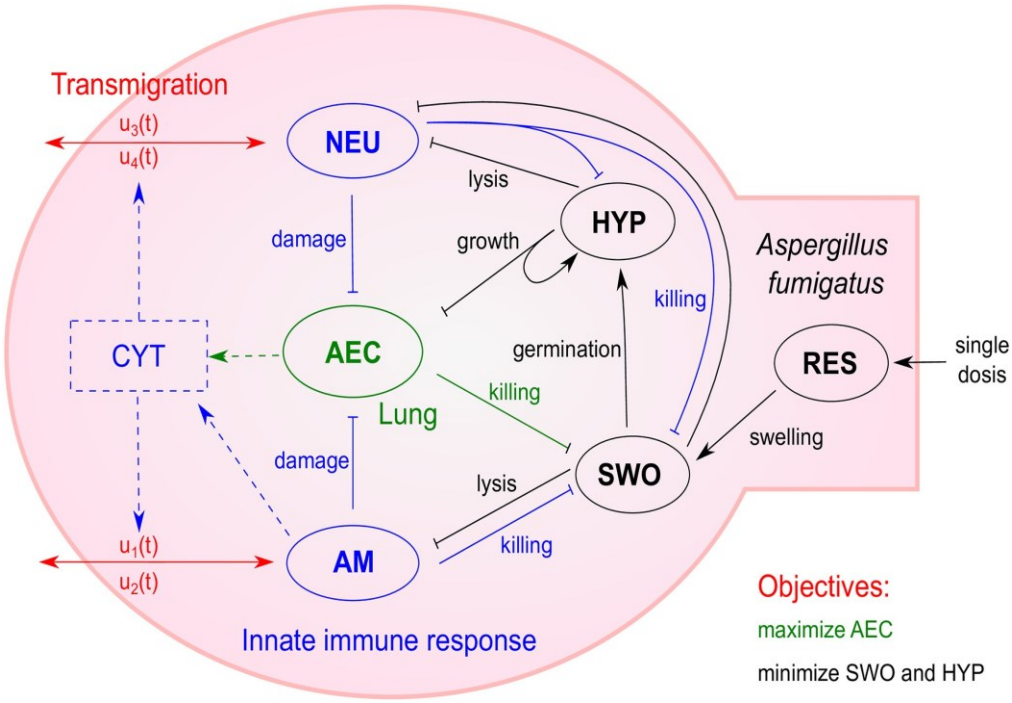

Fig 1. Model of invasive aspergillosis and the innate immune response as dynamic optimization problem. The different fungal growth states (black) including resting conidia (RES), swollen conidia (SWO) and hyphae (HYP) interact with alveolar epithelial cells (AEC, green) as well as with neutrophils (NEU, blue) or alveolar macrophages (AM, blue). Immune cell population is optimized via transmigration (red), which is linked to the cytokine level (CYT, blue), and optimal recruitment and depletion attain the trade-off between pathogen minimization and tissue integrity. Arrow heads indicate a positive interaction and bars show negative interactions.

https://doi.org/10.1371/journal.pcbi.1009645.g001

As host objectives we define two main goals, which are optimized during infection. Firstly, active fungal cells (swollen conidia and hyphae) should be minimized at all time points to avoid systemic infection. Secondly, unnecessary tissue damage *e.g.* due to hyperinflammation and collateral damage mediated by immune cells must be minimized. The consideration of only one of the objectives leads to undesired dynamics like continued hyphal growth or extensive tissue damage, as shown in S2 Appendix. Hence, we performed optimization with an equal weighting of both objectives. We did not opt for an alternative formulation of the objective function like the inclusion of energy requirements of the immune response or a more detailed quantification of the weighting between those objectives. This is mainly due to the difficulty of quantification of the related parameters (energy requirements) and the lack of time course data required for a multi-objective dynamic optimization (inverse optimal control) [40].

Parameters and time course of early immune response

For our dynamic optimization model of the innate immune response during early invasive aspergillosis, reference parameters were estimated based on an extensive study of existing data and literature (see S1 Appendix). The model focuses on the events in the alveoli during the first 24h and we normalize all cell populations per alveolus. Experimental studies and data reveal that the average number of AEC is 11.4 (type I and II combined) in a healthy mouse [41, 42]. Type I cells cover up to 95% of the alveolar surface and are more likely to come in contact

with conidia, while type II cells are more responsible for tissue repair and integrity [43]. Further, both types of cells can secrete pro-inflammatory cytokines upon stimulation [44]. Hence, we combined both cell types for the sake of simplicity as AEC in our model. On average in every third or fourth alveolus an AM, respectively a neutrophil, is resident [45]. In animal models of invasive aspergillosis typically initial conidia doses of 10^5 to 10^7 are applied as single dose [7, 37]. Since there are around $2.3 \cdot 10^6$ alveoli in a murine lung [42] and not all conidia reach an alveolus, one resting conidium per alveolus relates to a typical fungal burden during experiments.

To elucidate the general pattern of innate immune response during invasive aspergillosis, we simulated 500 randomized parameter sets, where each parameter follows a log-normal distribution with the estimated reference value as the mode (maximum of distribution). The calculated time courses of the dynamic optimization reveal that healthy mice are able to clear even high fungal burden without a complete destruction of the epithelial cell barrier (see Fig 2 and details of solving the dynamic optimization in Subsection Solving the optimization problem and parameter sensitivity). This is achieved by a rapid cytokine release by AM as well as AEC and recruitment of neutrophils after conidial swelling. After 10 to 15h, recruitment of neutrophils is stopped and the immune cells are depleted to avoid unnecessary tissue damage. In this regard, our model well reflects experimental observations [46] and depicts the trade-off between pathogen clearance and tissue damage by the innate immune response. In our model, interestingly, AM are not recruited in large quantities and are mostly depleted after germination of conidia. Based on our estimated parameters of the kinetic rates, this is mostly due to slower killing of conidia compared to neutrophils and the ability of AEC to release cytokines in large quantities.

Parameter sensitivity reveals importance of fungal growth parameters

To better understand the roles of immune cells and AEC, we analyzed parameter sensitivity and simulated several scenarios to study the effect of immunodeficiencies and dosage of conidia.

We determined decisive parameters for the outcome of infection by calculating the contribution to variance in the objective function of each randomized parameter (see Materials and methods, Subsection Solving the optimization problem and parameter sensitivity). Further, we simulated healthy mice and lack of immune cells as well as the influence of low or high doses of conidia. Across all scenarios the fungal parameters s_1 (germination time of a swollen conidium) and h_1 (hyphal growth rate) are most decisive for infection outcome since they explain more than 50% of the variance in the objective function (see Fig 3). This illustrates that fast germination of swollen conidia is a strong virulence attribute, because it is the most vulnerable growth state of the pathogen. The growth rate of hyphae is in addition crucial in the race between neutrophils (recruitment and hyphal killing) and *A. fumigatus*.

On the host side, the importance of some parameters differs significantly when the initial fungal burden is altered. Interestingly, at lower doses immune cell parameters like the number of resident neutrophils $N(0)$ or rate of hyphal killing h_2 are important (see Fig 3). However, at higher doses parameters of AEC, such as conidia phagocytosis (s_4) or cytokine release (c_2), are more important for the infection outcome and contribute nearly 20% to the variance in the objective function. The parameter sensitivity and time course of infection indicate that at low doses the control of hyphal growth is most important, while at high doses AEC are crucial to lower the number of swollen conidia. These results are noteworthy since parameters related to functions of AM only show even when combined a minor influence on the infection outcome (3.7% at high dose and 9.5% at low dose). Typically, AM are extensively studied since they

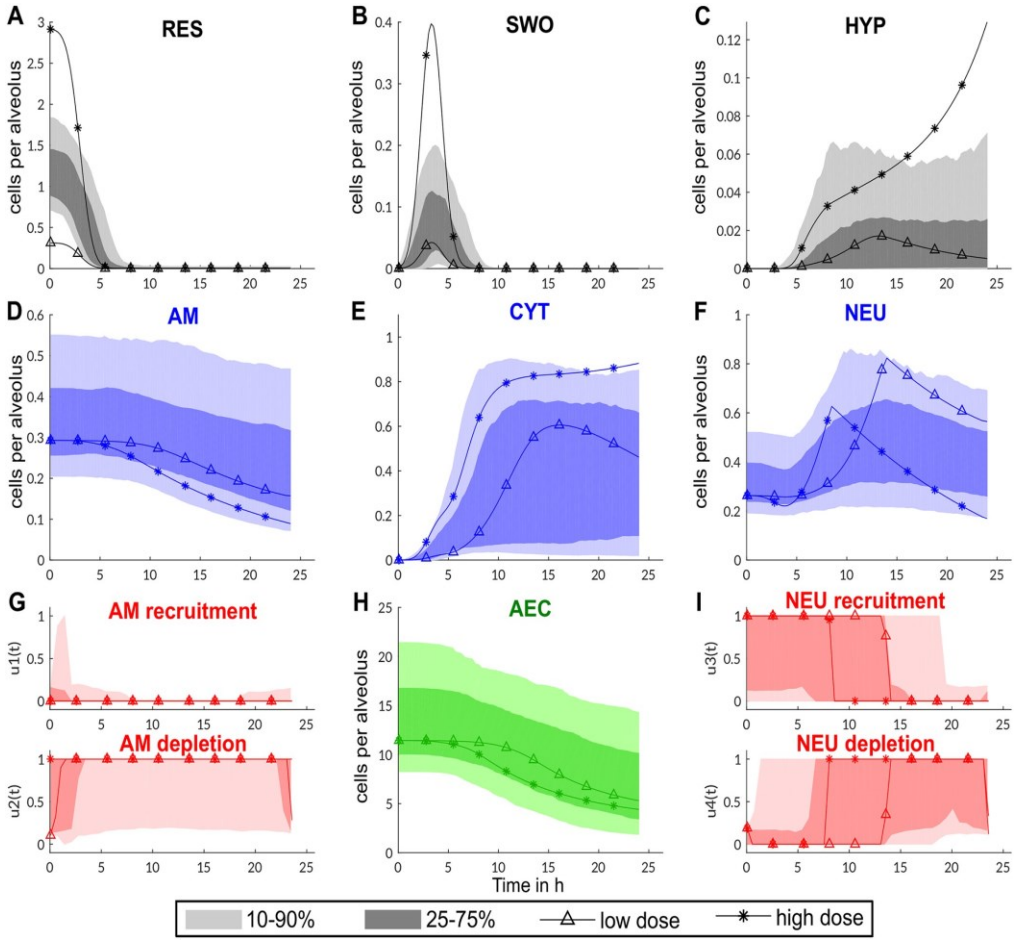

Fig 2. Dynamics of innate immune response of the murine host for varying parameters (shadings) and two dose scenarios of conidia based on the reference parameter set (lines). **A-C** Dynamics of fungal cells per alveolus. **D, F** show the dynamics of the immune cells per alveolus which are influenced by the optimized recruitment and depletion rates in panels **G** and **I** (rates between 1, maximal, and 0, no recruitment/depletion). Recruitment and depletion potential is dependent on the cytokine level (**E**). Cytokines are produced by alveolar macrophages (**D**) and alveolar epithelial cells (**H**) in response to swollen conidia (**B**) or hyphae (**C**). The simulations of 500 parameter sets are depicted with shadings indicating the confidence intervals of time courses.

https://doi.org/10.1371/journal.pcbi.1009645.g002

belong to the first line of defense. However, our parameter sensitivity results do not disclose a singular and distinctive role and we therefore performed additional analyses in the following sections.

Further insights were gained by studying the changes in parameter influence under scenarios of immunodeficiencies like the lack of monocytes (progenitor cells of AM) or neutrophils which were simulated as reduced immune cell populations and recruitment rates (1% of normal value). In both scenarios simulating monocytopenia or neutropenia, fungal virulence factors are even more important for infection outcome (see Fig 3). But there are different tendencies as to which factor is more important. During monocytopenia, here for simplicity expressed as a lack of AM, the time span for germination, s_1, is more important. This suggests that AM are mainly involved in the control of swollen conidia (see Fig 3). In contrast, during

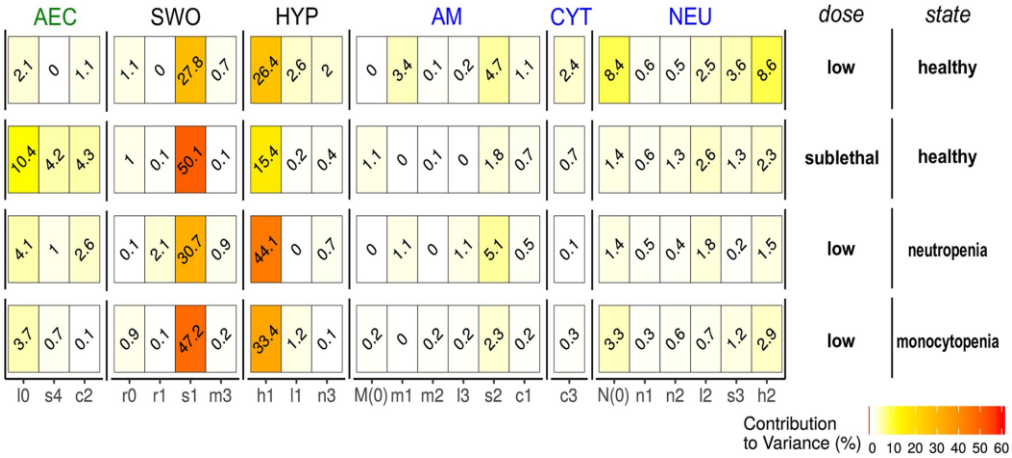

Fig 3. Influence of parameters on the outcome of infection depicted by the contribution to variance (colored from white, yellow to red from no to high influence). This relative contribution is based on a Spearman rank correlation of the parameter value and the objective value of the optimal solution (see Materials and methods, Subsection Solving the optimization problem and parameter sensitivity). Parameters are grouped based on their relation to cell types: alveolar epithelial cells (AEC), resting (RES) or swollen conidia (SWO), hyphae (HYP), alveolar macrophages (AM) and neutrophils (NEU). In addition the cytokine (CYT) property c_3 (decay rate) is listed.

https://doi.org/10.1371/journal.pcbi.1009645.g003

neutropenia the hyphal growth rate is more decisive for the infection outcome (see Fig 3) supporting the observation that neutrophils are crucial to prevent filamentous growth.

To support the findings established by modeling, we performed an experimental investigation of fungal virulence parameters by the comparison of different *Aspergillus* species. As revealed by the parameter sensitivity analysis, a key virulence factor is fast germination to minimize the time period of the vulnerable swollen-conidia state. The common species *A. fumigatus*, *A. nidulans*, *A. niger* and *A. terreus* show differences in their germination kinetics at 37°*C*, where *A. nidulans* is fastest, *A. fumigatus* as well as *A. niger* are around 1–2h slower and *A. terreus* is by far the slowest with an average germination time of $> 24h$ (see Fig 4A and 4B). Our model predicts here a non-linear but distinctive relationship between the germination time and epithelial damage after 24h (see Fig 4C). It suggests that virulence expressed as epithelial damage is strongly reduced if the germination time is longer than 10h.

Strikingly, in an experimental set-up where human (A549 cell line) and murine (T7 cell line) lung AEC are co-incubated with *Aspergillus spp*. for 24h, only those species with fast germination showed a pronounced host cell damage (see Fig 4D and 4E and *cf.* S1 Fig for different multiplicities of infection). Moreover, cytotoxicity against human cells coincides with germination speed and strongly supports model prediction. However, we observed a higher cytotoxicity of *A. fumigatus* against murine AEC while other species show comparable results (see Fig 4E). This underlines the importance of further investigations to understand differences between the human host and rodent model organisms. Further, it suggests an avoidance of elevated epithelial damage by *A. fumigatus* and its ability to hide and escape in AEC during the human immune response.

The accordance of prediction based on modeling with experimental data on germination as well as cytotoxicity shows that our dynamic optimization approach is able to identify key parameters of invasive aspergillosis. However, since *A. fumigatus* is the most common cause of invasive aspergillosis [10] in spite of its slightly slower germination than *A. nidulans*, the interaction of fungal pathogens with host cells and parameters defining this process require additional decisive factors for infection outcome.

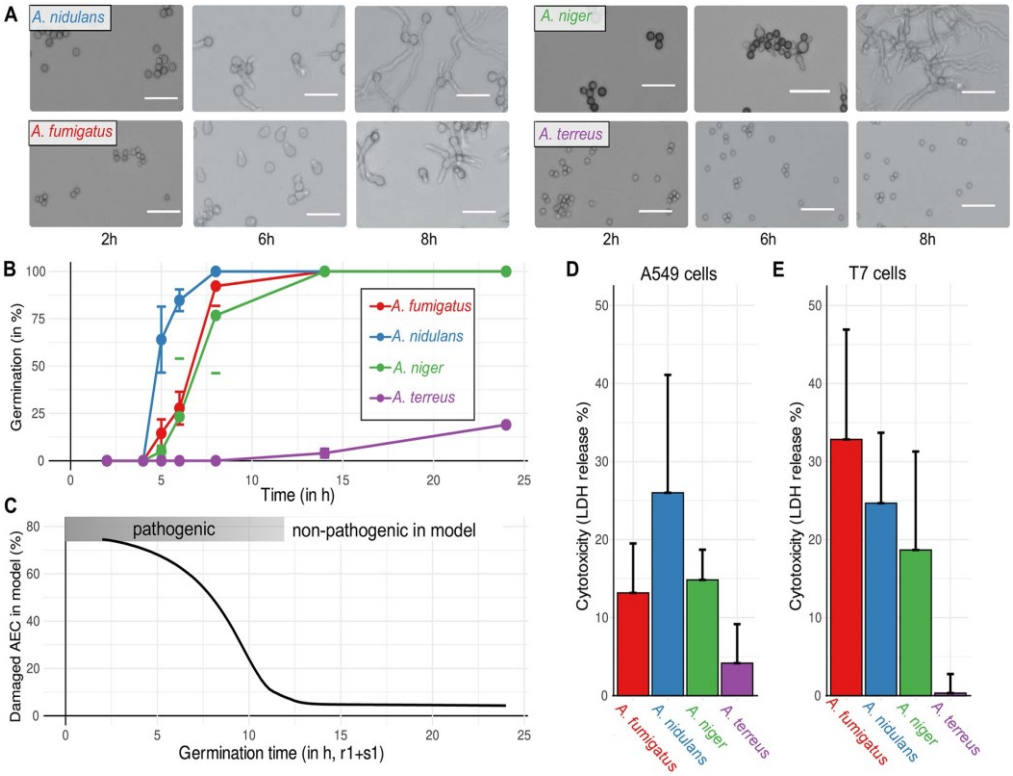

Fig 4. Germination kinetics of *Aspergillus spp*. and its impact on epithelial cytotoxicity. **A** Microscopic images (white scale bar, 20μm) of germination assays on RPMI medium to automatically count and derive germination kinetics as shown in **B** for the species *A. fumigatus* (red), *A. nidulans* (blue), *A. niger* (green) and *A. terreus* (purple). Error bars represent the standard deviation of four replicates. **C** the relation of germination time and damage of AEC after 24h in the dynamic optimization model and parameter range with expected pathogenicity. Model prediction in **C** is compared to experimental cytotoxicity of *Aspergillus spp*. by lactate-dehydrogenase (LDH) release measurements after 24h co-incubation with human A549 epithelial cells in **D** and with murine T7 epithelial cells in **E**. Error bars represent the standard deviation of six replicates.

https://doi.org/10.1371/journal.pcbi.1009645.g004

To this end, in the following part the specific roles and functions of host cells are investigated by modeling and supported by experimental investigations.

Neutrophils and epithelial cells primarily promote fungal clearance and cytokine release

The advantage of our model is that we can suppress a host cell population or function *in silico* to study their role and importance for infection outcome. This way we can simulate animal models with immunodeficiencies like neutropenia that is triggered by usage of cyclophosphamide and cortisone acetate in murine models of invasive aspergillosis [47]. The analysis of parameter sensitivity provides a global overview about the correlation between infection parameters and infection outcome. However, the causality of parameter influence is not explained. To this end, we performed additional *in silico* experiments with varying conidial doses to understand and link host cell functions to infection outcome.

The conidia dose-response-curves clearly indicate that lack of neutrophils heavily worsens infection outcome across all dose scenarios and host damage is barely dose-dependent (see Fig 5A and 5B). Further, both objectives, *i.e.*, the preservation of tissue and reduction of the fungal

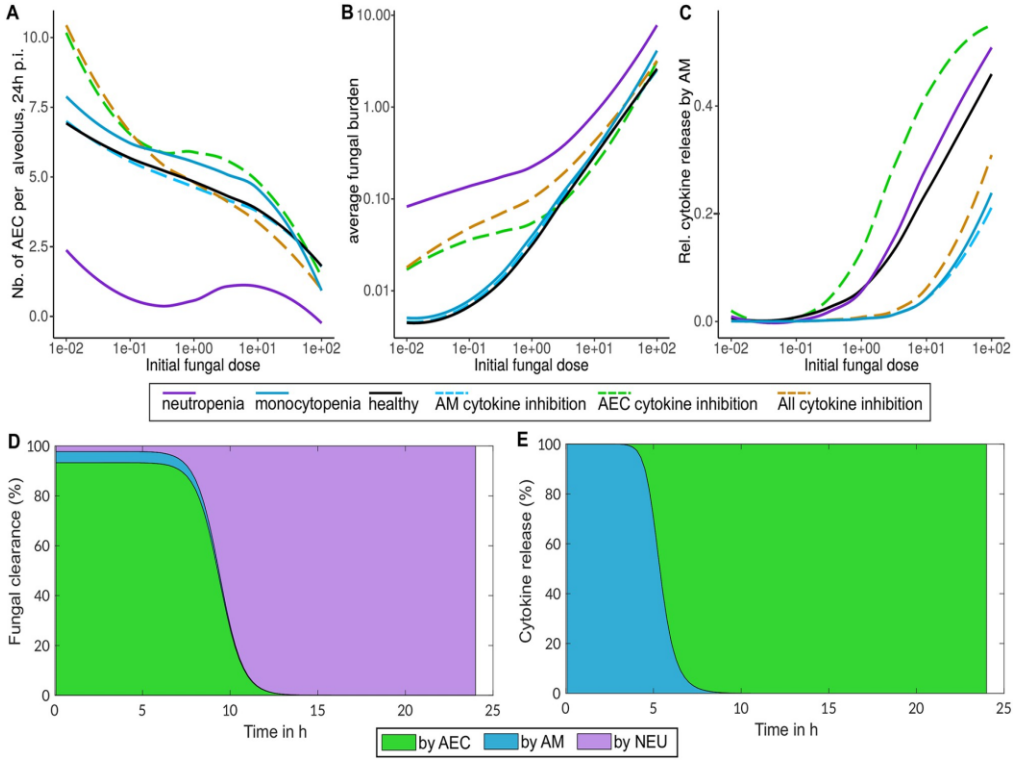

Fig 5. Relative contribution of host cells during infection. A-C Dose-response-curves with varying conidia doses (x-axis) and the remaining number of epithelial cells at the end of simulation in **A** or the average fungal burden during simulation in **B**. The relative contribution of alveolar macrophages to cytokine release depending on the initial conidia dose in **C**. Response curves were determined for the following disturbances: lack of immune cells (1% neutrophils, solid violet; 1% macrophages solid light blue) and cytokine release inhibition (1% of cytokine release by alveolar macrophages (AM, dashed light blue), 1% release by alveolar epithelial cells (AEC, dashed green) or 1% release from both (dashed brown). **D, E** Role of macrophages (AM), neutrophils (NEU) and epithelial cells (AEC) in fungal clearance **D** and cytokine release **E** in the dynamic optimization model over time as percentage of total at each time point. Fungal clearance is calculated as the sum of killing all fungal cell types (conidia and hyphae).

https://doi.org/10.1371/journal.pcbi.1009645.g005

burden, are more impaired by neutropenia than by all other deficiency scenarios including lack of AM or an inhibition of cytokine release. Interestingly, lack of AM or an inhibition of cytokine release by AM show no major differences in the infection outcome compared to the reference parameter set of healthy mice (see Fig 5A and 5B). The optimization results for the inhibition of cytokine release by AEC or by both, AEC and AM, indicate a shift in the immune objective at low conidia dosage. In comparison to healthy mice, lung tissue is more preserved at low conidia concentrations, but with the drawback of a higher average of fungal burden during the simulated time of infection.

In our model AM and AEC exhibit overlapping functions and duties during infection. Both are able to clear swollen conidia and to release cytokines for immune cell recruitment. However, their contribution is different depending on the initial fungal burden and during the dynamic stages of infection. When the dose of conidia is low, the relative contribution of AM to cytokine production is nearly zero and most importantly, germination and hyphal growth are recognized by AEC (see Fig 5C). The relative contribution to cytokine release by AM rises to > 40% at very high conidia concentrations (see Fig 5C) indicating that AM are more important when a high number of swollen conidia is present (10–100 spores per alveolus).

This finding is supported by the relative contribution of each cell type to fungal clearance and cytokine release over the time course of infection (see Fig 5D). During infection, according to our model, AM are responsible for early recognition of conidia, whereas AEC are the main cytokine releasing cells after germination. However, the low quantity of AM compared to AEC, lead to a much higher cytokine release by AEC compared to AM in absolute and relative terms during infection (see Fig 5E).

The prominent role of AEC in pro-inflammatory cytokine production and their major contribution to phagocytosis is not captured by other models of invasive aspergillosis [19, 21] and indicates an underestimated importance of these cells for the immune response. To quantify and support findings predicted by our model, *ex vivo* experiments with murine cells were performed and pro-inflammatory cytokines (TNF)-α and (IL)-6 were measured upon stimulation with *A. fumigatus* by enzyme-linked immunosorbent assay (ELISA). These cytokines were selected because of their prominent role during invasive aspergillosis in mice [46, 48–50]. Whereas AM mainly produce (TNF)-α after 6h of infection with conidia, murine AEC mainly produce (IL)-6 after 10h (see Fig 6A). At similar cell counts AM produce earlier (6h versus 10h), but less in absolute terms in comparison to AEC when excess release upon conidial challenge of both cytokines, (TNF)-α and (IL)-6, is combined (see Fig 6B). Considering the higher number of AEC than AM in an alveolus, these experimental findings strongly support our model that AEC are important mediators of the immune response.

Moreover, our model reveals that AEC are important phagocytes and are predicted to be the main cell type clearing fungal spores in the first hours of infection (see Fig 5D). Nevertheless, after germination neutrophils are decisive for fungal clearance by killing hyphae. These findings highlight that the alveolar epithelial cells fulfill a major role in fungal clearance but also in immune cell recruitment by cytokine release.

Discussion

In this study we deduced a unique model based on dynamic optimization to better understand the innate immune response during invasive aspergillosis. Main and distinctive features of the model are the optimization of the recruitment of immune cells depicting the trade-off between tissue integrity and pathogen clearance (dynamic optimization) as well as the active role of lung AEC in the immune response. While there is uncertainty in the kinetic description of the infection dynamics, it clearly provides a time-resolved insight into the roles of host cells and factors contributing to virulence. Further, the possibility to consider several cell types and inclusion of non-metabolic processes is a big advantage over other modeling techniques like flux balance analysis or statistical thermodynamics [51, 52].

The simulations and analyses of our model revealed key parameters and distinctive roles of host cells during the innate immune response against *A. fumigatus* and other Aspergilli. We identified the morphotype 'swollen conidia' to be most vulnerable for the attack by the host. Hence, the duration of this state is minimized by the fungus in order to escape phagocytosis and, subsequently, outcompete host cells by fast growth of hyphae. While this was indicated by experimental studies linking fungal traits with clinical observations [53, 54], we here report a quantification of this relationship. Further, we provide experimental evidence by determining the germination kinetics of different *Aspergillus spp*.. Further evidence for our model is given by data on the cytotoxicity against human and murine AEC by these fungi. Our results support the finding that the highly virulent strain of *A. fumigatus* CEA10 possesses a faster and higher germination rate in the lung environment accompanied with a more extensive lung damage than the less virulent strain Af293 [55]. Interestingly, in our and other studies *A. nidulans* showed fastest germination and a rather high damage to AEC. Since *A. nidulans* is not the

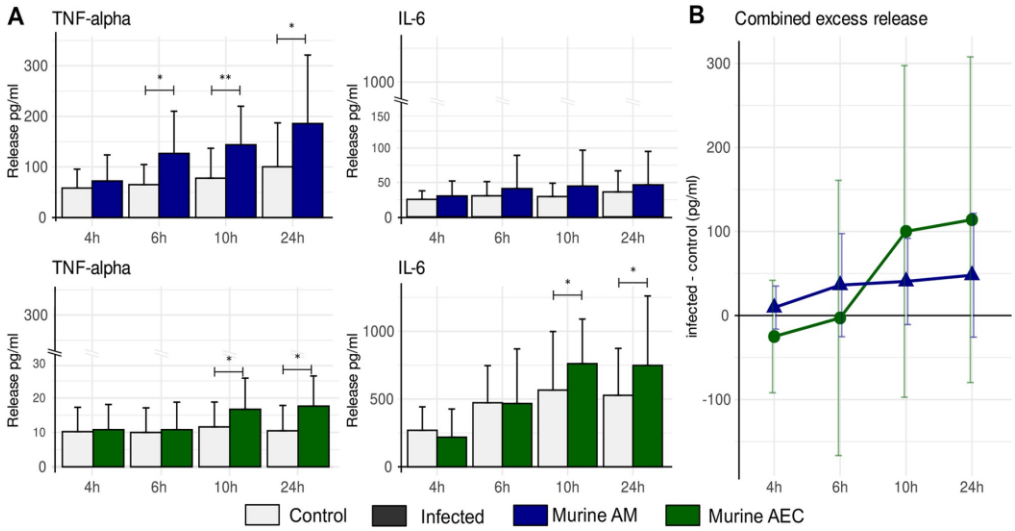

Fig 6. ***Ex vivo*** **cytokine release of isolated murine alveolar macrophages (AM, blue) and epithelial cells (AEC, green) upon infection with** ***A. fumigatus*****. A** Release of (TNF)-α and (IL)-6 over time in infected and control cells measured by ELISA. Significant differences between control and infected cells were determined by a two-tailed and paired t-test indicated by * ($p < 0.05$) and ** ($p < 0.01$). Error bars represent the standard deviation from nine mice used for cell isolation. **B** Combined cytokine release of both (TNF)-α and (IL)-6 in excess over spontaneous release over time to depict contribution during early and later stages of fungal infection.

https://doi.org/10.1371/journal.pcbi.1009645.g006

leading cause of invasive aspergillosis in humans [56], it is likely that this species lacks immune evasion mechanisms in comparison to *A. fumigatus* [38]. Hence, important fungal virulence traits of *A. fumigatus* are presumably linked to an efficient escape or inhibition of phagocytosis in comparison to *A. nidulans*. This conclusion is supported by the observation that *A. fumigatus* showed stronger cytotoxicity against murine cells in comparison to human AEC (see Fig 4D and 4E). While this indicates an adaption of *A. fumigatus* to hide and reside in human AEC from other immune cells, further investigation is necessary to understand the differences between the human host and rodent model organisms.

As crucial host parameters for infection outcome we reaffirmed the importance of neutrophils to control filamentous growth of *A. fumigatus* which confirms that dysfunctional hyphal killing by lack of neutrophils or non-functional neutrophils is a major risk factor for invasive aspergillosis [28, 57]. In addition to immune effector cells, we found that lung AEC significantly contribute to the immune response by phagocytosis of conidia and cytokine release in response to fungal germination. While this finding was partially observed and suggested in previous studies, we here present the first model which quantifies the role of AEC. Together with experimental measurements that compare the cytokine release of AM and AEC, we conclude that the role of AEC is underestimated. This conclusion is largely based on the observation that the number of AEC per alveolus is higher than the number of AM or neutrophils at early stages of infections, while phagocytosis rates and cytokine release are comparable or even higher than observed with AM (see Fig 6).

The functions and roles of macrophages during invasive aspergillosis were the focus of experimental studies as well as computational models which indicate a key role in fungal clearance and recognition [23, 58]. Our results suggest that AM are mainly involved in early recognition of swollen conidia and contribute less to fungal clearance than neutrophils and AEC.

We observe a slightly higher importance of AM in low dose scenarios that indicates the importance of dosage in animal models of invasive aspergillosis to ensure transferability of results. However, our results are in line with the observation that in murine infection models neutrophil depletion, but not AM depletion, increases mortality rates [28]. A possible explanation for the underestimated role of AM in our model is that it is based on ordinary differential equations. Therefore, it is not designed to resolve spatial and stochastic phenomena, while agent-based models are suitable to reflect such effects and were applied previously for the confrontation of AM and conidia in the lung [20, 21, 23, 59]. For example, clumping of conidia (*cf.* Fig 4A) in or outside the alveoli may influence the innate immune response.

Since our model focuses on the innate immune response and builds on a simplification of complex interactions during fungal infection, additional functions of AM are potentially not represented in the model. Such functions of AM involve *e.g.* the balance of pro- and anti-inflammatory signaling as well as the support of tissue repair [60, 61]. Further, AM link innate immunity to the adaptive immune system and are important versatile cells to maximize the robustness of the immune system [62, 63]. Further, due to the simplification of signaling, recruitment and orchestration of immune response in our model, specific roles in these cascades of AM as well as other cell types like monocytes and dendritic cells [64] are not covered.

Additional *in silico* and *in vivo* studies are needed to fully understand the roles of AM as well as lung AEC during invasive aspergillosis. Such models and the model presented here are very valuable to develop new treatment approaches and to determine optimal treatment regimens by a combination of approaches. Dynamic optimization has been previously applied to calculate an optimal time-course of treatment protocols for combating infections. This was based on the determination of an optimal usage of antimicrobials and therapies boosting the immune response [65]. For such purposes, our model provides an excellent starting point to identify time-optimal treatment strategies of invasive aspergillosis.

Materials and methods

Model formulation

To formulate a precise but simplistic kinetic model of the innate immune response during invasive aspergillosis, we choose constant, linear or bilinear rate laws depending on the number of influencing entities. This principle ensures a broad functionality of the model while keeping the number of parameters and complexity as low as possible.

We consider three different states, *i.e.*, resting ($\dot{R}$) and swollen conidia ($\dot{S}$) as well as hyphae ($\dot{H}$). Resting conidia are administered to the host's lung at varying quantity R_0. After 3–4h conidia swell in lung alveoli and can be recognized and phagocytosed by host cells [66]. To correctly include the time needed for swelling of conidia, we model the swelling rate as a normal distribution with the mean at time point r_1 = 4h and variance 1h:

$$\dot{R} = \underbrace{-R_0\, f_n\,(t\,|\,r_1, 1h)}_{\text{swelling}}, \quad f_n(t\,|\,\mu, \sigma^2) = \frac{1}{\sqrt{2\pi\sigma^2}}\, e^{-\frac{(t-\mu)^2}{2\sigma^2}}. \tag{1}$$

The time delay of the swelling process cannot be fully resolved by simple linear kinetics which are typically used for growth rates. Further, individual spores do not swell or germinate at the same time delay, as can be seen from germination experiments in our study (see Fig 4B) and others [53]. Hence, we assume as an approximation that the time delay of swelling and germination of spores follows a normal distribution.

Subsequent to swelling, conidia germinate after an additional delay of $s_1 = 3h$ to hyphae [66, 67]. The phagocytosis by immune as well as AEC is modeled by simple bilinear terms with the

specific rates (s_{2-4}):

$$\dot{S} = \underbrace{R_0 f_n(t \mid r_1, 1h)}_{\text{swelling}} \underbrace{-S f_n(t \mid r_1 + s_1, 1h)}_{\text{germination}} \underbrace{-S(s_2 M + s_3 N + s_4 L)}_{\text{phagocytosis}}. \tag{2}$$

In the multicellular growth state of hyphae the number of *A. fumigatus* cells depends on the rate of germination as well as the growth rate (h_1) of hyphae, which we link to the presence of AEC as a resource for growth. We model killing of hyphae by neutrophils and obtain the following description of hyphal dynamics:

$$\dot{H} = \underbrace{S f_n(t \mid r_1 + s_1, 1h)}_{\text{germination}} \underbrace{+h_1 \frac{L}{L_0} H}_{\text{growth}} \underbrace{-h_2 H N}_{\text{killing}}. \tag{3}$$

In our model the number of AEC ($\dot{L}$) is influenced by the lysis induced by fungal hyphae and the damage originating from active AM and neutrophils. The tissue damage by immune cells is often ignored in computational models, but is crucial to understand recruitment and, in particular, depletion of immune cells [68]. To this end, we further connect tissue damage with the pro-inflammatory cytokine level C:

$$\dot{L} = \underbrace{-l_1 L H}_{\text{dissemination}} \underbrace{-L C(l_2 N + l_3 M)}_{\text{tissue damage}}. \tag{4}$$

AM are of relevance for recognition and phagocytosis of swollen conidia. In addition to tissue-resident cells, more AM are recruited by transmigration and differentiation of monocytes which circulate in the blood. We assume that this recruitment has a maximal rate of m_1 cells per hour and depends on the pro-inflammatory cytokine level C and macrophage recruitment is further optimized *via* the control variable $u_1(t)$. This time dependent control variable is optimized by dynamic optimization and can vary between 0 (no macrophage recruitment) to 1 (maximal recruitment) at each time point. In a similar way active depletion or deactivation of AM is modeled ($u_2(t)$). Lastly, the number of AM ($\dot{M}$) also depends on the lysis initiated by germinating conidia and therefore we model macrophage dynamics as:

$$\dot{M} = \underbrace{m_1 C u_1}_{\text{recruitment}} \underbrace{-m_2 (C) u_2}_{\text{depletion}} \underbrace{-m_3 M(S f_n(t \mid r_1 + s_1, 1h))}_{\text{lysis by germinating conidia}}. \tag{5}$$

An important role of AM is the release of pro-inflammatory cytokines in response to fungal cells. However, AEC in addition release cytokines and mediate neutrophil recruitment. Thus, we model the dynamics of a pro-inflammatory cytokine level ($\dot{C}$) ranging from 0 (no inflammation) to 1 (maximum inflammation) as follows:

$$\dot{C} = \underbrace{c_1 (S + H) M (1 - C)}_{\text{inflammation by AMs}} \underbrace{+c_2 H L (1 - C)}_{\text{inflammation by AECs}} \underbrace{-c_3 C}_{\text{decay}}. \tag{6}$$

It is important to note that based on experimental observations, AEC start releasing cytokines only after conidia had germinated [30] and AM already in response to swollen conidia [7].

Although neutrophils also reside in lung tissue, they are recruited in large quantities from the blood in response to a fungal infection by pro-inflammatory cytokines like interleukin 8

[30]. The kinetics of a neutrophil population($\dot{N}$) is described by:

$$\dot{N} = \underbrace{n_1\, C\, u_3}_{\text{recruitment}} \underbrace{-n_2\,(C)\, u_1}_{\text{depletion}} \underbrace{-n_3\, N\,(S+H)}_{\text{lysis by fungi}} \tag{7}$$

The kinetic parameters are cumbersome to be determined due to the inclusion of optimal control variables and experimental inaccessibility of *in vivo* infection parameters. Nevertheless, we carefully and extensively reviewed published experiments to estimate each parameter (see S1 Appendix). Parameters and cell numbers are determined per murine alveolus.

The above described ODE system and parameters are available as SBML file in S1 File and are stored in the database BioModels [69] under the accession MODEL2105110001.

Constraints and objective of optimization problem. To determine the optimal innate immune response during invasive aspergillosis, the above described dynamic system has to fulfill the following constraints and objectives. Intuitively, state variables describing cell numbers are positive, pro-inflammatory cytokine level as well as control variables describing recruitment and depletion of immune cells range between 0 and 1:

$$0 \leq \begin{pmatrix} L(t) \\ R(t) \\ S(t) \\ H(t) \\ M(t) \\ N(t) \end{pmatrix} \begin{matrix} \text{alveolar epithelial cells} \\ \text{resting conidia} \\ \text{swollen conidia} \\ \text{hyphae} \\ \text{alveolar macrophages} \\ \text{neutrophils} \end{matrix}, \quad \underbrace{0 \leq C(t) \leq 1}_{\text{cytokines}}, \quad \underbrace{0 \leq u_{1-4}(t) \leq 1}_{\text{transmigration}} \tag{8}$$

Host evolution led to the development of immunity which optimizes a trade-off between costs and benefits. Intuitively, minimization of pathogen load is crucial for the host to survive and tissue damage as well as immune functions are costly. By this reasoning we defined two main goals of the host organism. Firstly, active fungal cells (swollen conidia and hyphae) should be minimized at all time points to reduce the risk of systemic infection. Secondly, unnecessary tissue damage *e.g.* by hyperinflammation and collateral damage mediated by immune cells must be avoided. We formalize as objective function:

$$F = \min_{u_{1-4}} \int_0^{T_{max}} \left(o_2 \cdot \frac{S(t)}{r_0} + o_3 \cdot \frac{H(t)}{r_0} - o_1 \cdot \frac{L(t)}{l_0} \right) dt. \tag{9}$$

Here, the calculation as a time integral ensures an optimization over time, rather than an unrealistic end-point minimization. The normalization to the initial cell numbers and equal weighting $o_{1-3} = 0.5$ ensures a balanced and biological meaningful optimization result. As shown in S2 Appendix, considering only one of the objectives leads to undesired dynamics like continued hyphal growth or extensive tissue damage. While the difference between the weightings o_{1-3} influences optimal control dynamics, the magnitude does not change the optimal control qualitatively. Hence, the value $o_{1-3} = 0.5$ is chosen as scaling factor for technical reasons so that numerical issues during optimization are avoided.

Solving the optimization problem and parameter sensitivity

The resulting dynamic optimization problem with continuous state and control variables was solved by a quasi-sequential approach established and implemented by Bartl *et al.* [70]. This

gradient-based method has proven its capability in several previous applications to biological systems [24, 71–74] and ensures fast and robust calculation of the optimal control. To avoid local optima, we perform for each parameter set at least 100 randomizations of the initial solution, which is used to start the optimization process.

To determine the sensitivity of parameters, we sampled 500 parameter sets according to a log-normal distribution, where for each parameter the respective mode (maximum of the density function) corresponds to the literature-based parameter value (see S1 Appendix). The latter ensures that parameter sensitivity is determined in the proximity of the reference parameter set and parameter values are always non-negative. The parameter sensitivity is expressed as the contribution to variance [75] and is based on the Spearman correlation $\rho(p)$ between the parameter value p and the objective function value:

$$ctv_p = \frac{\rho(p)^2}{\sum_p \rho(p)^2}. \tag{10}$$

Our model enables the exploration of different scenarios like different conidia doses and immunodeficiencies. For mice we use as initial conidia burden a dose of 1 conidium per alveolus as 'sublethal' and in low dose scenarios 0.1 which are comparable to *in vivo* experiments. A lack of immune cells like neutropenia or monocytopenia (lack of AM) is simulated by a reduced (1%) initial cell number and rate of recruitment. In a similar way, cytokine release inhibition is simulated by reducing the rates to 1% of the reference value.

Experimental evaluation of fungal and host infection parameters

Fungal strains and cultivation. *Aspergillus fumigatus* CEA10, *Aspergillus nidulans* FGSC A4, *Aspergillus niger* ATCC 1015 and *Aspergillus terreus* SBUG 844 were grown on *Aspergillus* minimal medium (AMM; containing $70mM\ NaNO_3$, $11.2mM\ KH_2PO_4$, $7mM\ KCl$, $2mM\ MgSO_4$, and $1^{\mu L}/_{mL}$ trace element solution at pH 6.5) and agar plates with 1% (w/v) glucose for 5 days at $37^\circ C$. The trace element solution was composed of $1g\ FeSO_4 \cdot 7H_2O$, $8.8g\ ZnSO_4 \cdot 7H_2O$, $0.4g\ CuSO_4 \cdot 5H_2O$, $0.15g\ MnSO_4 \cdot H_2O$, $0.1g\ NaB_4O_7 \cdot 10H_2O$, $0.05g\ (NH_4)_6 Mo_7O_{24} \cdot 4H_2O$, and ultra-filtrated water to $1000mL$ [76]. All conidia were harvested in sterile, autoclaved water, then filtered through $30\mu m$ filters (MACS Milteny Biotec) and counted with a Thoma chamber.

Germination assay. Germination assay was performed by inoculating $1 \cdot 10^6$ conidia per mL in RPMI without phenol red (Thermo Fisher Scientific). At different time points pictures were taken using a Keyence BZ-X800 microscope and the number of germinated spores was determined by counting the ratio of spores undergoing germination (germ-tube formation) per field (100 cells).

Cytotoxicity assay. Human lung AEC A549 (ATCC-CCL 185) were maintained in F12K nutrient medium (Thermo Fisher Scientific) with the addition of 10% (v/v) fetal bovine serum (FBS) (HyClone, GE Life science) at $37^\circ C$ with 5% (v/v) CO_2. Cells of the mouse lung epithelial cell line T7 (ECACC 07021402) were maintained in F12K nutrient medium (Thermo Fisher Scientific) with the addition of 0.5% (v/v) FBS (HyClone, GE Life science) and 0.02% (v/v) Insulin-Transferin-Sodium Selenite (Sigma Aldrich). $2 \cdot 10^5$ cells per well were seeded in 24 well plate $18h$ prior to the experiment. Before infection cells were washed once with sterile phosphate buffered saline (PBS) 1X (Gibco, Thermo Fisher Scientific) and then incubated with conidia based on the different MOIs in DMEM without phenol red (Gibco, Thermo Fisher Scientific) with the addition of 10% (v/v) FBS. Cells and conidia were incubated for $20h$ at $37^\circ C$ with 5% (v/v) CO_2. LDH release was measured using the CyQuant LDH cytotoxicity

assay (Thermo Fisher Scientific) using the manufacturer instructions. The absorbance was determined using a Tecan Infinite 200 (LabX).

Isolation of alveolar epithelial type II cells and AM from mice. A total of eighteen male and female 12–18 weeks old C57BL/6J (The Jackson Laboratory) mice were used. Mice were cared for in accordance with the principles outlined by the European Convention for the Protection of Vertebrate Animals Used for Experimental and Other Scientific Purposes (European Treaty Series, no.123). All animal experiments were in compliance with the German animal protection law and were approved by the responsible federal state authority "Thüringer Landesamt für Lebensmittelsicherheit und Verbraucherschutz" and ethics committee "Beratende Kommission nach §15 Abs. 1 Tierschutzgesetz" (permit no. 03–027/16).

Mice were sacrificed using $125\mu L$ ketamine/xylazine per 20g and the lungs were obtained as previously described [77]. After isolation, the lungs lobes were digested for $45min$ at room temperature in $1mL$ of dispase (Corning) and then the lung parenchyma was separated with the help of tweezers in $7mL$ of DMEM/F12K (Thermo Fisher Scientific) containing $0.01mg$ of DNase (Sigma Aldrich). The cell suspension was first filtered twice: through a $70\mu m$ and then through a $30\mu m$ (MACS, Miltenyi Biotec) filter and finally centrifuged. The pellet was lysed using a red blood cell (RBC) lysis buffer and re-centrifuged.

For their separation cells underwent a double magnetic labeling selection. At first, they were negatively labeled using CD45 (macrophages), CD16/32 (B/NK cells), anti-Ter (erythrocytes), CD31 (endothelial cells) (Miltyenyi Biotec) and anti-t1α (alveolar epithelial type I cells) (Novus Biologicals), biotin-linked antibodies. Secondly the negative fraction was collected and positively selected for alveolar epithelial type II cells using a CD326/EpCAM antibody (eBioscience). Both labeling steps were perfomed at $4^{\circ}C$ for $30min$, and followed by a second labeling with Anti-Biotin Microbeads Ultrapure (Miltenyi Biotec) for $15min$ at $4^{\circ}C$. The separation was performed using an autoMACS Pro Separator machine (Miltyenyi Biotec). The final cell suspension containing type II AEC was resuspended in mouse tracheal epithelial cells (MTEC) basic medium [78]: DMEM-F12K +1% HEPES, Na-bicarbonate, L-glutamine, penicillin-streptomycin, 0.1% amphotericin B (Gibco) supplemented with 0.001% Insulin-transferrin (Gibco), $0.1^{\mu g}/_{mL}$ cholera toxin (Sigma Aldrich), $25^{ng}/_{mL}$ epidermal growth factor (Invitrogen) and mice fibroblast growth factor 7 (R&D system), $30^{\mu g}/_{mL}$ bovine pituitary extract (Gibco), $30^{ng}/_{mL}$ multilinear hemopoietic growth factor, $50^{ng}/_{mL}$ human fibroblastic growth factor 10 (R&D system), 5% FBS, $0.01\mu M$ retinoic acid (Sigma Aldrich) and $10\mu M$ Rho kinase inhibitor (ROCK) (Thermo Fisher Scientific).

The isolation of AM was performed similarly, only using the first labeling step with CD45 antibodies. AM were re-suspended in MTEC basic medium with the addition of 10% (v/v) FBS.

Due to the necessity of using all the cells for experiment, the purity of the isolated cells was not assessed after every experiment, but as previously demonstrated this protocol assures a purity between 98—99% [77]. The percentage of viable cells was measured using Trypan blue and it was between 75—90% depending on the mice. From each mouse, a total of $1 \cdot 10^6$ cells were seeded onto 8 well Millicells slides (Merc, Millipore), pre-coated with $100^{\mu g}/_{mL}$ of fibronectin (Sigma Aldrich), for AEC, and incubated at $37^{\circ}C$ and 5% (v/v) CO_2. The medium was changed every 2 days and the cells were left to rest for 7 days prior the experiment.

Infection with *A. fumigatus* and cytokine measurement. Alveolar epithelial type II cells were infected with *A. fumigatus* CEA10 conidia at a multiplicity of infection (MOI) of 5, for 4, 6, 10, and 24h. At these time points the supernatant was collected, centrifuged at $300 \cdot g$ for 5 min and then stored at -20$^{\circ}C$ for 24h until measurements. The levels of interleukin (IL)-6 and tumor necrosis factor (TNF)-α were detected using ELISA kits (Biolegend) following the manufacturer's instructions.

Supporting information

S1 Appendix. Parameter estimation. Documentation of parameter estimation and calculation.
(PDF)

S2 Appendix. Objective function weighting. Influence of weighting innate immune response objectives.
(PDF)

S1 File. SBML model description. The described model of invasive aspergillosis is provided as SBML and COPASI file. To enable simulation, control variables u_{1-4} are fixed. Further, the model is archived in EBI BioModels under the accession MODEL2105110001.
(XML)

S1 Fig. Influence of MOI on cytotoxicity of *Aspergillus spp*. against epithelial cells. In addition to the depicted LDH release measurements of epithelial cells upon 24h co-incubation with *Aspergillus spp*. at an *MOI* = 5 (main text Fig 4D and 4E), cytotoxicity was measured for *MOI* = 2 and *MOI* = 10 for human A549 cells to demonstrate the influence of fungal burden.
(TIF)

Acknowledgments

We thank Elina Wiechens for an initial parameter search in the literature and thank Pedro Moura-Alves, MPIIB Berlin, for providing us the mouse T7 alveolar lung cells. In addition, we thank Dr. Maria Straßburger for the help with mouse experiments.

Author Contributions

Conceptualization: Jan Ewald, Axel A. Brakhage, Christoph Kaleta.

Data curation: Jan Ewald, Flora Rivieccio.

Formal analysis: Jan Ewald.

Funding acquisition: Stefan Schuster, Axel A. Brakhage.

Investigation: Jan Ewald, Flora Rivieccio.

Methodology: Jan Ewald, Flora Rivieccio, Lukáš Radosa.

Resources: Stefan Schuster, Axel A. Brakhage.

Software: Jan Ewald.

Supervision: Stefan Schuster, Axel A. Brakhage, Christoph Kaleta.

Validation: Flora Rivieccio, Lukáš Radosa.

Visualization: Jan Ewald.

Writing – original draft: Jan Ewald, Christoph Kaleta.

Writing – review & editing: Flora Rivieccio, Lukáš Radosa, Stefan Schuster, Axel A. Brakhage, Christoph Kaleta.

References

1. Mizgerd JP. Lung infection—a public health priority. PLoS Medicine. 2006; 3(2):e76. https://doi.org/10.1371/journal.pmed.0030076 PMID: 16401173

2. Vento S, Cainelli F, Temesgen Z. Lung infections after cancer chemotherapy. The Lancet Oncology. 2008; 9(10):982–992. https://doi.org/10.1016/S1470-2045(08)70255-9 PMID: 19071255

3. Brakhage AA, Langfelder K. Menacing mold: the molecular biology of *Aspergillus fumigatus*. Annual Reviews in Microbiology. 2002; 56(1):433–455. https://doi.org/10.1146/annurev.micro.56.012302.160625 PMID: 12142473

4. Tekaia F, Latgé JP. *Aspergillus fumigatus*: saprophyte or pathogen? Current Opinion in Microbiology. 2005; 8(4):385–392. https://doi.org/10.1016/j.mib.2005.06.017 PMID: 16019255

5. Dagenais TR, Keller NP. Pathogenesis of *Aspergillus fumigatus* in invasive aspergillosis. Clinical Microbiology Reviews. 2009; 22(3):447–465. https://doi.org/10.1128/CMR.00055-08 PMID: 19597008

6. Scharf DH, Heinekamp T, Remme N, Hortschansky P, Brakhage AA, Hertweck C. Biosynthesis and function of gliotoxin in *Aspergillus fumigatus*. Applied Microbiology and Biotechnology. 2012; 93(2):467–472. https://doi.org/10.1007/s00253-011-3689-1 PMID: 22094977

7. Latgé JP, Chamilos G. *Aspergillus fumigatus* and Aspergillosis in 2019. Clinical Microbiology Reviews. 2019; 33(1). https://doi.org/10.1128/cmr.00140-18 PMID: 31722890

8. Osherov N. Interaction of the pathogenic mold *Aspergillus fumigatus* with lung epithelial cells. Frontiers in Microbiology. 2012; 3:346. https://doi.org/10.3389/fmicb.2012.00346 PMID: 23055997

9. Balloy V, Chignard M. The innate immune response to *Aspergillus fumigatus*. Microbes and Infection. 2009; 11(12):919–927. https://doi.org/10.1016/j.micinf.2009.07.002 PMID: 19615460

10. Brown SP, Cornforth DM, Mideo N. Evolution of virulence in opportunistic pathogens: generalism, plasticity, and control. Trends in Microbiology. 2012; 20(7):336–342. https://doi.org/10.1016/j.tim.2012.04.005 PMID: 22564248

11. Dragonetti G, Criscuolo M, Fianchi L, Pagano L. Invasive Aspergillosis in Acute Myeloid Leukemia: Are We Making Progress in Reducing Mortality? Medical Mycology. 2017; 55(1):82–86. https://doi.org/10.1093/mmy/myw114 PMID: 27915304

12. Taccone FS, Van den Abeele AM, Bulpa P, Misset B, Meersseman W, Cardoso T, et al. Epidemiology of invasive aspergillosis in critically ill patients: clinical presentation, underlying conditions, and outcomes. Critical Care. 2015; 19(1):7. https://doi.org/10.1186/s13054-014-0722-7 PMID: 25928694

13. Bartoletti M, Pascale R, Cricca M, Rinaldi M, Maccaro A, Bussini L, et al. Epidemiology of invasive pulmonary aspergillosis among COVID-19 intubated patients: a prospective study. Clinical Infectious Diseases. 2020. https://doi.org/10.1093/cid/ciaa1065 PMID: 32719848

14. Weir HK, Thompson TD, Soman A, Møller B, Leadbetter S. The past, present, and future of cancer incidence in the United States: 1975 through 2020. Cancer. 2015; 121(11):1827–1837. https://doi.org/10.1002/cncr.29258 PMID: 25649671

15. Mistry M, Parkin D, Ahmad AS, Sasieni P. Cancer incidence in the United Kingdom: projections to the year 2030. British Journal of Cancer. 2011; 105(11):1795. https://doi.org/10.1038/bjc.2011.430 PMID: 22033277

16. Wynn JJ, Alexander CE. Increasing organ donation and transplantation: the US experience over the past decade. Transplant International. 2011; 24(4):324–332. https://doi.org/10.1111/j.1432-2277.2010.01201.x PMID: 21208297

17. Granich R, Gupta S, Hersh B, Williams B, Montaner J, Young B, et al. Trends in AIDS deaths, new infections and ART coverage in the top 30 countries with the highest AIDS mortality burden; 1990–2013. PloS One. 2015; 10(7):e0131353. https://doi.org/10.1371/journal.pone.0131353 PMID: 26147987

18. Hoenigl M. Invasive fungal disease complicating coronavirus disease 2019: when it rains, it spores. Clinical Infectious Diseases. 2020. https://doi.org/10.1093/cid/ciaa1342 PMID: 32887998

19. Tanaka RJ, Boon NJ, Vrcelj K, Nguyen A, Vinci C, Armstrong-James D, et al. *In silico* modeling of spore inhalation reveals fungal persistence following low dose exposure. Scientific Reports. 2015; 5:13958. https://doi.org/10.1038/srep13958 PMID: 26364644

20. Pollmächer J, Figge MT. Deciphering chemokine properties by a hybrid agent-based model of *Aspergillus fumigatus* infection in human alveoli. Frontiers in Microbiology. 2015; 6:503. https://doi.org/10.3389/fmicb.2015.00503 PMID: 26074897

21. Oremland M, Michels KR, Bettina AM, Lawrence C, Mehrad B, Laubenbacher R. A computational model of invasive aspergillosis in the lung and the role of iron. BMC Systems Biology. 2016; 10(1):34. https://doi.org/10.1186/s12918-016-0275-2 PMID: 27098278

22. Pollmächer J, Timme S, Schuster S, Brakhage AA, Zipfel PF, Figge MT. Deciphering the counterplay of *Aspergillus fumigatus* infection and host inflammation by evolutionary games on graphs. Scientific Reports. 2016; 6:27807. https://doi.org/10.1038/srep27807 PMID: 27291424

23. Blickensdorf M, Timme S, Figge MT. Comparative Assessment of Aspergillosis by Virtual Infection Modeling in Murine and Human Lung. Frontiers in Immunology. 2019; 10. https://doi.org/10.3389/fimmu.2019.00142 PMID: 30804941

24. Ewald J, Sieber P, Garde R, Lang SN, Schuster S, Ibrahim B. Trends in mathematical modeling of host–pathogen interactions. Cellular and Molecular Life Sciences. 2019; p. 1–14. https://doi.org/10.1007/s00018-019-03382-0 PMID: 31776589

25. Blickensdorf M, Timme S, Figge MT. Hybrid agent-based modeling of *Aspergillus fumigatus* infection to quantitatively investigate the role of pores of Kohn in human alveoli. Frontiers in Microbiology. 2020; 11:1951. https://doi.org/10.3389/fmicb.2020.01951 PMID: 32903715

26. Philippe B, Ibrahim-Granet O, Prevost M, Gougerot-Pocidalo M, Perez MS, Van der Meeren A, et al. Killing of *Aspergillus fumigatus* by alveolar macrophages is mediated by reactive oxidant intermediates. Infection and Immunity. 2003; 71(6):3034–3042. https://doi.org/10.1128/IAI.71.6.3034-3042.2003 PMID: 12761080

27. Taramelli D, Malabarba M, Sala G, Basilico N, Cocuzza G. Production of cytokines by alveolar and peritoneal macrophages stimulated by *Aspergillus fumigatus* conidia or hyphae. Journal of Medical and Veterinary Mycology. 1996; 34(1):49–56. https://doi.org/10.1080/02681219680000081 PMID: 8786471

28. Mircescu MM, Lipuma L, van Rooijen N, Pamer EG, Hohl TM. Essential role for neutrophils but not alveolar macrophages at early time points following *Aspergillus fumigatus* infection. The Journal of Infectious Diseases. 2009; 200(4):647–656. https://doi.org/10.1086/600380 PMID: 19591573

29. Wasylnka JA, Moore MM. *Aspergillus fumigatus* conidia survive and germinate in acidic organelles of A549 epithelial cells. Journal of Cell Science. 2003; 116(8):1579–1587. https://doi.org/10.1242/jcs.00329 PMID: 12640041

30. Balloy V, Sallenave JM, Wu Y, Touqui L, Latgé JP, Si-Tahar M, et al. *Aspergillus fumigatus*-induced interleukin-8 synthesis by respiratory epithelial cells is controlled by the phosphatidylinositol 3-kinase, p38 MAPK, and ERK1/2 pathways and not by the toll-like receptor-MyD88 pathway. Journal of Biological Chemistry. 2008; 283(45):30513–30521. https://doi.org/10.1074/jbc.M803149200

31. Jhingran A, Kasahara S, Shepardson KM, Junecko BAF, Heung LJ, Kumasaka DK, et al. Compartment-specific and sequential role of MyD88 and CARD9 in chemokine induction and innate defense during respiratory fungal infection. PLoS Pathogens. 2015; 11(1):e1004589. https://doi.org/10.1371/journal.ppat.1004589 PMID: 25621893

32. Shudo E, Iwasa Y. Dynamic optimization of host defense, immune memory, and post-infection pathogen levels in mammals. Journal of Theoretical Biology. 2004; 228(1):17–29. https://doi.org/10.1016/j.jtbi.2003.12.001 PMID: 15064080

33. Lenhart S, Workman JT. Optimal control applied to biological models. CRC press; 2007.

34. Dühring S, Ewald J, Germerodt S, Kaleta C, Dandekar T, Schuster S. Modelling the host–pathogen interactions of macrophages and *Candida albicans* using Game Theory and dynamic optimization. Journal of The Royal Society Interface. 2017; 14(132):20170095. https://doi.org/10.1098/rsif.2017.0095 PMID: 28701506

35. McDade TW, Georgiev AV, Kuzawa CW. Trade-offs between acquired and innate immune defenses in humans. Evolution, Medicine, and Public Health. 2016; 2016(1):1–16. https://doi.org/10.1093/emph/eov033 PMID: 26739325

36. Desoubeaux G, Cray C. Rodent models of invasive aspergillosis due to *Aspergillus fumigatus*: still a long path toward standardization. Frontiers in Microbiology. 2017; 8:841. https://doi.org/10.3389/fmicb.2017.00841 PMID: 28559881

37. Desoubeaux G, Cray C. Animal models of aspergillosis. Comparative Medicine. 2018; 68(2):109–123. PMID: 29663936

38. Heinekamp T, Schmidt H, Lapp K, Pähtz V, Shopova I, Köster-Eiserfunke N, et al. Interference of *Aspergillus fumigatus* with the immune response. In: Seminars in Immunopathology. vol. 37. Springer; 2015. p. 141–152.

39. Knox BP, Huttenlocher A, Keller NP. Real-time visualization of immune cell clearance of *Aspergillus fumigatus* spores and hyphae. Fungal Genetics and Biology. 2017; 105:52–54. https://doi.org/10.1016/j.fgb.2017.05.005 PMID: 28559109

40. Tsiantis N, Balsa-Canto E, Banga JR. Optimality and identification of dynamic models in systems biology: an inverse optimal control framework. Bioinformatics. 2018; 34(14):2433–2440. https://doi.org/10.1093/bioinformatics/bty139 PMID: 29522196

41. Stone KC, Mercer RR, Gehr P, Stockstill B, Crapo JD, et al. Allometric relationships of cell numbers and size in the mammalian lung. American Journal of Respiratory Cell and Molecular Biology. 1992; 6(2):235–43. https://doi.org/10.1165/ajrcmb/6.2.235 PMID: 1540387

42. Knust J, Ochs M, Gundersen HJG, Nyengaard JR. Stereological estimates of alveolar number and size and capillary length and surface area in mice lungs. The Anatomical Record: Advances in Integrative Anatomy and Evolutionary Biology: Advances in Integrative Anatomy and Evolutionary Biology. 2009; 292(1):113–122. https://doi.org/10.1002/ar.20747 PMID: 19115381

43. Guillot L, Nathan N, Tabary O, Thouvenin G, Le Rouzic P, Corvol H, et al. Alveolar epithelial cells: master regulators of lung homeostasis. The International Journal of Biochemistry & Cell Biology. 2013; 45 (11):2568–2573. https://doi.org/10.1016/j.biocel.2013.08.009 PMID: 23988571

44. Wong MH, Johnson MD. Differential response of primary alveolar type I and type II cells to LPS stimulation. PLoS One. 2013; 8(1):e55545. https://doi.org/10.1371/journal.pone.0055545 PMID: 23383221

45. Amich J, Mokhtari Z, Strobel M, Vialetto E, Sheta D, Yu Y, et al. Three-dimensional light sheet fluorescence microscopy of lungs to dissect local host immune-*Aspergillus fumigatus* interactions. mBio. 2020; 11(1). https://doi.org/10.1128/mBio.02752-19 PMID: 32019790

46. Kalleda N, Amich J, Arslan B, Poreddy S, Mattenheimer K, Mokhtari Z, et al. Dynamic immune cell recruitment after murine pulmonary *Aspergillus fumigatus* infection under different immunosuppressive regimens. Frontiers in Microbiology. 2016; 7:1107. https://doi.org/10.3389/fmicb.2016.01107 PMID: 27468286

47. Sheppard DC, Rieg G, Chiang LY, Filler SG, Edwards JE, Ibrahim AS. Novel inhalational murine model of invasive pulmonary aspergillosis. Antimicrobial Agents and Chemotherapy. 2004; 48(5):1908–1911. https://doi.org/10.1128/AAC.48.5.1908-1911.2004 PMID: 15105158

48. Duong M, Ouellet N, Simard M, Bergeron Y, Olivier M, Bergeron MG. Kinetic study of host defense and inflammatory response to *Aspergillus fumigatus* in steroid-induced immunosuppressed mice. The Journal of Infectious Diseases. 1998; 178(5):1472–1482. https://doi.org/10.1086/314425 PMID: 9780270

49. Borger P, Koeter G, Timmerman J, Vellenga E, Tomee J, Kauffman H. Proteases from *Aspevgillus fumigatus* Induce Interleukin (IL)-6 and IL-8 Production in Airway Epithelial Cell Lines by Transcriptional Mechanisms. The Journal of Infectious Diseases. 1999; 180(4):1267–1274. https://doi.org/10.1086/315027 PMID: 10479157

50. Cenci E, Mencacci A, Casagrande A, Mosci P, Bistoni F, Romani L. Impaired antifungal effector activity but not inflammatory cell recruitment in interleukin-6-deficient mice with invasive pulmonary aspergillosis. The Journal of Infectious Diseases. 2001; 184(5):610–617. https://doi.org/10.1086/322793 PMID: 11494166

51. Song HS, Cannon WR, Beliaev AS, Konopka A. Mathematical modeling of microbial community dynamics: a methodological review. Processes. 2014; 2(4):711–752. https://doi.org/10.3390/pr2040711

52. Cannon WR. Simulating metabolism with statistical thermodynamics. PLoS One. 2014; 9(8):e103582. https://doi.org/10.1371/journal.pone.0103582 PMID: 25089525

53. Araujo R, Rodrigues AG. Variability of germinative potential among pathogenic species of *Aspergillus*. Journal of Clinical Microbiology. 2004; 42(9):4335–4337. https://doi.org/10.1128/JCM.42.9.4335-4337.2004 PMID: 15365039

54. Rhodes JC. *Aspergillus fumigatus*: growth and virulence. Medical Mycology. 2006; 44(Supplement_1): S77–S81. https://doi.org/10.1080/13693780600779419 PMID: 17050423

55. Caffrey-Carr AK, Kowalski CH, Beattie SR, Blaseg NA, Upshaw CR, Thammahong A, et al. Interleukin 1α is critical for resistance against highly virulent *Aspergillus fumigatus* isolates. Infection and immunity. 2017; 85(12):e00661–17. https://doi.org/10.1128/IAI.00661-17 PMID: 28947643

56. Paulussen C, Hallsworth JE, Álvarez-Pérez S, Nierman WC, Hamill PG, Blain D, et al. Ecology of aspergillosis: insights into the pathogenic potency of *Aspergillus fumigatus* and some other *Aspergillus* species. Microbial Biotechnology. 2017; 10(2):296–322. https://doi.org/10.1111/1751-7915.12367 PMID: 27273822

57. Bonnett CR, Cornish EJ, Harmsen AG, Burritt JB. Early neutrophil recruitment and aggregation in the murine lung inhibit germination of *Aspergillus fumigatus* conidia. Infection and Immunity. 2006; 74 (12):6528–6539. https://doi.org/10.1128/IAI.00909-06 PMID: 16920786

58. Rosowski EE, Raffa N, Knox BP, Golenberg N, Keller NP, Huttenlocher A. Macrophages inhibit *Aspergillus fumigatus* germination and neutrophil-mediated fungal killing. PLoS Pathogens. 2018; 14(8): e1007229. https://doi.org/10.1371/journal.ppat.1007229 PMID: 30071103

59. Tokarski C, Hummert S, Mech F, Figge MT, Germerodt S, Schroeter A, et al. Agent-based modeling approach of immune defense against spores of opportunistic human pathogenic fungi. Frontiers in Microbiology. 2012; 3:129. https://doi.org/10.3389/fmicb.2012.00129 PMID: 22557995

60. Wynn TA, Vannella KM. Macrophages in tissue repair, regeneration, and fibrosis. Immunity. 2016; 44 (3):450–462. https://doi.org/10.1016/j.immuni.2016.02.015 PMID: 26982353

61. Allard B, Panariti A, Martin JG. Alveolar macrophages in the resolution of inflammation, tissue repair, and tolerance to infection. Frontiers in Immunology. 2018; 9:1777. https://doi.org/10.3389/fimmu.2018.01777 PMID: 30108592

62. Sales-Campos H, Tonani L, Cardoso CRB, Kress MRVZ. The immune interplay between the host and the pathogen in *Aspergillus fumigatus* lung infection. BioMed Research International. 2013; 2013. https://doi.org/10.1155/2013/693023 PMID: 23984400

63. Espinosa V, Rivera A. First line of defense: innate cell-mediated control of pulmonary aspergillosis. Frontiers in Microbiology. 2016; 7:272. https://doi.org/10.3389/fmicb.2016.00272 PMID: 26973640

64. Guo Y, Kasahara S, Jhingran A, Tosini NL, Zhai B, Aufiero MA, et al. During Aspergillus infection, monocyte-derived DCs, neutrophils, and plasmacytoid DCs enhance innate immune defense through CXCR3-dependent crosstalk. Cell Host & Microbe. 2020; 28(1):104–116. https://doi.org/10.1016/j.chom.2020.05.002 PMID: 32485165

65. Stengel RF, Ghigliazza RM, Kulkarni NV. Optimal enhancement of immune response. Bioinformatics. 2002; 18(9):1227–1235. https://doi.org/10.1093/bioinformatics/18.9.1227 PMID: 12217914

66. Dague E, Alsteens D, Latgé JP, Dufrêne YF. High-resolution cell surface dynamics of germinating *Aspergillus fumigatus* conidia. Biophysical Journal. 2008; 94(2):656–660. https://doi.org/10.1529/biophysj.107.116491 PMID: 17890393

67. Kwon-Chung KJ, Sugui JA. *Aspergillus fumigatus*—what makes the species a ubiquitous human fungal pathogen? PLoS Pathogens. 2013; 9(12):e1003743. https://doi.org/10.1371/journal.ppat.1003743 PMID: 24348239

68. Cicchese JM, Evans S, Hult C, Joslyn LR, Wessler T, Millar JA, et al. Dynamic balance of pro-and anti-inflammatory signals controls disease and limits pathology. Immunological Reviews. 2018; 285(1):147–167. https://doi.org/10.1111/imr.12671 PMID: 30129209

69. Malik-Sheriff RS, Glont M, Nguyen TV, Tiwari K, Roberts MG, Xavier A, et al. BioModels—15 years of sharing computational models in life science. Nucleic Acids Research. 2020; 48(D1):D407–D415. https://doi.org/10.1093/nar/gkz1055 PMID: 31701150

70. Bartl M, Li P, Biegler LT. Improvement of state profile accuracy in nonlinear dynamic optimization with the quasi-sequential approach. AIChE Journal. 2011; 57(8):2185–2197. https://doi.org/10.1002/aic.12437

71. Wessely F, Bartl M, Guthke R, Li P, Schuster S, Kaleta C. Optimal regulatory strategies for metabolic pathways in *Escherichia coli* depending on protein costs. Molecular Systems Biology. 2011; 7(1). https://doi.org/10.1038/msb.2011.46 PMID: 21772263

72. Bartl M, Kötzing M, Schuster S, Li P, Kaleta C. Dynamic optimization identifies optimal programmes for pathway regulation in prokaryotes. Nature Communications. 2013; 4:2243. https://doi.org/10.1038/ncomms3243 PMID: 23979724

73. Bartl M, Pfaff M, Ghallab A, Driesch D, Henkel SG, Hengstler JG, et al. Optimality in the zonation of ammonia detoxification in rodent liver. Archives of Toxicology. 2015; 89(11):2069–2078. https://doi.org/10.1007/s00204-015-1596-4 PMID: 26438405

74. Ewald J, Bartl M, Kaleta C. Deciphering the regulation of metabolism with dynamic optimization: an overview of recent advances. Biochemical Society Transactions. 2017; 45(4):1035–1043. https://doi.org/10.1042/BST20170137 PMID: 28754658

75. Groen EA, Bokkers EA, Heijungs R, de Boer IJ. Methods for global sensitivity analysis in life cycle assessment. The International Journal of Life Cycle Assessment. 2017; 22(7):1125–1137. https://doi.org/10.1007/s11367-016-1217-3

76. Brakhage AA, Van den Brulle J. Use of reporter genes to identify recessive trans-acting mutations specifically involved in the regulation of *Aspergillus nidulans* penicillin biosynthesis genes. Journal of Bacteriology. 1995; 177(10):2781–2788. https://doi.org/10.1128/jb.177.10.2781-2788.1995 PMID: 7677843

77. Sinha M, Lowell CA. Isolation of highly pure primary mouse alveolar epithelial type II cells by flow cytometric cell sorting. Bio-protocol. 2016; 6(22). https://doi.org/10.21769/BioProtoc.2013 PMID: 28180137

78. You Y, Richer EJ, Huang T, Brody SL. Growth and differentiation of mouse tracheal epithelial cells: selection of a proliferative population. American Journal of Physiology-Lung Cellular and Molecular Physiology. 2002; 283(6):L1315–L1321. https://doi.org/10.1152/ajplung.00169.2002 PMID: 12388377

Supplemental information

S1 Appendix

Documentation of parameter estimation and calculation

$L(0), L_0$ Average number of AEC (type I and II) per alveolus. The total number of AEC in several mammalian species was elucidated by Stone et al. [1] and reports for murine lungs $11.6 + 14.8 = 26.4 \cdot 10^6\, cells$ (type I and II). Knust et al. [2] determined $2.31 \cdot 10^6$ alveoli for mice with a comparable weight ($20\, g$) and we estimate $L(0) = L_0 = \frac{26.4}{2.31} = 11.43\, cells$.

l_1 Rate of hyphae destroying AEC. In [3], epithelial damage was assessed in mice by LDH release in bronchial lavage showing a 2.5 fold change of damage after 24h. The rate is calculated by $l_1 = \frac{ln(fold\, change)}{\cdot 24h} = 0.0382\, cells^{-1}\, h^{-1}$.

l_2 Rate of neutrophils damaging AEC. In [4], neutrophils were stimulated *in vivo* with LPS and cell damage in lungs was assessed as free elastase activity in BALF. The relative damage was 72% after 12h and we estimate $l_2 = \frac{ln(1-0.72)}{12h} = 0.1061\, cells^{-1}\, h^{-1}$

l_3 As l_2 but for AM. Host damage mediated by AM is less frequently measured and we therefore rely on data of Hirano [5]. In that study rat epithelial cells (SV40T2) were co-cultured with rat alveolar macrophages and stimulated by LPS. The damage was determined by transepithelial resistance and dropped from $11\, \Omega cm^2$ to $0.5\, \Omega cm^2$ within 24h. To this end, we calculate $l_3 = \dfrac{ln(\frac{11}{0.5})}{24h} = 0.1288\, cells^{-1}\, h^{-1}$.

$R(0), R_0$ Initial dose of resting conidia. Value depends on the scenarios. *In vivo* experiments with mice typically challenged with 10^5-10^7 conidia. Therefore, alveolus occupation is typically 0.1 - 10 conidia per alveolus. A detailed calculation is also provided by Blickensdorf et al. [6].

r_1 Average time for swelling of conidia. After 3h the conidial rodlet layer is disrupted [7].

s_1 Average time for germination of swollen conidia. Total time from resting conidia to germination is on average 7h [8]. Therefore $s_1 = 7h - r_1 = 4h$.

s_2 Killing rate of swollen conidia by AM. Intensively studied, but rates show high variation across studies [9]. In contrast, the killing rate of conidia by AEC is more rarely calculated. However, in [10] both was investigated. Accordingly, murine AM showed faster killing than AEC along all timepoints. For murine AM, conidia survival was 0.6% after 12h of interaction and we calculate $s_2 = \frac{ln(0.006)}{12h} = 0.4263\, cells^{-1}\, h^{-1}$.

s_3 Killing rate of swollen conidia by neutrophils. Phagocytosis and killing rate of conidia by neutrophils have been frequently studied. However, in the study of Alflen et al. [11] the killing rate of conidia and hyphae was compared and murine neutrophils were used. Conidial viability dropped to 39% after 4h of co-incubation and we calculate $s_3 = -\frac{0.39}{4h} = 0.2354\, cells^{-1}\, h^{-1}$.

s_4 Killing rate of swollen conidia by AEC. From the same study as for s_2 [10], AEC possessed a slower killing rate and we calculate $s_2 = \frac{ln(0.065)}{12h} = 0.2278\, cells^{-1}\, h^{-1}$.

h_1 Growth rate of hyphae. The increase of hyphal length with time is a good estimator for doubling times of cells since cell size is rather constant. In glucose medium and at $37°$C the length of hyphae doubles every 1h [12]. The rate is then $h_1 = \frac{ln(2}{1h} = 0.6533\, h^{-1}$.

h_2 Killing rate of hyphae by neutrophils. From the same study as used to estimate s_3 [11], the viability of hyphae was measured after co-incubation with neutrophils. After 4h 68% of initial fungal cells were viable, which equals a rate of $-\frac{0.68}{4h} = 0.0964\, cells^{-1}\, h^{-1}$. However, hyphae are growing at the same time and therefore we estimate $h_2 = h_1 \cdot 1\, cells + 0.0964$ since neutrophil killing outpaces hyphal growth by the above calculated rate during a fungal challenge of one fungal cell per alveolus.

$M(0)$ Number of resident AM per alveolus in an uninfected host. Recently, Amich et al. [13] were able to use 3D light sheet fluorescence microscopy to investigate invasive aspergillosis in *in vivo* mouse models. Due to this imaging approach one can precisely determine the number of immune cells within an alveolus. On average they find $M(0) = 0.2926\, cells$ AM per alveolus. Note, that in the agent-based model of Blickensdorf et al. [6] a slightly higher number of AM per murine alveolus (0.74) was calculated based on whole tissue cell counts [1].

m_1 Rate of recruitment of AM by influx and maturation of monocytes or even proliferation of resident macrophages. To complement data used for $M(0)$ and $N(0)$, we estimate the recruitment rates of AM and neutrophils based on data from a previous publication [14] of the same group of authors, which performed 3D light sheet fluorescence microscopy [13]. In that publication a similar murine infection model of invasive aspergillosis was used, but cell numbers were quantified by fluorescence-activated cell sorting (FACS) of lung tissue samples. For AM a rise from 2.75 to $9\, 10^5 cells$ in 4h after a mild dose of conidia was reported. We estimate $m_1 = M(0)\frac{9}{2.75 \cdot 4h} = 0.2394\, cells\, h^{-1}$.

m_2 Rate of alveolar macrophage depletion. Based on the same study as m_1 [14] macrophage level was on control level after 12h of peak inflammation. So we calculate $m_2 = M(0)\frac{9}{2.75 \cdot 12h} = 0.0798\, cells\, h^{-1}$.

m_3 Lysis rate of AM by swollen conidia. While phagocytosis and killing rate by AM are frequently reported the *vice versa* scenario is rarely depicted. For mice cytotoxicity of swollen conidia was reported [15] to be 84% after 24 h that corresponds to a rate of $m_3 = -\frac{ln(1-0.84)}{\cdot 24} = 0.0764\, cells^{-1}\, h^{-1}$.

c_1 Release rate of pro-inflammatory cytokines by AM. We intentionally do not model a single cytokine due to the complex network of cytokine functions and signaling to recruit neutrophils. Based on several studies investigating the time course of prominent pro-inflammatory cytokines we decided to set the cytokine release rate to $c_1 = 1\, cells^{-2}\, h^{-1}$ to mimic the peak in cytokine concentration at 5-10h after infection or stimulation with LPS.

c_2 Release rate of pro-inflammatory cytokines by lung AEC. Cytokine release of lung AEC is not well understood and only covered by few studies. A pioneering study [16] investigated the potential of human lung AM and AEC to recruit neutrophils when stimulated by LPS. Since AEC showed a 43.75% higher number of recruited neutrophils under similar conditions, we set $c_2 = 1.14375\, cells^{-2}\, h^{-1}$.

c_3 Decay rate of pro-inflammatory cytokines. As for c_1 we estimated the decay rate based on the investigation of several time courses and observed that decay is slower than release. For reference we set $c_3 = 0.1\,h^{-1}$.

$N(0)$ Number of tissue resident neutrophils. As described for $M(0)$ microscopy data of murine lungs reported a neutrophil density of $N(0) = 0.2628\,cells$ neutrophils per alveolus [13].

n_1 Rate of neutrophil recruitment by influx of leukocytes. Similar to the definition of m_1 an increase of neutrophils is reported in [14] from $1.9 \cdot 10^5 cells$ to $7.6 \cdot 10^5 cells$. To this end, we calculate $n_1 = N(0)\frac{7.6\cdot}{1.9\cdot 4h} = 0.2628\,cells\,h^{-1}$.

n_2 Rate of neutrophil depletion. Based on the same study as n_1 [14] neutrophil level was on control level after 12h of peak inflammation. So we calculate $n_2 = N(0)\frac{7.6\cdot}{2.8\cdot 12h} = 0.0594 cells\,h^{-1}$.

n_3 Lysis rate of neutrophils by fungal cells. In [17] induced decondensation of nuclei of neutrophils ($1 \cdot 10^6 cells$) was measured in response to short hyphae ($750CFU$ with length of $10 - 100\mu m$). After 6h of co-incubation 28 % of neutrophil nuclei were decondensed. Based on the assumption that hyphae contain around 10 nuclei at the reported length, we estimate an MOI of 1:10 and calculate the rate as $n_3 = -\frac{ln(1-0.28)}{0.1\cdot 6h} = 0.5475\,cells^{-1}\,h^{-1}$.

References

[1] K. C. Stone, R. R. Mercer, P. Gehr, B. Stockstill, J. D. Crapo, et al., Allometric relationships of cell numbers and size in the mammalian lung, American Journal of Respiratory Cell and Molecular Biology 6 (2) (1992) 235–43.

[2] J. Knust, M. Ochs, H. J. G. Gundersen, J. R. Nyengaard, Stereological estimates of alveolar number and size and capillary length and surface area in mice lungs, The Anatomical Record: Advances in Integrative Anatomy and Evolutionary Biology: Advances in Integrative Anatomy and Evolutionary Biology 292 (1) (2009) 113–122.

[3] M. Bertuzzi, M. Schrettl, L. Alcazar-Fuoli, T. C. Cairns, A. Muñoz, L. A. Walker, S. Herbst, M. Safari, A. M. Cheverton, D. Chen, et al., The pH-responsive PacC transcription factor of *Aspergillus fumigatus* governs epithelial entry and tissue invasion during pulmonary aspergillosis, PLoS Pathogens 10 (10) (2014) e1004413.

[4] M. Saffarzadeh, C. Juenemann, M. A. Queisser, G. Lochnit, G. Barreto, S. P. Galuska, J. Lohmeyer, K. T. Preissner, Neutrophil extracellular traps directly induce epithelial and endothelial cell death: a predominant role of histones, PloS One 7 (2) (2012) e32366.

[5] S. Hirano, Interaction of rat alveolar macrophages with pulmonary epithelial cells following exposure to lipopolysaccharide, Archives of Toxicology 70 (3-4) (1996) 230–236.

[6] M. Blickensdorf, S. Timme, M. T. Figge, Comparative Assessment of Aspergillosis by Virtual Infection Modeling in Murine and Human Lung, Frontiers in Immunology 10.

[7] E. Dague, D. Alsteens, J.-P. Latgé, Y. F. Dufrêne, High-resolution cell surface dynamics of germinating *Aspergillus fumigatus* conidia, Biophysical journal 94 (2) (2008) 656–660.

[8] K. J. Kwon-Chung, J. A. Sugui, *Aspergillus fumigatus*—what makes the species a ubiquitous human fungal pathogen?, PLoS pathogens 9 (12) (2013) e1003743.

[9] B. Philippe, O. Ibrahim-Granet, M. Prevost, M. Gougerot-Pocidalo, M. S. Perez, A. Van der Meeren, J. Latge, Killing of *Aspergillus fumigatus* by alveolar macrophages is mediated by reactive oxidant intermediates, Infection and Immunity 71 (6) (2003) 3034–3042.

[10] J. A. Wasylnka, M. M. Moore, *Aspergillus fumigatus* conidia survive and germinate in acidic organelles of A549 epithelial cells, Journal of Cell Science 116 (8) (2003) 1579–1587.

[11] A. Alflen, S. Prüfer, K. Ebner, S. Reuter, P. A. Lopez, I. Scharrer, F. Banno, M. Stassen, H. Schild, K. Jurk, et al., ADAMTS-13 regulates neutrophil recruitment in a mouse model of invasive pulmonary aspergillosis, Scientific Reports 7 (1) (2017) 7184.

[12] T. T. Ng, G. D. Robson, D. W. Denning, Hydrocortisone-enhanced growth of *Aspergillus spp.*: implications for pathogenesis, Microbiology 140 (9) (1994) 2475–2479.

[13] J. Amich, Z. Mokhtari, M. Strobel, E. Vialetto, D. Sheta, Y. Yu, J. Hartweg, N. Kalleda, K. J. Jarick, C. Brede, et al., Three-dimensional light sheet fluorescence microscopy of lungs to dissect local host immune-*Aspergillus fumigatus* interactions, mBio 11 (1).

[14] N. Kalleda, J. Amich, B. Arslan, S. Poreddy, K. Mattenheimer, Z. Mokhtari, H. Einsele, M. Brock, K. G. Heinze, A. Beilhack, Dynamic immune cell recruitment after murine pulmonary *Aspergillus fumigatus* infection under different immunosuppressive regimens, Frontiers in Microbiology 7 (2016) 1107.

[15] S. Slesiona, M. Gressler, M. Mihlan, C. Zaehle, M. Schaller, D. Barz, B. Hube, I. D. Jacobsen, M. Brock, Persistence versus escape: *Aspergillus terreus* and *Aspergillus fumigatus* employ different strategies during interactions with macrophages, PloS One 7 (2) (2012) e31223.

[16] A. J. Thorley, P. A. Ford, M. A. Giembycz, P. Goldstraw, A. Young, T. D. Tetley, Differential regulation of cytokine release and leukocyte migration by lipopolysaccharide-stimulated primary human lung alveolar type II epithelial cells and macrophages, The Journal of Immunology 178 (1) (2007) 463–473.

[17] M. Röhm, M. J. Grimm, A. C. D'Auria, N. G. Almyroudis, B. H. Segal, C. F. Urban, NADPH oxidase promotes neutrophil extracellular trap formation in pulmonary aspergillosis, Infection and Immunity 82 (5) (2014) 1766–1777.

S2 Appendix

Influence of weightings in the innate immune response objectives.

Model behavior with no fungal burden minimization and only minimization of tissue damage.

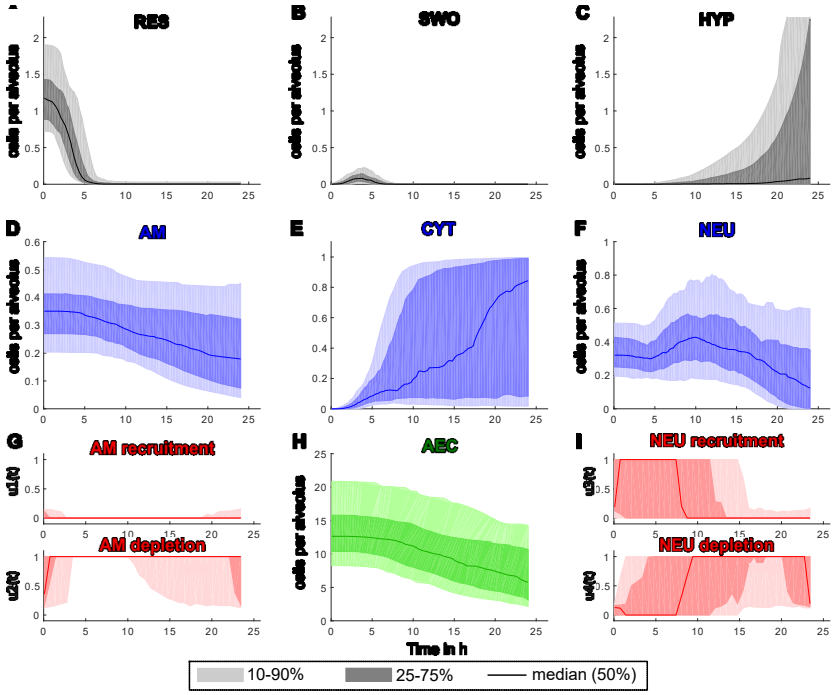

Figure A: Dynamics of innate immune response of the murine host challenged with a high dose of conidia (one per alveolus). The solution space of 100 parameter sets is depicted with shadings indicating the confidence intervals of time courses. Colors as in previous figures and equations.

Model behavior with only fungal burden minimization and no minimization of tissue damage.

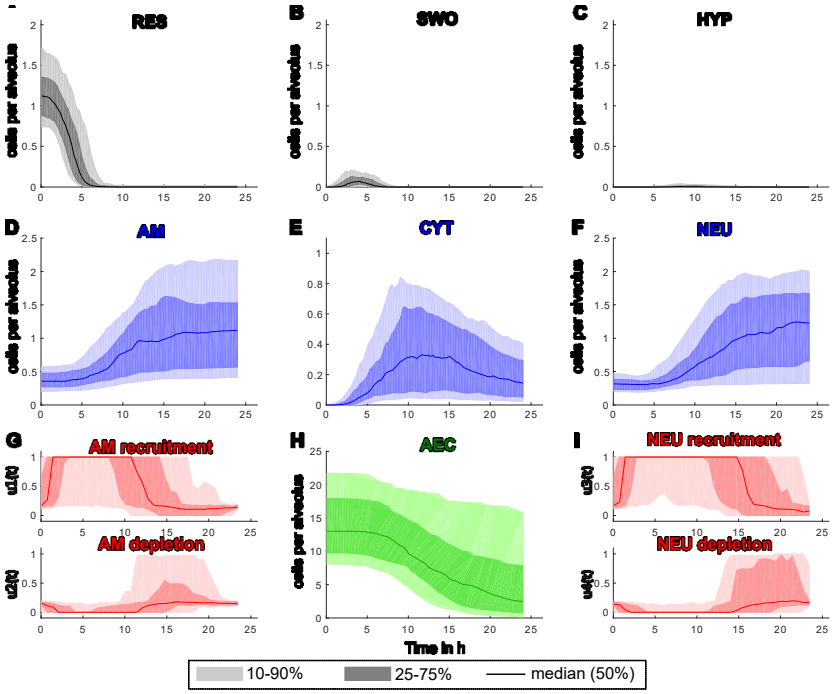

Figure B: Dynamics of innate immune response of the murine host challenged with a high dose of conidia (one per alveolus). The solution space of 100 parameter sets is depicted with shadings indicating the confidence intervals of time courses. Colors as in previous figures and equations.

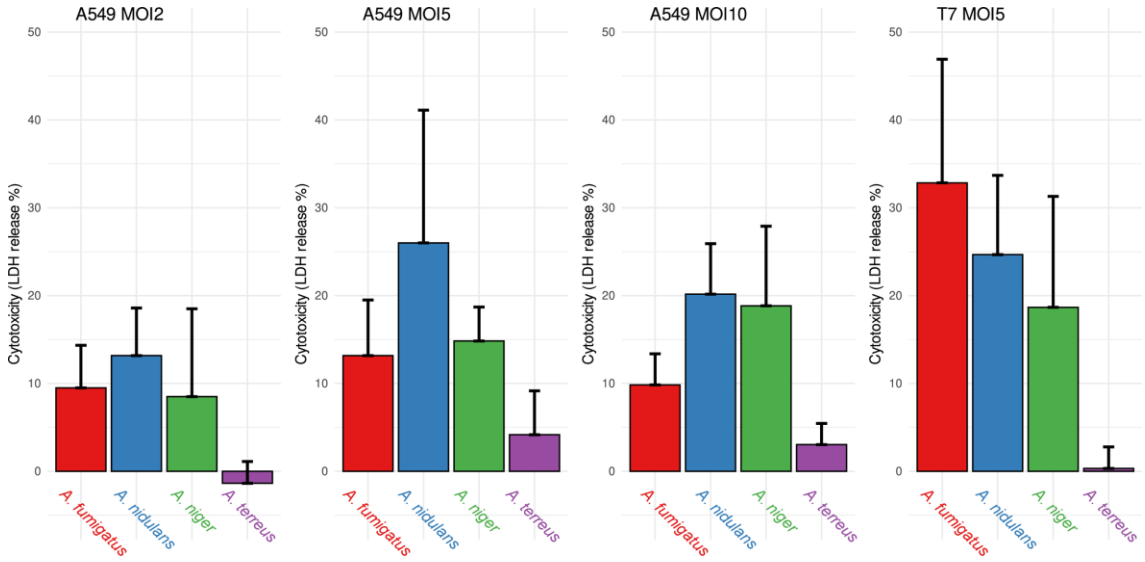
A549 MOI2
A549 MOI5
A549 MOI10
T7 MOI5
Cytotoxicity (LDH release %)
0
10
20
30
40
50
A. fumigatus
A. nidulans
A. niger
A. terreus

3. Manuscripts

3.5 Manuscript E

Selective DHN-melanin-dependent antifungal activity of neutrophil-derived extracellular vesicles against *Aspergillus fumigatus*

Rivieccio F, Zimmermann A-K, Cseresnyés Z, Rafiq M, Krüger T, Höppener S, Van den Brulle J, Kniemeyer O, Figge M.T, Von Lilienfeld-Toal M, Blango MG, Brakhage A.A.

Manuscript in preparation

Summary:

Polymorphonuclear leukocytes after contact with *A. fumigatus* conidia secrete extracellular vesicles which proved to be antifungal when applied to hyphae. In this study we further characterize these vesicles, showing that their killing activity is specific against *A. fumigatus* hyphae. Furthermore, we show that DHN-melanin present on the surface of conidia is triggering the release of antifungal EVs from neutrophils and that the most antifungal EV subpopulation is enriched for the tetraspanin CD81.

Additionally, investigation on neutrophils derived from immunosuppressed patients revealed that their EVs are not capable anymore, of inducing hyphal damage.

Contribution to the manuscript:

Flora Rivieccio participated in execution of all experiments. She contributed to design and optimization of protocols for EV staining, metabolic assay, isolation of EV-subpopulation and co-incubation experiments with different pathogens. Additionally, she contributed to writing and editing the manuscript.

Estimated contribution in percentage:

Author	Conceptual	Data analysis	Experimental	Writing the manuscript	Provision of material
Rivieccio F.	**20%**	**35%**	**40%**	**35%**	**0%**
Zimmermann A-K	10%	15%	20%	10%	0%
Cseresnyés Z	5%	20%	0%	5%	0%
Rafiq M	5%	12%	15%	5%	0%
Krüger T.	5%	8%	15%	5%	0%
Blango MG.	15%	5%	0%	15%	0%
Brakhage A.A	35%	0%	0%	20%	100%
Others	5%	5%	10%	5%	0%
Total:	100%	100%	100%	100%	100%

Selective, DHN-melanin-dependent antifungal activity of neutrophil-derived extracellular vesicles against *Aspergillus fumigatus*

Flora Rivieccio[1,2], Ann-Kathrin Zimmermann[1,2], Zoltán Cseresnyés[3], Rafiq Muhammad[1,2], Thomas Krüger[1], Stephanie Höppener[4,5], Jan Van den Brulle[6], Olaf Kniemeyer[1], Marc Thilo Figge [2,3], Marie von Lilienfeld-Toal[7,8,9], Matthew G. Blango[10], Axel A. Brakhage[1,2*]

[1] Department of Molecular and Applied Microbiology, Leibniz Institute for Natural Product Research and Infection Biology (Leibniz-HKI), Jena, Germany.

[2] Department of Microbiology and Molecular Biology, Institute of Microbiology, Friedrich Schiller University, Jena, Germany.

[3] Research Group Applied Systems Biology, Leibniz Institute for Natural Product Research and Infection Biology (Leibniz-HKI), Jena, Germany

[4] Laboratory of Organic and Macromolecular Chemistry (IOMC), Friedrich Schiller University, Jena, Germany.

[5] Jena Center for Soft Matter (JCSM), Friedrich Schiller University, Jena, Germany.

[6] T-CURX GmbH, Würzburg, Germany.

[7] Klinik für Innere Medizin II, Abteilung für Hämatologie und Internistische Onkologie, Universitätsklinikum Jena, Germany.

[8] Infections in Hematology and Oncology, Leibniz Institute for Natural Product Research and Infection Biology (Leibniz-HKI), Jena, Germany.

[9] National Reference Center for Invasive Fungal Infections (NRZMyk), Leibniz Institute for Natural Product Research and Infection Biology (Leibniz-HKI), Jena, Germany.

[10] Junior Research Group RNA Biology of Fungal Infections, Leibniz Institute for Natural Product Research and Infection Biology (Leibniz-HKI), Jena, Germany.

Running Title: Selective killing of neutrophil-derived EVs

Key Words: fungi, PMNs, extracellular vesicles, conidia, *Aspergillus fumigatus*, *Pseudomonas aeruginosa*, *Staphylococcus aureus*, *Aspergillus nidulans*, opsonization, DHN-melanin

*Correspondence: E-mail axel.brakhage@leibniz-hki.de

Tel. +49 (0)3641-532 1001.

Abstract

Fungal infections cause over 1.5 million deaths per year worldwide. Alarmingly these numbers continue to rise, and treatment of life-threatening fungal infections is often inefficient. Essential immune cells for defense are human polymorphonuclear granulocytes (PMNs). They release antifungal extracellular vesicles (afEVs) upon exposure to the important human fungal pathogen *Aspergillus fumigatus*. These afEVs prevent germination of asexual spores and kill hyphae. Here, we investigated the specificity of afEVs against microorganisms and their characteristics when isolated from patients. We demonstrate that the antifungal activity of afEVs requires conidial dihydroxynapthalene melanin as trigger and that these afEVs are only antifungal against DHN-melanin-producing Aspergillus species but not bacteria, or even other Aspergillus species like *Aspergillus nidulans*. Surprisingly, despite carrying a range of antimicrobial cargo proteins afEVs promoted yeast-to-hyphal transition of the pathogenic yeast *Candida albicans*. Proteomics and selective EV enrichment strategies indicated that the afEV population was enriched for tetraspanin CD81. Furthermore, staining of EVs with the self-quenching membrane dye MemGlow revealed that afEVs primarily associate with the remnants of the conidia where germination starts, suggesting a model whereby targeting of EVs to the specific pathogen is required for delivery of antifungal cargo. Finally, we tested the antifungal activity of afEVs derived from PMNs of corticosteroid-treated patients that are at risk for an A. *fumigatus* infection. We observed that certain treatment regimens of patients abolished the antifungal activity of *A. fumigatus*-induced EVs. In conclusion, human PMNs produce afEVs after association with DHN-melanized *A. fumigatus* conidia that exhibit target specificity. Their reduced antifungal activity likely contributes to the susceptibility of corticosteroid-treated patients for invasive fungal infections.

Introduction

Invasive aspergillosis (IA), mainly caused by the filamentous fungus *Aspergillus fumigatus*, is the mold infection most frequently found in immunocompromised patients (Brakhage 2005, Brown et al 2012, Kwon-Chung & Sugui 2013, Latge & Chamilos 2019). IA is a critical condition with exceedingly high fatality rates, and, in the last years, recognized as a complication in patients infected with the SARS-CoV-2 virus (Lahmer et al 2021, Latge & Chamilos 2019, Nasir et al 2020). Polymorphonuclear granulocytes (PMNs), primarily neutrophils, are immune cells essential for the clearance of *A. fumigatus* (Kalleda et al 2016, Marciano et al 2015, Mircescu et al 2009). The importance of PMNs in antifungal defense was deduced from studies with neutropenic mouse infection models, which show high susceptibility to *Aspergillus* infections, and from the high infection rate of patients with neutropenia or chronic granulomatous disease (King et al 2016, Segal & Romani 2009, Stephens-Romero et al 2005). PMNs rapidly phagocytose conidia and subsequently release cytokines, granules, and reactive oxygen species (ROS) to limit fungal spread and further alert the immune system (Braem et al 2015, Drummond et al 2014, Levitz & Farrell 1990, Shlezinger et al 2017). As the spores germinate and grow into hyphae too large to be phagocytosed, PMNs provide an additional layer of defense through the formation of neutrophil extracellular traps (NETs) and granules (Branzk & Papayannopoulos 2013, Bruns et al 2010). NETs consist of extracellular DNA and antimicrobial proteins and are usually released upon pathogens stimulation (Rosazza et al 2021). Surprisingly, despite containing antifungal proteins, NETs only act mildly fungistatic on *A. fumigatus* (McCormick et al 2010).

Recently, it was discovered that PMNs also produce a diverse group of secreted particles known as extracellular vesicles (EVs) (Brakhage et al 2021, Kolonics et al 2021). EVs are small lipid bilayer nanoparticles that can exert various functions in

vivo (Headland et al 2015, Letsiou et al 2021), including antibacterial and antiviral activity (Lim et al 2015, Lőrincz Á et al 2020, Timár et al 2013). Depending on the stimulus applied to the cells, they carry different surface markers, which can be used for the diagnosis of diseases, like sepsis or cancer (Headland et al 2015, Herrmann et al 2015, Kolonics et al 2020, Letsiou et al 2021, Manojlovic et al 2020).

Previously, we discovered that human PMNs secrete particles with a mean size of 200 nm after having encountered conidia of *A. fumigatus* (Shopova et al 2020). Proteome analysis showed that antifungal EVs (afEVs) derived from infected PMNs are enriched for antimicrobial peptides like azurocidin, cathepsin G, and defensin compared to spontaneously released EVs (sEVs). Further investigation revealed that afEVs were associated with the fungal cell wall and that a portion traversed the cell wall and even reached the fungal cytoplasm. Interestingly co-incubation of hyphae of a mitochondrial GFP-tagged strain of *A. fumigatus* with afEVs, but not sEVs, led to inhibition of fungal growth and fragmentation of mitochondria, suggesting killing of hyphae.

Here, we demonstrate that afEVs derived from primary PMNs infected with *A. fumigatus*, are highly specific against *A. fumigatus* and that the molecule triggering the antifungal activity of afEVs is dihydroxynaphthalene (DHN) melanin present on the surface of conidia. Furthermore, we tracked the entry of afEVs into fungal hyphae in detail and define the CD81+ EV subset as key in delivering antifungal cargo (Théry et al 2018). Lastly, we demonstrate that afEVs derived from PMNs of patients undergoing immunosuppressive treatment lack the antifungal activity in response to the fungal challenge, potentially refining our understanding of the susceptibility of these patients for fungal infections and providing an intervention point for design of future therapeutics.

Materials and Methods

Fungal strains and cultivation

Cultivation of all strains listed in **Table 1** was performed on malt extract (Sigma-Aldrich) agar plates supplemented with 2% (wt/vol) agar for 5 days at 37°C. The only exception was *Aspergillus clavatus* which was incubated at 25°C. Conidia were harvested in sterile, autoclaved water, filtered through 30-µm filters (MACS Milteny Biotec), and counted with a Thoma chamber. Cultivation of the *Candida albicans* wild-type strain SC5314 or of the strain constitutively expressing a cytoplasmic GFP under the control of the alcohol dehydrogenase (ADH1) promoter (kindly provided by Bernard Hube, Leibniz-HKI, Jena) was performed on YPD agar (10 g/L Yeast extract, 20 g/L peptone, 20 g/L dextrose and 20 g/L of agar) for 20 h at 30°C.

Bacterial strains and their cultivation

Staphylococcus aureus HG003 and *Pseudomonas aeruginosa* PAO1 (ATCC BAA-47) were streaked from -80°C glycerol stocks on Lysogeny broth (LB; Sigma Aldrich) medium agar plates and incubated at 37°C for 16 h. Before co-incubation with EVs, fresh bacterial colonies were inoculated in LB medium and cultured at 37°C with 200 rpm shaking for 5 h. The turbidity of the culture broth was measured at 600 nm using a spectrophotometer. For determination of colony forming units (CFUs), bacterial growth was stopped when an optical density (OD) of 0.3 was reached. Bacteria were spun down at 1500 x g for 5 min, washed once with PBS, and resuspended in 1 ml of Hank's balanced salt solution (HBSS) with Ca^{2+} and Mg^{2+} (HyClone, GE Healthcare). For each condition, 250 µl of this bacterial suspension was mixed with 50 µl of EVs derived from PMNs infected with *A. fumigatus* (afEVs) or spontaneously derived EVs (sEVs) and incubated for 1 h at 37°C with 100 rpm shaking. As positive control, bacteria were mixed with 50 µl of HBSS containing 0.3% (v/v) of hydrogen peroxide

(Carl Roth). At the end of the co-incubation time, serial dilutions in LB medium were plated on LB agar plates. The agar plates were incubated at 37°C for 16 h.

Viability assay for bacteria

Bacteria were grown until an OD of 0.1 was reached, then spun down, washed once with PBS, and resuspended in HBSS buffer. 150 µl of bacterial suspension per well was filled in an 8-well micro chamber slide (Ibidi) and co-incubated with 50 µl of EVs (afEVs or sEVs) for 1 h at 37°C. In the remaining wells, 50 µl of HBSS or 0.2% (v/v) hydrogen peroxide for *P. aeruginosa* and 0.4 % (v/v) for *S. aureus* was added as a positive control. After 1 h, bacteria were stained using the LIVE/DEAD™ BacLight™ Bacterial Viability Kit (Thermo Fischer Scientific) according to the manufacturer's instructions. Imaging was performed using a Zeiss LSM 780 confocal microscope.

Determination of CFUs of *Candida albicans* and microscopical analysis

To determine CFUs of *C. albicans*, 10 ml of YPD liquid medium were inoculated with fresh colonies of the *C. albicans* wild-type strain grown on YPD agar plates. Cultures were incubated at 30°C with 200 rpm until an OD=2.0 was reached. Cells were then spun down by centrifugation, washed once with PBS, and were re-suspended in 1 ml of HBSS. *C. albicans* cells were counted with a Thoma chamber and $1x10^7$ cells/condition were re-suspended in HBSS up to 250 µl and mixed with 50 µl of EVs (afEVs or sEVs) for 1 h at 30°C. As a positive control, 50 µl of HBSS containing 0.3% (v/v) of hydrogen peroxide (Carl Roth) was added. After the co-incubation time serial dilutions were performed in YPD liquid medium, plated on YPD agar plates, and incubated at 30°C for 48 h.

To determine the effects of EVs on *C. albicans*, a GFP strain kindly provided by

Bernhard Hube (Leibniz-HKI, Jena) was used. The strain was cultured as described above. Then, 10^5 cells were re-suspended in 150 µl of HBSS, added to an 8-well chamber slide (Ibidi) and co-incubated with 50 µl of EVs (afEVs or sEVs) or HBSS containing 0.2% (v/v) of hydrogen peroxide. Images were captured after 3 and 20 h using a Zeiss LSM 780 confocal microscope.

Opsonization of conidia

Conidia (900 µl in PBS) were opsonized with 100 µL pooled normal human serum (Merck Millipore) for 30 min at 37°C, 500 rpm. After opsonization, conidia were sedimented by centrifugation (5 min, 4°C, 1800 x g), and washed with PBS three times.

Isolation of human PMNs

Isolation of primary PMNs from the blood of healthy donors between 20 and 35 years of age, non-smokers, was performed as described before (Rafiq et al 2022). This study was approved by the Jena University Hospital Institutional Review Board (approval number 5074-02/17) in agreement with the Declaration of Helsinki.

After approval from the local institutional review board (approval number 2020-1965) and written informed consent, 5 patients with hematological malignancies were recruited for this study. All patients had neutrophil counts >1.5 G/l and no or a mild impairment in the full blood count. Three groups of patients were recruited to account for different factors: the first patient suffered from relapsed multiple myeloma with currently active disease and received immunosuppressive chemotherapy with short term high dose steroid treatment. The second group consisted of patients with recent allogeneic stem cell transplantation, no evidence of graft-versus-host disease (GvHD) and no steroid treatment but ongoing immunosuppressive therapy with cyclosporine.

The third group had received allogeneic stem cell transplantation >2 years prior to the study and suffered from chronic GvHD that made long term steroid treatment as well as immunosuppression with everolimus necessary. For details on the immunosuppressive status of recruited patients, see **Table S2**.

Isolation of extracellular vesicles

EVs were prepared essentially as described previously (Shopova et al 2020). Briefly, after co-incubation of PMNs with conidia, the samples were centrifuged with 1000 x g for 10 min at 4°C. The supernatant was filtered through 5-µm filters (Merck-Millipore) and then re-centrifuged for 20 min with 19,500 x g at 4°C. Finally, the EV pellet was re-suspended in 100 µl of HBSS buffer with Ca^{2+} and Mg^{2+} (HyClone, GE Healthcare) and added to the fungus for the fungal inhibition assay. For protein analysis, the pellet was resuspended in 100 µl of PBS and stored at -20°C. For isolation of EV subpopulations, EVs were selected for tetraspanin proteins present on their surface. For this purpose, after the filtration step, 50 µl of microbeads covered with antibodies against CD9, CD81, CD63 (Miltenyi biotec) were added to the EV flow through and left at room temperature for 1 h. Then, EVs were enriched by magnetic columns following the manufacturer's instructions and eluted from the columns. Then the eluted solution was ultracentrifuged at 4°C for 20 min at 19,500 x g. The obtained pellet was resuspended in either HBSS buffer or PBS as described above.

Fluorescent labeling of EVs

EVs were fluorescently labeled using MemGlow™ 560 (Cytoskeleton, Inc.). After ultracentrifugation, EVs were resuspended in 100 µl of HBSS and mixed with 200 nM of MemGlow reagent. The solution was added to hyphae of a mitochondrial-GFP

reporter strain of *A. fumigatus* that allows to detect inhibition and killing of hyphae (AfS35/pJW103; (Ruf et al 2018), as previously described (Shopova et al., 2020). The co-culture was left at room temperature for 10 min and was finally incubated at 37°C for 16 h. Microscopy Z-stacks were taken using a Zeiss LSM 780 confocal microscope (Carl Zeiss).

Fungal inhibition and killing assays

To assess the antifungal killing capacity of EVs derived from PMNs co-incubated with *A. fumigatus*, *A. clavatus* or melanin ghosts, we used the mitochondrial-GFP reporter strain AfS35/pJW103 (Ruf et al 2018). For some experiments EVs derived from PMNs infected either with *A. fumigatus* or *A. nidulans* WT were added to a mitochondrial-GFP strain of *A. nidulans*. This strain was created by translationally fusing the GFP with the N-terminus of the *SUAPRGA1* protein (AN3034) which is localized in mitochondria (**Fig. 1D**) (Van den Brulle et al 1999). To this aim, the *A. nidulans pyrG89* strain, with an auxotrophy for uracil, was co-transformed with plasmids pKTB1 and p123. pKTB1 encodes a functional *pyrG* gene, for complementation of the *pyrG89* mutation, and the β lactamase resistance gene. Plasmid p123 encodes the N-terminus (amino acids 1-95) of the *SUAPRGA1* protein translationally fused with an eGFP gene. The gene fusion is controlled by the translation elongation factor gene (tef) promoter of *Ustilago maydis* which is constitutively expressed in *A. nidulans*.

For co-cultivation of fungus and EVs, $5x10^4$ conidia/well in an 8-well chamber slide (Ibidi) were resuspended in 150 µl of RPMI without phenol red (Thermo Fischer Scientific) and incubated at 37°C + 5% (v/v) CO_2 for 8 h. Then 100 µl of EVs in HBSS buffer were added to the wells and as negative and positive controls, HBSS alone or with 0.4% (v/v) H_2O_2, respectively. After 16 h the fungal cell wall was

stained with calcofluor white and microscopy Z-stacks were taken using a Zeiss LSM 780 confocal microscope.

To monitor inhibition of fungal activity after addition of EVs, the conversion of the blue nonfluorescent compound, resazurin (Sigma Aldrich), into the highly fluorescent pink resorufin was measured (Monteiro et al 2012). After 16 h of co-incubation with EVs, the supernatant was removed from the Ibidi wells and 300 µl/well of RPMI without phenol red containing 20 ng/ml of resazurin (Sigma Aldrich) were added. The slide was placed for additional 20 h at 37°C + 5% (v/v) CO2. After incubation, 100 µl were transferred in each well of a 96-well plate and the absorbance was measured at both 590 and 615 nm using a Tecan Infinite 200 (LabX) microplate reader. The metabolic conversion of resazurin by hyphae treated with sEVs and afEVs was calculated in comparison with the fungus left untreated as a negative control and with the fungus treated with H_2O_2 as a positive control.

Isolation of melanin ghosts

Melanin ghosts from *A. fumigatus* CEA10 were prepared according to the method previously described (Thywißen et al 2011) with few modifications. The fungus was cultivated for 5 days at 37°C on malt agar plates. The produced spores were harvested and washed twice with PBS + 0.1% (v/v) Tween 20. The cell wall was digested overnight with 10 mg/ml vinotaste (Novozymes) and 5 mg/ml Yatalase (Takara) dissolved in 10 ml of 0.1 M sodium citrate and 1 M sorbitol at 30°C. The generated protoplasts were washed 3 times in PBS + 0.1% (v/v) Tween 20 and incubated overnight with 4 M guanidine thiocyanate (Sigma-Aldrich) at room temperature. After three washing steps the particles generated were digested with 1 mg/ml of Proteinase K in 10 mM of Tris pH 7.8, 1 mM $CaCl_2$ and 0.5% (w/v) SDS, overnight at 37°C. Particles were washed again as before and boiled in 6 M hydrochloric acid

overnight. To get rid of any remaining impurities, the ghosts were washed 3 times with methanol (polar organic solvent) and three times with hexane (apolar organic solvent). After these washing steps, solvents were completely evaporated, and the melanin ghosts were resuspended in water and stored at 4°C.

Nanoparticle tracking analysis

Particle concentration and size distribution of particles were analyzed using a nanoparticle tracking analyzer (NTA) NS300 device with a 650 nm laser (Malvern Instruments Ltd., UK). Samples were measured with a constant flow rate of 20 and a temperature set to 25°C. Four videos 40 seconds each were recorded with a camera level of 11. Videos were then analyzed with the NTA 3.2.16 software using a detection threshold of 5.

Protein isolation and LC-MS/MS analysis

Proteins of EVs were isolated by delipidation and proteolytically digested as described previously (Rafiq et al 2022). LC-MS/MS analysis was performed on an Ultimate 3000 nano RSLC system connected to a Q Exactive Plus (#1) and Q Exactive HF (#2) mass spectrometer (both Thermo Fisher Scientific). Each sample was measured in triplicate (three analytical replicates) as previously described (Rafiq et al 2022) with the following changes. Precursor ions were monitored at m/z 300 to 1500 at a resolution of 140,000 (#1) or 120,000 (#2) FWHM (full width at half maximum). MS2 ions were scanned at 17,500 (#1) or 15,000 (#2) FWHM.

Database search and data analysis

Tandem mass spectra were searched against the UniProt database of *Homo sapiens* (https://www.uniprot.org/proteomes/UP000005640; 8 Dec 2021) and *Neosartorya*

fumigate Aspergillus fumigatus (https://www.uniprot.org/proteomes/UP000002530; 8 Dec 2021) using Proteome Discoverer (PD) 2.4 (Thermo) and the algorithms of Mascot 2.4.1 (Matrix Science), Sequest HT (version of PD2.4), MS Amanda 2.0, and MS Fragger 3.4 as previously described (Rafiq et al 2022). For label-free protein quantification, the Minora algorithm of PD2.4 was used. Significant differences in protein abundance were defined when the following three requirements were reached: at least a 2-fold change in abundance (up and down), a ratio-adjusted P value of <0.05, and identified in at least two of three replicates of the sample group with the highest abundance.

Data availability

The mass spectrometry proteomics data have been deposited to the ProteomeXchange Consortium via the PRIDE partner repository (Perez-Riverol et al 2022) with the data set identifier PXD033496.

Bioinformatic analysis

Images were provided for quantitative analysis in the Carl Zeiss Image (CZI) 3D native format. In the first step of processing (see **Suppl. Fig. S4**), images were deconvolved using the Huygens Professional software (SVI, Hilversum, The Netherlands, https://www.svi.nl). The software utilized the measured point spread function (PSF; see **Suppl. Fig. 5A**), which was acquired in the same sample as the actual experiments, using 170 nm fluorescent plastic beads with excitation and emission wavelengths that matched those of the biological samples: excitation at 488 nm (mitochondria), 560 nm (transmitted light; EVs), 405 nm (hyphae). The deconvolved images were saved automatically in the Imaris (Bitplane, Zürich, Switzerland, https://www.bitplane.com) native .ims file format, using the batch

processing mode of Huygens. The deconvolved files were further processed in Imaris 9.9.0 and 9.9.1, using home-developed batch processing scripts (**Suppl. Fig. 4**). Each processed image was manually checked for possible segmentation errors and corrected by rerunning the adjusted segmentation script when necessary. Comparing the raw and deconvolved hyphae (**Suppl. Fig. 5B**) and mitochondria (**Suppl. Fig. 5C**) images reveals that the most noticeable effect of deconvolution is in the Z direction, where the raw segmentation expands larger. The deconvolved images were segmented both with a stricter and a more lenient threshold (**Suppl. Fig. 4**). The strict hyphae segmentation revealed the actual wall boundaries, whereas the lenient hyphae reconstruction provided the properly closed volume necessary to correctly estimate the hyphae volume that was compared with the lenient mitochondria volume (**Suppl. Fig. 6**). The strict hyphae volume was used to measure the EVs' spatial position relative to the hyphal cell wall (**Suppl. Fig. 7**).

The health status of the hyphae was characterized by measuring the volume of the intact (brightly fluorescent) mitochondria (**Suppl. Fig. 5 A-B**) relative to the that of the hyphae (**Suppl. Fig. 6C**). Additional measures were also made available by the segmentation, including area, aspect ratio, ellipticity, etc. These measures were deduced for the various biological conditions and their distributions plotted for the entire population in order allow objective conclusions to be drawn regarding the possible differences assignable to the various circumstances. For the quantitative analysis of the EVs, the deconvolved fluorescence signal (**Suppl. Fig. 7A**) was segmented as Spots in Imaris (**Suppl. Fig. 7B**), and the location of the Spots were compared to the nearest position of the strict hyphal membrane (**Suppl. Fig. 7C**). The Spots were allowed to have various radii, in order to account for the possible presence of unresolvable small EV clusters (**Suppl. Fig. 7B**). The Spots were color-coded according to the mean intensity of the hyphae fluorescence measured inside the Spots.

These measurements were made more objective and quantifiable by using a masked channel of the hyphae signal: here the raw fluorescence volume signal of the hyphae was masked with the reconstructed hyphae surfaces, making all voxels outside the hyphae surface equal zero, whereas setting the voxels inside the surface equal to 10. This way the mean value of the masked hyphal signal inside the individual EVs quantitatively characterized the proportion of the Spots volume occupied by hyphal signal. *E.g.*, with Spots that were full embedded in the hyphae wall, the mean value of the masked signal equaled 10, whereas the Spots that were outside the hyphae showed a mean value of 0. A Spot that was 40% embedded into the hyphae wall would show the mean value of 4.0 (0.4 * 10). This simple method allowed us to quantify the proportion of EV Spots that were fully or partially embedded in the hyphae wall, compared to those that were outside the fungal cell wall. The EV analysis was limited to the bulbous, based on the observation that the EVs were attached exclusively to this part of the fungi.

Cryo-EM

Cryo-TEM samples were prepared utilizing a Vitrobot Mark IV (FEI, The Netherlands) plunge freezer. 9 µL of the solution was blotted onto a precleaned Quantifoil R2/2 (Quantifoil, Germany). Cleaning was performed in Argon plasma for 2 minutes (Diener Electronics, Germany). Excess of the liquid was removed utilizing the Vitrobot (-2 mm blot force, 1 sec blotting time) and samples were rapidly immersed in liquid ethane serving as a cryogen. Samples were transferred to the cryo holder (Gatan 626, US) utilizing the Gatan cryo stage and are finally transferred to the microscope. After vitrification the temperature was maintained below -173°C at all times.

Cryo-TEM investigations were performed on a FEI Tecnai G^2 20 at an acceleration

voltage of 200 kV. Images were acquired on a Megaview (OSIS, Olympus Soft Imaging Systems, Japan) or a 4x4 k Eagle CCD camera. Image analysis and contrast optimization were performed with ImageJ (Version V1.47v).

Statistical Analysis

To plot and analyze the data GraphPad Prism software 5.0 (GraphPad Software) was used. Significance between two groups was calculated with the Student's t test. Differences were considered significant at a P value of <0.05. Throughout the article, significance is denoted as follows: *, $P \leq 0.05$; **, $P \leq 0.01$, ***, $P \leq 0.001$; ns, not significant.

Results

***A. fumigatus*-induced afEVs of human polymorphonuclear leukocytes (PMNs) specifically target *A. fumigatus*.**

PMNs respond to A. *fumigatus* infection with the production of afEVs (Shopova et al 2020). To assess whether the killing capacity of such afEVs is restricted to *A. fumigatus*, we tested their activity on a series of bacterial and fungal pathogens. Therefore, afEVs were isolated from primary PMNs and were co-incubated for 1 h with *Pseudomonas aeruginosa*, *Staphylococcus aureus*, and *Candida albicans* followed by plating of serial dilutions on agar plates and determination of colony forming units (CFUs). Because there was no significant difference of CFUs in treated and untreated cultures, we concluded that afEVs do not harm any of these pathogens over this co-incubation time (**Fig. 1A, Suppl. Fig. 1A**). To confirm these findings, we applied live/death staining with Syto 9 and propidium iodide. Both dyes bind DNA, but while Syto 9 is able to permeate intact membranes, the cell-impermeable PI dye can only cross damaged membranes. *S. aureus* and *P. aeruginosa* were stained

with both dyes after treatment with either afEVs or sEVs. As shown in **Fig. 1B**, *P. aeruginosa* exhibited only green signals in samples untreated, treated with afEVs and sEVs, suggesting that membrane integrity of bacteria was not compromised under any of these conditions. Surprisingly, despite no change in CFUs, *S. aureus* treated with afEVs showed both green and red fluorescence similar to the positive control that was treated with hydrogen peroxide (**Suppl. Fig. 1B**).

We next determined the effect of EVs on *C. albicans* using a GFP-expressing strain. Confocal laser scanning microscopy revealed that both sEVs and afEVs induced formation of hyphae after 3 h that was even more visible after 20 h of co-incubation (**Fig. 1C**). To check whether induction of hyphae formation was dependent on intact vesicles, we lysed EVs with Triton X-100. This treatment completely abolished the phenotype, indicating that an intact EV membrane is required for the induction of the yeast-to-hypha transition (**Suppl. Fig. 1C**).

Lastly, we tested the antifungal effect of afEVs on another member of the Aspergilli, *i.e.*, *Aspergillus nidulans*. *A. nidulans* has a few key differences to *A. fumigatus*, including an apparently different melanin polymer on conidia (Valiante et al 2016). To analyze the effect of afEVs on *A. nidulans* we generated a mitochondrially tagged-GFP strain that has the suAprgA1 gene translationally fused with the GFP gene. As shown in **Fig. 1D**, this strain worked as well as the corresponding *A. fumigatus* strain. Treatment with H_2O_2 led to the disappearance of the mitochondrial network. By contrast, treatment with afEVs for 16 h did not show a significant change in the mitochondrial network or in the length of hyphae compared to the untreated control, indicating that afEVs did not have a major effect on *A. nidulans* (**Fig. 1D**).

DHN-melanin induces formation of antifungal EVs.

Our previous study suggested that EVs derived from human PMNs infected with a

DHN-melanin deficient of *A. fumigatus*, the *ΔpksP* mutant strain, did not exhibit antifungal activity (Shopova et al 2020). Therefore, it appeared likely that DHN-melanin is an important inducer of the antifungal activity of EVs. To further address this question, we isolated DHN-melanin ghosts from conidia, and added them to human PMNs. After co-incubation for 2 h we isolated EVs potentially induced by DHN-melanin ghosts (mg-EVs) and analyzed the mg-EVs for their antifungal activity using the mitochondrial GFP reporter strain of *A. fumigatus*. As shown in **Fig. 2A**, incubation of hyphae with mg-EVs triggered fragmented mitochondria and a reduced length of hyphae. This data suggested that in fact DHN-melanin is important as a stimulus for production of afEVs. To confirm this finding, we infected PMNs with another member of the Aspergilli, *Aspergillus clavatus* that apparently is the second known Aspergillus species that encodes the DHN-melanin gene cluster and thus most likely produces DHN-melanin (Valiante et al. 2016). As expected, EVs isolated from PMNs infected with conidia of *A. clavatus* exhibited antifungal activity (**Fig. 2A**). For comparison, we infected PMNs with *A. nidulans* conidia, whose conidial melanin significantly differs from DHN-melanin (Gonçalves et al 2012, Strycker et al 2021). EVs derived from this co-incubation (anEVs), were not able to kill *A. fumigatus* or *A. nidulans* itself, suggesting specificity in both the inducing signal for formation of afEVs and their target microorganisms (**Suppl. Fig. 2**).

Although visual inspection of the mitochondrial GFP strains by confocal laser scanning microscopy allowed the detection of differences in antifungal capacity between EV populations, we decided to quantify this effect by adapting a bioinformatic algorithm. This algorithm allowed to deconvolve and reconstruct the signal from all hyphae observed in one microscopy Z-stack and then to evaluate the volume of both hyphae and mitochondria. As shown in **Fig. 2C**, this analysis highlighted the damage to mitochondria and the growth inhibition induced by afEVs

compared to sEVs or to untreated controls. The values for mg-EVs and *A. clavatus*-derived EVs were also comparable to afEVs although, for the melanin ghosts, slightly higher values were observed. This may be due to the tendency of ghosts to clump and form aggregates, leading to an insufficient stimulation of PMNs (**Fig. 2C**).

EVs strongly associate with hyphae near the site of conidia germination.

Since their discovery visualization of EVs has been a real challenge (Reclusa et al 2020). In previous work we showed that annexin V-stained afEVs primarily associated with the cell wall of the fungus and to a much lesser extent were internalized (Shopova et al 2020). Due to difficulties in removing excess dye from EV samples during washing, these staining experiments are typically aggravated by the loss of the sample, high background fluorescence, and artifacts (Simonsen 2019). Here, to stain EVs we took advantage of a newer generation of lipophilic dye called MemGlow. These self-quenching dyes intercalate into lipid bilayers, where they then emit a fluorescence signal. The advantage of staining EVs is the minimal background observed when the dye is not bound to membranes.

After incubation with fungal germlings for 16 h, afEVs stained with MemGlow accumulated on the former conidium head of *A. fumigatus* and apparently used this site for entry into the cytoplasm (**Fig. 3A**). Since afEVs do not kill *A. nidulans*, we wondered if this was due to their cargo or to their lack of affinity to the cell wall of *A. nidulans* and at the same time to their affinity for *A. fumigatus*. Therefore, we co-incubated Memglow-stained afEVs with the mitochondrial GFP strain of *A. nidulans*. As seen in **Fig. 3B**, afEVs were not internalized into this fungus but were rather enriched at the bottom of the well. The intensity of the EV signal inside or outside of the cell wall of *A. fumigatus* and the amount of signal present on the conidia head or directly on hyphae, was again quantified. As shown in **Fig. 3C**, most of the signal

from all EV populations derives from outside the hyphae. However, the percentage of afEVs completely embedded into *A. fumigatus* hyphae was much higher compared to sEVs or afEVs embedded into *A. nidulans* hyphae. Thus, this quantification proves that afEVs have a higher affinity to the cell wall of *A. fumigatus*.

Antifungal activity is most potent in a CD81+ labelled EV subpopulation.

The tetraspanins CD9, CD81, and CD63 are well-established EV markers used in both research and the clinics (Théry et al 2018). Although being almost ubiquitously present on EVs from different cells and tissues, these tetraspanins are not equally distributed on the surface of EVs (Mathieu et al 2021). In some cases, EV populations are enriched for particular tetraspanin proteins, which seems to correlate with specific cargos in these EVs (Andreu & Yáñez-Mó 2014, Mizenko et al 2021).

To characterize the subpopulations of PMN-derived EVs, we isolated afEVs and sorted them with CD9, CD81, CD63 antibody-coated beads. Cryo-EM imaging on each tetraspanin-enriched fraction assured the integrity of EVs in the samples (**Fig. 4A**).

The thus obtained different EV populations appeared dissimilar, suggesting different cargos in these afEV subsets. This led us wonder whether the subpopulations differ in their antifungal effects. This was in fact the case, when the GFP-tagged *A. fumigatus* strain was confronted with different afEV subpopulations. As shown in **Fig. 4B**, the CD81-afEVs always proved to show the highest antifungal activity, leading to a complete disappearance of the mitochondrial GFP signal after 16 h of co-incubation with the fungus. The CD9-enriched afEVs on the other hand were hardly antifungal, whereas the CD63-enriched population displayed a mild antifungal effect. To define the contents of the strongly antifungal CD81-afEV subpopulation, we performed proteome analysis by comparing sEVs and afEVs

isolated without beads and sEVs and afEVs enriched with CD81 antibodies. LC-MS/MS analyses allowed to detect a total of 817 proteins (see dataset S1). As expected, most of these proteins were shared between sEVs and afEVs total population, while a small number were exclusively found in afEVs isolated with beads (**Fig. 4C**). Interestingly, we observed the presence of 14 common proteins more highly abundant in both total afEVs and the afEVs-CD81 subpopulation (**Fig. 4D**). Among these proteins, we found several complement proteins and immunoglobulins (**Table 1**).

afEVs from immunosuppressed patients do not exhibit antifungal activity.

Patients undergoing organ or stem-cell transplantation need to follow a strict medication regimen to suppress their immune system and prevent allograft rejection (Tönshoff 2020). Treatment with immunosuppressive drugs impairs the functionality of the immune system and makes treated patients susceptible for the development of infectious diseases like invasive aspergillosis (Fraczek et al 2018, Lewis & Kontoyiannis 2009, Palmer et al 1991). As our data suggests that afEVs play an important role for the defense against *A. fumigatus*, thus we studied the ability of PMNs isolated from immunosuppressed patients to produce afEVs. Patient P1 only underwent a short-term high dose steroid treatment. In contrast, the patients P2 and P3 received an allogeneic stem cell transplantation without developing graft-versus-host disease (GvHD) and received no steroid treatment but ongoing immunosuppressive therapy. Patients P4 and P5 underwent allogeneic stem cell transplantation and also suffered from GvHD. Hence, they were daily treated with steroids and immunosuppressants.

As shown by nanoparticle tracking analysis (**Suppl. Fig. 3A**), PMNs of these patients produced EVs spontaneously and after co-incubation with conidia. Their numbers

were comparable to those counted from healthy individuals, as previously reported (Rafiq et al 2022), with a mean diameter of 200 nm. We then tested afEVs of patients for the ability to inhibit hyphal growth and induce fragmentation of mitochondria and thus killing as demonstrated for afEVs secreted from PMNs of heathy donors. The immunosuppressive treatments apparently abolished the killing ability of afEVs from PMNs of these patients (**Fig. 5A**). The notable exception were afEVs from patient P1, that still had impaired fungal metabolic activity in one of the three measurements. This particular measurement was performed with PMNs obtained after only one cycle of immunosuppression of this patient. However, after additional rounds of treatment with immunosuppressants, afEVs isolated from this patient also proved to be ineffective in fungal killing, further corroborating the detrimental effect of immunosuppressive therapy on the antifungal activity of afEVs. Fungal damage was additionally evaluated by quantification of the metabolic activity of fungi by employing the reduction of resazurin as a readout. The obtained data confirmed the ineffectiveness of afEVs from patients to harm *A. fumigatus* hyphae (**Fig. 5B**). These data show that despite the different treatments and underlying diseases, the same phenotype in these patients was observed, i.e., lack of antifungal activity of afEVs.

To get first hints on the molecular basis of the differences seen in afEVs between healthy individuals and patients, label-free LC-MS/MS proteomic analysis of spontaneously released and afEVs was carried out. We detected in total 1086 proteins from these patients (dataset S2). Comparison of the significantly increased proteins in the afEV samples from healthy donors with those from immunosuppressed patients, revealed that most of the proteins were not shared between the two groups, suggesting a major difference in protein cargo (**Fig. 5C**). The148 proteins uniquely found in the afEVs from healthy donors included components of the C1 complement pathway and the afEVs/afEVs-CD81-enriched proteins found in the above-described

analysis (**see Table 1**) (**Table 2**). In addition to the lack of these complement proteins in afEVs from patients, gene ontology analysis also revealed decreased abundances of several signal transduction pathways required for immune defense. This might contribute to the observed loss of antifungal activity in patient-derived afEVs (**Suppl. Fig. 3B**).

Discussion

In this study, we show that afEVs derived from PMNs infected with *A. fumigatus* are highly specific against *A. fumigatus*. They failed to inhibit the growth of bacteria like *P. aeruginosa*, the opportunistic yeast pathogen *C. albicans*, or even of another Aspergillus species, *i.e.*, *A. nidulans*. Using various methods, we confirmed and quantified the antimicrobial potential of afEVs. CFU-based killing assays and fluorescent viability staining of the bacteria revealed that *P. aeruginosa* was not inhibited or killed by either sEVs or afEVs, whereas *S. aureus* showed an increase in membrane permeabilization after treatment with afEVs demonstrated by imaging. However, this was not reflected by the number of CFUs. It was previously shown that EVs derived from PMNs infected with *S. aureus* proved to be also effective against *S. aureus* itself and *Escherichia coli* but not against other bacteria like *Proteus mirabilis* (Timár et al 2013). This finding also suggested a certain level of specific antimicrobial activity of PMN-derived EVs, which was further substantiated by our findings. The effect of afEVs and sEVs on *C. albicans* was observed by microscopical inspection using a GFP-tagged *C. albicans* strain. After contact with these EVs, *C. albicans* displayed a near-complete morphological switch from yeast-to-hyphal growth, which resulted in very long hyphae after 20 h of incubation. This result is in line with data showing that EVs derived from primary monocytes infected with *C. albicans*, and even fungal-derived vesicles from *C. albicans* itself are capable of

promoting hyphal growth (Halder et al 2022, Honorato et al).

The observed lack of killing of *A. nidulans* by afEVs was surprising. A partial explanation for this finding may come from the alternative types of melanin found on the surface of different *Aspergillus* conidia. As previously shown, co-incubation of PMNs with an *A. fumigatus* mutant lacking the surface pigment, DHN-melanin, led to the production of EVs that were no longer antifungal (Shopova et al 2020). Here, we extended this finding by showing that the presence of DHN-melanin is required for the stimulation of PMNs and formation of afEVs. The interaction of PMNs with melanin ghosts alone or with *A. clavatus*, another DHN-melanin harboring strain (Valiante et al 2016), was sufficient for the induction of afEVs. Furthermore, stimulation of PMNs with *A. nidulans* conidia did not lead to this phenotype. This finding fully agrees with our assumption since the conidial melanin of *A. nidulans* does not contain DHN in its melanin (Klejnstrup et al 2012, Langfelder et al 2003, Wheeler & Bell 1988). Further, our findings corroborate the hypothesis that DHN-melanin, being one of the most important virulence factors of *A. fumigatus* (Heinekamp et al 2015), has an additional function as an inducer of the biogenesis and protein cargo selection of afEVs from human PMNs. The fact that *A. nidulans* is only rarely found to infect immunocompromised patients (Henriet et al 2012) suggests a lack of effective virulence determinants like DHN-melanin.

Another interesting finding from our comparison with *A. nidulans* derived from tracking of stained EVs after their addition to fungal hyphae. For this, we employed a self-quenching lipophilic dye called MemGlow that causes minimal background signals. These staining experiments revealed that EVs derived from *A. fumigatus* infected PMNs (afEVs) accumulate on the conidial sites of *A. fumigatus* hyphae where the germination initiated. Interestingly, when the same experiment was performed with *A. nidulans*, the fungus appeared to be surrounded by afEVs which,

however, did not permeate the mycelium . This unexpected result suggests that the antifungal effect of EVs relies on both their ability to enter hyphae and on their cargo, since internalized sEVs were not able to kill hyphae.

In order to better define the antifungal cargo of the afEVs, we performed additional LC-MS/MS-based proteomics analysis of different EV subsets. The tetraspanins CD9, CD81, and CD63 play a crucial role in EV protein cargo selection (Chen et al 2021), therefore we tested the antifungal potential of EV populations enriched for each of these three tetraspanins. From this assay we observed that the CD81+ afEVs showed the highest antifungal activity. Thus, the presence of CD81 on the surface of EVs might lead to incorporation of a specific cargo that is particularly toxic to the fungus. Indeed, it was already shown for other cell types, like B lymphocytes, that the selective enrichment of tetraspanins, including CD81, 82, and 63 can favor the enrichment of proteins in EVs like MHC class proteins, which can stimulate T-cells (Escola et al 1998).

Proteomic analysis of the CD81 subpopulation identified here as being the most antifungal, highlighted the presence of shared proteins between all afEVs and the afEVs-CD81 subpopulation. Of note, two of these proteins are subunits of the C1q complement factor. The complement protein C1q is known to trigger chemotaxis of PMNs and their ROS production (Goodman et al 1995, Hooshmand et al 2017, Leigh et al 1998). Furthermore, phagocytosis of *A. fumigatus* conidia after C1q surface deposition is one of the preferential mechanisms employed by PMNs to recognize and eliminate the fungus (Braem et al 2015). The abundance of C1q in the EV proteome led us to hypothesize that the enrichment of C1q in afEVs might direct them to the fungal cell wall and aid in delivery of antifungal cargo; however, more work is required to prove this intriguing hypothesis.

The antimicrobial activity of PMNs is known to be highly impaired after

immunosuppressive treatment (Imbert et al 2016, Vymazal et al 2021). In our study, we demonstrate that regimens of immunosuppression strongly affect their ability to produce antifungal EVs. For most of the patients we tested, our data obtained with the mitochondrial reporter strain of *A. fumigatus* indicated no detrimental effect on the fungus by its treatment with afEVs. The only exception was patient P1 whose PMNs obtained after only one immunosuppressive cycle, produced EVs capable of inducing some mitochondrial fragmentation. However, this antifungal activity was lost in afEVs from PMNs isolated after three immunosuppressive cycles. This patient is the only individual who did not receive a daily immunosuppression, but discontinuously once a week for the course of three weeks, with a one month break in between. This break in treatment might allow for some recovery of antifungal activity between regimens, resulting in afEVs that still show some antifungal activity. We wondered if the loss of antifungal activity was due to the absence of a specific cargo protein. To address this question, we compared of proteomic datasets obtained from EVs of immunosuppressed patients with previous data on EVs from healthy donors. There was only little overlap between the two groups, with a large number of proteins exclusively found in one group. Notably, the C1q subunits together with other C1 pathway components were lacking in the patient-derived afEVs, strengthening our hypothesis on the potentially important role of this complement proteins. Together, our data help to explain the lack of antifungal activity observed in immunosuppressed patients and refine our understanding of the role of PMNs in antifungal defense in healthy individuals.

Acknowledgements

We thank all anonymous blood donors and Katherine González Rojas for the excellent support in blood drawing. We also thank Johannes Wagener for providing

the *A. fumigatus* mitochondrial-GFP strain, and Bernard Hube for providing the *C. albicans* cytosolic-GFP reporter strain. Natascha Wilker is gratefully acknowledged for excellent technical assistance.

This work was supported by the Deutsche Forschungsgemeinschaft (DFG)-funded Collaborative Research Center/Transregio 124 FungiNet (project number 210879364, projects A1 and Z2) and the DFG-funded ANR project AfuInf. M.G.B. was supported by the Federal Ministry for Education and Research (BMBF: https://www.bmbf.de/), Germany, Project FKZ 01K12012 "RFIN – RNA-Biologie von Pilzinfektionen." The funders had no role in the study design, data collection and analysis, decision to publish, or preparation of the manuscript. The authors declare no conflicts of interest.

Figure Legends

Figure 1. Specificity of afEVs. (A) Number of CFUs of *P. aeruginosa* and *C. albicans* after 1 h of confrontation with spontaneously released extracellular vesicles (sEVs) or extracellular vesicles isolated from primary human PMNs infected with *A. fumigatus* (afEVs). Data is presented as means +/- SEM from four replicates. Statistical significance is indicated as follows: ns, not significant. **(B)** Confocal microscopy image showing *P. aeruginosa* stained with propidium iodide (PI) (red) and Syto 9 (green). **(C)** Confocal microscopy images of *C. albicans*-GFP strain after 3 and 20 h co-incubation with sEVs or afEVs. **(D)** Confocal microscopy image of *A. nidulans* hyphae expressing the mitochondrially located GFP (green). The strain was grown for 8 h and then confronted for 16 h with sEVs or afEVs. The hyphal cell walls were stained with CFW (blue). As a control, all pathogens were treated with H_2O_2. Images are representative of three independent biological experiments. Bars, 10 µm.

Figure 2. DHN-melanin as inducer of afEVs. (A) The *A. fumigatus* mitochondrial

GFP reporter strain (green) was grown for 8 h and then incubated overnight with sEVs or with EVs derived from PMNs treated with melanin ghosts (mg_EVs) or with *A. clavatus* conidia (Cl_EVs). Fungal hyphae were stained with CFW (blue). As a positive control, hyphae were treated with H_2O_2. An intact mitochondrial network is indicated by long lines of green mitochondria, whereas fragmented green spots or the lack of any green fluorescence marks ´dead hyphae. Images are representative of eight independent biological experiments with PMNs from different donors. Bars, 10 µm. **(B)** Examples of the bioinformatic analysis performed on *A. fumigatus* mitochondrial-GFP strain treated with the different indicated EVs. **(C)** Quantification of the values of hyphal volume against mitochondrial volume based on microscopy Z-stacks from 5 different donors.

Figure 3. Internalization of EVs into fungal hyphae. (A) Confocal laser scanning microscopy showing *A. fumigatus* mitochondrial GFP reporter strain (green) after overnight incubation with either sEVs or afEVs that were stained with Memglow (red). Images are representative of seven biological replicates. **(B)** Hyphae of the *A. nidulans* strain with mitochondrially tagged GFP (green) confronted with sEVs or afEVs (red). Cell walls were visualized by CFW staining (blue). Images are representative of four biological replicates with PMNs of different donors. Scale bars, 10 µm. **(C)** Quantification of the signal derived from microscopy Z-stacks from 2 biological replicates of EVs (afEVs and sEVs) stained with Memglow co-incubated with *A. fumigatus* mitochondrial-GFP strain or *A. nidulans* mitochondrial-GFP strain; signals derived from EVs, and the hyphal cell wall were deconvolved.

Figure 4. Characterization of different tetraspanin-enriched afEV populations. (A) Cryo-EM picture showing afEVs pulled out with anti-CD63, -CD9 and -CD81

antibody-coated beads. **(B)** *A. fumigatus* mitochondrial GFP reporter strain (green) was incubated with afEVs sorted with the different beads from 3 different donors and visualized after 16 h by CLSM. Hyphae were stained with CFW (blue). Bars, 10 µm. **(C)** Proteins identified in sEVs and afEVs using the complete EV population or the CD81 subpopulation were compared using UpSetR. The green bar indicates proteins that were found in all four samples. **(D)** Venn diagram intersecting only the proteins with a higher than 2-fold increase in afEVs of both indicated EV populations.

Figure 5. Effect of immunosuppressive treatment on the formation of afEVs from PMNs. (A) CLSM images showing hyphae of the *A. fumigatus* mitochondrially tagged GFP strain (green). The fungal strain was grown for 8 h and then incubated overnight with sEVs or afEVs from PMNs isolated from 5 patients undergoing immunosuppressive treatments. The cell wall was stained with CFW (blue) and hyphal damage was evaluated by CLSM. Scale bars, 10 µm. **(B)** Quantification of resazurin reduction by hyphae after their confrontation with either sEVs or afEVs from patients or healthy donors. As a positive control, H_2O_2 was added to the wells. Data is presented as means +/- SEM from three independent replicates for each patient and five biological replicates for healthy donors. Statistical significance is indicated as follows: *, $P \leq 0.05$; ns, not significant. **(C)** Venn diagram of intersecting proteins with a higher than 2-fold increase in afEVs from patients and healthy donors.

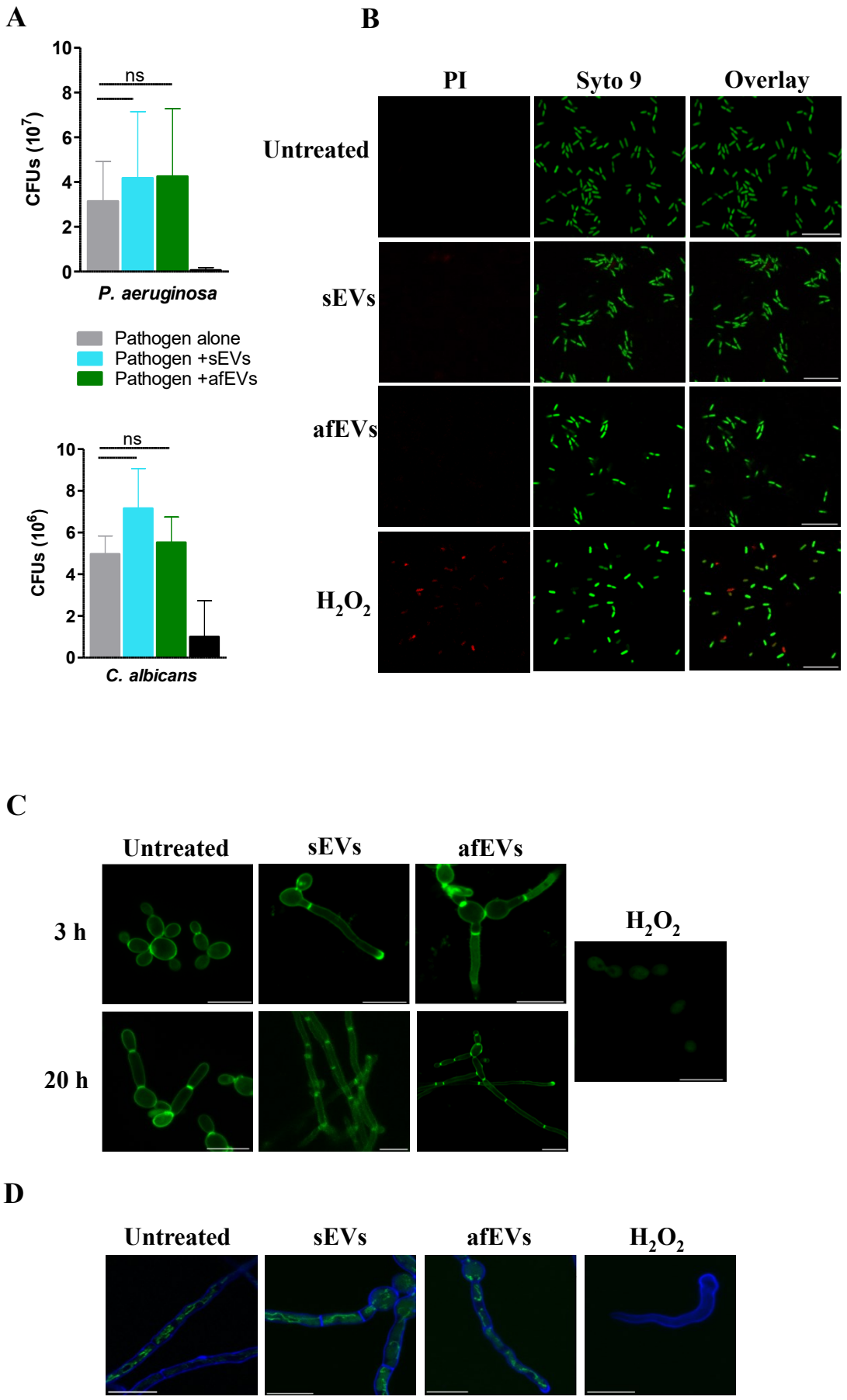
A
B
CFUs (10^7)
ns
P. aeruginosa
Pathogen alone
Pathogen +sEVs
Pathogen +afEVs
CFUs (10^6)
ns
C. albicans
PI
Syto 9
Overlay
Untreated
sEVs
afEVs
H_2O_2
C
Untreated
sEVs
afEVs
H_2O_2
3 h
20 h
D
Untreated
sEVs
afEVs
H_2O_2

Figure 1

A

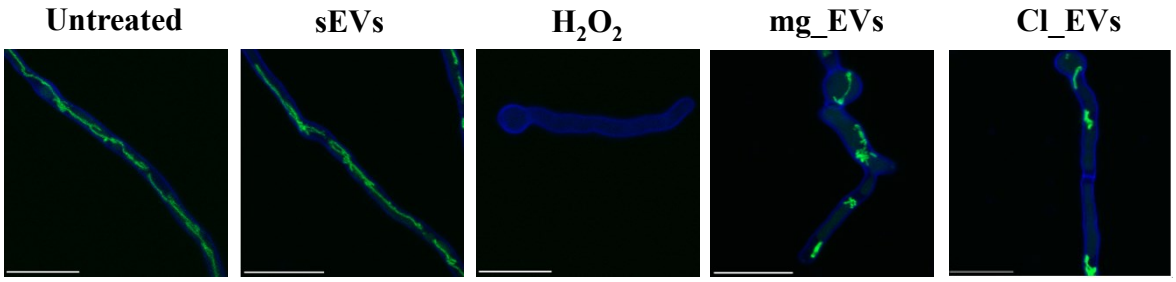
Untreated
sEVs
H_2O_2
mg_EVs
Cl_EVs

B

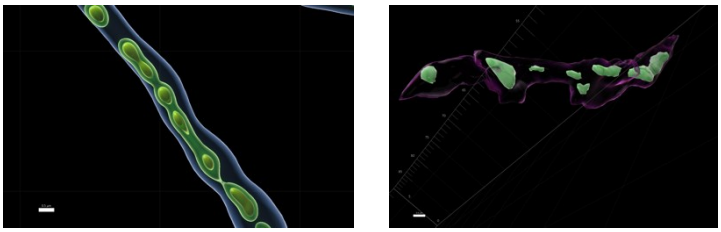

C

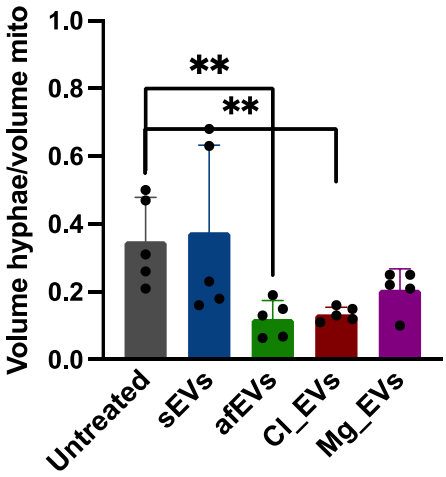
Volume hyphae/volume mito
1.0
0.8
0.6
0.4
0.2
0.0
**
**
Untreated
sEVs
afEVs
Cl_EVs
Mg_EVs

Figure 2

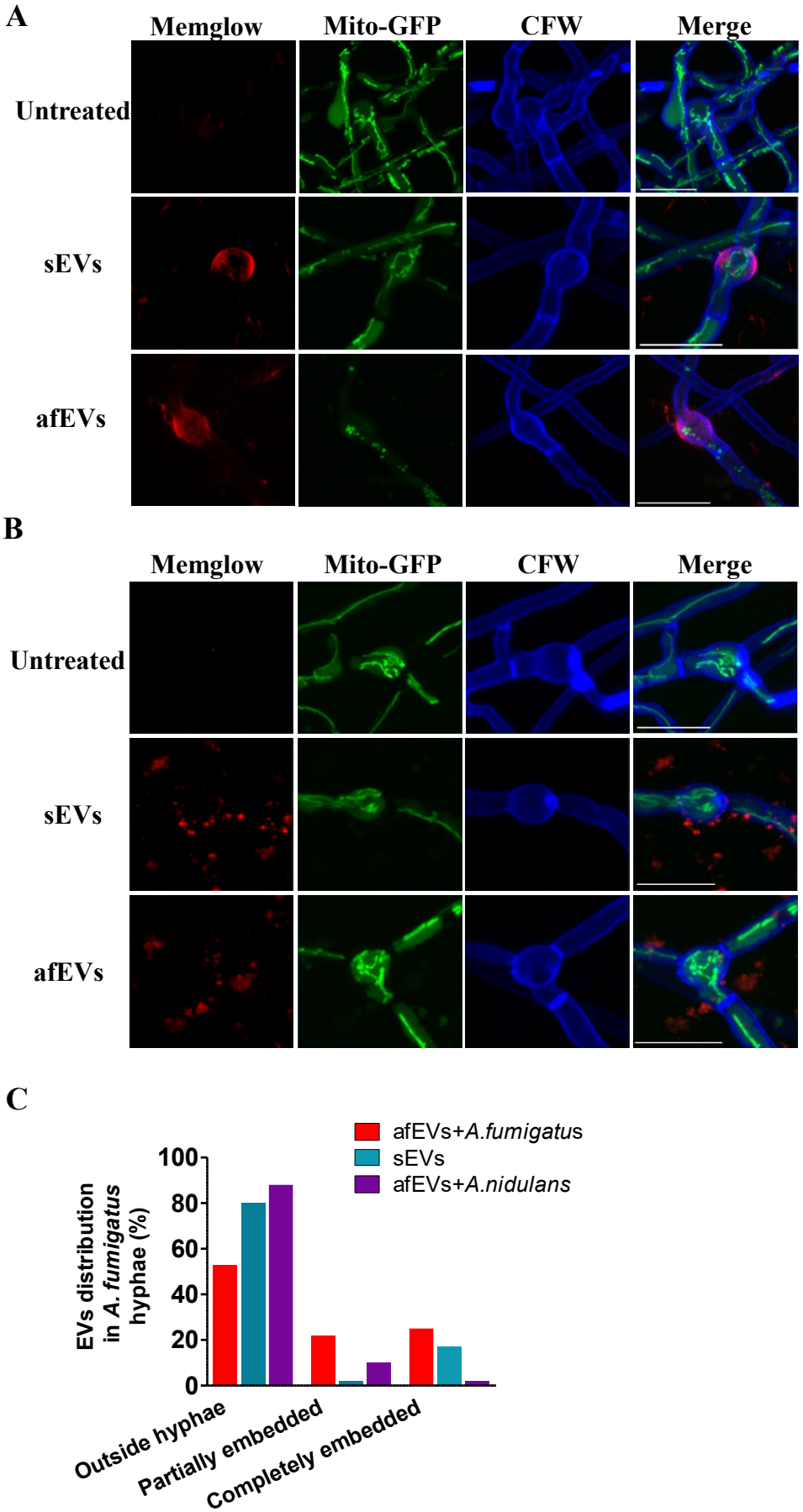
A
Memglow
Mito-GFP
CFW
Merge
Untreated
sEVs
afEVs
B
Memglow
Mito-GFP
CFW
Merge
Untreated
sEVs
afEVs
C
afEVs+A.fumigatus
sEVs
afEVs+A.nidulans
EVs distribution in A. fumigatus hyphae (%)
100
80
60
40
20
0
Outside hyphae
Partially embedded
Completely embedded

Figure 3

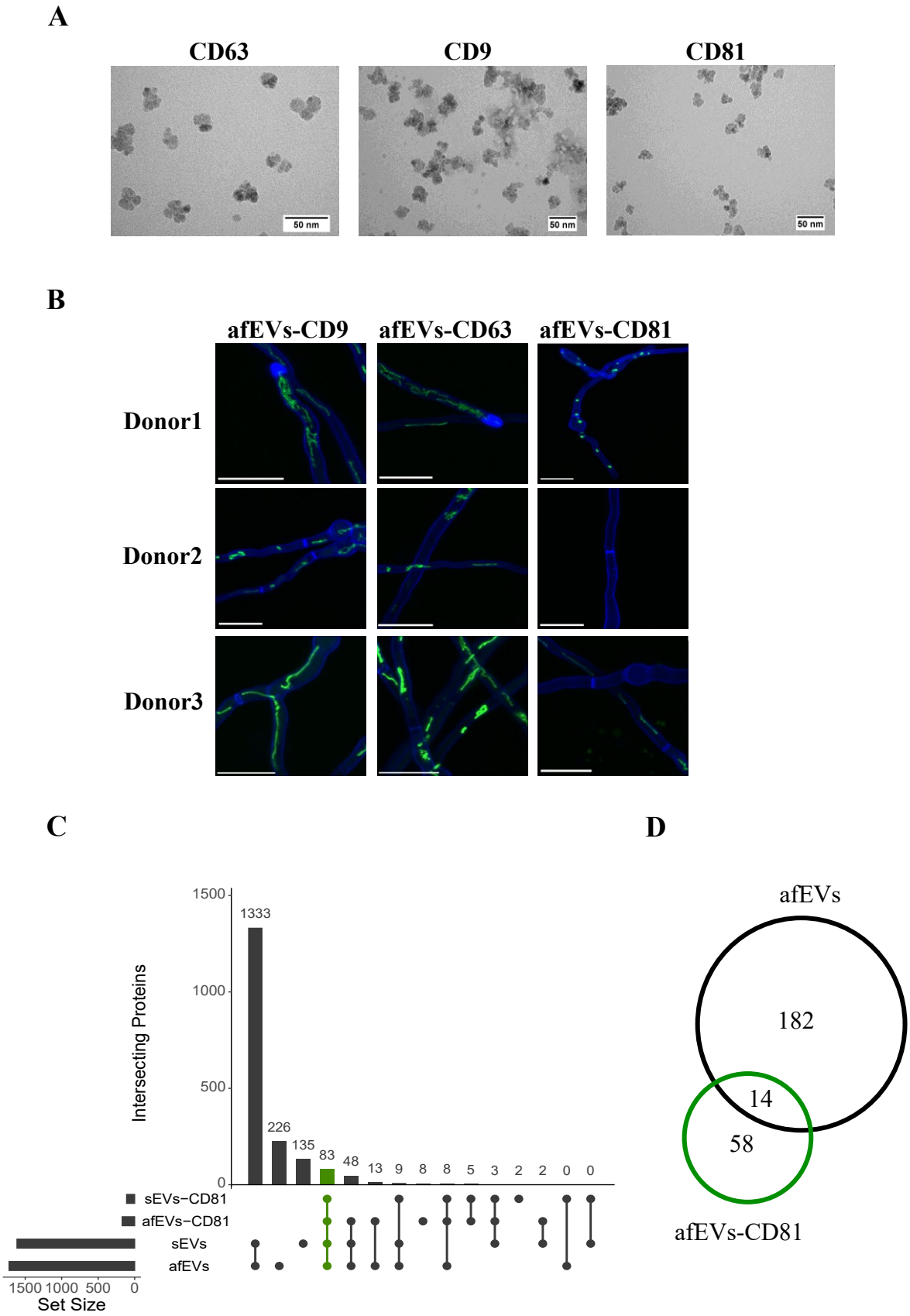
A
CD63
CD9
CD81
50 nm
B
afEVs-CD9
afEVs-CD63
afEVs-CD81
Donor1
Donor2
Donor3
C
Intersecting Proteins
1500
1000
500
0
1333
226
135
83
48
13
9
8
8
5
3
2
2
0
0
sEVs−CD81
afEVs−CD81
sEVs
afEVs
1500 1000 500 0
Set Size
D
afEVs
182
14
58
afEVs-CD81

Figure 4

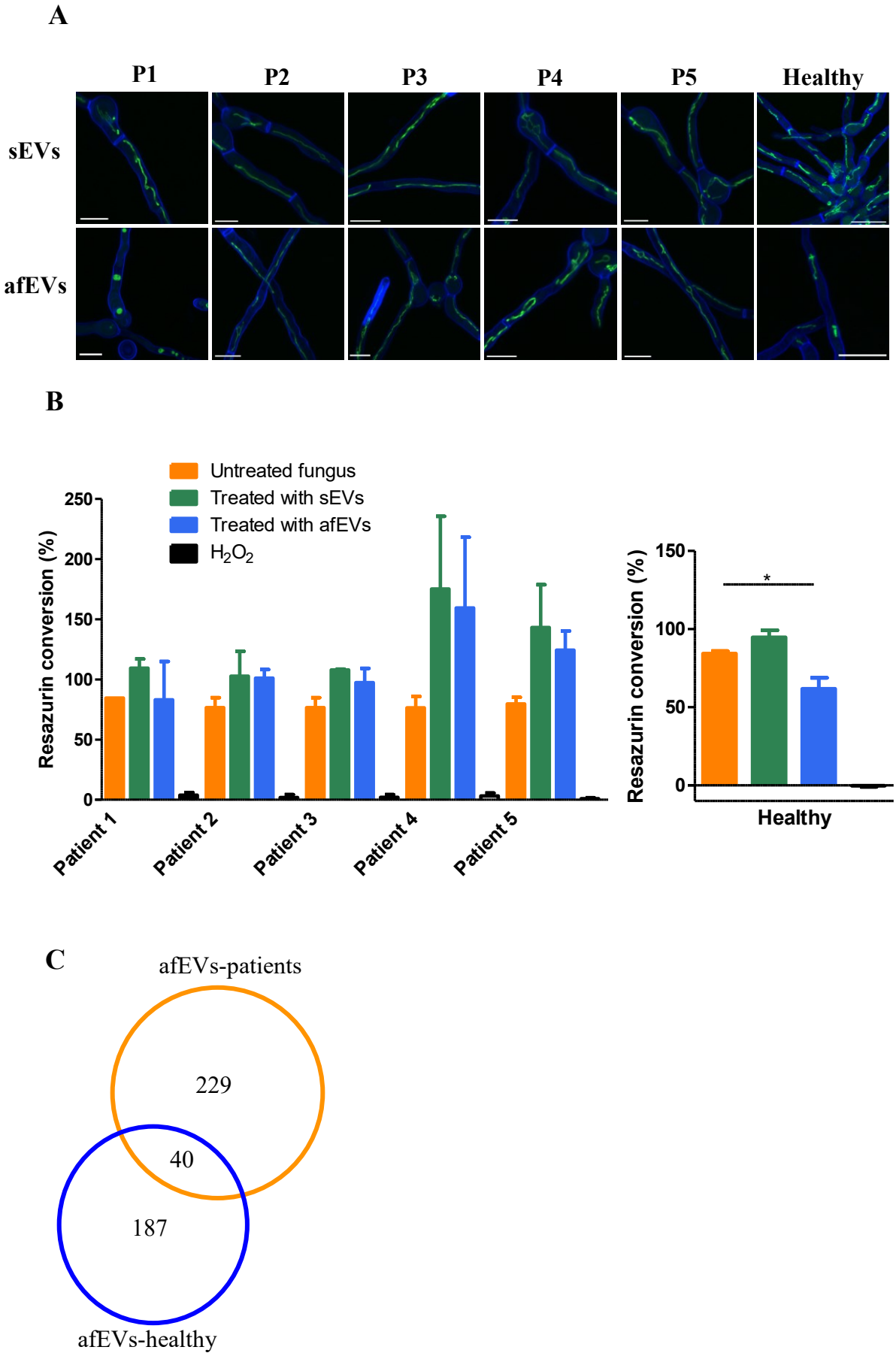
A
P1
P2
P3
P4
P5
Healthy
sEVs
afEVs
B
Untreated fungus
Treated with sEVs
Treated with afEVs
H_2O_2
Resazurin conversion (%)
250
200
150
100
50
0
Patient 1
Patient 2
Patient 3
Patient 4
Patient 5
Resazurin conversion (%)
150
100
50
0
*
Healthy
C
afEVs-patients
229
40
187
afEVs-healthy

Figure 5

Supplemental Materials

Legends to the Supplemental Figures

Figure S1. Effect of afEVs on *S. aureus* and *C. albicans*. (A) Number of CFUs of *S. aureus* after 1 h confrontation with sEVs or afEVs. Data represent the mean +/- SEM from four replicates. Statistical significance is indicated as follows: ns, not significant. **(B)** Confocal microscopy images showing *S. aureus* stained with propidium iodide (PI) (red) and Syto 9 (green). Treatment with H_2O_2 was used as positive control. **(C)** CLSM image of *C. albicans*-GFP strain after 3 and 20 h of co-incubation with sEVs or afEVs in the presence of Triton X-100. Images are representative of three replicates. Scale bars, 10 µm.

Figure S2. Antifungal capacity of *A. nidulans*-induced EVs. After overnight incubation of the *A. nidulans* strain producing mitochondrially tagged GFP (green) **(A)**, or of the *A. fumigatus* mitochondrial-tagged GFP strain (green) **(B)**, with sEVs or EVs from primary human PMNs infected with *A. nidulans* (anEVs), CLSM images were taken. Hyphal cell wall was stained with CFW (blue). Images are representative of four biological replicates. Bars, 10 µm.

Figure S3. Analysis of EVs released from PMNs of immunosuppressed patients. (A) EVs spontaneously released or released after infection with opsonized *A. fumigatus* conidia (afEVs) from PMNs of corticosteroid-treated patients were co-incubated with conidia for 2 h. Then, EVs were isolated and quantified by nanoparticle tracking analysis (NTA). Data represents the mean +/- SEM from three independent replicates for each patient. **(B)** GO analysis indicating biological processes in which the upregulated proteins in afEVs from healthy donors (blue) and

immunosuppressed patients (orange) are involved.

Figure S4. **Flowchart of the pipeline used to analyze the hyphal, mitochondrial, and EV-linked fluorescence signals from 3D confocal microscopy images.** The images were provided as CZI, deconvolved in Huygens, and the three channels separated, corresponding to the hyphae (blue blocks), mitochondria (green blocks) and EVs (orange blocks). All three compartments were segmented both leniently and more strictly. The strict segmentations were used to measure distances and characterize relative localizations, whereas the lenient surfaces served the purpose of shape and volume measurements.

Figure S5. Deconvolution of mitochondria. The measured PSF **(A)** was used to deconvolve the mitochondrial volume signal. **(B)** The transparent purple surface shows the reconstructed raw signal, with the skin-like surface indicating the deconvolved signal. **(C)** The same PSF was used to deconvolve the mitochondria, with the purple transparent surface corresponding to the raw signal, and the solid green surface indicating the deconvolved mitochondrial signal.

Figure S6. **Reconstructing the mitochondria as Surfaces in Imaris.** The deconvolved volume signal **(A)** was used to create Surfaces objects in Imaris (**B**, yellow surfaces). **(C)** The corresponding reconstructed hyphal membrane are shown in transparent blue.

Figure S7. The reconstruction of afEVs as Spots in Imaris. The deconvolved volume signal of afEVs **(A)** was used to create Spots objects with various radii **(B)** to describe the localization of the individual and small-clustered afEVs. **(C)** The strict

reconstruction of the corresponding hyphae is shown in form of blue transparent surfaces. In **(B)** and **(C)**, the color-coding of the Spots indicates the mean intensity of the masked hyphal signal (scaled between 0 and 10): values close to 0 are in blue and indicate that the EV is not embedded; values close to 10 are in red, and these characterize EVs that are (nearly) fully embedded in the hyphal cell wall.

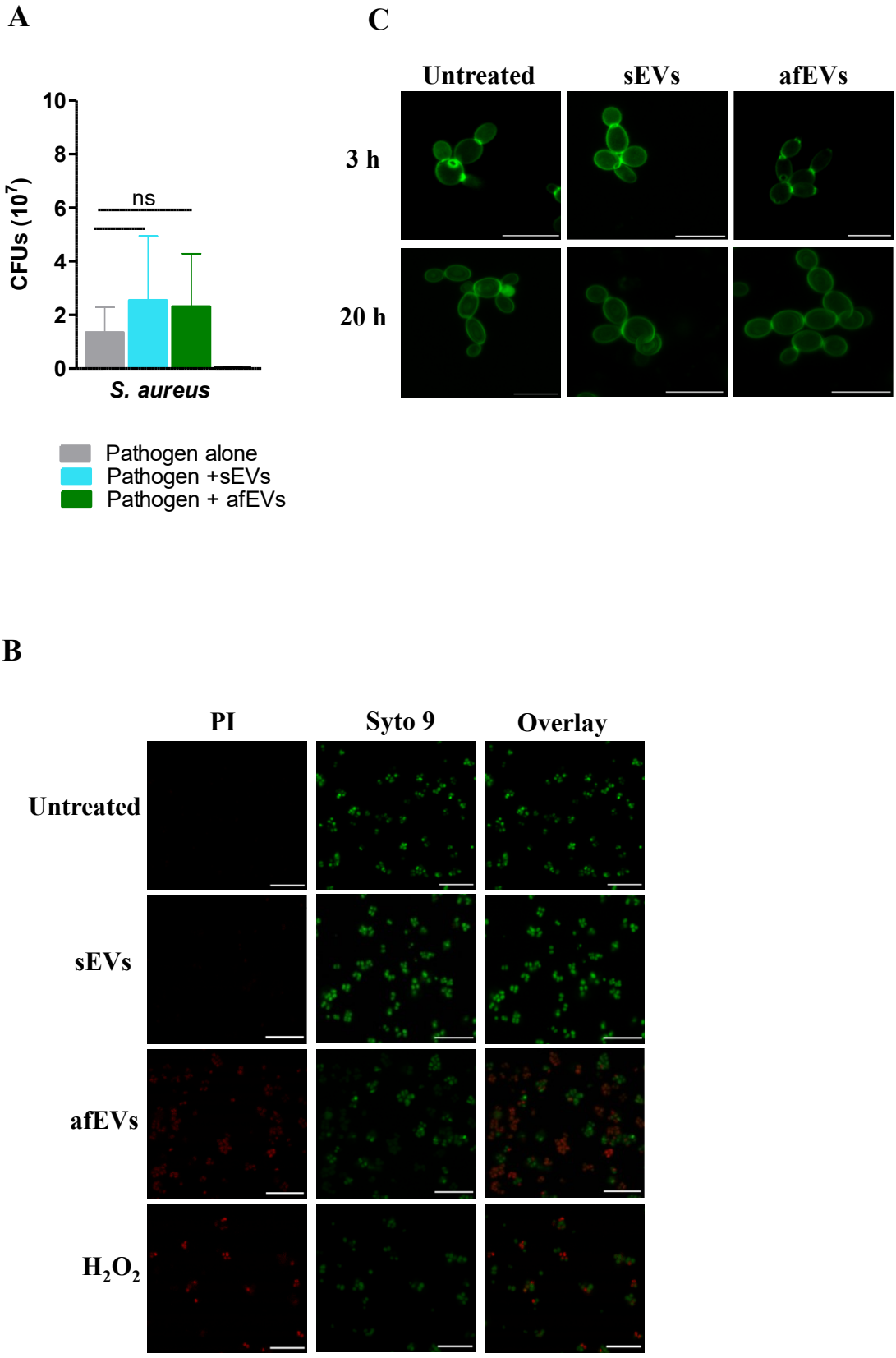
A
C
Untreated
sEVs
afEVs
3 h
20 h
CFUs (10^7)
10
8
6
4
2
0
ns
S. aureus
Pathogen alone
Pathogen +sEVs
Pathogen + afEVs
B
PI
Syto 9
Overlay
Untreated
sEVs
afEVs
H_2O_2

Figure S1

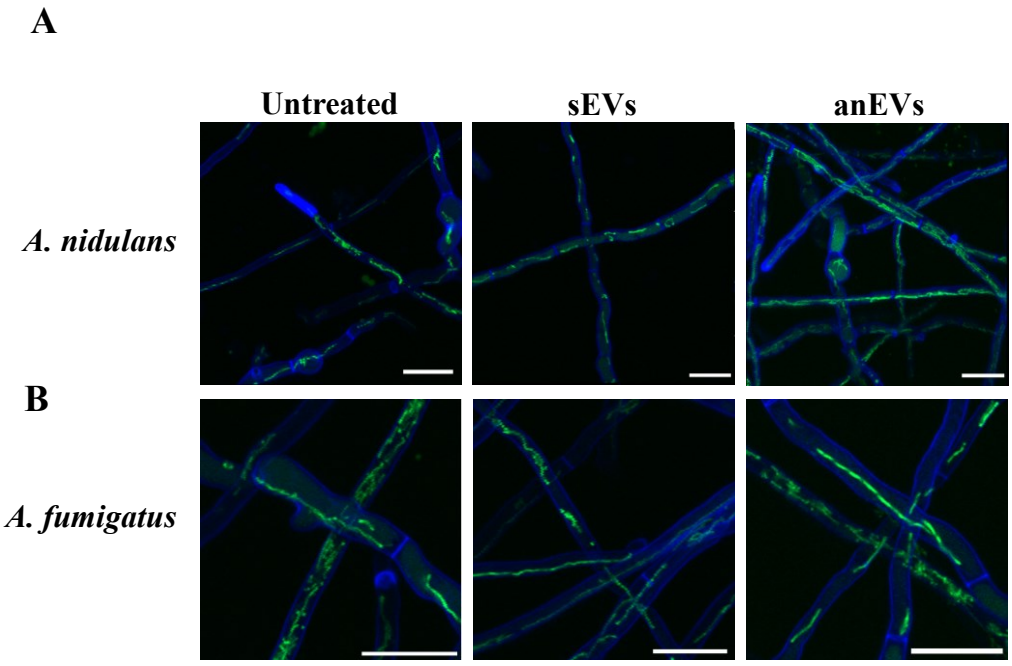

Figure S2

A

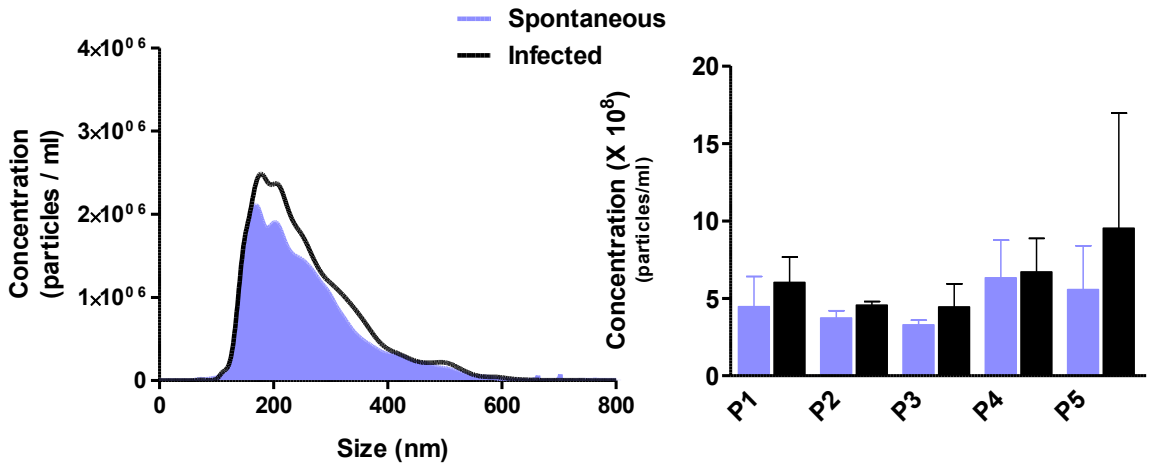
Spontaneous
Infected
Concentration (particles / ml)
4×10^06
3×10^06
2×10^06
1×10^06
0
0
200
400
600
800
Size (nm)
Concentration (X 10^8) (particles/ml)
20
15
10
5
0
P1
P2
P3
P4
P5

B

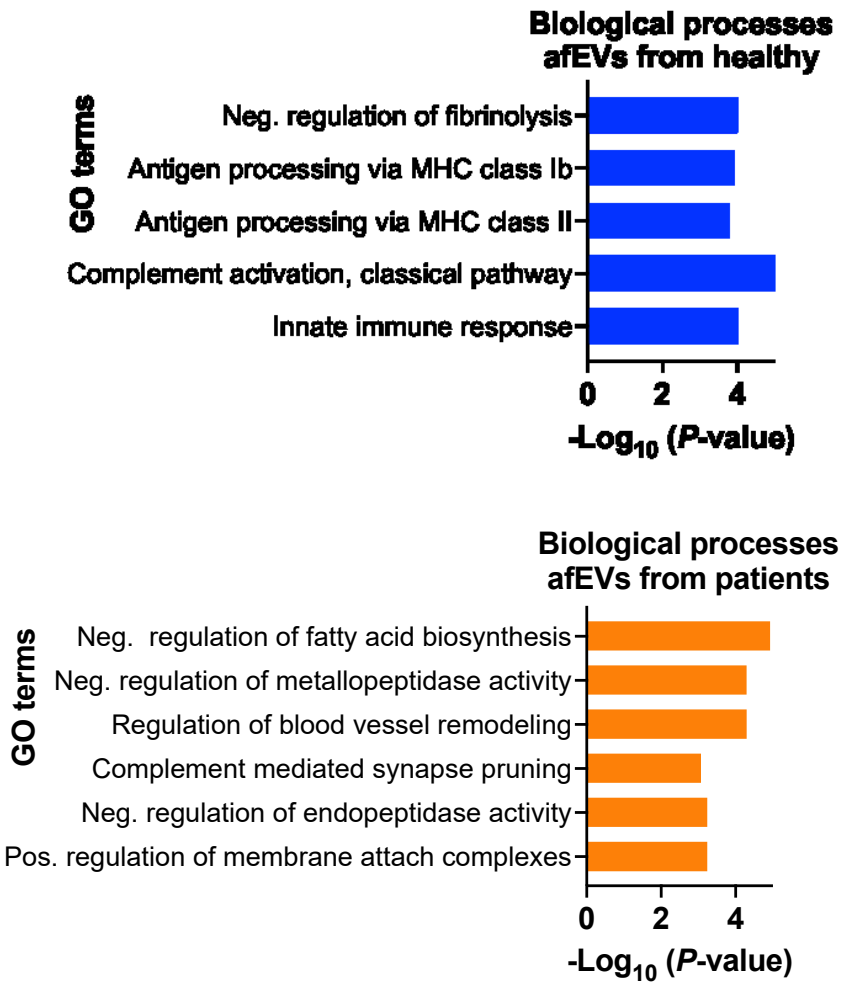
Biological processes afEVs from healthy
GO terms
Neg. regulation of fibrinolysis
Antigen processing via MHC class Ib
Antigen processing via MHC class II
Complement activation, classical pathway
Innate immune response
0
2
4
-Log10 (P-value)
Biological processes afEVs from patients
GO terms
Neg. regulation of fatty acid biosynthesis
Neg. regulation of metallopeptidase activity
Regulation of blood vessel remodeling
Complement mediated synapse pruning
Neg. regulation of endopeptidase activity
Pos. regulation of membrane attach complexes
0
2
4
-Log10 (P-value)

Figure S3

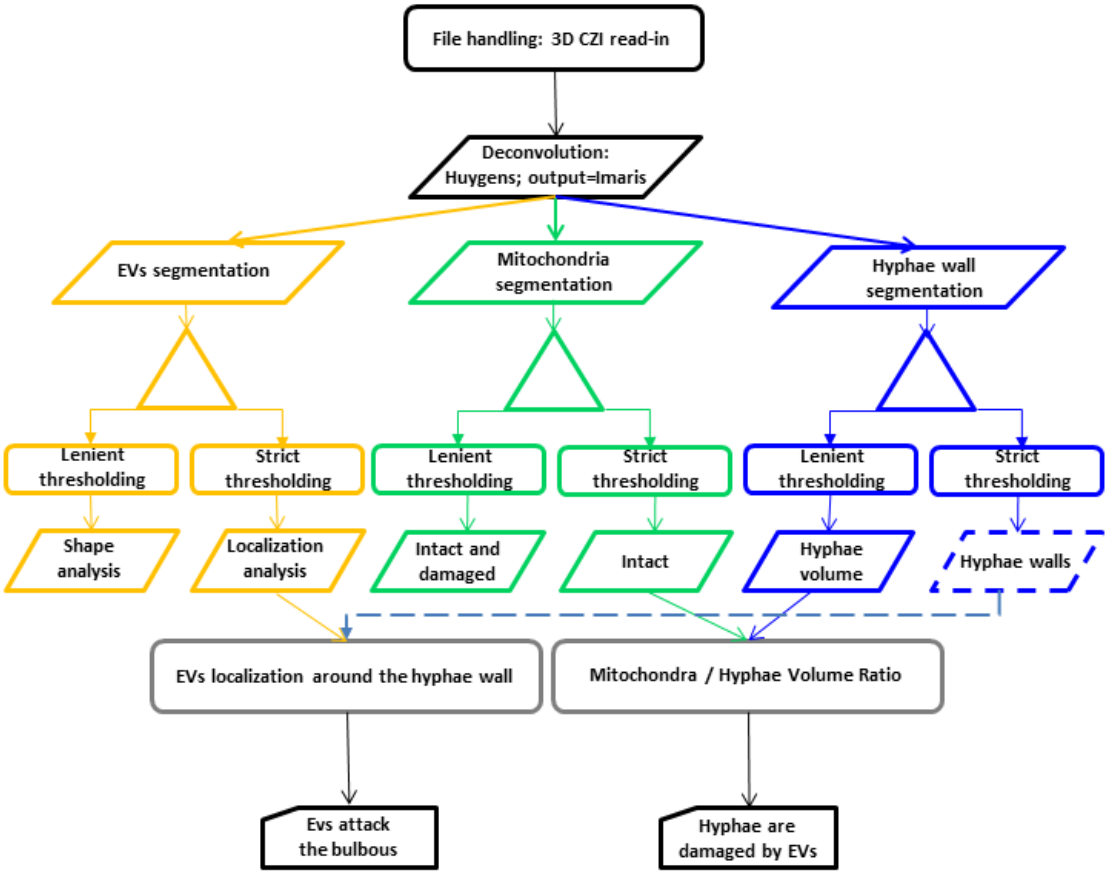
File handling: 3D CZI read-in
Deconvolution: Huygens; output=Imaris
EVs segmentation
Mitochondria segmentation
Hyphae wall segmentation
Lenient thresholding
Strict thresholding
Lenient thresholding
Strict thresholding
Lenient thresholding
Strict thresholding
Shape analysis
Localization analysis
Intact and damaged
Intact
Hyphae volume
Hyphae walls
EVs localization around the hyphae wall
Mitochondra / Hyphae Volume Ratio
Evs attack the bulbous
Hyphae are damaged by EVs

Figure S4

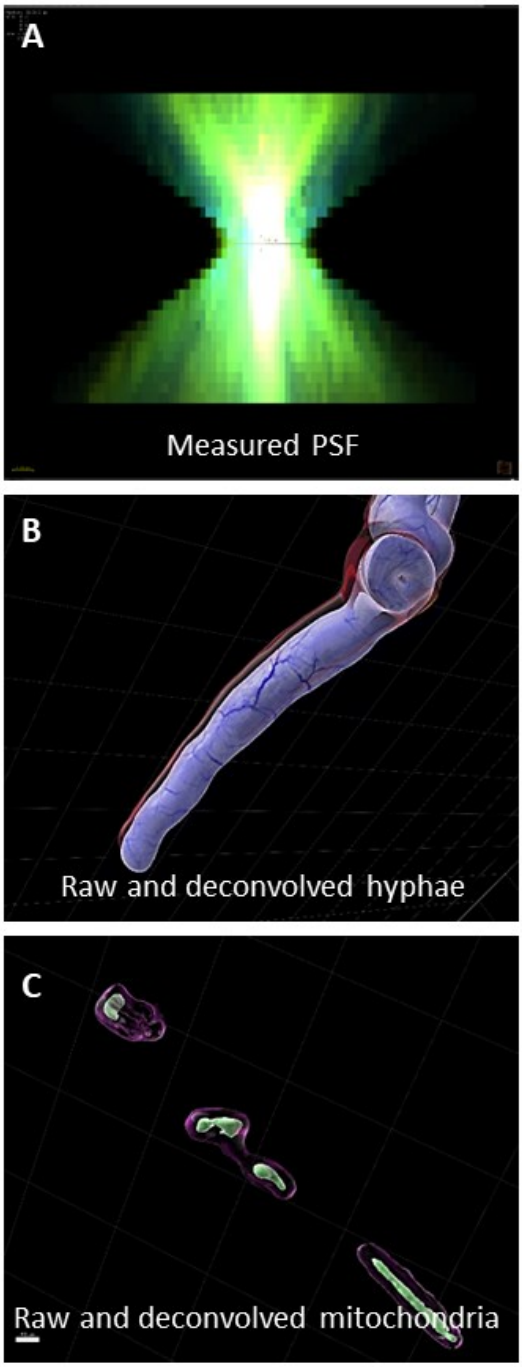
A
Measured PSF
B
Raw and deconvolved hyphae
C
Raw and deconvolved mitochondria

Figure S5

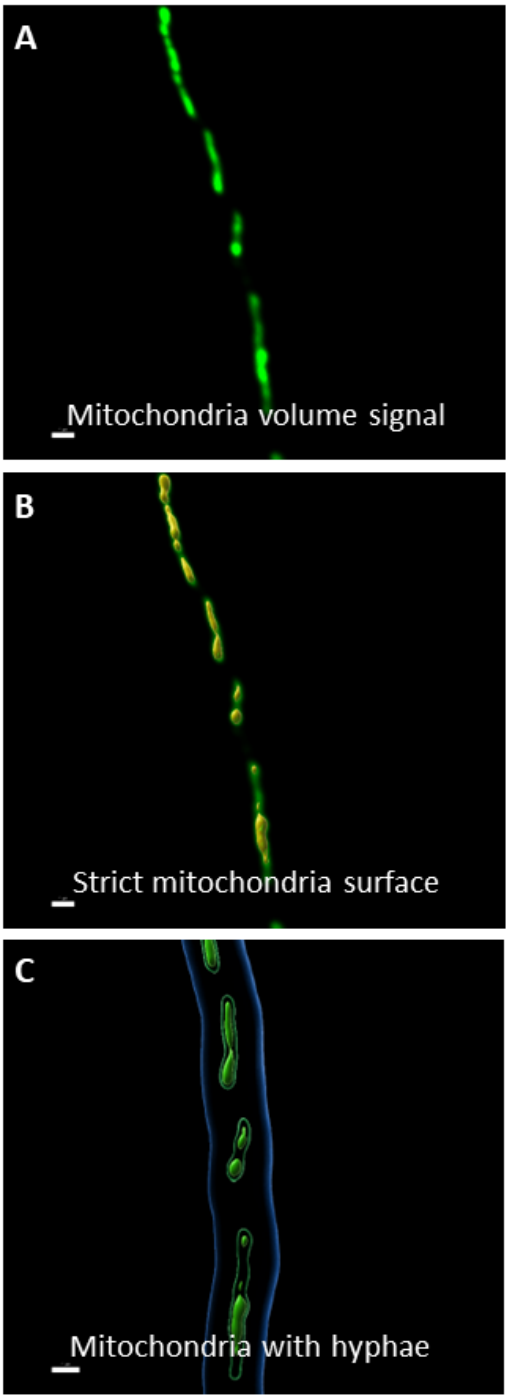
A
Mitochondria volume signal
B
Strict mitochondria surface
C
Mitochondria with hyphae

Figure S6

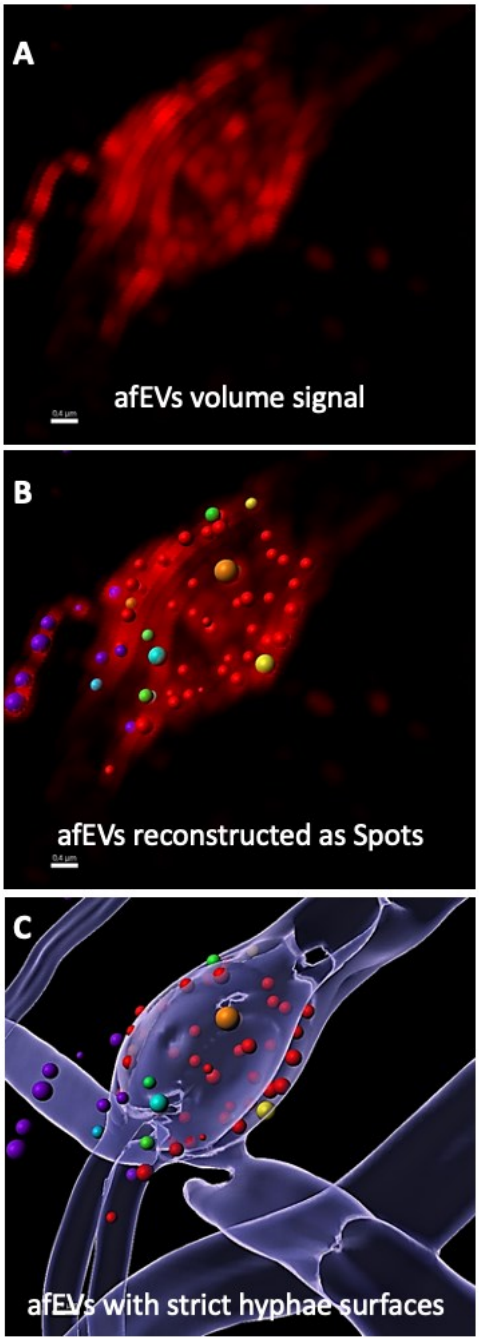
A
afEVs volume signal
B
afEVs reconstructed as Spots
C
afEVs with strict hyphae surfaces

Figure S7

Tables

Table 1 Selected examples of upregulated proteins in afEVs and the afEVs-CD81 subpopulation.

Uniprot accession no.	Protein	Fold change afEVs/sEVs	Fold change afEVs/sEVs CD81
P47929	Galectin-7	4.8	48.2
P01871	Immunoglobulin heavy constant mu	4.3	11.1
P02745	Complement C1q subcomponent subunit A	133.6	2.4
Q08188	Protein-glutamine gamma-glutamyltransferase	3.7	4.0
A0A0A0MSV6	Complement C1q subcomponent subunit B	21.1	2.0
P01040	Cystatin-A	3.4	4.1
P04792	Heat shock protein beta-1	2.0	128.4
A0A804HKE0	Glutamate dehydrogenase 1, mitochondrial	3.2	14.6
P30048	Thioredoxin-dependent peroxide reductase, mitochondrial	2.1	9.5
Q08477	Cytochrome P450	2.0	5.3

Table 2 Proteins upregulated in afEVs from healthy donors and absent in afEVs from patients.

Uniprot accession no	**Protein**	**Fold change afEVs/sEVs**
P02745	Complement C1q subcomponent subunit A	133.6
P02741	C-reactive protein	96.7
O14556	Glyceraldehyde-3-phosphate dehydrogenase	88.3
F5H053	Phospholipase B-like	57.8
P09525-2	Isoform 2 of annexin A4	51.7
A0A0A0MSV6	Complement C1q subcomponent subunit B	21.1
O75947	ATP synthase subunit d, mitochondrial	14.2
A0A0C4DG89	RNA helicase	9.4
B4DPQ0	Complement subcomponent C1r	6.1

Table S1. **Fungal strains used in this study.**

Strain	Genotype/Phenotype	Source
CEA10	*A. fumigatus* wild type	Fungal Genetics Stock Center (A1163)
AfS35/pJW103	*A. fumigatus* mitochondrial GFP	Shopova et al. 2020
FGSC A4	*A. nidulans* wild type	JMRC collection
GFPsuA\N4	*A. nidulans* mitochondrial GFP	J. Van Den Brulle. Dissertation 1999; this study
FSU 1270	*A. clavatus* wild type	JMRC collection

Table S2.

Pat. No.	**1**	**3**	**2**	**5**	**4**
Sex	female	male	male	male	female
Age (years)	72	66	71	50	63
Diagnosis	Multiple Myeloma	Primary Myelofibrosis	Acute Myeloid Leukemia	Acute Myeloid Leukemia	Acute B-Lymphoblastic Leukemia
Current disease status	relapse, active disease	first complete remission	first complete remission	first complete remission	second complete remission
Allogeneic stem-cell transplantation	no	yes	yes	yes	yes
Duration from allo-SCT (months)		3	3	29	30
Chronic GvHD	no	no	no	yes	yes
Ongoing chemotherapy	cyclophosphamide 300mg/m^2 weekly carfilzomib 36mg/m^2 twice weekly	no	no	no	no
Ongoing immunosuppression	no	yes	yes	yes	yes
Immunosuppressive drug	no	cyclosporine	cyclosporine	everolimus	everolimus

Plasma concentration	n.a.	267 µg/l, tapering	138 µg/l, tapering	3-7 µg/l, ongoing	4-5 µg/l, ongoing
Steroid treatment	short term	no	no	long term	long term
Steroid dose	dexamethasone 40mg/day once weekly			prednisolone 20mg/d	prednisolone 20mg/d

References

Andreu Z, Yáñez-Mó M. 2014. Tetraspanins in extracellular vesicle formation and function. *Front Immunol* 5: 442

Braem SG, Rooijakkers SH, van Kessel KP, de Cock H, Wösten HA, et al. 2015. Effective Neutrophil Phagocytosis of Aspergillus fumigatus Is Mediated by Classical Pathway Complement Activation. *J Innate Immun* 7: 364-74

Brakhage AA. 2005. Systemic fungal infections caused by Aspergillus species: epidemiology, infection process and virulence determinants. *Curr Drug Targets* 6: 875-86

Brakhage AA, Zimmermann A-K, Rivieccio F, Visser C, Blango MG. 2021. Host-derived extracellular vesicles for antimicrobial defense. *microLife* 2

Branzk N, Papayannopoulos V. 2013. Molecular mechanisms regulating NETosis in infection and disease. *Semin Immunopathol* 35: 513-30

Brown GD, Denning DW, Gow NA, Levitz SM, Netea MG, White TC. 2012. Hidden killers: human fungal infections. *Sci Transl Med* 4: 165rv13

Bruns S, Kniemeyer O, Hasenberg M, Aimanianda V, Nietzsche S, et al. 2010. Production of extracellular traps against Aspergillus fumigatus in vitro and in infected lung tissue is dependent on invading neutrophils and influenced by hydrophobin RodA. *PLoS Pathog* 6: e1000873

Chen Y, Zhao Y, Yin Y, Jia X, Mao L. 2021. Mechanism of cargo sorting into small extracellular vesicles. *Bioengineered* 12: 8186-201

Drummond RA, Gaffen SL, Hise AG, Brown GD. 2014. Innate Defense against Fungal Pathogens. *Cold Spring Harb Perspect Med* 5

Escola J-M, Kleijmeer MJ, Stoorvogel W, Griffith JM, Yoshie O, Geuze HJ. 1998. Selective Enrichment of Tetraspan Proteins on the Internal Vesicles of Multivesicular Endosomes and on Exosomes Secreted by Human B-lymphocytes*. *Journal of Biological Chemistry* 273: 20121-27

Fraczek MG, Chishimba L, Niven RM, Bromley M, Simpson A, et al. 2018. Corticosteroid treatment is associated with increased filamentous fungal burden in allergic fungal disease. *J Allergy Clin Immunol* 142: 407-14

Gonçalves RC, Lisboa HC, Pombeiro-Sponchiado SR. 2012. Characterization of melanin pigment produced by Aspergillus nidulans. *World J Microbiol Biotechnol* 28: 1467-74

Goodman EB, Anderson DC, Tenner AJ. 1995. C1q triggers neutrophil superoxide production by a unique CD18-dependent mechanism. *J Leukoc Biol* 58: 168-76

Halder LD, Babych S, Palme DI, Mansouri-Ghahnavieh E, Ivanov L, et al. 2022. Candida albicans Induces Cross-Kingdom miRNA Trafficking in Human

Monocytes To Promote Fungal Growth. *mBio* 13: e03563-21

Headland SE, Jones HR, Norling LV, Kim A, Souza PR, et al. 2015. Neutrophil-derived microvesicles enter cartilage and protect the joint in inflammatory arthritis. *Sci Transl Med* 7: 315ra190

Heinekamp T, Schmidt H, Lapp K, Pahtz V, Shopova I, et al. 2015. Interference of Aspergillus fumigatus with the immune response. *Semin Immunopathol* 37: 141-52

Henriet SSV, Verweij PE, Warris A. 2012. Aspergillus nidulans and Chronic Granulomatous Disease: A Unique Host–Pathogen Interaction. *The Journal of Infectious Diseases* 206: 1128-37

Herrmann IK, Bertazzo S, O'Callaghan DJ, Schlegel AA, Kallepitis C, et al. 2015. Differentiating sepsis from non-infectious systemic inflammation based on microvesicle-bacteria aggregation. *Nanoscale* 7: 13511-20

Honorato L, Araujo JFDd, Ellis CC, Piffer AC, Pereira Y, et al. Extracellular Vesicles Regulate Biofilm Formation and Yeast-to-Hypha Differentiation in Candida albicans. *mBio* 0: e00301-22

Hooshmand MJ, Nguyen HX, Piltti KM, Benavente F, Hong S, et al. 2017. Neutrophils Induce Astroglial Differentiation and Migration of Human Neural Stem Cells via C1q and C3a Synthesis. *The Journal of Immunology* 199: 1069-85

Imbert S, Bresler P, Boissonnas A, Gauthier L, Souchet L, et al. 2016. Calcineurin inhibitors impair neutrophil activity against Aspergillus fumigatus in allogeneic hematopoietic stem cell transplant recipients. *J Allergy Clin Immunol* 138: 860-68

Kalleda N, Amich J, Arslan B, Poreddy S, Mattenheimer K, et al. 2016. Dynamic Immune Cell Recruitment After Murine Pulmonary Aspergillus fumigatus Infection under Different Immunosuppressive Regimens. *Front Microbiol* 7: 1107

King J, Henriet SSV, Warris A. 2016. Aspergillosis in Chronic Granulomatous Disease. *J Fungi (Basel)* 2

Klejnstrup ML, Frandsen RJN, Holm DK, Nielsen MT, Mortensen UH, et al. 2012. Genetics of Polyketide Metabolism in Aspergillus nidulans. *Metabolites* 2: 100-33

Kolonics F, Kajdacsi E, Farkas VJ, Veres DS, Khamari D, et al. 2021. Neutrophils produce proinflammatory or anti-inflammatory extracellular vesicles depending on the environmental conditions. *J Leukoc Biol* 109: 793-806

Kolonics F, Szeifert V, Timár CI, Ligeti E, Lőrincz Á M. 2020. The Functional Heterogeneity of Neutrophil-Derived Extracellular Vesicles Reflects the Status of the Parent Cell. *Cells* 9

Kwon-Chung KJ, Sugui JA. 2013. Aspergillus fumigatus--what makes the species a ubiquitous human fungal pathogen? *PLoS Pathog* 9: e1003743

Lahmer T, Kriescher S, Herner A, Rothe K, Spinner CD, et al. 2021. Invasive pulmonary aspergillosis in critically ill patients with severe COVID-19 pneumonia: Results from the prospective AspCOVID-19 study. *PLoS One* 16: e0238825

Langfelder K, Streibel M, Jahn B, Haase G, Brakhage AA. 2003. Biosynthesis of fungal melanins and their importance for human pathogenic fungi. *Fungal Genet Biol* 38: 143-58

Latge JP, Chamilos G. 2019. Aspergillus fumigatus and Aspergillosis in 2019. *Clin Microbiol Rev* 33

Leigh LE, Ghebrehiwet B, Perera TP, Bird IN, Strong P, et al. 1998. C1q-mediated

chemotaxis by human neutrophils: involvement of gClqR and G-protein signalling mechanisms. *The Biochemical journal* 330 (Pt 1): 247-54

Letsiou E, Teixeira Alves LG, Felten M, Mitchell TJ, Muller-Redetzky HC, et al. 2021. Neutrophil-Derived Extracellular Vesicles Activate Platelets after Pneumolysin Exposure. *Cells* 10

Levitz SM, Farrell TP. 1990. Human neutrophil degranulation stimulated by Aspergillus fumigatus. *J Leukoc Biol* 47: 170-5

Lewis RE, Kontoyiannis DP. 2009. Invasive aspergillosis in glucocorticoid-treated patients. *Medical Mycology* 47: S271-S81

Lim K, Hyun YM, Lambert-Emo K, Capece T, Bae S, et al. 2015. Neutrophil trails guide influenza-specific $CD8^+$ T cells in the airways. *Science* 349: aaa4352

Lőrincz Á M, Bartos B, Szombath D, Szeifert V, Timár CI, et al. 2020. Role of Mac-1 integrin in generation of extracellular vesicles with antibacterial capacity from neutrophilic granulocytes. *J Extracell Vesicles* 9: 1698889

Manojlovic M, Juto A, Jonasdottir A, Colic J, Vojinovic J, et al. 2020. Microparticles expressing myeloperoxidase as potential biomarkers in anti-neutrophil cytoplasmic antibody (ANCA)-associated vasculitides (AAV). *J Mol Med (Berl)* 98: 1279-86

Marciano BE, Spalding C, Fitzgerald A, Mann D, Brown T, et al. 2015. Common severe infections in chronic granulomatous disease. *Clin Infect Dis* 60: 1176-83

Mathieu M, Névo N, Jouve M, Valenzuela JI, Maurin M, et al. 2021. Specificities of exosome versus small ectosome secretion revealed by live intracellular tracking of CD63 and CD9. *Nat Commun* 12: 4389

McCormick A, Heesemann L, Wagener J, Marcos V, Hartl D, et al. 2010. NETs formed by human neutrophils inhibit growth of the pathogenic mold Aspergillus fumigatus. *Microbes Infect* 12: 928-36

Mircescu MM, Lipuma L, van Rooijen N, Pamer EG, Hohl TM. 2009. Essential role for neutrophils but not alveolar macrophages at early time points following Aspergillus fumigatus infection. *J Infect Dis* 200: 647-56

Mizenko RR, Brostoff T, Rojalin T, Koster HJ, Swindell HS, et al. 2021. Tetraspanins are unevenly distributed across single extracellular vesicles and bias sensitivity to multiplexed cancer biomarkers. *Journal of Nanobiotechnology* 19: 250

Monteiro MC, de la Cruz M, Cantizani J, Moreno C, Tormo JR, et al. 2012. A new approach to drug discovery: high-throughput screening of microbial natural extracts against Aspergillus fumigatus using resazurin. *J Biomol Screen* 17: 542-9

Nasir N, Farooqi J, Mahmood SF, Jabeen K. 2020. COVID-19-associated pulmonary aspergillosis (CAPA) in patients admitted with severe COVID-19 pneumonia: An observational study from Pakistan. *Mycoses* 63: 766-70

Palmer LB, Greenberg HE, Schiff MJ. 1991. Corticosteroid treatment as a risk factor for invasive aspergillosis in patients with lung disease. *Thorax* 46: 15-20

Perez-Riverol Y, Bai J, Bandla C, García-Seisdedos D, Hewapathirana S, et al. 2022. The PRIDE database resources in 2022: a hub for mass spectrometry-based proteomics evidences. *Nucleic Acids Res* 50: D543-D52

Rafiq M, Rivieccio F, Zimmermann AK, Visser C, Bruch A, et al. 2022. PLB-985 Neutrophil-Like Cells as a Model To Study Aspergillus fumigatus Pathogenesis. *mSphere*: e0094021

Reclusa P, Verstraelen P, Taverna S, Gunasekaran M, Pucci M, et al. 2020. Improving extracellular vesicles visualization: From static to motion. *Sci Rep* 10: 6494

Rosazza T, Warner J, Sollberger G. 2021. NET formation – mechanisms and how they relate to other cell death pathways. *The FEBS Journal* 288: 3334-50

Ruf D, Brantl V, Wagener J. 2018. Mitochondrial Fragmentation in Aspergillus fumigatus as Early Marker of Granulocyte Killing Activity. *Front Cell Infect Microbiol* 8: 128

Segal BH, Romani LR. 2009. Invasive aspergillosis in chronic granulomatous disease. *Medical Mycology* 47: S282-S90

Shlezinger N, Irmer H, Dhingra S, Beattie SR, Cramer RA, et al. 2017. Sterilizing immunity in the lung relies on targeting fungal apoptosis-like programmed cell death. *Science* 357: 1037-41

Shopova IA, Belyaev I, Dasari P, Jahreis S, Stroe MC, et al. 2020. Human Neutrophils Produce Antifungal Extracellular Vesicles against Aspergillus fumigatus. *mBio* 11

Simonsen JB. 2019. Pitfalls associated with lipophilic fluorophore staining of extracellular vesicles for uptake studies. *J Extracell Vesicles* 8: 1582237

Stephens-Romero SD, Mednick AJ, Feldmesser M. 2005. The pathogenesis of fatal outcome in murine pulmonary aspergillosis depends on the neutrophil depletion strategy. *Infect Immun* 73: 114-25

Strycker BD, Han Z, Bahari A, Pham T, Lin X, et al. 2021. Raman Characterization of Fungal DHN and DOPA Melanin Biosynthesis Pathways. *J Fungi (Basel)* 7

Théry C, Witwer KW, Aikawa E, Alcaraz MJ, Anderson JD, et al. 2018. Minimal information for studies of extracellular vesicles 2018 (MISEV2018): a position statement of the International Society for Extracellular Vesicles and update of the MISEV2014 guidelines. *J Extracell Vesicles* 7: 1535750

Thywißen A, Heinekamp T, Dahse HM, Schmaler-Ripcke J, Nietzsche S, et al. 2011. Conidial Dihydroxynaphthalene Melanin of the Human Pathogenic Fungus Aspergillus fumigatus Interferes with the Host Endocytosis Pathway. *Front Microbiol* 2: 96

Timár CI, Lorincz AM, Csépányi-Kömi R, Vályi-Nagy A, Nagy G, et al. 2013. Antibacterial effect of microvesicles released from human neutrophilic granulocytes. *Blood* 121: 510-8

Tönshoff B. 2020. Immunosuppressants in Organ Transplantation. *Handb Exp Pharmacol* 261: 441-69

Valiante V, Baldin C, Hortschansky P, Jain R, Thywißen A, et al. 2016. The Aspergillus fumigatus conidial melanin production is regulated by the bifunctional bHLH DevR and MADS-box RlmA transcription factors. *Mol Microbiol* 102: 321-35

Van Den Brulle J, Steidl S, Brakhage AA. 1999. Cloning and characterization of an Aspergillus nidulans gene involved in the regulation of penicillin biosynthesis. *Applied and environmental microbiology* 65: 5222-28

Vymazal O, Bendíčková K, De Zuani M, Vlková M, Hortová-Kohoutková M, Frič J. 2021. Immunosuppression Affects Neutrophil Functions: Does Calcineurin-NFAT Signaling Matter? *Frontiers in Immunology* 12

Wheeler MH, Bell AA. 1988. Melanins and their importance in pathogenic fungi. *Curr Top Med Mycol* 2: 338-87

4. Discussion

4.1 Neutrophil derived EVs are specific against *A. fumigatus*

In this thesis I aimed to investigate more in detail the role of EVs derived from neutrophils and epithelial cells in the context of *A. fumigatus* infection. Extensive research on EVs over the past decade has shown that their active release from cells is always associated with a specific cargo of RNA, DNA, proteins and lipids that exerts a distinctive function when delivered to the recipient cell (Anand et al 2019). The investigation of this cargo enables not only the understanding of the complex communication between cells under physiological and pathological conditions, but also the possibility of its manipulation for the benefit of the host.

The discovery that neutrophils release afEVs after contact with *A. fumigatus* conidia and that these afEVs are antifungal when applied to hyphae, opened up the possibility also to a future application of such afEVs for the treatment of invasive aspergillosis. Manuscript E revealed that the afEVs produced after co-incubation of PMNs with melanized conidia of *A. fumigatus* are specifically antimicrobial against *A. fumigatus* hyphae. This finding is particularly surprising considering that most of the killing mechanisms employed by neutrophils are extremely potent against a variety of microbes. The addition of afEVs to *P. aeruginosa* revealed that the bacterium was not affected in its growth. A similar result was obtained with the yeast *Candida albicans* which however, after contact with afEVs, exhibited a marked transition from the yeast to the hyphal form. The phenotypical switch and promotion of fungal growth induced by EVs has also been observed with EVs secreted from monocytes infected with *C. albicans,* theorizing a generalized counter-response of the yeast to immune cell-derived EVs (Halder et al 2022). Unexpectedly, a species closely related to *A. fumigatus*, *A. nidulans*, also showed no susceptibility to afEVs. The only pathogen tested that appeared to be sensitive was *S. aureus*. The study by (Timár et al 2013) showed that co-incubation of neutrophils with *S. aureus* also resulted in the production of EVs that could reduce its viability, it is therefore possible, that *S. aureus* is generally susceptible to particles secreted by neutrophils. In addition, the mentioned research provides further evidence for EV-specificity, as EVs induced by *S. aureus* were antibacterial against *Escherichia coli* but not *Proteus mirabilis*. Another example of how specific the response of immune cells against a pathogen can be,

comes from macrophages infected with *Mycobacterium tuberculosis*. After ingestion of the bacterium in fact the cells produced exosomes containing mycobacterial components, such as PAMPs, which were then taken up by naïve macrophages and activated their pro-inflammatory response (Wang et al 2019).

4.1.1 DHN-melanin as inducer of antifungal EVs

An important question concerns the molecule of *A. fumigatus* that triggers the specificity of afEVs. As previously shown the interaction between neutrophils and the *ΔpksP* mutant strain of *A. fumigatus* lacking the DHN-melanin on the surface of conidia, led to the production of EVs which were no longer antifungal (Shopova et al 2020). This finding is strongly supported in this thesis by further evidence, that co-incubation of neutrophils with melanin ghosts, which are composed mainly of pure melanin fibers, could also induce antifungal EVs. Furthermore, another DHN-melanin synthetizing fungus, *A. clavatus* showed an equivalent outcome, it also induced formation of functional afEVs. The role of DHN-melanin in the intracellular modulation of *A. fumigatus* infection was very well characterized in macrophages. In these cells, DHN-melanin interferes with the acidification of conidia-containing phagosomes, inhibiting the vATPase assembly, and thereby activation of proteolytic enzymes (Schmidt et al 2020, Thywißen et al 2011). The same phenotype has also been observed in primary neutrophils, but whether it affects vesicle biogenesis remains still unsolved. What we know is that the absence of this molecule alters the protein load of EVs. EVs derived from *ΔpksP*-infected neutrophils do not show a major antifungal activity and contain less antimicrobial peptides (Shopova et al 2020). In addition to inhibition of acidification, melanin could hamper the normal processing of conidia, starting with phagocytosis. The receptor that binds DHN-melanin on the surface of neutrophils is not known, but as demonstrated by *Akoumianaki et al.,* melanin can block LC3-mediated phagocytosis, which normally promotes fungal killing (Akoumianaki et al 2016). Furthermore, mutations in the pksP gene, involved in DHN-melanin biosynthesis, led to the production of a mutant strain that was phagocytosed by neutrophils to a much greater extent than the WT (Luther et al 2007, Tsai et al 1998). Additionally, melanin can apparently bind $Ca2^{+}$ or $Mg2^{+}$, which are important for MVBs formation and exocytosis (Taylor et al 2020).

4.1.2 Affinity of EVs for *A. fumigatus* hyphae and cargo delivery

The specificity of EVs derived from neutrophils infected with *A. fumigatus* was further investigated, by analyzing binding of EVs to fungal hyphae. Using a new generation dye to stain the EV lipid membrane, it was possible to visualize the interaction and internalization of the entire EV population within the fungal hyphae (Manuscript E), without losing any part of the sample through washing steps. This experiment revealed an unprecedented finding, *i.e.*, the accumulation of the dye signal where germination from conidia had started. Microscopic observations, accompanied by image analysis, indicated that a consistent number of afEVs are completely embedded in the cell wall of the hypha, whereas spontaneously formed EVs are mostly outside the cell wall or only partially embedded. Nevertheless, it remains to be shown by which mechanism afEVs are internalized and why they have a special affinity for the indicated part of the hyphae. Several studies have described a receptor-mediated internalization of EVs. Notably, neutrophil-derived EVs in the context of bacterial infections were found to be directly internalized into platelets *via* the Mac-1 receptor and to shuttle arachidonic acid (Rossaint et al 2016). Furthermore, inhibition of the αvβ3-integrin on tumor cell-derived EVs impaired their uptake by non-malignant cells (Altei et al 2020). In the case of *A. fumigatus*, a molecule present on the cell wall, CalA, was identified as a binder for human α5β1-integrin on both endothelial and epithelial cells (Liu et al 2016). It thus might play a role in uptake of afEVs and can be tested in the future.

Moreover, one of the preferred pathways by which EVs are taken up by cells is endocytosis mediated by clathrin or lipid rafts (Gurung et al 2021). Filamentous fungi are known to grow exclusively at the tip of hyphae by adding cell wall and membrane components. The conventional wisdom was that this growth occurs only through exocytosis at the Spitzenkörper, a part of the hyphae filled with secretory vesicles. However, recent discoveries have shown that another area called the sub-apical collar area, is also enriched for endocytic vesicles and therefore is also required for hyphal growth. Thus, it is now generally accepted that hyphal growth is not a random process and that it depends on the balance between endocytosis and exocytosis (Commer & Shaw 2020, Steinberg 2014). Thereby, a second hypothesis, is that EVs might be taken up by the fungus through endocytosis during the process of hyphal extension. However, such a scenario would not explain why afEVs accumulate at the former conidial head and not at the tip of the hyphae.

What is more likely is that there is some unique feature in the composition of the *A. fumigatus* cell wall which favors the internalization of afEVs. In agreement, when I performed the same experiment with afEVs applied to *A. nidulans*, afEVs mostly surrounded the fungal hyphae and were not located to distinct areas. Unfortunately, even after decades of studies aimed to characterize in detail the cell wall of both fungi, several aspects remain a mystery. It is known that they share some similarities and that the main difference seems to be the production level of some galactosaminogalactans (GAGs) (Guest & Momany 2000, Speth et al 2019). The role of GAGs in the interaction between *A. fumigatus* and neutrophils was already described. It was shown that GAGs induce neutrophils apoptosis and more interestingly they mediate the fungal resistance to extracellular killing by NETs (Bianchi et al 2009, Robinet et al 2014). In particular while *A. fumigatus* is not killed by NETs, these chromatin fibers are antifungal against *A. nidulans.* The difference in GAG composition in *A. nidulans* seems to be due to the low expression levels of the uge3 of the *A. fumigatus* homolog, called ugeB. The encoded enzyme is a cytosolic glucose-4 epimerase involved in the first step of the sugar's biosynthesis. As it turned out overexpression of ugeB or heterologous expression of *A. fumigatus´*uge3, in *A. nidulans* made this fungus also resistant to NETs killing (Lee et al 2015). The hypothesis behind GAG-mediated resistance to NETs killing is that the positive charge of GAG might repulse the positively charged antimicrobial peptides present in the NET fibers. This hypothesis might on the other hand explain the affinity of afEVs for *A. fumigatus* hyphae, since the change of EVs under physiological conditions is negative (Midekessa et al 2020).

The surface charge of EVs is strongly correlated to their membrane protein composition, in particular it depends on the proteins of the tetraspanin family CD9, CD81 and CD63 (Yasui et al 2021). In our study, characterization of subpopulation of afEVs enriched for a single tetraspanin revealed that they possess different antifungal potential. Specifically, the CD81-enriched population exerted the strongest antifungal effect when applied to fungal hyphae. The presence of high levels of CD81 on the surface of these afEVs might either influence their charge or might be connected to a different cargo sorting into these afEVs. While the charge of the single subpopulation was not investigated, the protein content of the CD81 subpopulation was analyzed. Comparative analysis between the whole population of afEVs and the CD81-afEV subpopulation, highlighted the presence of some shared proteins which

might be accountable for inhibition of the fungal growth. The considerable amount of glycolytic enzymes found in the afEVs suggests that they might be metabolically active and could potentially modify the concentrations of critical nutrients for the fungus, affecting its physiology (Fridman et al 2022). This hypothesis is in part corroborated in this study by the metabolic resazurin assay performed on the hyphae treated with afEVs. The addition of the blue compound resazurin, to healthy hyphae, led to its conversion into the pink compound resorufin, which is an indicator of a normal mitochondrial chain activity (Smith et al 2016). This conversion was significantly reduced in hyphae treated with afEVs, suggesting that the metabolic activity of the fungus is compromised. The fact that EVs can be metabolically active or induce metabolic reprogramming of the recipient cell has been shown previously. In particular, *Iraci et al.* have demonstrated for the first time that EVs from neuronal cells are not only carriers of metabolic enzymes, but that they possess an intrinsic asparaginase activity (Iraci et al 2017). In the same line, exosomes from cancer cells appear to promote tumor progression and angiogenesis by stimulation of glycolysis in recipient non-tumorigenic cells (Yang et al 2020).

4.1.3 C1q as a possible target molecule for fungal hyphae?

Another feature we observed in this analysis was the presence in the afEVs of very high concentrations of all the components of the C1q complement protein (Figure 5). C1q belongs to the pattern recognition molecules family and can bind a variety of ligands, ranging from molecules on the surface of immune cells to molecules on the surface of pathogens. Its main role is to activate the classical complement pathway but the complex can also be involved in processes that are complement-independent (Nayak et al 2012). During *A. fumigatus* infection, the conidia are often opsonized by immunoglobulins or complement proteins to be better phagocytosed. As shown by *Rosbjerg et al.*, the classical complement pathway is the predominant pathway used in response to this fungus (Rosbjerg et al 2016). Hence, it is reasonable to assume that neutrophils attempt to load this complement protein into afEVs to efficiently target fungal hyphae. The employment of C1q to target the hyphae could also explain why afEVs are accumulating on hyphae where the former conidium head can be still seen. This observation indeed, agrees with a recent study, showing that the C1q together with immunoglobulins has a much higher affinity for curved surfaces than for flat surfaces (Zeuthen et al 2020). In line, with the importance of C1q during aspergillosis

infections, non-immunocompromised mice with genetic deficiency of C1q showed increased fungal burden in the lungs and enhanced susceptibility to IA (Garlanda et al 2002).

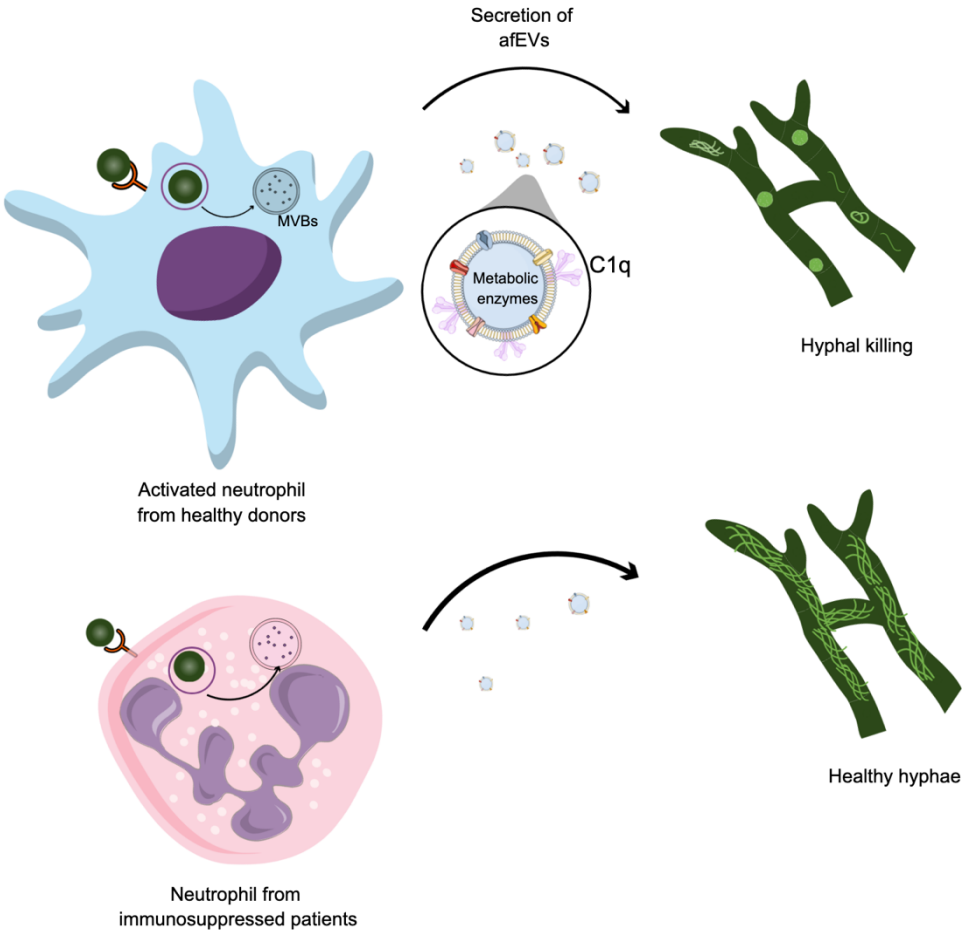

Figure 5 Interaction of neutrophils with *A. fumigatus* WT conidia and production of afEVs.

This model shows a healthy neutrophil in its active state, phagocytosing *A. fumigatus* WT melanized conidia. Phagocytosis occurs through elongation of uropods and this finally leads to the formation of MVBs. MVBs are vesicles-containing subcellular structures that fuse with the cytoplasmic membrane thereby releasing their content in the extracellular space. afEVs derived from neutrophils infected with WT conidia, are filled with metabolic enzymes and contain a high amount of the C1q complement protein. When delivered to fungal hyphae afEVs become internalized and cause a complete fragmentation of mitochondria and death of the hyphae. Neutrophils from immunosuppressed patients, after phagocytosis of WT conidia can also secrete EVs. Nevertheless, these EVs harbor a different protein cargo , in particular less C1q, and when delivered to hyphae are not able to kill them, as demonstrated by the presence of intact mitochondrial filaments inside hyphae.

4.1.4 Immunosuppressing treatment affects neutrophil production of afEVs by neutrophils

Our study on the role of afEVs for defence against *A. fumigatus* led us to investigate the effect of immunosuppressive drugs on the functionality of neutrophils, specifically on their ability to produce afEVs. Indeed, my work revealed that neutrophils isolated from 5 different patients treated with diverse classes of immunosuppressive drugs no longer generate "afEVs". This result might explain why such patients are highly susceptible for fungal exacerbations (Lionakis & Kontoyiannis 2003). The impairment of immune cells, in particular neutrophils, due to this kind of immunosuppressing treatment was intensively studied. It was shown that the treatment potently suppress processes dependent on the NF-κb transcription factor and on the NADPH-oxidase complex. In addition, co-incubation of healthy neutrophils with low amounts of dexamethasone for only 10 minutes already reduced their ability to kill hyphae by 20 %. Longer incubation times with the same drug also affected the production of pro-inflammatory cytokines and abolished completely hyphal killing (Bellocchio et al 2004b, Lewis & Kontoyiannis 2009). These results suggest that steroid drugs have a strong impact on the extracellular killing mechanisms, required for inhibition of hyphae, employed by neutrophils against *A. fumigatus*. In this thesis, I further define these killing mechanisms as killing by afEVs. This hypothesis is rather robust because the patients analyzed here were treated by different drugs and regimens. In fact, all patients who were in remission after stem cell transplantation, and underwent daily immunosuppression showed a complete loss of their "afEVs" antifungal activity. Hyphae incubated with either sEVs or "afEVs" were not inhibited in their growth and displayed an even higher metabolic activity compared to the untreated control. In this context a number of studies have previously shown a direct link between high-dose and prolonged treatment with glucocorticoids and a poor outcome of IA. The most affected population is composed of individuals receiving stem cell transplantations. For example, the administration of high doses of prednisone alone for 21 days increased the risk of developing IA sixfold compared to lower-dose regimens (O'Donnell et al 1994).

In contrast, one of the patients who did not receive a daily immunosuppressant, but only a weekly steroid dose over a period of three weeks, and who did not endure a stem cell transplantation displayed different results. This could be due to the fact that the intervals between doses might give the neutrophils time to

regain their activity and full functionality. For a deeper understanding of what might have caused the loss of antifungal activity of "afEVs", we analyzed once again their proteome content. What we gained from this analysis was that the majority of proteins differentially expressed in the "afEVs" from patients' neutrophils, were not shared with the afEVs from healthy donors' neutrophils. This finding suggests that immunosuppressive treatments in neutrophils are changing the protein sorting of afEVs. Several findings indicate that cells exposed to some kind of external stress can modify their EV content. The detrimental role of exosomes during atherosclerosis plaque formation is an example of how smooth muscle cells when constantly stimulated by oxidized LDL or TNF-alpha, secrete microparticles expressing ICAM-1. This molecule, through the vesicles, gets transferred to endothelial cells, and increases their adhesion to monocytes, thereby promoting, even more, the plaque formation (Fu et al 2017).

Of note, by intersecting the two proteomic datasets, we observed that some subunits of the C1q were missing in the patient-derived "afEVs". Hence, we hypothesize that these EVs might also not be antifungal because they lack this component and are therefore unable to be internalized into the fungal hyphae (Figure 5).

In summary, several aspects of the antifungal activity of afEVs remain to be investigated, in particular how they act specifically on *A. fumigatus* hyphae and what makes them cytotoxic to the fungus.

4.2 PLB-985 cells: a valid model to investigate *A. fumigatus* pathogenesis

As discussed in the previous section, neutrophils are very important cells in the defense against *A. fumigatus*. Despite that, their numerous functions have so far only been studied in primary neutrophils isolated from healthy donors or animals.
The involved procedures to isolate human neutrophils are laborious and time-consuming and have on the one hand the advantage of investigating mechanisms and pathways in primary cells, but on the other hand, the disadvantage of the availability of only a limited amount of cells, and their short half-life which prevents experiments with long incubation times from being carried out (Lahoz-Beneytez et al 2016). For these reasons the prospect of using a neutrophil cell line as a model has always been compelling and would be a valuable addition to studies on neutrophils. PLB-985 cells were originally described as cells isolated from a leukemic patient in 1987 (Tucker et al 1987). However, sequencing data revealed that they are actually a subline of the HL-60 cells, obtained from a patient with acute promyelocytic leukemia in 1977 (Drexler et al 2003). Following their structural characterization, they were shown to be able to differentiate into either monocytes or granulocytes in the presence of inducing agents (Collins et al 1978). The three, most commonly used, compounds responsible for maturation towards neutrophils are dibutyryl cyclic adenosine monophosphate (dbcAMP), dimethyl formamide (DMF) and dimethyl sulfoxide (DMSO) (Hazan-Eitan et al 2006, Katschinski et al 1999). Several studies have shown that all three agents induce the neutrophil phenotype, but each of them can enhance a specific cellular function. Furthermore, they do not have a major impact on cell viability, an important factor to consider when using them for functional assays. Through RNA-sequencing it was also known that after differentiation both HL-60 and PLB-985 cells display high similarities in their gene expression with primary neutrophils, strengthening their value as substitutes in the neutrophil research (Rincón et al 2018). In the context of infectious diseases PLB-985 cells appeared to be a worthy model to study the generation of NETs in response to *Escherichia coli* and *Candida albicans* (Amulic et al 2017, Marin-Esteban et al 2012). The only work based on a neutrophil-cell line in combination with *A. fumigatus*, was published by *Baistrocchi et al.*, for investigation on the antifungal potential of HL-60 cells treated with different concentrations of posaconazole (Baistrocchi et al 2016). Hence, in Manuscript C, the PLB-985 cells were used for the first time to analyze *A. fumigatus*

pathogenesis. To this aim we evaluated the response of DMF-differentiated PLB-985 cells (dPLBs) to *A. fumigatus* conidia and hyphae. Specifically, I analyzed the phagocytosis rate of the cells when confronted with either WT or *ΔpksP* conidia, and the secretion of pro-inflammatory cytokines both in comparison with primary neutrophils. The phagocytosis analysis, performed with a combination of image flow cytometry and confocal laser scanning microscopy, showed that dPLBs phagocytose more non-melanized *ΔpksP* conidia compared to WT conidia. This phenotype was also observed in primary neutrophils, and it is in accordance with the role of DHN-melanin in the prevention of phagocytosis from professional phagocytes (Aimanianda et al 2009, Luther et al 2007, Romani 2011). Nevertheless, the total amount of engulfed conidia after two hours of co-incubation was much lower in the dPLBs compared to primary neutrophils. This might be due to the compound we used for cell differentiation, in fact, DMF-differentiated cells exhibited lower phagocytic activity compared to DMSO-differentiated PLBs (Pivot-Pajot et al 2010). I next examined whether the interaction between dPLBs and conidia would lead to an upregulation of the immune response measured by the production of the pro-inflammatory cytokines IL-8 and IL-1β. The results revealed that the levels of secreted cytokines were generally higher in dPLBs compared to primary neutrophils. However, WT conidia induced, in both cells, the secretion of high levels of IL-8 and not IL-1β , and the trend of secretion was also equally comparable. In fact, a significant accumulation of IL-8 in the supernatant of infected dPLBs and primary neutrophils was only reached after six hours of co-incubation, with a very high peak after 24 hours. The finding that neutrophils do not secrete high levels of IL-1β after contact with *A. fumigatus* is not surprising, this cytokine is indeed released during *Aspergillus* infection mainly from monocytes or macrophages by a two-step process involving expression and synthesis of pro-IL-1β and the NLRP3 inflammasome and caspase-1 activation (Griffiths et al 2021, Saïd-Sadier et al 2010). Although, neutrophils do not secrete a high amount of IL-1β, they can bind this cytokine through IL1R and this seems to be crucial for their survival and inhibition of apoptosis (Ralph et al 2021). Whereas IL-8, as one of the most potent pro-inflammatory cytokines, is produced in considerate amounts from different immune cells, including neutrophils. Generally a single activated monocyte generates up to 70-fold more IL-8 compared to a single neutrophil, however since the recruitment and abundance of neutrophils during infection is always much higher than that of monocytes, their secreted IL-8 has a greater and more significant impact on

the resolution of infection (Fujishima et al 1993). Indeed, a fundamental role of neutrophil-secreted IL-8 is to induce migration and recruitment of other neutrophils from the blood to the damaged tissue, therefore amplifying the inflammation cascade (de Oliveira et al 2013). Furthermore, in agreement with our results with dPLBs, primary neutrophils, stimulated with opsonized L-ficolin particles also displayed a significantly higher release of IL-8 compared to IL-1β (Bidula et al 2016). Ultimately my results together with those of other colleagues, show the ability of DMF-differentiated PLB-985 cells to generate hyphal-directed NETs, secrete afEVs, and acidify conidia-containing phagosomes in a manner similar to primary neutrophils. Together, this suggests that the PLB-985 cell line can be a useful model to study the dynamic interaction between the pathogenic fungus *A. fumigatus* and neutrophils.

4.3 Epithelial cells as key regulators of cytokine cascades

Alveolar and bronchial epithelial cells belong to the first barrier encountered by fungal conidia after inhalation and penetration in the lungs. Nevertheless, there are very few studies on the factors involved in this interaction and the downstream signals activated in the cells. In Manuscript D we have combined mathematical and modeling observations with experimental data, to decipher the key fungal virulence determinants that make *A. fumigatus* a human pathogen compared to other Aspergilli, as well as the role of cytokines secreted by epithelial cells for the outcome of infection. This combined approach proved to be useful for predicting immune evasion mechanisms employed by pathogens such as *C. albicans* or *S. aureus* in a human whole-blood infection model or for predicting the role of Pores of Kohn during *A. fumigatus* infections (Blickensdorf et al 2020, Lehnert et al 2021). Our dynamic optimization model which took into account several parameters like, immune status of the host, the depletion of alveolar macrophages or neutrophils and the influence of high and low conidial doses, showed that the germination rate of the fungus is among the most crucial fungal virulence factors for the establishment of infection. To experimentally prove this computer finding, I tested the germination rate of four Aspergillus species: *A. fumigatus, A. nidulans, A. niger,* and *A. terreus*, which indeed displayed different germination kinetics at 37 °C. While the germination of *A. nidulans* was among the fastest, starting after only 4 hours, the germination of *A. fumigatus* and *niger* was delayed by1 or 2 hours, and *A. terreus* was by far the slowest, with not even one germinating conidia after 24 hours. To test whether their growth dynamics was related to their ability to damage the epithelial barrier, the release of lactate-dehydrogenase (LDH) from human alveolar epithelial cells (A549) and mouse alveolar epithelial cells (T7) was measured after 24 hours of co-incubation. This experiment confirmed the model prediction that a fast-germinating fungus is more likely to cause harm to the host than a slow germinating one. The faster growth of *A. nidulans* partly explains why this fungus is less successful in causing infections in humans compared to *A. fumigatus* (Kwon-Chung & Sugui 2013). Indeed, the conidia of *A. nidulans* grow faster because they are less phagocytosed and processed than the conidia of *A. fumigatus*. However, this induces a much more robust cytokine response and oxidative burst in the cells leading to more efficient clearance of the fungus (Gresnigt et al 2018). It also needs to be taken into consideration that even if engulfment of *A. fumigatus* happens more rapidly, the fungus can reside for longer

times inside phagosomes, by inhibiting their acidification and immune activation (Schoen et al 2019). Together with *A. fumigatus, A. niger* showed a comparable germination rate and damage to epithelial cells. Nevertheless, RNA-seq data revealed that the gene expression of cells differs after contact with both fungi. In particular, most genes involved in cytokine and chemokine release are downregulated by *A. fumigatus* and upregulated by *A. niger*, confirming that *A. fumigatus* reprograms the epithelium to be immunologically silent (Escobar et al 2018).
Among the tested aspergilli, *A. terreus* was the slowest and least damaging. This result supports the observation in the interaction with alveolar macrophages, where *A. terreus* after being efficiently phagocytosed due to the high exposure of beta 1-3 glucan on its surface, remained viable inside the phagosomes limiting germination and causing lower cytotoxicity (Slesiona et al 2012).

However, the data from the LDH assay obtained with human alveolar epithelial cells, were not in accordance with the data obtained with mouse cells where *A. fumigatus* induced the highest secretion of LDH. This finding highlights the fact that the response of human and mouse cells to *A. fumigatus*, is different, and that these differences must be taken into account when conducting a study (Hellmann et al 2017). They also prove that *A. fumigatus* can adapt much better to the human host, avoiding cell damage and recognition than to a rodent organism (Ballard et al 2018).

Most of the mathematical models of IA exclude the contribution of epithelial cells and focus mostly on neutrophils and alveolar macrophages (Oremland et al 2016, Tanaka et al 2015). Conversely, our dynamic optimization approach predicted a valuable contribution of epithelial cells in cytokine secretion after germination of conidia and depletion of alveolar macrophages. When measuring the levels of secreted IL-6 and TNF-alpha from alveolar macrophages and epithelial cells derived from mouse lungs we detected a consistent amount of secreted TNF-alpha from infected macrophages at 6 hours post-infection, whereas a significant level was reached from epithelial cells after a longer incubation period. Despite the longer time required, epithelial cells secreted greater amounts of both TNF-alpha and IL-6 after 10 hours and even more after 24 hours of infection. In contrast, the latter cytokine was almost undetectable in the supernatant of infected macrophages, suggesting that epithelial cells are the major source. The importance of both cytokines in mouse infection models of aspergillosis has been previously documented by their high concentrations found in the homogenized lungs of corticosteroid-treated mice

infected with *A. fumigatus* and by the observation that IL-6 deficient mice are more susceptible to IA showing an increased fungal burden (Cenci et al 2001, Duong et al 1998, Kalleda et al 2016). Overall, our findings are consistent with this literature, and strongly support a model in which epithelial cells are crucial for the immune response against *A. fumigatus*.

4.3.1 Bronchial epithelial cells-derived EVs: additional information carriers

In the course of the investigation on EVs, I also characterized EVs secreted by bronchial epithelial cells (BECs) in response to *A. fumigatus* (see Appendix).

EVs derived from BECs have been shown to play an important role in some pathological conditions and to be beneficial or detrimental for the lung tissue depending on the stimulus acting on the cells (Bartel et al 2020). For instance, they display antifibrotic activity in the course of a severe lung disease, called idiopathic pulmonary fibrosis (IPF), by inhibiting TGF-β induction in myofibroblasts (Kadota et al 2021). Contrarily, exposure to cigarette smoke induces the secretion of EVs from BECs carrying a specific miRNA that promotes fibrosis and airway remodeling, contributing to COPD exacerbations (Fujita et al 2015). Nevertheless, there are no studies to date on the role of BECs-derived EVs after confrontation with *A. fumigatus*.

In our methodology for studying EVs, it is essential to minimize cell death after infection with conidia, to limit the inclusion of apoptotic bodies in our analysis, as well as to obtain a large amount of EVs for follow-up investigations. To achieve both objectives, BECs were confronted for 24 hours with mutants of *A. fumigatus* incapable of germinating in the absence or uracil, the *pyrG*- mutant, and the corresponding non-melanized *ΔpksP* mutant (Weidner et al 1998). Initial examination of the number and diameter of these vesicles showed that the amount had not changed significantly after any of the different co-incubations and that the particle diameter was around 150 nm. From work on afEVs derived from primary neutrophils we know that infection with *A. fumigatus* does not necessarily increase the number of secreted vesicles, but rather their content (Rafiq et al 2022, Shopova et al 2020). Through LC-MS/MS analysis of these EVs, we found that most proteins matched between all groups, in particular, the differences between *pyrG*-derived EVs and sEVs were minor. The only outlier was EVs from *ΔpksP*-infected BECs, which possessed a large number of unique proteins. However, based on gene ontology annotations we could not assign a pro-inflammatory or immune-related function to them. They were mostly

involved in metabolic processes or intercellular transport. Again, our finding was consistent with what was observed with *ΔpksP*-derived EVs from primary neutrophils, which contained a great amount of unique proteins without antifungal potential (Shopova et al 2020). This led us to hypothesize that, similar to neutrophil granulocytes, *ΔpksP* conidia might be engulfed by BECs more efficiently than WT conidia, leading to upregulation of cell metabolisms and incorporation of all these enzymes into EVs. However, our hypothesis was refuted by image stream quantification which revealed significantly higher phagocytosis of WT conidia. Enhanced conidia uptake induced by DHN-melanin has also been described in alveolar epithelial cells (AECs). Our result together with previous findings thus indicate that this phenotype is common to all human lung epithelial cells (Amin et al 2014). Furthermore, in this study on AECs, it was shown that after ingestion, WT-melanized conidia could survive for longer inside cells by inhibiting phagosome acidification. Although further experimental evidence is needed to support this hypothesis, we speculate that DHN-melanin may exert the same inhibitory effect on BECs. Therefore, a large amount of metabolic enzymes in EVs could come from the cells trying to digest the non-melanized conidia after phagocytosis.

4.3.2 *PyrG*-derived EVs as inducer of pro-inflammatory cytokines

Systemic body functions are constantly influenced by cytokines, as they facilitate communication between cells. In recent years EVs have been identified as cytokine carriers or inducers in physiological and pathological states (Barnes & Somerville 2020). Indeed, our co-incubation experiment of naïve BECs with EVs derived from BECs infected with either WT or *ΔpksP* conidia demonstrated that only EVs derived from WT infected cells stimulated naïve cells to produce more IL-6 and IL-8. Previous findings have also shown that EVs play a role in the modulation of cytokines during fungal infection, in particular, EVs secreted by monocytes following *C. albicans* infection, and containing TGF-β1, can down-modulate the response of M1 macrophages, whereas our results show activation of the pro-inflammatory response (Halder et al 2020).

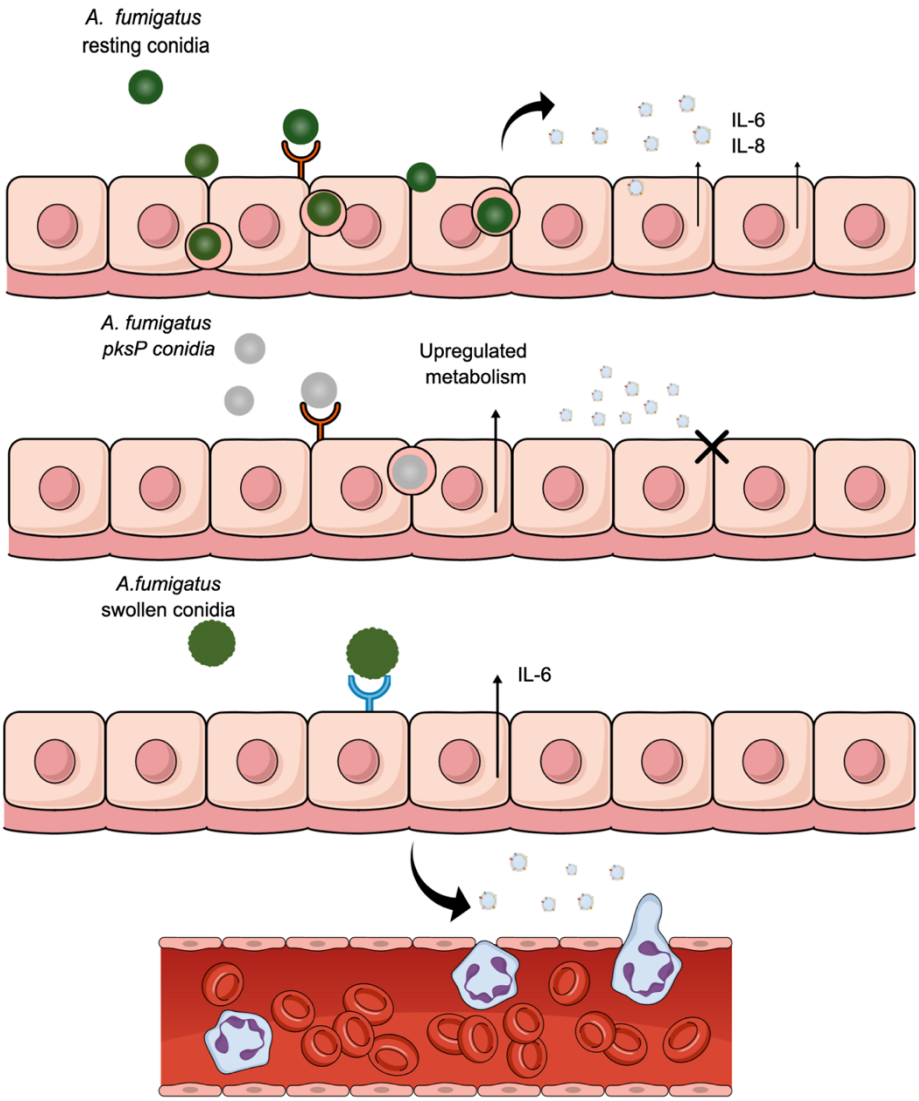

Figure 6 Model summarizing the interaction of BECs with *A. fumigatus* conidia.

After phagocytosis of resting WT conidia BECs secrete EVs which are then internalized into naïve neighboring cells, up-regulating their pro-inflammatory response. Contrarily, phagocytosis of Δ*pksP* conidia, happens at slower rates and leads to the generation of EVs with no obvious function on neighboring cells, but which are filled with metabolic enzymes. Lastly, exposure of beta 1-3 glucan on the surface of swollen conidia, induces a strong activation of BECs and loading into EVs of cytokines and proteins with the potential role of recruiting cells to the site of infection.

In addition, we measured the amount of cytokines released in the extracellular space after contact with the conidia.

Through this estimation we were able to determine that *ΔpksP* conidia, do not stimulate cytokine production by BECs. Surprisingly, the amount of IL-8 and IL-6

induced by WT conidia was also quite low and almost comparable to the baseline amount secreted by uninfected cells.

As shown previously, the production of pro-inflammatory mediators from airway epithelial cells is reduced in the presence of the DHN-melanin and rodlet layers, and only increases after 6 or 8 hours of infection, a time corresponding to the swelling and germination of conidia (Balloy et al 2008, Bigot et al 2020b, Tomee et al 1997). Hence, we hypothesize that co-incubation of BECs with swollen conidia, exposing more beta 1-3 glucan, could lead to higher activation and alteration of their EV profile. Indeed, infection of cells with swollen conidia enhanced cytokine secretion and led to the generation of EVs which were also filled with pro-inflammatory cytokines such as IL-6 and TNF-alpha. Examination on the biological processes in which their unique protein content was involved, revealed their engagement in neutrophils aggregation, zinc sequestration, and nitric oxide generation. The role of epithelial cells in neutrophil recruitment was shown before, and in this case, could be a defense strategy to eliminate the threat more rapidly. Instead, the proteins associated with zinc sequestration and nitric oxide production could be signals of the stress induced by the swollen conidia in the cells, as zinc proved to be fundamental in maintaining the integrity of the epithelial barrier, and nitric oxide to have important antioxidant functions (Bao & Knoell 2006, Schieler et al 2019, Szabady & McCormick 2013).

In conclusion, the human body is a very complex but perfect system. The human cells as gears of this system, work tirelessly to keep it healthy and eliminate any possible threat. This work provides evidence that each cell, especially when confronted with *A. fumigatus*, contributes in its own way to eradicating the fungus. Further understanding of how cells communicate with each other, either *via* EVs or simply through secreted molecules could support future research to develop targeted strategies to combat aspergillosis infections and new approaches to protect susceptible patients.

5. References

Adrover JM, Nicolás-Ávila JA, Hidalgo A. 2016. Aging: A Temporal Dimension for Neutrophils. *Trends Immunol* 37: 334-45

Aimanianda V, Bayry J, Bozza S, Kniemeyer O, Perruccio K, et al. 2009. Surface hydrophobin prevents immune recognition of airborne fungal spores. *Nature* 460: 1117-21

Akoumianaki T, Kyrmizi I, Valsecchi I, Gresnigt MS, Samonis G, et al. 2016. Aspergillus Cell Wall Melanin Blocks LC3-Associated Phagocytosis to Promote Pathogenicity. *Cell Host Microbe* 19: 79-90

Alekseeva L, Huet D, Féménia F, Mouyna I, Abdelouahab M, et al. 2009. Inducible expression of beta defensins by human respiratory epithelial cells exposed to Aspergillus fumigatusorganisms. *BMC Microbiology* 9: 33

Altei WF, Pachane BC, dos Santos PK, Ribeiro LNM, Sung BH, et al. 2020. Inhibition of αvβ3 integrin impairs adhesion and uptake of tumor-derived small extracellular vesicles. *Cell Communication and Signaling* 18: 158

Amich J, Calera JA. 2014. Zinc acquisition: a key aspect in Aspergillus fumigatus virulence. *Mycopathologia* 178: 379-85

Amin S, Thywissen A, Heinekamp T, Saluz HP, Brakhage AA. 2014. Melanin dependent survival of Apergillus fumigatus conidia in lung epithelial cells. *International Journal of Medical Microbiology* 304: 626-36

Amulic B, Knackstedt SL, Abu Abed U, Deigendesch N, Harbort CJ, et al. 2017. Cell-Cycle Proteins Control Production of Neutrophil Extracellular Traps. *Dev Cell* 43: 449-62.e5

Anand S, Samuel M, Kumar S, Mathivanan S. 2019. Ticket to a bubble ride: Cargo sorting into exosomes and extracellular vesicles. *Biochimica et Biophysica Acta (BBA) - Proteins and Proteomics* 1867: 140203

Anand S, Samuel M, Mathivanan S. 2021. Exomeres: A New Member of Extracellular Vesicles Family. *Subcell Biochem* 97: 89-97

and AAB, Langfelder K. 2002. Menacing Mold: The Molecular Biology of Aspergillus fumigatus. *Annual Review of Microbiology* 56: 433-55

Bainton DF, Ullyot JL, Farquhar MG. 1971. The development of neutrophilic polymorphonuclear leukocytes in human bone marrow. *J Exp Med* 134: 907-34

Baistrocchi SR, Lee MJ, Lehoux M, Ralph B, Snarr BD, et al. 2016. Posaconazole-Loaded Leukocytes as a Novel Treatment Strategy Targeting Invasive Pulmonary Aspergillosis. *J Infect Dis* 215: 1734-41

Ballard E, Melchers WJG, Zoll J, Brown AJP, Verweij PE, Warris A. 2018. In-host microevolution of Aspergillus fumigatus: A phenotypic and genotypic analysis. *Fungal genetics and biology : FG & B* 113: 1-13

Balloy V, Chignard M. 2009. The innate immune response to Aspergillus fumigatus. *Microbes and Infection* 11: 919-27

Balloy V, Sallenave JM, Wu Y, Touqui L, Latgé JP, et al. 2008. Aspergillus fumigatus-induced interleukin-8 synthesis by respiratory epithelial cells is controlled by the phosphatidylinositol 3-kinase, p38 MAPK, and ERK1/2 pathways and not by the toll-like receptor-MyD88 pathway. *J Biol Chem* 283: 30513-21

Balloy V, Si-Tahar M, Takeuchi O, Philippe B, Nahori M-A, et al. 2005. Involvement of Toll-Like Receptor 2 in Experimental Invasive Pulmonary Aspergillosis. *Infection and Immunity* 73: 5420-25

Bao S, Knoell DL. 2006. Zinc modulates cytokine-induced lung epithelial cell barrier permeability. *Am J Physiol Lung Cell Mol Physiol* 291: L1132-41

Barnes BJ, Somerville CC. 2020. Modulating Cytokine Production via Select Packaging and Secretion From Extracellular Vesicles. *Frontiers in Immunology* 11

Bartel S, Deshane J, Wilkinson T, Gabrielsson S. 2020. Extracellular Vesicles as Mediators of Cellular Cross Talk in the Lung Microenvironment. *Frontiers in Medicine* 7

Basu S, Hodgson G, Katz M, Dunn AR. 2002. Evaluation of role of G-CSF in the production, survival, and release of neutrophils from bone marrow into circulation. *Blood* 100: 854-61

Bayry J, Aimanianda V, Guijarro JI, Sunde M, Latgé J-P. 2012. Hydrophobins—Unique Fungal Proteins. *PLOS Pathogens* 8: e1002700

Bellocchio S, Montagnoli C, Bozza S, Gaziano R, Rossi G, et al. 2004a. The Contribution of the Toll-Like/IL-1 Receptor Superfamily to Innate and Adaptive Immunity to Fungal Pathogens In Vivo. *The Journal of Immunology* 172: 3059

Bellocchio S, Moretti S, Perruccio K, Fallarino F, Bozza S, et al. 2004b. TLRs govern neutrophil activity in aspergillosis. *J Immunol* 173: 7406-15

Ben-Ghazzi N, Moreno-Velásquez S, Seidel C, Thomson D, Denning DW, et al. 2021. Characterisation of Aspergillus fumigatus Endocytic Trafficking within Airway Epithelial Cells Using High-Resolution Automated Quantitative Confocal Microscopy. *J Fungi (Basel)* 7

Bhabhra R, Askew DS. 2005. Thermotolerance and virulence of Aspergillus fumigatus: role of the fungal nucleolus. *Med Mycol* 43 Suppl 1: S87-93

Bianchi M, Hakkim A, Brinkmann V, Siler U, Seger RA, et al. 2009. Restoration of NET formation by gene therapy in CGD controls aspergillosis. *Blood* 114: 2619-22

Bidula S, Sexton DW, Abdolrasouli A, Shah A, Reed A, et al. 2015. The serum opsonin L-ficolin is detected in lungs of human transplant recipients following fungal infections and modulates inflammation and killing of Aspergillus fumigatus. *J Infect Dis* 212: 234-46

Bidula S, Sexton DW, Schelenz S. 2016. Serum opsonin ficolin-A enhances host-fungal interactions and modulates cytokine expression from human monocyte-derived macrophages and neutrophils following Aspergillus fumigatus challenge. *Med Microbiol Immunol* 205: 133-42

Bigot J, Guillot L, Guitard J, Ruffin M, Corvol H, et al. 2020a. Bronchial Epithelial Cells on the Front Line to Fight Lung Infection-Causing Aspergillus fumigatus. *Frontiers in Immunology* 11

Bigot J, Guillot L, Guitard J, Ruffin M, Corvol H, et al. 2020b. Respiratory Epithelial Cells Can Remember Infection: A Proof-of-Concept Study. *J Infect Dis* 221: 1000-05

Blease K, Kunkel SL, Hogaboam CM. 2001. IL-18 modulates chronic fungal asthma in a murine model; putative involvement of Toll-like receptor-2. *Inflammation Research* 50: 552-60

Blickensdorf M, Timme S, Figge MT. 2020. Hybrid Agent-Based Modeling of Aspergillus fumigatus Infection to Quantitatively Investigate the Role of Pores of Kohn in Human Alveoli. *Front Microbiol* 11: 1951

Borregaard N, Cowland JB. 1997a. Granules of the Human Neutrophilic Polymorphonuclear Leukocyte. *Blood* 89: 3503-21

Borregaard N, Cowland JB. 1997b. Granules of the human neutrophilic

polymorphonuclear leukocyte. *Blood* 89: 3503-21

Borregaard N, Sehested M, Nielsen BS, Sengelϕv H, Kjeldsen L. 1995. Biosynthesis of Granule Proteins in Normal Human Bone Marrow Cells. Gelatinase Is a Marker of Terminal Neutrophil Differentiation. *Blood* 85: 812-17

Boyle KB, Stephens LR, Hawkins PT. 2012. Activation of the neutrophil NADPH oxidase by Aspergillus fumigatus. *Ann N Y Acad Sci* 1273: 68-73

Braedel S, Radsak M, Einsele H, Latgé J-P, Michan A, et al. 2004. Aspergillus fumigatus antigens activate innate immune cells via toll-like receptors 2 and 4. *British Journal of Haematology* 125: 392-99

Braem SGE, Rooijakkers SHM, van Kessel KPM, de Cock H, Wösten HAB, et al. 2015. Effective Neutrophil Phagocytosis of Aspergillus fumigatus Is Mediated by Classical Pathway Complement Activation. *Journal of Innate Immunity* 7: 364-74

Brakhage AA, Bruns S, Thywissen A, Zipfel PF, Behnsen J. 2010. Interaction of phagocytes with filamentous fungi. *Current Opinion in Microbiology* 13: 409-15

Brakhage AA, Zimmermann A-K, Rivieccio F, Visser C, Blango MG. 2021. Host-derived extracellular vesicles for antimicrobial defense. *microLife* 2

Brandon M, Howard B, Lawrence C, Laubenbacher R. 2015. Iron acquisition and oxidative stress response in aspergillus fumigatus. *BMC Systems Biology* 9: 19

Bratton DL, Henson PM. 2011. Neutrophil clearance: when the party is over, clean-up begins. *Trends Immunol* 32: 350-7

Brinkmann V, Reichard U, Goosmann C, Fauler B, Uhlemann Y, et al. 2004. Neutrophil extracellular traps kill bacteria. *Science* 303: 1532-5

Brown GD, Herre J, Williams DL, Willment JA, Marshall AS, Gordon S. 2003. Dectin-1 mediates the biological effects of beta-glucans. *J Exp Med* 197: 1119-24

Brown GD, Taylor PR, Reid DM, Willment JA, Williams DL, et al. 2002. Dectin-1 is a major beta-glucan receptor on macrophages. *J Exp Med* 196: 407-12

Bruns S, Kniemeyer O, Hasenberg M, Aimanianda V, Nietzsche S, et al. 2010. Production of extracellular traps against Aspergillus fumigatus in vitro and in infected lung tissue is dependent on invading neutrophils and influenced by hydrophobin RodA. *PLoS Pathog* 6: e1000873

Campitelli M, Zeineddine N, Samaha G, Maslak S. 2017. Combination Antifungal Therapy: A Review of Current Data. *J Clin Med Res* 9: 451-56

Carvalho LO, Aquino EN, Neves AC, Fontes W. 2015. The Neutrophil Nucleus and Its Role in Neutrophilic Function. *J Cell Biochem* 116: 1831-6

Cenci E, Mencacci A, Casagrande A, Mosci P, Bistoni F, Romani L. 2001. Impaired antifungal effector activity but not inflammatory cell recruitment in interleukin-6-deficient mice with invasive pulmonary aspergillosis. *J Infect Dis* 184: 610-7

Chai LY, Kullberg BJ, Vonk AG, Warris A, Cambi A, et al. 2009. Modulation of Toll-like receptor 2 (TLR2) and TLR4 responses by Aspergillus fumigatus. *Infect Immun* 77: 2184-92

Chai LYA, Netea MG, Sugui J, Vonk AG, van de Sande WWJ, et al. 2010. Aspergillus fumigatus Conidial Melanin Modulates Host Cytokine Response. *Immunobiology* 215: 915-20

Clark HR, Powell AB, Simmons KA, Ayubi T, Kale SD. 2019. Endocytic Markers Associated with the Internalization and Processing of Aspergillus fumigatus Conidia by BEAS-2B Cells. *mSphere* 4

Cohen J, Denning DW, Viviani MA, the EIFICG. 1993. Epidemiology of invasive aspergillosis in European cancer centres. *European Journal of Clinical Microbiology and Infectious Diseases* 12: 392-93

Cohen MS, Isturiz RE, Malech HL, Root RK, Wilfert CM, et al. 1981. Fungal infection in chronic granulomatous disease. The importance of the phagocyte in defense against fungi. *Am J Med* 71: 59-66

Collins SJ, Ruscetti FW, Gallagher RE, Gallo RC. 1978. Terminal differentiation of human promyelocytic leukemia cells induced by dimethyl sulfoxide and other polar compounds. *Proceedings of the National Academy of Sciences of the United States of America* 75: 2458-62

Commer B, Shaw BD. 2020. Current views on endocytosis in filamentous fungi. *Mycology* 12: 1-9

Cowland JB, Borregaard N. 1999. Isolation of neutrophil precursors from bone marrow for biochemical and transcriptional analysis. *Journal of Immunological Methods* 232: 191-200

Culibrk L, Croft CA, Toor A, Yang SJ, Singhera GK, et al. 2019. Phagocytosis of Aspergillus fumigatus by Human Bronchial Epithelial Cells Is Mediated by the Arp2/3 Complex and WIPF2. *Front Cell Infect Microbiol* 9: 16

Dąbrowska D, Jabłońska E, Garley M, Ratajczak-Wrona W, Iwaniuk A. 2016. New Aspects of the Biology of Neutrophil Extracellular Traps. *Scandinavian Journal of Immunology* 84: 317-22

Dagenais TRT, Keller NP. 2009. Pathogenesis of Aspergillus fumigatus in Invasive Aspergillosis. *Clinical Microbiology Reviews* 22: 447-65

Dancey JT, Deubelbeiss KA, Harker LA, Finch CA. 1976. Neutrophil kinetics in man. *J Clin Invest* 58: 705-15

de Castro PA, Colabardini AC, Manfiolli AO, Chiaratto J, Silva LP, et al. 2020. Aspergillus fumigatus calcium-responsive transcription factors regulate cell wall architecture promoting stress tolerance, virulence and caspofungin resistance. *PLOS Genetics* 15: e1008551

de Oliveira S, Reyes-Aldasoro CC, Candel S, Renshaw SA, Mulero V, Calado A. 2013. Cxcl8 (IL-8) mediates neutrophil recruitment and behavior in the zebrafish inflammatory response. *J Immunol* 190: 4349-59

Denning DW, Park S, Lass-Florl C, Fraczek MG, Kirwan M, et al. 2011. High-frequency Triazole Resistance Found In Nonculturable Aspergillus fumigatus from Lungs of Patients with Chronic Fungal Disease. *Clinical Infectious Diseases* 52: 1123-29

Diamond RD, Krzesicki R, Epstein B, Jao W. 1978. Damage to hyphal forms of fungi by human leukocytes in vitro. A possible host defense mechanism in aspergillosis and mucormycosis. *Am J Pathol* 91: 313-28

Drexler HG, Dirks WG, Matsuo Y, MacLeod RA. 2003. False leukemia-lymphoma cell lines: an update on over 500 cell lines. *Leukemia* 17: 416-26

Drummond RA, Brown GD. 2011. The role of Dectin-1 in the host defence against fungal infections. *Current Opinion in Microbiology* 14: 392-99

Dubourdeau M, Athman R, Balloy V, Philippe B, Sengmanivong L, et al. 2006. Interaction of Aspergillus fumigatus with the alveolar macrophage. *Medical Mycology* 44: S213-S17

Dumestre-Pérard C, Lamy B, Aldebert D, Lemaire-Vieille C, Grillot R, et al. 2008. Aspergillus conidia activate the complement by the mannan-binding lectin C2 bypass mechanism. *J Immunol* 181: 7100-5

Duong M, Ouellet N, Simard M, Bergeron Y, Olivier M, Bergeron MG. 1998. Kinetic study of host defense and inflammatory response to Aspergillus fumigatus in

steroid-induced immunosuppressed mice. *J Infect Dis* 178: 1472-82

Edgar JR, Eden ER, Futter CE. 2014. Hrs- and CD63-Dependent Competing Mechanisms Make Different Sized Endosomal Intraluminal Vesicles. *Traffic* 15: 197-211

Eken C, Martin PJ, Sadallah S, Treves S, Schaller M, Schifferli JA. 2010. Ectosomes released by polymorphonuclear neutrophils induce a MerTK-dependent anti-inflammatory pathway in macrophages. *J Biol Chem* 285: 39914-21

Eken C, Sadallah S, Martin PJ, Treves S, Schifferli JA. 2013. Ectosomes of polymorphonuclear neutrophils activate multiple signaling pathways in macrophages. *Immunobiology* 218: 382-92

Elmore S. 2007. Apoptosis: a review of programmed cell death. *Toxicol Pathol* 35: 495-516

Escobar N, Valdes ID, Keizer EM, Ordonez SR, Ohm RA, et al. 2018. Expression profile analysis reveals that Aspergillus fumigatus but not Aspergillus niger makes type II epithelial lung cells less immunological alert. *BMC Genomics* 19: 534

Ewald J, Rivieccio F, Radosa L, Schuster S, Brakhage AA, Kaleta C. 2021. Dynamic optimization reveals alveolar epithelial cells as key mediators of host defense in invasive aspergillosis. *PLOS Computational Biology* 17: e1009645

Faro-Trindade I, Willment JA, Kerrigan AM, Redelinghuys P, Hadebe S, et al. 2012. Characterisation of Innate Fungal Recognition in the Lung. *PLOS ONE* 7: e35675

Feigelson SW, Grabovsky V, Shamri R, Levy S, Alon R. 2003. The CD81 tetraspanin facilitates instantaneous leukocyte VLA-4 adhesion strengthening to vascular cell adhesion molecule 1 (VCAM-1) under shear flow. *J Biol Chem* 278: 51203-12

Fekkar A, Balloy V, Pionneau C, Marinach-Patrice C, Chignard M, Mazier D. 2012. Secretome of Human Bronchial Epithelial Cells in Response to the Fungal Pathogen Aspergillus fumigatus Analyzed by Differential In-Gel Electrophoresis. *J Infect Dis* 205: 1163-72

Feng D, Zhao W-L, Ye Y-Y, Bai X-C, Liu R-Q, et al. 2010. Cellular Internalization of Exosomes Occurs Through Phagocytosis. *Traffic* 11: 675-87

Ferwerda B, Ferwerda G, Plantinga TS, Willment JA, van Spriel AB, et al. 2009. Human Dectin-1 Deficiency and Mucocutaneous Fungal Infections. *New England Journal of Medicine* 361: 1760-67

Fisher MC, Alastruey-Izquierdo A, Berman J, Bicanic T, Bignell EM, et al. 2022. Tackling the emerging threat of antifungal resistance to human health. *Nature Reviews Microbiology*

Frankel EB, Audhya A. 2018. ESCRT-dependent cargo sorting at multivesicular endosomes. *Seminars in Cell & Developmental Biology* 74: 4-10

French KC, Antonyak MA, Cerione RA. 2017. Extracellular vesicle docking at the cellular port: Extracellular vesicle binding and uptake. *Seminars in cell & developmental biology* 67: 48-55

Fridman ES, Ginini L, Gil Z. 2022. The Role of Extracellular Vesicles in Metabolic Reprogramming of the Tumor Microenvironment. *Cells* 11

Fu Z, Zhou E, Wang X, Tian M, Kong J, et al. 2017. Oxidized low-density lipoprotein-induced microparticles promote endothelial monocyte adhesion via intercellular adhesion molecule 1. *Am J Physiol Cell Physiol* 313: C567-c74

Fuchs TA, Abed U, Goosmann C, Hurwitz R, Schulze I, et al. 2007. Novel cell death program leads to neutrophil extracellular traps. *J Cell Biol* 176: 231-41

Fujishima S, Hoffman AR, Vu T, Kim KJ, Zheng H, et al. 1993. Regulation of neutrophil interleukin 8 gene expression and protein secretion by LPS, TNF-alpha, and IL-1 beta. *J Cell Physiol* 154: 478-85

Fujita Y, Araya J, Ito S, Kobayashi K, Kosaka N, et al. 2015. Suppression of autophagy by extracellular vesicles promotes myofibroblast differentiation in COPD pathogenesis. *J Extracell Vesicles* 4: 28388

Gaboriaud C, Juanhuix J, Gruez A, Lacroix M, Darnault C, et al. 2003. The crystal structure of the globular head of complement protein C1q provides a basis for its versatile recognition properties. *J Biol Chem* 278: 46974-82

Gantner BN, Simmons RM, Canavera SJ, Akira S, Underhill DM. 2003. Collaborative induction of inflammatory responses by dectin-1 and Toll-like receptor 2. *J Exp Med* 197: 1107-17

García-Martínez M, Vázquez-Flores L, Álvarez-Jiménez VD, Castañeda-Casimiro J, Ibáñez-Hernández M, et al. 2019. Extracellular vesicles released by J774A.1 macrophages reduce the bacterial load in macrophages and in an experimental mouse model of tuberculosis. *International journal of nanomedicine* 14: 6707-19

Garlanda C, Hirsch E, Bozza S, Salustri A, De Acetis M, et al. 2002. Non-redundant role of the long pentraxin PTX3 in anti-fungal innate immune response. *Nature* 420: 182-86

Gasser O, Hess C, Miot S, Deon C, Sanchez JC, Schifferli JA. 2003. Characterisation and properties of ectosomes released by human polymorphonuclear neutrophils. *Exp Cell Res* 285: 243-57

Gazendam RP, van Hamme JL, Tool AT, Hoogenboezem M, van den Berg JM, et al. 2016. Human Neutrophils Use Different Mechanisms To Kill Aspergillus fumigatus Conidia and Hyphae: Evidence from Phagocyte Defects. *J Immunol* 196: 1272-83

Geijtenbeek TBH, Gringhuis SI. 2009. Signalling through C-type lectin receptors: shaping immune responses. *Nature Reviews Immunology* 9: 465-79

Genster N, Præstekjær Cramer E, Rosbjerg A, Pilely K, Cowland JB, Garred P. 2016. Ficolins Promote Fungal Clearance in vivo and Modulate the Inflammatory Cytokine Response in Host Defense against Aspergillus fumigatus. *Journal of Innate Immunity* 8: 579-88

Gerson SL, Talbot GH, Hurwitz S, Strom BL, Lusk EJ, Cassileth PA. 1984. Prolonged granulocytopenia: the major risk factor for invasive pulmonary aspergillosis in patients with acute leukemia. *Ann Intern Med* 100: 345-51

Gersuk GM, Underhill DM, Zhu L, Marr KA. 2006. Dectin-1 and TLRs permit macrophages to distinguish between different Aspergillus fumigatus cellular states. *J Immunol* 176: 3717-24

Gomez I, Ward B, Souilhol C, Recarti C, Ariaans M, et al. 2020. Neutrophil microvesicles drive atherosclerosis by delivering miR-155 to atheroprone endothelium. *Nature Communications* 11: 214

Goodridge HS, Reyes CN, Becker CA, Katsumoto TR, Ma J, et al. 2011. Activation of the innate immune receptor Dectin-1 upon formation of a 'phagocytic synapse'. *Nature* 472: 471-75

Goodridge HS, Underhill DM, Touret N. 2012. Mechanisms of Fc receptor and dectin-1 activation for phagocytosis. *Traffic* 13: 1062-71

Gout E, Moriscot C, Doni A, Dumestre-Pérard C, Lacroix M, et al. 2011. M-ficolin interacts with the long pentraxin PTX3: a novel case of cross-talk between soluble pattern-recognition molecules. *J Immunol* 186: 5815-22

Gresnigt MS, Becker KL, Leenders F, Alonso MF, Wang X, et al. 2018. Differential

Kinetics of Aspergillus nidulans and Aspergillus fumigatus Phagocytosis. *Journal of Innate Immunity* 10: 145-60

Griffiths JS, Camilli G, Kotowicz NK, Ho J, Richardson JP, Naglik JR. 2021. Role for IL-1 Family Cytokines in Fungal Infections. *Frontiers in Microbiology* 12

Gringhuis SI, Kaptein TM, Wevers BA, Theelen B, van der Vlist M, et al. 2012. Dectin-1 is an extracellular pathogen sensor for the induction and processing of IL-1β via a noncanonical caspase-8 inflammasome. *Nat Immunol* 13: 246-54

Guegan H, Prat E, Robert-Gangneux F, Gangneux J-P. 2021. Azole Resistance in Aspergillus fumigatus: A Five-Year Follow Up Experience in a Tertiary Hospital With a Special Focus on Cystic Fibrosis. *Frontiers in Cellular and Infection Microbiology* 10

Guest GM, Momany M. 2000. Analysis of cell wall sugars in the pathogen Aspergillus fumigatus and the saprophyte Aspergillus nidulans. *Mycologia* 92: 1047-50

Guinea J, Torres-Narbona M, Gijón P, Muñoz P, Pozo F, et al. 2010. Pulmonary aspergillosis in patients with chronic obstructive pulmonary disease: incidence, risk factors, and outcome. *Clin Microbiol Infect* 16: 870-7

Gurung S, Perocheau D, Touramanidou L, Baruteau J. 2021. The exosome journey: from biogenesis to uptake and intracellular signalling. *Cell Communication and Signaling* 19: 47

Hackam DJ, Rotstein OD, Grinstein S. 1999. Phagosomal acidification mechanisms and functional significance In *Advances in Cellular and Molecular Biology of Membranes and Organelles*, ed. S Gordon, pp. 299-319: JAI

Hakkim A, Fuchs TA, Martinez NE, Hess S, Prinz H, et al. 2011. Activation of the Raf-MEK-ERK pathway is required for neutrophil extracellular trap formation. *Nature Chemical Biology* 7: 75-77

Halder LD, Babych S, Palme DI, Mansouri-Ghahnavieh E, Ivanov L, et al. 2022. Candida albicans Induces Cross-Kingdom miRNA Trafficking in Human Monocytes To Promote Fungal Growth. *mBio* 13: e0356321

Halder LD, Jo EAH, Hasan MZ, Ferreira-Gomes M, Krüger T, et al. 2020. Immune modulation by complement receptor 3-dependent human monocyte TGF-β1-transporting vesicles. *Nat Commun* 11: 2331

Hammond EE, McDonald CS, Vestbo J, Denning DW. 2020. The global impact of Aspergillus infection on COPD. *BMC Pulm Med* 20: 241

Hasenberg M, Behnsen J, Krappmann S, Brakhage A, Gunzer M. 2011. Phagocyte responses towards Aspergillus fumigatus. *Int J Med Microbiol* 301: 436-44

Hazan-Eitan Z, Weinstein Y, Hadad N, Konforty A, Levy R. 2006. Induction of Fc gammaRIIA expression in myeloid PLB cells during differentiation depends on cytosolic phospholipase A2 activity and is regulated via activation of CREB by PGE2. *Blood* 108: 1758-66

Headland SE, Jones HR, Norling LV, Kim A, Souza PR, et al. 2015. Neutrophil-derived microvesicles enter cartilage and protect the joint in inflammatory arthritis. *Science translational medicine* 7: 315ra190-315ra190

Heijink IH, Vellenga E, Borger P, Postma DS, De Monchy JGR, Kauffman HF. 2002. Interleukin-6 promotes the production of interleukin-4 and interleukin-5 by interleukin-2-dependent and -independent mechanisms in freshly isolated human T cells. *Immunology* 107: 316-24

Heinekamp T, Thywissen A, Macheleidt J, Keller S, Valiante V, Brakhage A. 2013. Aspergillus fumigatus melanins: interference with the host endocytosis pathway and impact on virulence. *Frontiers in Microbiology* 3

Hellmann A-M, Lother J, Wurster S, Lutz MB, Schmitt AL, et al. 2017. Human and Murine Innate Immune Cell Populations Display Common and Distinct Response Patterns during Their In Vitro Interaction with the Pathogenic Mold Aspergillus fumigatus. *Frontiers in Immunology* 8

Hess C, Sadallah S, Hefti A, Landmann R, Schifferli JA. 1999. Ectosomes released by human neutrophils are specialized functional units. *J Immunol* 163: 4564-73

Hidalgo A, Chilvers ER, Summers C, Koenderman L. 2019. The Neutrophil Life Cycle. *Trends Immunol* 40: 584-97

Hohl TM. 2017. Immune responses to invasive aspergillosis: new understanding and therapeutic opportunities. *Curr Opin Infect Dis* 30: 364-71

Hong C-W. 2018. Extracellular Vesicles of Neutrophils. *Immune network* 18: e43-e43

Ibrahim-Granet O, Philippe B, Boleti H, Boisvieux-Ulrich E, Grenet D, et al. 2003. Phagocytosis and Intracellular Fate of Aspergillus fumigatus Conidia in Alveolar Macrophages. *Infection and Immunity* 71: 891-903

Iraci N, Gaude E, Leonardi T, Costa ASH, Cossetti C, et al. 2017. Extracellular vesicles are independent metabolic units with asparaginase activity. *Nat Chem Biol* 13: 951-55

Jahn B, Boukhallouk F, Lotz J, Langfelder K, Wanner G, Brakhage AA. 2000. Interaction of human phagocytes with pigmentless Aspergillus conidia. *Infection and immunity* 68: 3736-39

Jahn B, Koch A, Schmidt A, Wanner G, Gehringer H, et al. 1997. Isolation and characterization of a pigmentless-conidium mutant of Aspergillus fumigatus with altered conidial surface and reduced virulence. *Infect Immun* 65: 5110-7

Jahn B, Langfelder K, Schneider U, Schindel C, Brakhage AA. 2002. PKSP-dependent reduction of phagolysosome fusion and intracellular kill of Aspergillus fumigatus conidia by human monocyte-derived macrophages. *Cell Microbiol* 4: 793-803

Jankovičová J, Sečová P, Michalková K, Antalíková J. 2020. Tetraspanins, More than Markers of Extracellular Vesicles in Reproduction. *International journal of molecular sciences* 21: 7568

Jenks JD, Hoenigl M. 2018. Treatment of Aspergillosis. *J Fungi (Basel)* 4: 98

Jeong JS, Lee KB, Kim SR, Kim DI, Park HJ, et al. 2018. Airway epithelial phosphoinositide 3-kinase-δ contributes to the modulation of fungi-induced innate immune response. *Thorax* 73: 758

Johnson MD, Perfect JR. 2010. Use of Antifungal Combination Therapy: Agents, Order, and Timing. *Curr Fungal Infect Rep* 4: 87-95

Juvvadi PR. 2017. Balancing iron and calcium: Flavin carrier family proteins in Aspergillus fumigatus virulence. *Virulence* 8: 621-24

Kadota T, Fujita Y, Araya J, Watanabe N, Fujimoto S, et al. 2021. Human bronchial epithelial cell-derived extracellular vesicle therapy for pulmonary fibrosis via inhibition of TGF-β-WNT crosstalk. *J Extracell Vesicles* 10: e12124

Kalleda N, Amich J, Arslan B, Poreddy S, Mattenheimer K, et al. 2016. Dynamic Immune Cell Recruitment After Murine Pulmonary Aspergillus fumigatus Infection under Different Immunosuppressive Regimens. *Frontiers in Microbiology* 7

Kasahara S, Jhingran A, Dhingra S, Salem A, Cramer RA, Hohl TM. 2016. Role of Granulocyte-Macrophage Colony-Stimulating Factor Signaling in Regulating Neutrophil Antifungal Activity and the Oxidative Burst During Respiratory Fungal Challenge. *J Infect Dis* 213: 1289-98

Katschinski DM, Robins HI, Schad M, Frede S, Fandrey J. 1999. Role of tumor necrosis factor alpha in hyperthermia-induced apoptosis of human leukemia cells. *Cancer Res* 59: 3404-10

Keller NP. 2019. Fungal secondary metabolism: regulation, function and drug discovery. *Nat Rev Microbiol* 17: 167-80

Kerr SC, Fischer GJ, Sinha M, McCabe O, Palmer JM, et al. 2016. FleA Expression in Aspergillus fumigatus Is Recognized by Fucosylated Structures on Mucins and Macrophages to Prevent Lung Infection. *PLOS Pathogens* 12: e1005555

King J, Henriet SSV, Warris A. 2016. Aspergillosis in Chronic Granulomatous Disease. *J Fungi (Basel)* 2: 15

Klein J, Rello J, Dimopoulos G, Bulpa P, Blot K, et al. 2022. Invasive pulmonary aspergillosis in solid-organ transplant patients in the intensive care unit. *Transpl Infect Dis* 24: e13746

Knutsen AP, Slavin RG. 2011. Allergic bronchopulmonary aspergillosis in asthma and cystic fibrosis. *Clin Dev Immunol* 2011: 843763

Kolonics F, Kajdácsi E, Farkas VJ, Veres DS, Khamari D, et al. 2021. Neutrophils produce proinflammatory or anti-inflammatory extracellular vesicles depending on the environmental conditions. *Journal of leukocyte biology* 109: 793-806

Kwon-Chung KJ, Sugui JA. 2013. Aspergillus fumigatus—What Makes the Species a Ubiquitous Human Fungal Pathogen? *PLOS Pathogens* 9: e1003743

Lahoz-Beneytez J, Elemans M, Zhang Y, Ahmed R, Salam A, et al. 2016. Human neutrophil kinetics: modeling of stable isotope labeling data supports short blood neutrophil half-lives. *Blood* 127: 3431-8

Lai CP, Mardini O, Ericsson M, Prabhakar S, Maguire C, et al. 2014. Dynamic biodistribution of extracellular vesicles in vivo using a multimodal imaging reporter. *ACS Nano* 8: 483-94

Langfelder K, Jahn B, Gehringer H, Schmidt A, Wanner G, Brakhage AA. 1998. Identification of a polyketide synthase gene (pksP) of Aspergillus fumigatus involved in conidial pigment biosynthesis and virulence. *Med Microbiol Immunol* 187: 79-89

Langfelder K, Streibel M, Jahn B, Haase G, Brakhage AA. 2003. Biosynthesis of fungal melanins and their importance for human pathogenic fungi. *Fungal Genetics and Biology* 38: 143-58

Lass-Flörl C. 2019. How to make a fast diagnosis in invasive aspergillosis. *Medical Mycology* 57: S155-S60

Latgé J-P, Chamilos G. 2019. Aspergillus fumigatus and Aspergillosis in 2019. *Clinical Microbiology Reviews* 33: e00140-18

Latifkar A, Hur YH, Sanchez JC, Cerione RA, Antonyak MA. 2019. New insights into extracellular vesicle biogenesis and function. *J Cell Sci* 132

Lee MJ, Liu H, Barker BM, Snarr BD, Gravelat FN, et al. 2015. The Fungal Exopolysaccharide Galactosaminogalactan Mediates Virulence by Enhancing Resistance to Neutrophil Extracellular Traps. *PLOS Pathogens* 11: e1005187

Lehnert T, Prauße MTE, Hünniger K, Praetorius JP, Kurzai O, Figge MT. 2021. Comparative assessment of immune evasion mechanisms in human whole-blood infection assays by a systems biology approach. *PLoS One* 16: e0249372

Lehrer RI, Jan RG. 1970. Interaction of Aspergillus fumigatus Spores with Human Leukocytes and Serum. *Infection and Immunity* 1: 345-50

Lessing F, Kniemeyer O, Wozniok I, Loeffler J, Kurzai O, et al. 2007. The Aspergillus fumigatus Transcriptional Regulator AfYap1 Represents

the Major Regulator for Defense against Reactive Oxygen Intermediates but Is Dispensable for Pathogenicity in an Intranasal Mouse Infection Model. *Eukaryotic Cell* 6: 2290-302

Levitz SM, Farrell TP. 1990. Human neutrophil degranulation stimulated by Aspergillus fumigatus. *J Leukoc Biol* 47: 170-5

Lewis RE, Cahyame-Zuniga L, Leventakos K, Chamilos G, Ben-Ami R, et al. 2013. Epidemiology and sites of involvement of invasive fungal infections in patients with haematological malignancies: a 20-year autopsy study. *Mycoses* 56: 638-45

Lewis RE, Kontoyiannis DP. 2009. Invasive aspergillosis in glucocorticoid-treated patients. *Medical Mycology* 47: S271-S81

Li S-P, Lin Z-X, Jiang X-Y, Yu X-Y. 2018. Exosomal cargo-loading and synthetic exosome-mimics as potential therapeutic tools. *Acta pharmacologica Sinica* 39: 542-51

Li Y, Karlin A, Loike JD, Silverstein SC. 2002. A critical concentration of neutrophils is required for effective bacterial killing in suspension. *Proceedings of the National Academy of Sciences* 99: 8289-94

Liew PX, Kubes P. 2019. The Neutrophil's Role During Health and Disease. *Physiological Reviews* 99: 1223-48

Lin SJ, Schranz J, Teutsch SM. 2001. Aspergillosis case-fatality rate: systematic review of the literature. *Clin Infect Dis* 32: 358-66

Lionakis MS, Kontoyiannis DP. 2003. Glucocorticoids and invasive fungal infections. *Lancet* 362: 1828-38

Little JS, Weiss ZF, Hammond SP. 2021. Invasive Fungal Infections and Targeted Therapies in Hematological Malignancies. *J Fungi (Basel)* 7: 1058

Liu H, Lee MJ, Solis NV, Phan QT, Swidergall M, et al. 2016. Aspergillus fumigatus CalA binds to integrin α5β1 and mediates host cell invasion. *Nature Microbiology* 2: 16211

Lőrincz Á M, Schütte M, Timár CI, Veres DS, Kittel Á, et al. 2015. Functionally and morphologically distinct populations of extracellular vesicles produced by human neutrophilic granulocytes. *J Leukoc Biol* 98: 583-9

Luther K, Torosantucci A, Brakhage AA, Heesemann J, Ebel F. 2007. Phagocytosis of Aspergillus fumigatus conidia by murine macrophages involves recognition by the dectin-1 beta-glucan receptor and Toll-like receptor 2. *Cell Microbiol* 9: 368-81

Ma YJ, Doni A, Hummelshøj T, Honoré C, Bastone A, et al. 2009. Synergy between Ficolin-2 and Pentraxin 3 Boosts Innate Immune Recognition and Complement Deposition*. *Journal of Biological Chemistry* 284: 28263-75

Mah J-H, Yu J-H. 2006. Upstream and Downstream Regulation of Asexual Development in Aspergillus fumigatus. *Eukaryotic Cell* 5: 1585-95

Máiz L, Vendrell M, Olveira C, Girón R, Nieto R, Martínez-García MA. 2015. Prevalence and Factors Associated with Isolation of Aspergillus and Candida from Sputum in Patients with Non-Cystic Fibrosis Bronchiectasis. *Respiration* 89: 396-403

Mambula SS, Sau K, Henneke P, Golenbock DT, Levitz SM. 2002. Toll-like receptor (TLR) signaling in response to Aspergillus fumigatus. *J Biol Chem* 277: 39320-6

Manley HR, Keightley MC, Lieschke GJ. 2018. The Neutrophil Nucleus: An Important Influence on Neutrophil Migration and Function. *Frontiers in immunology* 9: 2867-67

Marciano BE, Spalding C, Fitzgerald A, Mann D, Brown T, et al. 2015. Common

severe infections in chronic granulomatous disease. *Clin Infect Dis* 60: 1176-83

Marin-Esteban V, Turbica I, Dufour G, Semiramoth N, Gleizes A, et al. 2012. Afa/Dr Diffusely Adhering Escherichia coli Strain C1845 Induces Neutrophil Extracellular Traps That Kill Bacteria and Damage Human Enterocyte-Like Cells. *Infection and Immunity* 80: 1891-99

Marr KA, Balajee SA, Hawn TR, Ozinsky A, Pham U, et al. 2003. Differential role of MyD88 in macrophage-mediated responses to opportunistic fungal pathogens. *Infection and immunity* 71: 5280-86

Mayadas TN, Cullere X, Lowell CA. 2014. The multifaceted functions of neutrophils. *Annu Rev Pathol* 9: 181-218

Mayer AK, Muehmer M, Mages J, Gueinzius K, Hess C, et al. 2007. Differential Recognition of TLR-Dependent Microbial Ligands in Human Bronchial Epithelial Cells. *The Journal of Immunology* 178: 3134

McCormick A, Heesemann L, Wagener J, Marcos V, Hartl D, et al. 2010. NETs formed by human neutrophils inhibit growth of the pathogenic mold Aspergillus fumigatus. *Microbes Infect* 12: 928-36

Mehrad B, Strieter RM, Moore TA, Tsai WC, Lira SA, Standiford TJ. 1999. CXC chemokine receptor-2 ligands are necessary components of neutrophil-mediated host defense in invasive pulmonary aspergillosis. *J Immunol* 163: 6086-94

Meier A, Kirschning CJ, Nikolaus T, Wagner H, Heesemann J, Ebel F. 2003. Toll-like receptor (TLR) 2 and TLR4 are essential for Aspergillus-induced activation of murine macrophages. *Cellular Microbiology* 5: 561-70

Midekessa G, Godakumara K, Ord J, Viil J, Lättekivi F, et al. 2020. Zeta Potential of Extracellular Vesicles: Toward Understanding the Attributes that Determine Colloidal Stability. *ACS omega* 5: 16701-10

Mir B, Goettsch C. 2020. Extracellular Vesicles as Delivery Vehicles of Specific Cellular Cargo. *Cells* 9: 1601

Misslinger M, Hortschansky P, Brakhage AA, Haas H. 2021. Fungal iron homeostasis with a focus on Aspergillus fumigatus. *Biochimica et Biophysica Acta (BBA) - Molecular Cell Research* 1868: 118885

Moalli F, Doni A, Deban L, Zelante T, Zagarella S, et al. 2010. Role of complement and Fc{gamma} receptors in the protective activity of the long pentraxin PTX3 against Aspergillus fumigatus. *Blood* 116: 5170-80

Mortensen KL, Johansen HK, Fuursted K, Knudsen JD, Gahrn-Hansen B, et al. 2011. A prospective survey of Aspergillus spp. in respiratory tract samples: prevalence, clinical impact and antifungal susceptibility. *European Journal of Clinical Microbiology & Infectious Diseases* 30: 1355

Mutua V, Gershwin LJ. 2021. A Review of Neutrophil Extracellular Traps (NETs) in Disease: Potential Anti-NETs Therapeutics. *Clinical reviews in allergy & immunology* 61: 194-211

Nayak A, Pednekar L, Reid KB, Kishore U. 2012. Complement and non-complement activating functions of C1q: a prototypical innate immune molecule. *Innate Immun* 18: 350-63

Nederveen JP, Warnier G, Di Carlo A, Nilsson MI, Tarnopolsky MA. 2021. Extracellular Vesicles and Exosomes: Insights From Exercise Science. *Front Physiol* 11

Netea MG, Warris A, Van der Meer JW, Fenton MJ, Verver-Janssen TJ, et al. 2003. Aspergillus fumigatus evades immune recognition during germination through loss of toll-like receptor-4-mediated signal transduction. *J Infect Dis*

188: 320-6

Netzker T, Flak M, Krespach MK, Stroe MC, Weber J, et al. 2018. Microbial interactions trigger the production of antibiotics. *Curr Opin Microbiol* 45: 117-23

Neupane AS, Willson M, Chojnacki AK, Vargas E Silva Castanheira F, Morehouse C, et al. 2020. Patrolling Alveolar Macrophages Conceal Bacteria from the Immune System to Maintain Homeostasis. *Cell* 183: 110-25.e11

O'Donnell MR, Schmidt GM, Tegtmeier BR, Faucett C, Fahey JL, et al. 1994. Prediction of systemic fungal infection in allogeneic marrow recipients: impact of amphotericin prophylaxis in high-risk patients. *J Clin Oncol* 12: 827-34

O'Gorman CM. 2011. Airborne Aspergillus fumigatus conidia: a risk factor for aspergillosis. *Fungal Biology Reviews* 25: 151-57

O'Gorman CM, Fuller HT, Dyer PS. 2009. Discovery of a sexual cycle in the opportunistic fungal pathogen Aspergillus fumigatus. *Nature* 457: 471-74

Oosthuizen JL, Gomez P, Ruan J, Hackett TL, Moore MM, et al. 2011. Dual organism transcriptomics of airway epithelial cells interacting with conidia of Aspergillus fumigatus. *PLoS One* 6: e20527

Oremland M, Michels KR, Bettina AM, Lawrence C, Mehrad B, Laubenbacher R. 2016. A computational model of invasive aspergillosis in the lung and the role of iron. *BMC Syst Biol* 10: 34

Ortiz SC, Pennington K, Thomson DD, Bertuzzi M. 2022. Novel Insights into Aspergillus fumigatus Pathogenesis and Host Response from State-of-the-Art Imaging of Host-Pathogen Interactions during Infection. *J Fungi (Basel)* 8

Osherov N. 2012. Interaction of the pathogenic mold Aspergillus fumigatus with lung epithelial cells. *Frontiers in Microbiology* 3

Øya E, Becher R, Ekeren L, Afanou AKJ, Øvrevik J, Holme JA. 2019. Pro-Inflammatory Responses in Human Bronchial Epithelial Cells Induced by Spores and Hyphal Fragments of Common Damp Indoor Molds. *Int J Environ Res Public Health* 16

Paoletti M, Rydholm C, Schwier EU, Anderson MJ, Szakacs G, et al. 2005. Evidence for sexuality in the opportunistic fungal pathogen Aspergillus fumigatus. *Curr Biol* 15: 1242-8

Parente R, Doni A, Bottazzi B, Garlanda C, Inforzato A. 2020. The complement system in Aspergillus fumigatus infections and its crosstalk with pentraxins. *FEBS Lett* 594: 2480-501

Paris S, Debeaupuis J-P, Crameri R, Carey M, Charlès F, et al. 2003. Conidial hydrophobins of Aspergillus fumigatus. *Appl Environ Microbiol* 69: 1581-88

Pérez-Cantero A, López-Fernández L, Guarro J, Capilla J. 2020. Azole resistance mechanisms in Aspergillus: update and recent advances. *International Journal of Antimicrobial Agents* 55: 105807

Perez-Cuesta U, Guruceaga X, Cendon-Sanchez S, Pelegri-Martinez E, Hernando FL, et al. 2021. Nitrogen, Iron, and Zinc Acquisition: Key Nutrients to Aspergillus fumigatus Virulence. *Journal of Fungi* 7: 518

Perfect JR, Cox GM, Lee JY, Kauffman CA, de Repentigny L, et al. 2001. The Impact of Culture Isolation of Aspergillus Species: A Hospital-Based Survey of Aspergillosis. *Clinical Infectious Diseases* 33: 1824-33

Phadke AP, Mehrad B. 2005. Cytokines in host defense against Aspergillus: recent advances. *Medical Mycology* 43: S173-S76

Philippe B, Ibrahim-Granet O, Prévost MC, Gougerot-Pocidalo MA, Sanchez Perez M, et al. 2003. Killing of Aspergillus fumigatus by alveolar macrophages is

mediated by reactive oxidant intermediates. *Infection and immunity* 71: 3034-42

Pihet M, Vandeputte P, Tronchin G, Renier G, Saulnier P, et al. 2009. Melanin is an essential component for the integrity of the cell wall of Aspergillus fumigatus conidia. *BMC Microbiology* 9: 177

Pitanga TN, de Aragão França L, Rocha VCJ, Meirelles T, Borges VM, et al. 2014. Neutrophil-derived microparticles induce myeloperoxidase-mediated damage of vascular endothelial cells. *BMC cell biology* 15: 21-21

Pivot-Pajot C, Chouinard FC, Amine El Azreq M, Harbour D, Bourgoin SG. 2010. Characterisation of degranulation and phagocytic capacity of a human neutrophilic cellular model, PLB-985 cells. *Immunobiology* 215: 38-52

Pollock JD, Williams DA, Gifford MA, Li LL, Du X, et al. 1995. Mouse model of X-linked chronic granulomatous disease, an inherited defect in phagocyte superoxide production. *Nat Genet* 9: 202-9

Post MJ, Lass-Floerl C, Gastl G, Nachbaur D. 2007. Invasive fungal infections in allogeneic and autologous stem cell transplant recipients: a single-center study of 166 transplanted patients. *Transplant Infectious Disease* 9: 189-95

Prüfer S, Weber M, Stein P, Bosmann M, Stassen M, et al. 2014. Oxidative burst and neutrophil elastase contribute to clearance of Aspergillus fumigatus pneumonia in mice. *Immunobiology* 219: 87-96

Radomski N, Karger A, Franzke K, Liebler-Tenorio E, Jahnke R, et al. 2019. Chlamydia psittaci-Infected Dendritic Cells Communicate with NK Cells via Exosomes To Activate Antibacterial Immunity. *Infect Immun* 88

Raffa N, Keller NP. 2019. A call to arms: Mustering secondary metabolites for success and survival of an opportunistic pathogen. *PLOS Pathogens* 15: e1007606

Rafiq M, Rivieccio F, Zimmermann A-K, Visser C, Bruch A, et al. 2022. PLB-985 Neutrophil-Like Cells as a Model To Study Aspergillus fumigatus Pathogenesis. *mSphere* 7: e00940-21

Ralph BA, Lehoux M, Ostapska H, Snarr BD, Caffrey-Carr AK, et al. 2021. The IL-1 Receptor Is Required to Maintain Neutrophil Viability and Function During Aspergillus fumigatus Airway Infection. *Frontiers in Immunology* 12

Raposo G, Stoorvogel W. 2013. Extracellular vesicles: exosomes, microvesicles, and friends. *J Cell Biol* 200: 373-83

Remijsen Q, Vanden Berghe T, Wirawan E, Asselbergh B, Parthoens E, et al. 2011. Neutrophil extracellular trap cell death requires both autophagy and superoxide generation. *Cell research* 21: 290-304

Richard N, Marti L, Varrot A, Guillot L, Guitard J, et al. 2018. Human Bronchial Epithelial Cells Inhibit Aspergillus fumigatus Germination of Extracellular Conidia via FleA Recognition. *Scientific Reports* 8: 15699

Rincón E, Rocha-Gregg BL, Collins SR. 2018. A map of gene expression in neutrophil-like cell lines. *BMC Genomics* 19: 573

Robinet P, Baychelier F, Fontaine T, Picard C, Debré P, et al. 2014. A Polysaccharide Virulence Factor of a Human Fungal Pathogen Induces Neutrophil Apoptosis via NK Cells. *The Journal of Immunology* 192: 5332

Rogacheva YA, Markelov VV, Popova MO, Volkova AG, Nikolaev IY, et al. 2021. Invasive Aspergillosis in Allogeneic Hematopoietic Stem Cell Transplantation Recipients: A Large Cohort Single-Center Study. *Blood* 138: 1801

Röhm M, Grimm MJ, D'Auria AC, Almyroudis NG, Segal BH, Urban CF. 2014. NADPH oxidase promotes neutrophil extracellular trap formation in

pulmonary aspergillosis. *Infection and immunity* 82: 1766-77

Romani L. 2011. Immunity to fungal infections. *Nature Reviews Immunology* 11: 275-88

Rosales C. 2018. Neutrophil: A Cell with Many Roles in Inflammation or Several Cell Types? *Front Physiol* 9: 113-13

Rosbjerg A, Genster N, Pilely K, Skjoedt M-O, Stahl GL, Garred P. 2016. Complementary Roles of the Classical and Lectin Complement Pathways in the Defense against Aspergillus fumigatus. *Frontiers in Immunology* 7

Rossaint J, Kühne K, Skupski J, Van Aken H, Looney MR, et al. 2016. Directed transport of neutrophil-derived extracellular vesicles enables platelet-mediated innate immune response. *Nat Commun* 7: 13464

Rowat AC, Jaalouk DE, Zwerger M, Ung WL, Eydelnant IA, et al. 2013. Nuclear envelope composition determines the ability of neutrophil-type cells to passage through micron-scale constrictions. *J Biol Chem* 288: 8610-18

Saïd-Sadier N, Padilla E, Langsley G, Ojcius DM. 2010. Aspergillus fumigatus stimulates the NLRP3 inflammasome through a pathway requiring ROS production and the Syk tyrosine kinase. *PloS one* 5: e10008-e08

Sainz J, Lupiáñez CB, Segura-Catena J, Vazquez L, Ríos R, et al. 2012. Dectin-1 and DC-SIGN polymorphisms associated with invasive pulmonary Aspergillosis infection. *PLoS One* 7: e32273

Schieler BM, Soni MV, Brown CM, Coolen MJL, Fredricks H, et al. 2019. Nitric oxide production and antioxidant function during viral infection of the coccolithophore Emiliania huxleyi. *The ISME Journal* 13: 1019-31

Schmidt F, Thywißen A, Goldmann M, Cunha C, Cseresnyés Z, et al. 2020. Flotillin-Dependent Membrane Microdomains Are Required for Functional Phagolysosomes against Fungal Infections. *Cell Rep* 32: 108017

Schmidt H, Vlaic S, Krüger T, Schmidt F, Balkenhol J, et al. 2018. Proteomics of Aspergillus fumigatus Conidia-containing Phagolysosomes Identifies Processes Governing Immune Evasion*. *Molecular & Cellular Proteomics* 17: 1084-96

Schnoor M, Vadillo E, Guerrero-Fonseca IM. 2021. The extravasation cascade revisited from a neutrophil perspective. *Current Opinion in Physiology* 19: 119-28

Schoen TJ, Rosowski EE, Knox BP, Bennin D, Keller NP, Huttenlocher A. 2019. Neutrophil phagocyte oxidase activity controls invasive fungal growth and inflammation in zebrafish. *J Cell Sci* 133

Schrettl M, Kim HS, Eisendle M, Kragl C, Nierman WC, et al. 2008. SreA-mediated iron regulation in Aspergillus fumigatus. *Mol Microbiol* 70: 27-43

Sha Q, Truong-Tran AQ, Plitt JR, Beck LA, Schleimer RP. 2004. Activation of Airway Epithelial Cells by Toll-Like Receptor Agonists. *American Journal of Respiratory Cell and Molecular Biology* 31: 358-64

Shamseddine AA, Airola MV, Hannun YA. 2015. Roles and regulation of neutral sphingomyelinase-2 in cellular and pathological processes. *Advances in Biological Regulation* 57: 24-41

Sheshachalam A, Srivastava N, Mitchell T, Lacy P, Eitzen G. 2014. Granule Protein Processing and Regulated Secretion in Neutrophils. *Frontiers in Immunology* 5

Shi J, Gilbert GE, Kokubo Y, Ohashi T. 2001. Role of the liver in regulating numbers of circulating neutrophils. *Blood* 98: 1226-30

Shin SH, Lee YH, Jeon CH. 2006. Protease-dependent activation of nasal polyp epithelial cells by airborne fungi leads to migration of eosinophils and

neutrophils. *Acta Otolaryngol* 126: 1286-94

Shlezinger N, Hohl TM, Mitchell AP. 2021. Mitochondrial Reactive Oxygen Species Enhance Alveolar Macrophage Activity against Aspergillus fumigatus but Are Dispensable for Host Protection. *mSphere* 6: e00260-21

Shopova IA, Belyaev I, Dasari P, Jahreis S, Stroe MC, et al. 2020. Human Neutrophils Produce Antifungal Extracellular Vesicles against Aspergillus fumigatus. *mBio* 11

Simpson RJ, Kalra H, Mathivanan S. 2012. ExoCarta as a resource for exosomal research. *J Extracell Vesicles* 1

Slesiona S, Gressler M, Mihlan M, Zaehle C, Schaller M, et al. 2012. Persistence versus Escape: Aspergillus terreus and Aspergillus fumigatus Employ Different Strategies during Interactions with Macrophages. *PLOS ONE* 7: e31223

Smith TM, Richie DL, Tao J. 2016. A Fluorescence-Based High-Throughput Screening Assay to Identify Growth Inhibitors of the Pathogenic Fungus Aspergillus fumigatus. *Methods Mol Biol* 1439: 171-9

Speth C, Rambach G, Lass-Flörl C, Howell PL, Sheppard DC. 2019. Galactosaminogalactan (GAG) and its multiple roles in Aspergillus pathogenesis. *Virulence* 10: 976-83

Steele C, Rapaka RR, Metz A, Pop SM, Williams DL, et al. 2005. The Beta-Glucan Receptor Dectin-1 Recognizes Specific Morphologies of Aspergillus fumigatus. *PLOS Pathogens* 1: e42

Stein JM, Luzio JP. 1991. Ectocytosis caused by sublytic autologous complement attack on human neutrophils. The sorting of endogenous plasma-membrane proteins and lipids into shed vesicles. *Biochem J* 274 (Pt 2): 381-6

Steinberg G. 2014. Endocytosis and early endosome motility in filamentous fungi. *Current Opinion in Microbiology* 20: 10-18

Sugui JA, Losada L, Wang W, Varga J, Ngamskulrungroj P, et al. 2011. Identification and Characterization of an Aspergillus fumigatus “Supermater” Pair. *mBio* 2: e00234-11

Sun WK, Lu X, Li X, Sun QY, Su X, et al. 2012. Dectin-1 is inducible and plays a crucial role in Aspergillus-induced innate immune responses in human bronchial epithelial cells. *European Journal of Clinical Microbiology & Infectious Diseases* 31: 2755-64

Svirshchevskaya EV, Shevchenko MA, Huet D, Femenia F, Latgé JP, et al. 2009. Susceptibility of mice to invasive aspergillosis correlates with delayed cell influx into the lungs. *Int J Immunogenet* 36: 289-99

Szabady R, McCormick B. 2013. Control of Neutrophil Inflammation at Mucosal Surfaces by Secreted Epithelial Products. *Frontiers in Immunology* 4

Szeifert V, Kolonics F, Bartos B, Khamari D, Vági P, et al. 2021. Mac-1 Receptor Clustering Initiates Production of Pro-Inflammatory, Antibacterial Extracellular Vesicles From Neutrophils. *Front Immunol* 12: 671995

Tanaka RJ, Boon NJ, Vrcelj K, Nguyen A, Vinci C, et al. 2015. In silico modeling of spore inhalation reveals fungal persistence following low dose exposure. *Sci Rep* 5: 13958

Tansey MR, Brock TD. 1972. The Upper Temperature Limit for Eukaryotic Organisms. *Proceedings of the National Academy of Sciences* 69: 2426-28

Taylor J, Azimi I, Monteith G, Bebawy M. 2020. Ca(2+) mediates extracellular vesicle biogenesis through alternate pathways in malignancy. *Journal of extracellular vesicles* 9: 1734326-26

Tekaia F, Latgé JP. 2005. Aspergillus fumigatus: saprophyte or pathogen? *Curr Opin*

Microbiol 8: 385-92

Thywißen A, Heinekamp T, Dahse H-M, Schmaler-Ripcke J, Nietsche S, et al. 2011. Conidial Dihydroxynaphthalene Melanin of the Human Pathogenic Fungus Aspergillus fumigatus Interferes with the Host Endocytosis Pathway. *Frontiers in Microbiology* 2

Timár CI, Lőrincz ÁM, Csépányi-Kömi R, Vályi-Nagy A, Nagy G, et al. 2013. Antibacterial effect of microvesicles released from human neutrophilic granulocytes. *Blood* 121: 510-18

Tomee JF, Wierenga AT, Hiemstra PS, Kauffman HK. 1997. Proteases from Aspergillus fumigatus induce release of proinflammatory cytokines and cell detachment in airway epithelial cell lines. *J Infect Dis* 176: 300-3

Tricarico C, Clancy J, D'Souza-Schorey C. 2017. Biology and biogenesis of shed microvesicles. *Small GTPases* 8: 220-32

Tsai HF, Chang YC, Washburn RG, Wheeler MH, Kwon-Chung KJ. 1998. The developmentally regulated alb1 gene of Aspergillus fumigatus: its role in modulation of conidial morphology and virulence. *J Bacteriol* 180: 3031-8

Tucker KA, Lilly MB, Heck L, Jr., Rado TA. 1987. Characterization of a new human diploid myeloid leukemia cell line (PLB-985) with granulocytic and monocytic differentiating capacity. *Blood* 70: 372-8

Tverdek FP, Kofteridis D, Kontoyiannis DP. 2016. Antifungal agents and liver toxicity: a complex interaction. *Expert Rev Anti Infect Ther* 14: 765-76

Ullmann AJ, Aguado JM, Arikan-Akdagli S, Denning DW, Groll AH, et al. 2018. Diagnosis and management of Aspergillus diseases: executive summary of the 2017 ESCMID-ECMM-ERS guideline. *Clinical Microbiology and Infection* 24: e1-e38

Valsecchi I, Dupres V, Stephen-Victor E, Guijarro JI, Gibbons J, et al. 2017. Role of Hydrophobins in Aspergillus fumigatus. *J Fungi (Basel)* 4: 2

van Bruggen R, Drewniak A, Jansen M, van Houdt M, Roos D, et al. 2009. Complement receptor 3, not Dectin-1, is the major receptor on human neutrophils for beta-glucan-bearing particles. *Mol Immunol* 47: 575-81

van de Veerdonk FL, Gresnigt MS, Romani L, Netea MG, Latgé J-P. 2017. Aspergillus fumigatus morphology and dynamic host interactions. *Nature Reviews Microbiology* 15: 661-74

van Niel G, Charrin S, Simoes S, Romao M, Rochin L, et al. 2011. The Tetraspanin CD63 Regulates ESCRT-Independent and -Dependent Endosomal Sorting during Melanogenesis. *Developmental Cell* 21: 708-21

Venkatraman Girija U, Gingras AR, Marshall JE, Panchal R, Sheikh MA, et al. 2013. Structural basis of the C1q/C1s interaction and its central role in assembly of the C1 complex of complement activation. *Proc Natl Acad Sci U S A* 110: 13916-20

von Vietinghoff S, Ley K. 2008. Homeostatic regulation of blood neutrophil counts. *J Immunol* 181: 5183-8

Wang J, Wang Y, Tang L, Garcia RC. 2019. Extracellular Vesicles in Mycobacterial Infections: Their Potential as Molecule Transfer Vectors. *Frontiers in Immunology* 10

Weidner G, d'Enfert C, Koch A, Mol PC, Brakhage AA. 1998. Development of a homologous transformation system for the human pathogenic fungus Aspergillus fumigatus based on the pyrG gene encoding orotidine 5'-monophosphate decarboxylase. *Curr Genet* 33: 378-85

Werner JL, Metz AE, Horn D, Schoeb TR, Hewitt MM, et al. 2009. Requisite role for the dectin-1 beta-glucan receptor in pulmonary defense against Aspergillus

fumigatus. *J Immunol* 182: 4938-46

Westman J, Grinstein S. 2021. Determinants of Phagosomal pH During Host-Pathogen Interactions. *Frontiers in Cell and Developmental Biology* 8

Williams C, Rajendran RK, Ramage G. 2016. Aspergillus Biofilms in Human Disease. *Advances in experimental medicine and biology* 931: 1-11

Yang E, Wang X, Gong Z, Yu M, Wu H, Zhang D. 2020. Exosome-mediated metabolic reprogramming: the emerging role in tumor microenvironment remodeling and its influence on cancer progression. *Signal Transduction and Targeted Therapy* 5: 242

Yasui T, Paisrisarn P, Yanagida T, Konakade Y, Nakamura Y, et al. 2021. Molecular profiling of extracellular vesicles via charge-based capture using oxide nanowire microfluidics. *Biosensors and Bioelectronics* 194: 113589

Yokoi A, Ochiya T. 2021. Exosomes and extracellular vesicles: Rethinking the essential values in cancer biology. *Seminars in Cancer Biology* 74: 79-91

Youngchim S, Morris-Jones R, Hay RJ, Hamilton AJ. 2004. Production of melanin by Aspergillus fumigatus. *Journal of Medical Microbiology* 53: 175-81

Zarember KA, Sugui JA, Chang YC, Kwon-Chung KJ, Gallin JI. 2007. Human polymorphonuclear leukocytes inhibit Aspergillus fumigatus conidial growth by lactoferrin-mediated iron depletion. *J Immunol* 178: 6367-73

Zeuthen CM, Shahrokhtash A, Fromell K, Ekdahl KN, Mohammad-Beigi H, Sutherland DS. 2020. C1q recognizes antigen-bound IgG in a curvature-dependent manner. *Nano Research* 13: 1651-58

Zhang J, Debets AJM, Verweij PE, Snelders E. 2021. Azole-Resistance Development; How the Aspergillus fumigatus Lifecycle Defines the Potential for Adaptation. *Journal of Fungi* 7: 599

6. Appendix

6.1 Additional results

6.2 Characterization of EVs derived from bronchial epithelial cells

Bronchial epithelial cells (BECs) were shown to interact with *A. fumigatus* by binding the FleA lectin on the surface of resting conidia, which leads to secretion of IL-8 and inhibition of conidial germination. However, the main signal inducing their full engagement in pro-inflammatory responses seems to be the beta 1-3 glucan exposed on swollen conidia. Furthermore, reactive oxygen species (ROS) and antimicrobial peptides like cathepsin D or N-acetyl-β-d-glucosaminidase were found in the secretome of BECs, after long incubation times with the fungus. These findings hint that epithelial cells may serve additional important roles beyond just providing a barrier function during *Aspergillus* infections. It was also observed that airway epithelial cells respond to toxins, stressors, and pathogens by secreting extracellular vesicles (EVs). In particular, the function of BECs-derived EVs in different contexts, *e.g.* during viral infection or chronic obstructive pulmonary disease (COPD) was shown to be important for the outcome of these pathologic conditions. Hence, we hypothesized that EVs derived from BECs after confrontation with *A. fumigatus* conidia might also exert a specific function during aspergillosis infections.

6.2.1 Bronchial epithelial cells do not alter EVs production after infection.

To test whether fungal infection causes an increased release of EVs in epithelial cells, BEAS-2B cells were infected for 24 hours with *A. fumigatus* CEA17 (FGSC 1152) carrying a point mutation in the *pyrG* gene or its derivative *A. fumigatus* CEA17 Δ*pksP*. Comparing the number and size distribution of EVs using NTA analysis between uninfected BEAS-2B cells and cells infected with *pyrG* wild-type (WT) conidia or a Δ*pksP* mutant, we saw that only the mutant was able to lead to a slightly increase in production of EVs, while the number was completely unchanged after confrontation with the WT (**Figure 7A**). The size distribution remained similar among all the samples with a peak around 150 nm (**Figure 7A**). To visualize the EVs, we performed cryo-transmission electron microscopy (cryo-TEM) imaging, which confirmed the exclusive presence in our samples of small vesicles surrounded by a single lipid bilayer (**Figure 7B**).

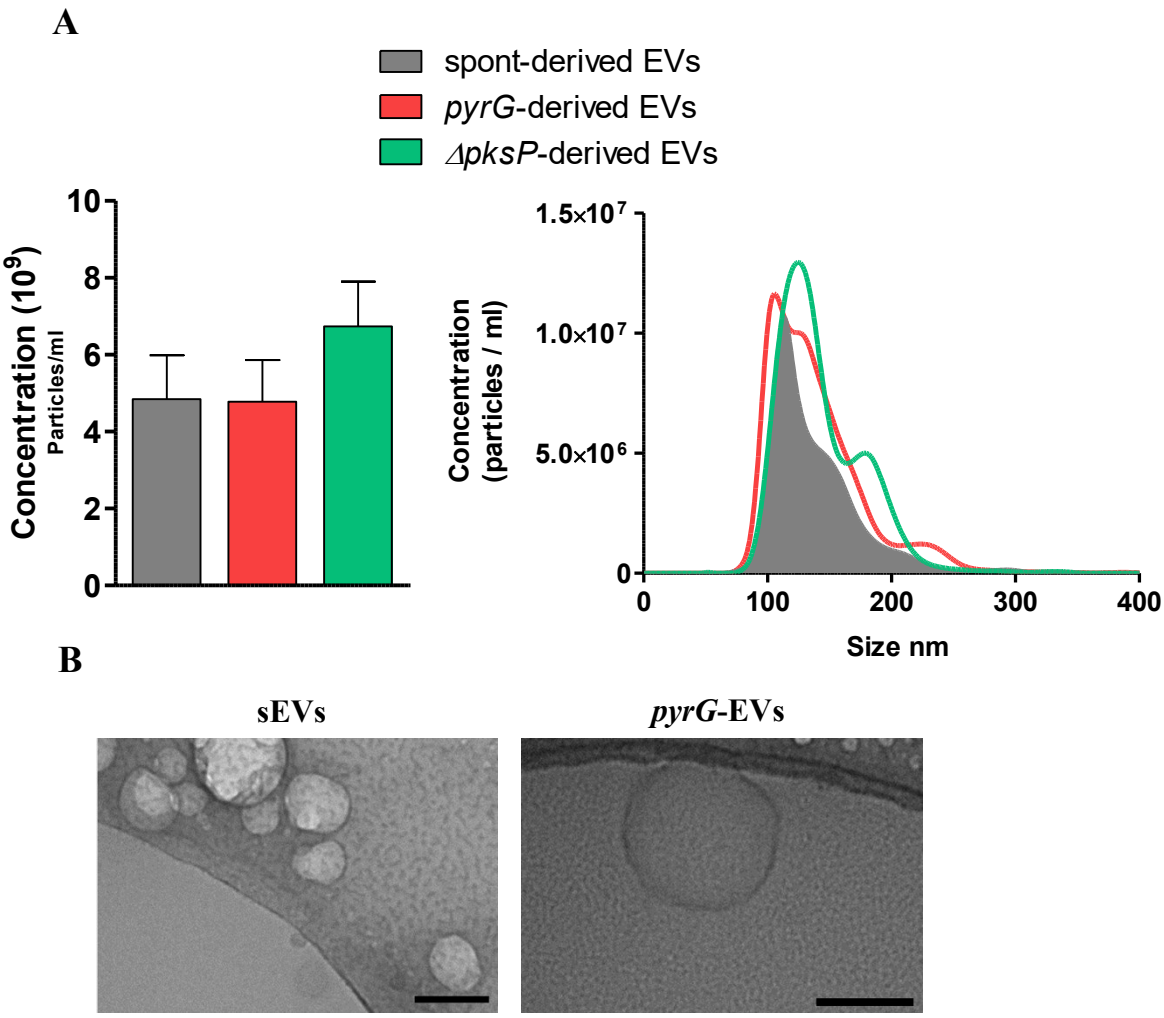

Figure 7 Concentration and size distribution of BEAS-2B cell-derived EVs.

(A) NTA analysis showing number and size distribution of extracellular vesicles released spontaneously or after infection with *pyrG*-WT or Δ*pksP* conidia, from BEAS-2B cells after 24 h. **(B)** Cryo-TEM showing spontaneously or infection-derived EVs from BEAS-2B cells. Scale bar 100 nm.

6.2.2 Proteomic analyses show changes in the EV cargo only in the *ΔpksP*-derived EVs.

To assess the protein cargo of these different EVs subsets LC-MS/MS analysis using label-free quantification was performed. Lipopolysaccharide (LPS)-induced EVs from BEAS-2B cells were included as a positive control for a pro-inflammatory state in these cells. A total of 464 proteins were detected, with 184 proteins shared between

all the samples **(Figure 8A)**. Surprisingly, the EVs derived from Δ*pksP*-infected BECs contained 160 unique proteins. Investigation of their annotated functions revealed that they were mostly involved in intercellular transport, cellular component biogenesis, and metabolic processes (**Figure 8B**). This highly active metabolic state of the cells led us to hypothesize that BECs might phagocytose conidia of the pigmentless Δ*pksP* strain better than of the WT strain. Hence, their phagocytosis capacity when confronted with the two different strains using image-based flow cytometry was tested with an ImageStream system. However, this analysis revealed that the melanized WT conidia are significantly more phagocytosed than the Δ*pksP* ones, so phagocytosis is not the factor inducing the BECs metabolic activation (**Figure 8C**).

A

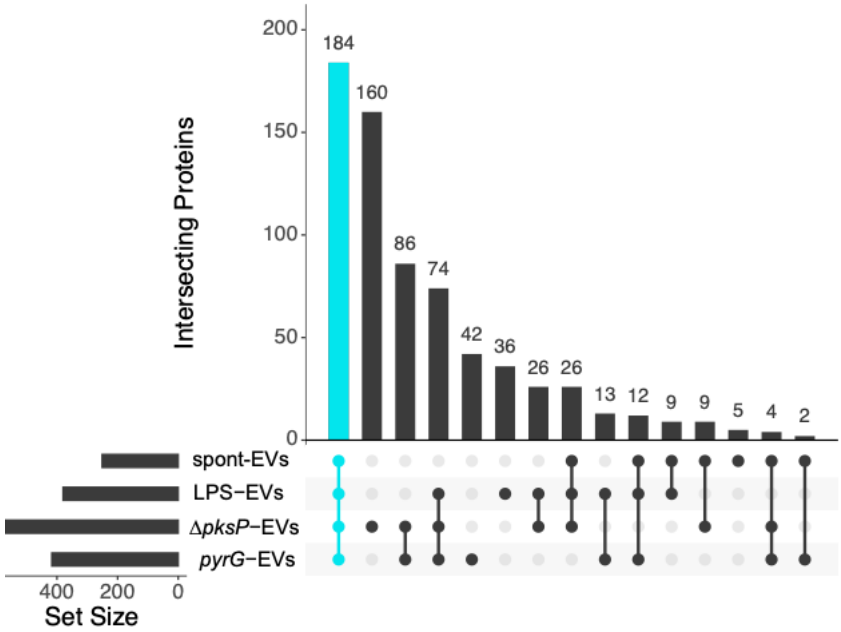

B

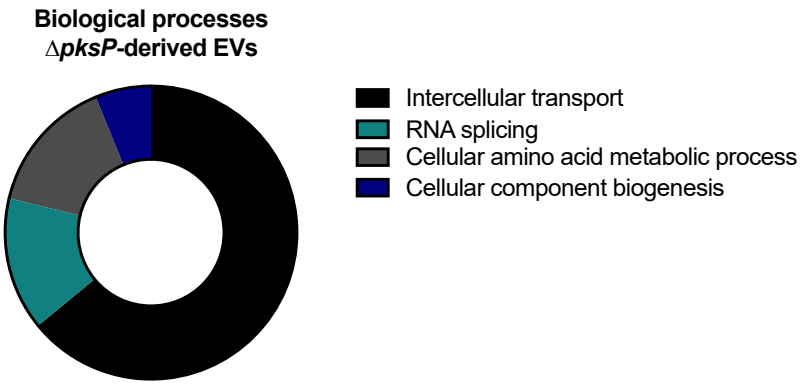

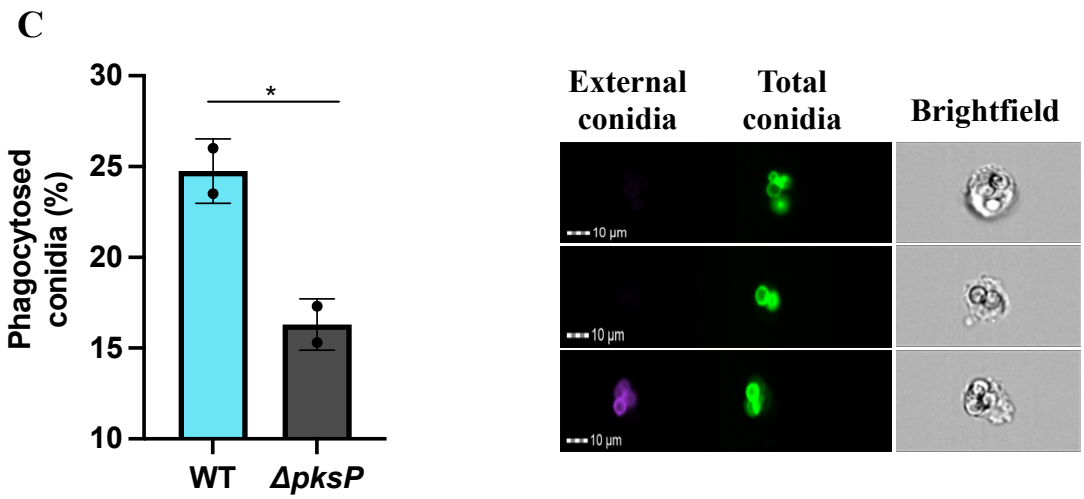

Figure 8 Proteomic analysis on different subsets of EVs.

(A) UpSetR plot displaying the proteins identified in spontaneously released extracellular vesicles (sEVs) and *pyrG*- or Δ*pksP* infection-derived extracellular vesicles (*pyrG*-EVs/Δ*pksP*-EVs) and LPS-induced EVs (LPS-EVs), from at least two replicates of a given sample. The light blue bar indicates proteins that were found in all four samples. **(B)** Gene ontology analysis of the biological processes in which the proteins found uniquely in the Δ*pksP*-derived EVs, are involved. **(C)** Quantification of either wild-type (WT) or Δ*pksP* conidia phagocytosis from BEAS-2B cells using the IDEAS software on 5,000 cells per condition. Values are means plus standard errors of the means (SEM) (error bars) of two independent experiments. Representative images of phagocytosed FITC-stained conidia (green) and external CFW-stained (purple) conidia.

6.2.3 *PyrG*-induced EVs promote IL-6 secretion from unstimulated BECs

Epithelial cells are known to secrete pro-inflammatory cytokines in response to fungal pathogens, likely to recruit or activate neighboring cells. For this reason, the ability of EVs derived from BEAS-2B cells infected with conidia of the WT or Δ*pksP* strain to induce the release of two proinflammatory cytokines, IL-6 and IL-8, from naïve BEAS-2B cells, was tested. This assay showed that only EVs derived from cells infected with WT conidia induced secretion of IL-6 and IL-8 from naïve BEAS-2B cells (**Figure 9A**). Of note, one of the proteins found exclusively in WT-derived EVs

was Disintegrin and Metalloproteinase (ADAM) 10, which is known to induce IL-6 receptor shedding. Furthermore, in measuring the amount of these cytokines released spontaneously from BECs in the extracellular space after contact with conidia, we observed quite low levels, in particular after infection with the Δ*pksP* strain when compared to the LPS treated samples (**Figure 9B**). These results suggest that extracellular vesicles are the means used by BECs to potentiate pro-inflammatory responses from neighboring cells, when confronted with *A. fumigatus* WT conidia. The lack of cytokine secretion from epithelial cells after encounter with conidia might be due to the fact that the dectin-1 agonist β-1-3 glucan is hidden behind a thick layer of dihydroxynaphthalene (DHN) melanin and RodA protein on the surface of resting conidia. Hence, the response of BECs after interaction with swollen conidia, was evaluated, revealing rapid release of the proinflammatory IL-6 cytokine (**Figure 9B**).

A

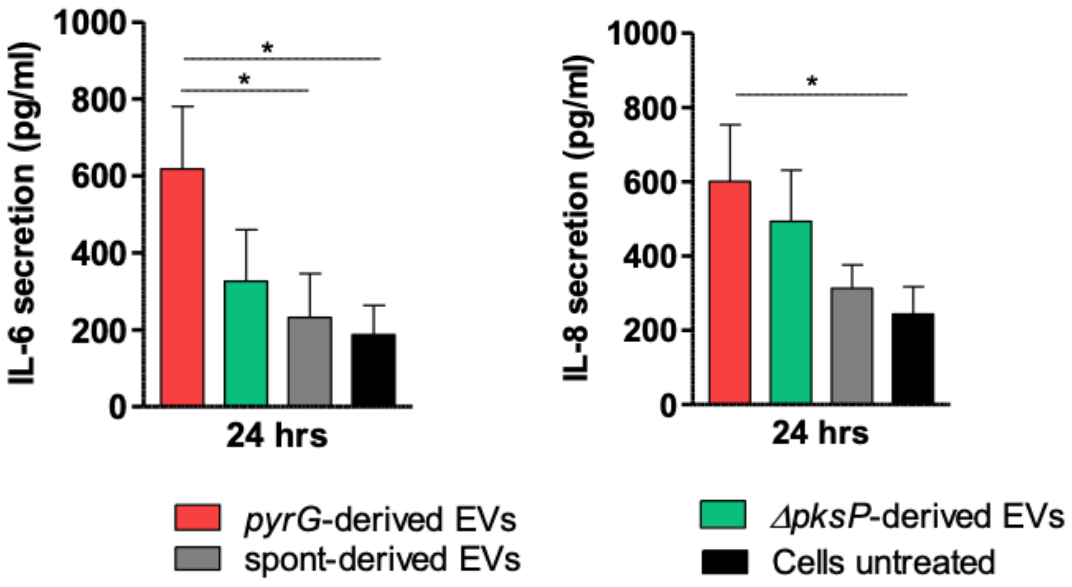

B

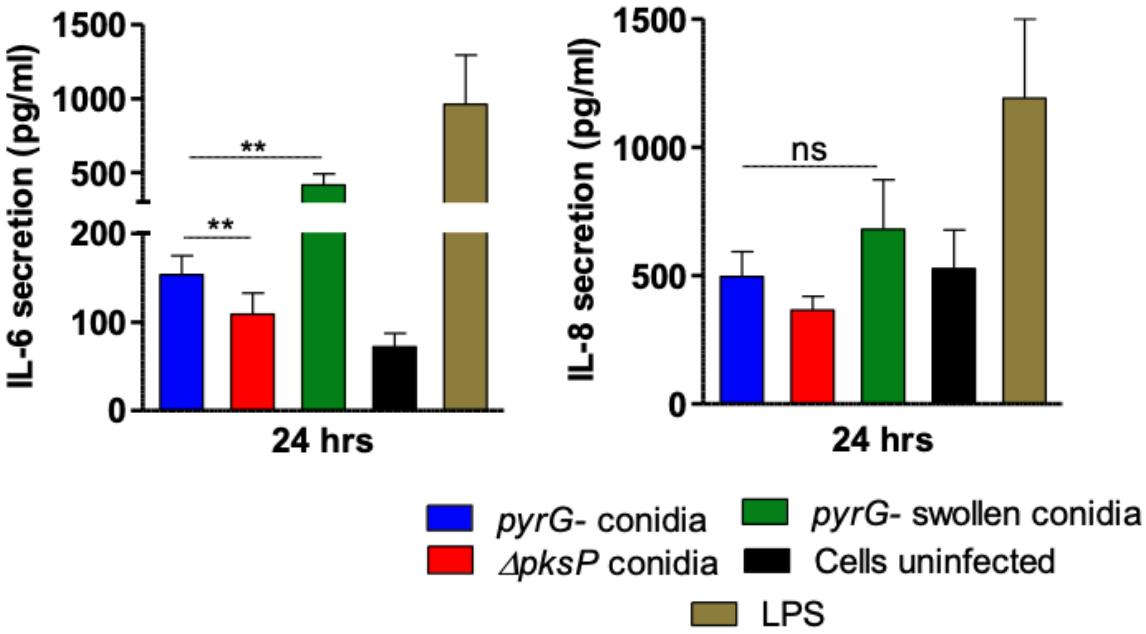

Figure 9 Evaluation of cytokines released from BEAS-2B cells.

(A) Measurement of IL-6 and IL-8 levels released from BEAS-2B cells after stimulation with different EV populations for 24 h. **(B)** Levels of IL-6 and IL-8 released from BEAS-2B cells after infection with *pyrG*-, Δ*pksP* or swollen conidia for 24 h. Lipopolysaccharide (LPS) was included as positive control. Data are presented as means ± SEM from four biological replicates Statistical significance is indicated as follows: *, $P \leq 0.05$; **, $P \leq 0.01$; ns, not significant.

6.2.4 Infection of BECs with swollen conidia changes the content of EVs.

The change in the activation profile of BECs when confronted with different morphotypes of *A. fumigatus* led us to investigate possible changes in their secreted extracellular vesicles. First, the cytokine content of EVs derived from infection with resting WT conidia with the EVs produced during infection with swollen WT conidia was compared. EVs were first lysed to release cytokines enclosed within the lipid bilayer and then incubated with a membrane-based antibody array for the simultaneous detection of 23 cytokines. This array showed that EVs produced in response to swollen conidia are filled with high levels of pro-inflammatory cytokines

like IL-6, IL-8, and TNF-alpha. Furthermore, other cytokines were also detected in both populations, like the granulocyte stimulating factor (GCSF), IL-3, and the monocyte chemoattractant protein 1 (MCP-1) (**Figure 10A**). Investigation on the protein content of these EVs also revealed that most of the proteins were shared between all the populations (**Figure 10B**), as in the previous analysis. However, gene ontology analysis on the proteins uniquely found in the swollen conidia-derived EVs highlighted the involvement of these proteins in some immune activation processes, like neutrophil aggregation or nitric oxide generation (**Figure 10C**).

A

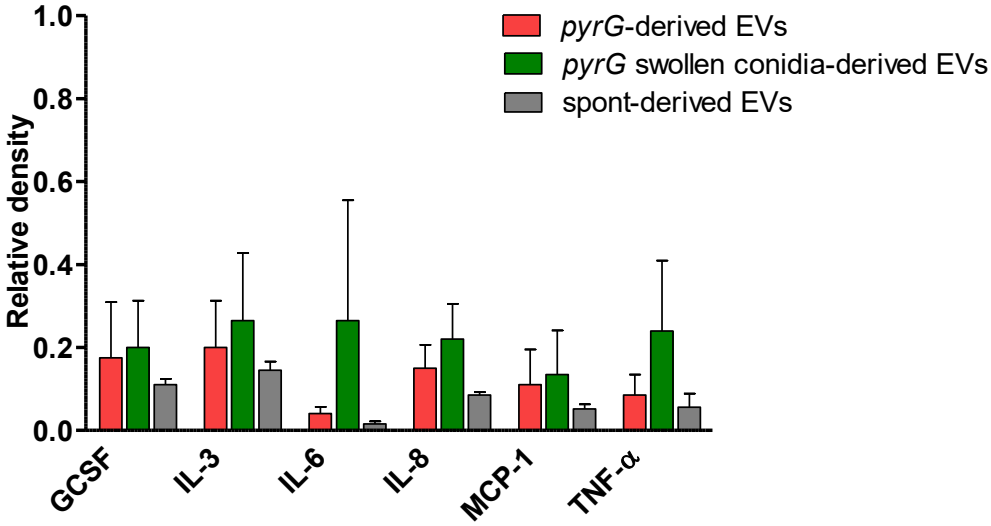

B

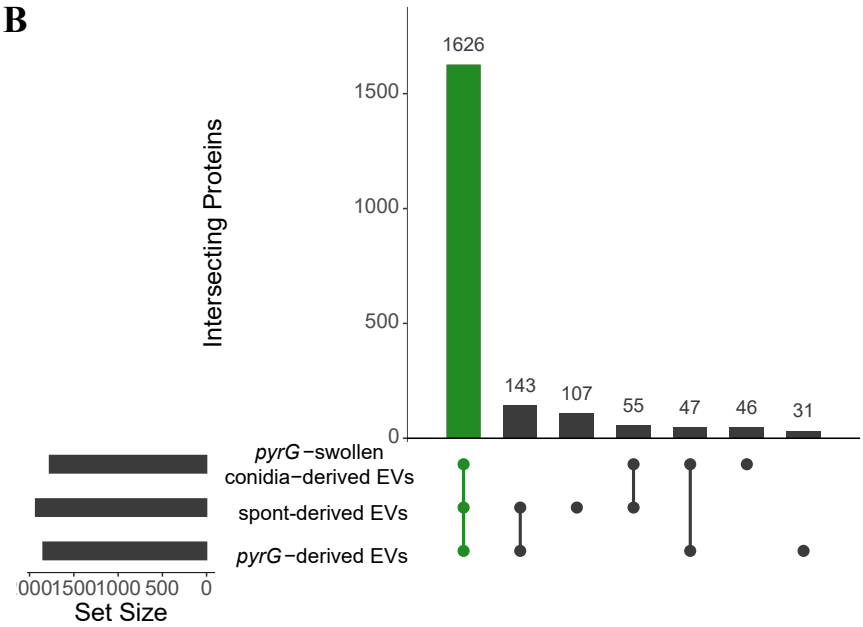

C

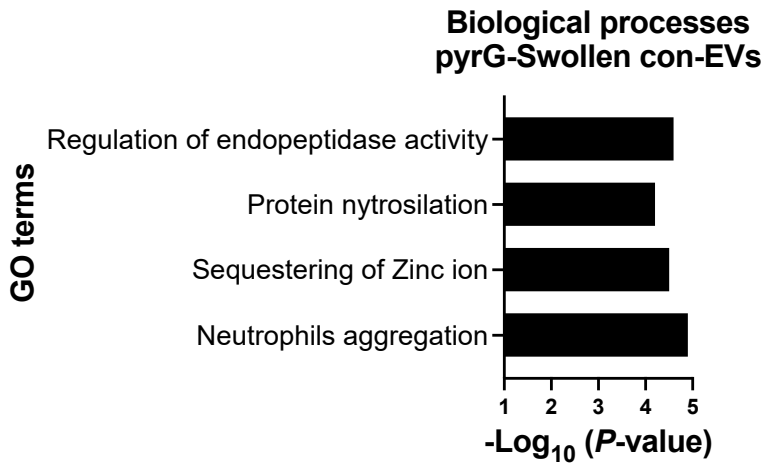

Figure 10 Analysis of EVs derived from BEAS-2B cells infected with swollen conidia.

(A) Cytokine array showing the integrated density of cytokines present in spontaneously, *pyrG*- or swollen conidia infection-derived EVs from BEAS-2B cells. Data are representative of two biological replicates. **(B)** UpSet R plot with intersected proteins found in spontaneously, *pyrG*- or swollen conidia infection-derived EVs. The green bar shows the proteins which were found in all three samples. **(C)** Gene ontology analysis on proteins found uniquely in the swollen conidia-derived EVs.

6.3 Contribution to Figures

Manuscript No. 1

Short reference Blango et al., (2020), *J. Proteome Res*.

Contribution of the doctoral candidate

Contribution of the doctoral candidate to figures reflecting experimental:

Figure: 3 and **Suppl Fig 3**	☐	100% (the data presented in this figure come entirely from experimental work carried out by the candidate)
	☐	0% (the data presented in this figure are based exclusively on the work of other co-authors)
	X	Approximate contribution of the doctoral candidate to the figure: **90** % Brief description of the contribution: I contributed to the phenotypic analysis of the KO mutants and complemented strain**.** (Panel A)

Figure: 1, 2, 4, 5 and **Suppl Fig 1, 2, 4**	☐	100% (the data presented in this figure come entirely from experimental work carried out by the candidate)
	X	0% (the data presented in this figure are based exclusively on the work of other co-authors)
	☐	Approximate contribution of the doctoral candidate to the figure: %

Manuscript No. 2

Short reference Brakhage et al., (2021), *eLife*.

Contribution of the doctoral candidate

Contribution of the doctoral candidate to figures reflecting experimental:

Figure: 1	X	100% (the data presented in this figure come entirely from experimental work carried out by the candidate)
	☐	0% (the data presented in this figure are based exclusively on the work of other co-authors)
	☐	Approximate contribution of the doctoral candidate to the figure: %

Figure: 2	☐	100% (the data presented in this figure come entirely from experimental work carried out by the candidate)
	X	0% (the data presented in this figure are based exclusively on the work of other co-authors)
	☐	Approximate contribution of the doctoral candidate to the figure: %

Manuscript No. 3

Short reference: Rafiq M., Rivieccio F., Zimmermann A-K. et al., (2022), *mSphere.*

Contribution of the doctoral candidate

Contribution of the doctoral candidate to figures reflecting experimental:

Figure: 1 and **Suppl Fig 1**	☐	100% (the data presented in this figure come entirely from experimental work carried out by the candidate)
	☐	0% (the data presented in this figure are based exclusively on the work of other co-authors)
	X	Approximate contribution of the doctoral candidate to the figure: **80** % Brief description of the contribution: I contributed to evaluation of phagocytosis via Image stream and cytokine measurements (Panel B-D)

Figure: **Suppl Fig 2**	X	100% (the data presented in this figure come entirely from experimental work carried out by the candidate)
	☐	0% (the data presented in this figure are based exclusively on the work of other co-authors)
	☐	Approximate contribution of the doctoral candidate to the figure: %

Figure: 2, 3, 4, 5, 6 and **Suppl Fig 3, 4, 5**	☐	100% (the data presented in this figure come entirely from experimental work carried out by the candidate)
	X	0% (the data presented in this figure are based exclusively on the work of other co-authors)
	☐	Approximate contribution of the doctoral candidate to the figure: %

Manuscript No. 4

Short reference Ewald J., Rivieccio F., et al. (2021), *Plos Comp. Biology*.

Contribution of the doctoral candidate

Contribution of the doctoral candidate to figures reflecting experimental:

Figure: 4 and **Fig 6**	☐	100% (the data presented in this figure come entirely from experimental work carried out by the candidate)
	☐	0% (the data presented in this figure are based exclusively on the work of other co-authors)
	X	Approximate contribution of the doctoral candidate to the figure: **90** % Brief description of the contribution: I contributed to the measurement of fungal germination and LDH release (Fig 4: panels A-B and D); and cytokine evaluation (Fig 6: panel A)

Figure: Suppl Fig 1	X	100% (the data presented in this figure come entirely from experimental work carried out by the candidate)
	☐	0% (the data presented in this figure are based exclusively on the work of other co-authors)
	☐	Approximate contribution of the doctoral candidate to the figure: %

Figure: 1, 2, 3, 5	☐	100% (the data presented in this figure come entirely from experimental work carried out by the candidate)
	X	0% (the data presented in this figure are based exclusively on the work of other co-authors)
	☐	Approximate contribution of the doctoral candidate to the figure: %

Manuscript No. 5

Short reference Rivieccio F. et al., In preparation.

Contribution of the doctoral candidate

Contribution of the doctoral candidate to figures reflecting experimental:

Figures: 1, 5 and **Suppl Fig 1-3**	X	100% (the data presented in this figure come entirely from experimental work carried out by the candidate)
	☐	0% (the data presented in this figure are based exclusively on the work of other co-authors)
	☐	Approximate contribution of the doctoral candidate to the figure: %

Figure: 2-4	☐	100% (the data presented in this figure come entirely from experimental work carried out by the candidate)
	☐	0% (the data presented in this figure are based exclusively on the work of other co-authors)
	X	Approximate contribution of the doctoral candidate to the figure: 80 % Brief description of the contribution: I performed the microscopy evaluations and proteomic analysis (Fig 2: panel A), (Fig 3: panels A-B), (Fig 4: panels B-D)

Figure: Suppl Fig 4, 5, 6, 7	☐	100% (the data presented in this figure come entirely from experimental work carried out by the candidate)
	X	0% (the data presented in this figure are based exclusively on the work of other co-authors)
	☐	Approximate contribution of the doctoral candidate to the figure: %

Scientific contributions

Peer reviewed publications

Blango MG, Pschibul A, **Rivieccio F**, Krüger T, Rafiq M, Jia L, Zheng T, Goldmann M, Voltersen V, Li J, Panagiotou G, Kniemeyer O, Brakhage AA (2020). Dynamic surface proteomes of allergenic fungal conidia. *Journal of Proteome Research*; 19(5), 2092-2104

Brakhage A.A, Zimmermann A.K, **Rivieccio F**, Visser C, Blango MG. (2021). Host-derived extracellular vesicles for antimicrobial defense. *microLife*, Volume 2 (review).

Ewald J*, **Rivieccio F***, Radosa L, Schuster S, Brakhage A.A, Kaleta C. (2021). Dynamic optimization reveals alveolar epithelial cells as key mediators of host defense in invasive aspergillosis. *Plos Computational biology* 17(12): e1009645.
*These authors contributed equally

Rafiq M*, **Rivieccio F***, Zimmermann A-K*, Visser C, Bruch A, Krüger T, González Rojas K, Kniemeyer O, Blango MG, Brakhage A.A. (2022). PLB-985 Neutrophil-Like cells as a model to study *Aspergillus fumigatus* pathogenesis. *mSphere* journal. 7(1):e0094021. *These authors contributed equally

Non-peer reviewed publications

Rivieccio F, Zimmermann A-K, Cseresnyés Z, Rafiq M, Krüger T, Höppener S, Kniemeyer O, Figge M.T, Von Lilienfeld-Toal M, Blango MG, Brakhage A.A. (2022). Selective DHN-melanin-dependent antifungal activity of neutrophil-derived extracellular vesicles against *Aspergillus fumigatus.* In preparation.

Rivieccio F, Rafiq M, González Rojas K, Zimmermann A-K, Visser C, Krüger T, Höppener S, Blango MG, Kniemeyer O, Brakhage A.A. (2022). Bronchial epithelial cells release extracellular vesicles in response to *Aspergillus fumigatus.* In preparation.

Kelani A, Bruch A, **Rivieccio F**, Visser C, Krüger T, Kniemeyer O, Bromley M, Bowyer P, Barber A, Brakhage A.A, Blango MG. (2022). Exploitation of the RNA interference pathway of the human fungal pathogen, *Aspergillus fumigatus*. In preparation.

Conference contributions

Rivieccio F. *Aspergillus fumigatus* triggers extracellular defense mechanisms in human lung epithelial cells. International Leibniz Research School symposium. October 2018. Talk.

Rivieccio F. Deciphering the role of host-derived extracellular vesicles in the fight against *Aspergillus fumigatus*. 56. Wissenschaftliche Tagung der Deutschsprachigen Mykologischen Gesellschaft. DmyK. September 2021. Talk.

Rivieccio F. Deciphering the role of host-derived extracellular vesicles in the fight against *Aspergillus fumigatus*. Jahrestagung der Vereinigung für Allgemeine und Angewandte Mikrobiologie. VAAM. February 2022. Talk.

Rivieccio F, Zimmermann A-K, Rafiq M, Visser C, Blango MG, Brakhage A.A. Deciphering the role of host-derived extracellular vesicles in the fight against *Aspergillus fumigatus*. Phagocyte-Centric Perspectives on Health and Disease: From Actin to Zebrafish. Oxnard, CA, USA. March 2022. Poster presentation.

Acknowledgements

First and foremost, I would like to thank my supervisor and mentor Prof. Dr. Axel A. Brakhage, for giving me the opportunity to work on such an interesting project, for his guidance and encouragement throughout my PhD, and especially for his patience and swift reply during this last time of writing the dissertation.

Secondly, I would like to thank Dr. Matthew Blango, who taught me a great deal about working with EVs and who was always there for suggestions and advices. I am very grateful for having him as one of my supervisors.

Thirdly, I thank Dr. Thomas Krüger and Dr. Zoltán Cseresnyés, for their help with proteomic procedures and microscopic data analysis.

Moreover, I am also grateful to all the members of the MAM department, who helped me when needed and created a pleasant working environment, especially to Anni for introducing me to the work with EVs and with the fungus and to Rafiq, Rahman, Kathy, Liuba, Dr. Maria Stroe and Dr. Michal Flak , for their friendship that motivated me through difficult times with laughter and funny moments, and for the numerous discussions that often helped to develop new ideas for projects.

Last but not least, I would like to thank my families. My italian family, “Grazie mamma, papà e Giuseppe”, for their limitless support and love, if I am where I am now is thanks to you. My german family, “Danke Christina, Peter und Hanni”, they accepted and loved me as a daughter from the start and always made me feel at home. My husband, who supported me in any way possible during my PhD time with love and understanding, even not being a scientist.

Ehrenwörtliche Erklärung

Ich erkläre hiermit, dass mir die Promotionsordnung der Fakultät der Biowissenschaften der Friedrich-Schiller-Universität bekannt ist. Ich habe die vorliegende Arbeit selbst angefertigt und keine Textabschnitte eines Dritten oder eigener Prüfungsarbeiten ohne Kennzeichnung übernommen. Alle benutzten Hilfsmittel, persönliche Mitteilungen und Quellen sind in der Arbeit angegeben. Unterstützung bei der Auswahl und Auswertung des Materials sowie bei der Herstellung des Manuskriptes habe ich durch die in der Danksagung erwähnten Personen erfahren. Ich versichere, dass keine Hilfe kommerzieller Promotionsvermittlungen in Anspruch genommen wurde und dass Dritte weder unmittelbar noch mittelbar geldwerte Leistung von mir für Arbeiten erhalten haben, die im Zusammenhang mit dem Inhalt der vorgelegten Dissertation stehen.
Diese Dissertation wurde von mir bisher weder für eine staatliche noch eine wissenschaftliche Prüfung eingereicht. Weder die gleiche, eine in wesentlichen Teilen ähnliche oder eine andere Abhandlung wurde bei einer anderen Hochschule oder anderen Fakultät als Dissertation von mir eingereicht.

Jena, den _____

_____

Flora Rivieccio